DDX11 HELICASE AS A SYNTHETIC LETHAL CANCER THERAPY TARGET

by

Leanne Amitzi

B.Sc., Tel Aviv University, Israel, 2004

M.Sc., Weizmann Institute of Science, Israel, 2007

A THESIS SUBMITTED IN PARTIAL FULFILLMENT OF

THE REQUIREMENTS FOR THE DEGREE OF

DOCTOR OF PHILOSOPHY

in

THE FACULTY OF GRADUATE AND POSTDOCTORAL STUDIES

(Medical Genetics)

THE UNIVERSITY OF BRITISH COLUMBIA

(Vancouver)

November 2021

The following individuals certify that they have read, and recommend to the Faculty of Graduate and Postdoctoral Studies for acceptance, the dissertation entitled:

DDX11 helicase as a synthetic lethal cancer therapy target

submitted by Leanne Amitzi in partial fulfillment of the requirements for

the degree of Doctor of Philosophy

in Medical Genetics

Examining Committee:

Philip Hieter, Medical Genetics, UBC
Supervisor

Peter Lansdorp, Medical Genetics, UBC
Supervisory Committee Member

Christopher Loewen, Cell and Developmental Biology, UBC
University Examiner

Colin Ross, Medical Genetics, UBC
University Examiner

Additional Supervisory Committee Members:

Samuel Aparicio, Pathology, UBC
Supervisory Committee Member

Michael Underhill, Cellular and Physiological Sciences, UBC
Supervisory Committee Member

Abstract

Genotype-driven therapies are a new paradigm for cancer treatment. These approaches rely on identification of genetic vulnerabilities and genotype-linked therapeutic agents. One approach utilizes synthetic lethality (SL), which occurs when disruption of two gene products individually is non-lethal, but simultaneous disruption of both gene products results in lethality. A synthetic lethal target identified in our lab is the helicase *DDX11*, the human homolog of yeast *CHL1*. In yeast, *CHL1* is a highly-connected synthetic lethal hub, that genetically interacts with many genes involved in processes often defective in tumours, such as sister-chromatid cohesion (SCC) and replication fork stability, and as such, would make a good synthetic lethal therapeutic target.

The overarching goal of this research is to advance development of DDX11 inhibition as a synthetic lethal therapeutic. Previous work in our lab identified a genetic interaction between cohesin mutations and *CHL1* in yeast. We first directly tested a potential genetic interaction between *DDX11* and the cancer-mutated cohesin gene *STAG2* in human cell lines and found that it did not result in synthetic lethality. We then conducted an unbiased screen for *DDX11* genetic interactions in human cells and identified many genes involved in SCC, supporting the conserved role of *DDX11*, as well as supporting DDX11 inhibition as a potential SL-based therapy for tumours with cohesion defects.

To date, only one SL-based drug has reached the clinic, PARP inhibitors, which trap PARP on the DNA creating a cytotoxic complex. Small molecule-induced trapping may represent a generalized mechanism for clinically relevant synthetic lethal interactions. We hypothesized that missense mutations that model such inhibitors can be utilized as an alternative to knock-out/knock-down based screens. As a proof-of principle, we expressed missense

mutations in *CHL1* that inhibited enzymatic activity but retained substrate binding, and found that these mutations elicited a dominant synthetic lethal phenotype consistent with the generation of cytotoxic intermediates. These results point to the utility of modeling trapping mutations in pursuit of more clinically relevant synthetic lethal interactions.

Finally, we developed a biochemical method for high-throughput screening for DDX11 inhibitors. Together, this work contributes to the development of DDX11 inhibition as an anti-cancer therapeutic.

Lay Summary

Cancer is an individualized disease - each patient's tumor is a unique combination of genetic changes that drive its development. Recent advances in DNA sequencing offer the promise of personalized treatments based on these changes; however most of the genetic changes do not currently have targeted treatments. A promising target identified in our lab is DDX11, a protein that unwinds DNA. In this study, we utilized genetic methods to study the interactions of DDX11 in human cells and to mimic the effect of a drug in yeast cells. We also developed a method to measure DDX11 activity for the purpose of searching for small-molecule inhibitors. This work further advances the development of DDX11 inhibition as an anti-cancer therapy.

Preface

Chapter 2: The research conducted in Chapter 2 was designed and performed mostly by me, with training and suggestions provided by M. Bailey. N. O'Neil and P. Hieter provided overall project direction. I designed, performed and analyzed all the experiments, with the exception of the experimental part of the CRISPR/Cas9 screen and initial bioinformatics analysis to generate the pi-scores, which was conducted by the Moffat lab at the University of Toronto. All figures and text included in this chapter of the dissertation were generated by L. Amitzi. These experiments involve cell lines, not human tissue, and do not require ethics approval.

Chapter 3: A modified version of the research conducted in Chapter 3 was published in the journal *Proceedings of the National Academy of Sciences* (PNAS). Hamza, A.*, Amitzi, L.*, Ma, L., Driessen, M. R. M., O'Neil, N. J., & Hieter, P. (2021). Modeling DNA trapping of anticancer therapeutic targets using missense mutations identifies dominant synthetic lethal interactions. *Proceedings of the National Academy of Sciences*, 118(14), e2100240118. https://doi.org/10.1073/pnas.2100240118. *These authors contributed equally to this work.

The paper was designed and written by L. Amitzi, A. Hamza and N. O'Neil under the supervision of P. Hieter. I performed all the *CHL1* experiments and A. Hamza performed all the *FEN1* experiments. M. Driessen and L. Ma constructed some of the strains tested in the paper.

The dosage/dominant synthetic lethal interaction screen method will be published as a detailed protocol (methods) paper: Hamza A., Amitzi L., Duffy S., & Hieter P. (2021) Mapping Synthetic Dosage Lethal Genetic Interactions in Saccharomyces cerevisiae. *Methods in Molecular Biology*. In press.

The methodology was developed by Hamza A., Amitzi L., and Duffy S. The paper was written by Hamza A., Amitzi L., and Duffy S., under the supervision of Hieter P.

Chapter 4: The research conducted in Chapter 4 was designed and conducted by me. N. O'Neil and P. Hieter provided overall project direction. I performed all the experiments and generated all of the text and figures for this chapter.

The synthetic lethal figure in Chapter 1 (Figure 1.2) was generated by N. O'Neil.

Table of Contents

List of Tables

List of Figures

List of Symbols, Abbreviations and Acronyms

Δ	Deletion, null mutant
ADC	Adenocarcinoma
ALF	A-like faker assay
APC/C	Anaphase Promoting Complex or Cyclosome
ATCC	American Type Culture Collection
ATP	adenosine triphosphate
AURKB	aurora kinase B
BCR-ABL1	Breakpoint-cluster-region – Abelson1 fusion gene
BLM	Bloom helicase
BPV	Bovine papillomavirus
BQQ	Benzoquinoquinoxaline
BRAF	B-RAF Proto-Oncogene
BRCA	BReast CAncer gene
BSA	Bovine Serum Albumin
CDK1	cyclin-dependent kinase 1
CHL	CHromosome Loss
CIP	Ctf4-interacting-protein
CML	chronic myelogenous leukemia
CONCR	cohesion regulator non-coding RNA
COSMIC	Catalogue of somatic mutations in cancer
cPu	cyclopurine deoxynucleoside
CRISPR	Clustered Regularly Interspaced Short Palindromic Repeats
CRISPRi	CRISPR-inhibition
CTCF	CCCTC-Binding Factor
CTF	Chromosome Transmission Fidelity
dCas9	Dead Cas9
DDX11	DEAD/H-Box Helicase 11
DMEM	Dulbecco's Modified Eagle Medium
DSB	Double strand break
DTT	Dithiothreitol
ECL	enhanced luminol-based chemiluminescent
EGFR	Epidermal Growth Factor
FACS	Fluorescence-activated cell sorting
FANC	Fanconi Anemia
FBS	Fetal Bovine Serum
FEN1	Flap Endonuclease 1
Fe-S	Iron-sulphur
FRET	Förster Resonance Energy Transfer
G4	G-quadruplex
GO	Gene Ontology
gRNA/sgRNA	Guide RNA/single guide RNA
HCC	hepatocellular carcinoma
HD	Helicase Domain
HER2	Human Epidermal growth factor Receptor 2

HPLC	High performance liquid chromatography
HPV	Human papillomavirus
HR	Homologous Recombination
HRDC	Helicase RNase D-like C-terminal
HRP	Horseradish Peroxidase
HU	Hydroxyurea
ICGC	International Cancer Genome Consortium
IMDM	Iscove's Modified Dulbecco's Medium
IPTG	isopropyl-ß-D-thio-galactoside
KD	Knock-down
KI	Knock-in
KO	Knock-out
KRAB	Krüppel-associated box
KRAS	Kirsten rat sarcoma
LFC	Log2 (fold-change)
MEK	Mitogen-activated protein kinase kinase
MMC	Mitomycin C
MMS	methylmethane sulfonate
NCI	National Cancer Institute
NGI	Negative Genetic Interactions
NHEJ	Non-homologous end-joining
NRAS	NRAS Proto-Oncogene
ORF	Open Reading Frame
PARP	Poly (ADP-ribose) polymerase
PCNA	Proliferating Cell Nuclear Antigen
PGI	Positive Genetic Interactions
PLK1	Polo-like kinase 1
PTE	alkyl phosphotriester
PVDF	Polyvinylidene difluoride
RAD	RADiation sensitive
RFC	Replication Factor C
RFU	Relative Fluorescent Units
RNAi	RNA interference
RPA	Replication protein A
RQC	RecQ C-terminal
RTK	Receptor tyrosine kinase
SBVS	Structure Based Virtual Screening
SCC	Sister chromatid cohesion
SCE	Sister chromatid exchange
SDS-PAGE	Sodium dodecyl-sulfate polyacrylamide gel electrophoresis
SF2	Super Family 2
SGA	Synthetic genetic array
shRNA	Short hairpin RNA
siRNA	Small inhibitory RNA
SL	Synthetic Lethality/Synthetic Lethal
SMC	Structural maintenance of chromosomes

SPA	Scintillation Proximity Assay
SSB	Single strand break
TCEP	Tris (2-carboxyethyl) phosphine hydrochloride
TCGA	The Cancer Genome Atlas
TKO	Toronto Knock Out
Top1	Topoisomerase 1
UV	Ultraviolet
VOUS	Variant of Unknown Significance
WB	Western Blot
WBA/WABS	Warsaw Breakage Syndrome
WRN	Werner helicase
YPD	Yeast extract, peptone, and dextrose
YPG	Yeast extract, peptone, and galactose
YPR	Yeast extract, peptone, and raffinose
YPRG	Yeast extract, peptone, and raffinose + galactose

Acknowledgements

I would like to thank my supervisor, Dr. Philip Hieter, for his guidance, patience and support during my PhD studies. Thank you for bearing with me when times were rough, and for your patience as I found my feet again during the pandemic while trying to balance family and graduate work.

I also thank my committee members, Dr. Sam Aparicio, Dr. Peter Lansdorp, and Dr. Michael Underhill for their scientific input and assistance in keeping my thesis on track.

I thank Dr. Yuliang Wu for his helpful correspondence while developing the DDX11 activity assay and the Moffat lab in Toronto for their collaboration.

I thank all the Hieter lab members I have worked with over the years. It was a pleasure to share a lab with you and discuss topics both related to science and outside of science. I am especially indebted to Dr. Nigel O'Neil for his unwavering support, advice and motivation throughout the years and particularly during the writing of this thesis, and to Dr. Melanie L. Bailey and Dr. Akil Hamza for their support and training.

I would also like to thank all the friends and colleagues I have met here at UBC for their friendship, and especially Naama Rotem-Kohavi and Sarah Brown, for their support and pep-talks over the last few years.

I acknowledge scholarship support in the form of the Government of Canada's Vanier Canada Graduate Scholarships (Vanier CGS) program, and the University of British Columbia's Graduate Entrance Scholarship and Four Year Fellowship awards.

And last, but definitely not least, I would like to thank my family near and far for their everlasting support, which filled me with strength and positivity. I especially wish to thank my

spouse, Liron Amitzi, for taking on such a major role in care-taking over the last few months, and giving me the physical and mental space I needed to complete the task of writing this thesis, and my children for being so understanding and loving throughout this process.

Dedication

To my family, near and far, for all your love and support, and in memory of my cousin, who was taken too young by cancer while I was working on this research.

Chapter 1: Introduction

Cancer is a disease of uncontrolled growth due to accumulation of multiple underlying defects in the somatic (and germline) genome. The sequencing of the human genome, and even more so, the advances in sequencing technologies and computational pipelines in recent years, have ushered in the era of personalized oncogenomics (Hyman et al., 2017). Key to this approach is both the ability to identify the genetic vulnerabilities of individual tumors, and the development of an arsenal of drugs poised to exploit these defects for selective killing of cancer cells versus healthy cells. Although much progress has been made on studying the landscape of genetic alterations that occur in cancers and identifying mutations driving development of tumours (Malone et al., 2020), there has been less progress on developing genetically targeted therapies.

Of the genetically targeted therapies available – the large majority target activated oncogenes (Zhong et al., 2021). Synthetic lethality (see below) provides an avenue for development of therapies targeting "undruggable" genetic vulnerabilities. This thesis utilizes several approaches to advance the study of DDX11 (DEAD/H-Box Helicase 11), a human helicase, as a synthetic lethal (SL) cancer therapy target.

1.1 The genetic basis of cancer

The history of cancer research is strongly entwined with the development of the field of genetics, and more recently, genomics (reviewed in Martínez-Jiménez et al. 2020). Advancing technologies enabled the identification of the first oncogenes, followed closely by identification of tumour suppressor genes, and the identification of mutations, chromosomal rearrangements and gene amplifications that cause the cancer cell phenotype (reviewed in MacConaill and

Garraway 2010). A 1988 landmark paper by Vogelstein and colleagues demonstrated that cancer is multigenic, with the progression of mutations accumulated during colorectal cancer development following a predictable path in which some mutations, such as loss of *TP53*, were always preceded by others, such as the mutation of *RAS* (Vogelstein et al. 1988).

Technological advances in molecular biology and recombinant DNA, driven in part by the ambitious goal of sequencing the entire human genome (Abdellah et al., 2004; Lander et al., 2001; Venter et al., 2001), lead to the discovery of many cancer genes and the first curated census of cancer genes (Futreal et al., 2004). This paper also raised the issue of distinguishing "driver" mutations, which contribute to tumour formation or survival, from "passenger" mutations, which are not involved in tumour biology, an issue that still exists today (Brown et al., 2019). Since the first publication in 2004, a continuous curation approach to the scientific literature has grown this resource into a comprehensive description of over 700 genes, detailing how each gene contributes to disease causation (Sondka et al., 2018). The latest release, COSMIC v86 (August 2018) describes 719 genes based on two lines of evidence – mutational patterns and biological function (Tate et al., 2019).

The growing list of cancer genes, and the multitude of pathways in which they are involved, led to a seminal proposal by Hanahan and Weinberg to catalogue them by "hallmarks" – essential alterations in cell physiology (that can be caused by a variety of underlying genetic defects) that collectively dictate malignant growth (Hanahan & Weinberg, 2000). These include self-sufficiency in growth signals, insensitivity to growth-inhibitory (antigrowth) signals, evasion of programmed cell death (apoptosis), limitless replicative potential, sustained angiogenesis, and tissue invasion and metastasis. The hallmarks of cancer were subsequently updated in 2011 adding reprogramming of energy metabolism and evading immune detection, as well as two

important underlying enabling characteristics: genome instability, which generates the genetic diversity that expedites acquisition of hallmarks, and inflammation, which fosters multiple hallmark functions (Hanahan & Weinberg, 2011).

As often happens in science, the ambitious goal of sequencing the entire human genome drove technological advances in sequencing and analysis, which in turn opened up new research questions and methodologies. Upon completion of the human genome project in 2004, an even more ambitious "cancer genome" project was launched, with the goal of obtaining a comprehensive understanding of the genomic alterations that underlie all major cancers. This encompasses multiple projects such as The Cancer Genome Atlas (TCGA), launched in 2005, exploring whole exome sequencing of multiple cancer types, with the aim of cataloging cancer-associated mutations from more than 20,000 matched tumour and normal samples across 33 cancer types. In 2008, the TCGA documented the first analysis of a single tumour type, glioblastoma, which identified three major pathways: Receptor Tyrosine Kinase (RTK) signalling, and the TP53 and Retinoblastoma (RB) tumour suppressor pathways (McLendon et al., 2008), followed closely by the analysis of other tumour types (Bass et al., 2014; Bell et al., 2011; Collisson et al., 2014; Hammerman et al., 2012; Koboldt et al., 2012; Muzny et al., 2012; Weinstein et al., 2014), and culminating in The Cancer Genome Atlas Pan-Cancer analysis, summarizing the first 12 tumour types profiled by the TCGA (Hoadley et al., 2014). The Pan-Cancer analysis was subsequently updated in 2018 to include 11,000 tumors from 33 of the most prevalent forms of cancer (Ding et al., 2018; Hoadley et al., 2018; Sanchez-Vega et al., 2018). In 2020, TCGA, together with International Cancer Genome Consortium (ICGC) added 2,658 whole-cancer genomes and their matching normal tissues across 38 tumour types studying driver mutations in both coding and non-coding regions (Campbell et al., 2020).

One of the most striking outcomes of the cancer sequencing projects is the discovery that each tumor genome is quite different from every other, and that while many contain alterations in a number of well-known cancer genes such as *TP53*, there is a long tail of genetic alterations, most of which are rare. However, the data also supports the concept of the "Hallmarks of Cancer" at the molecular level by demonstrating that, while the individual alterations themselves are rare, cancer exploits a recurring set of "hallmark" pathways. For example, a pan-cancer analysis, that focused on oncogenic drivers and integrated genomic analysis with a pathway-centric perspective, estimated that 90% of tumours have a driver mutation or alteration in at least one of ten hallmark signalling pathways and identified pathways that often cross-talk by studying co-occurrence and mutual exclusivity between molecular alterations in various pathways (Sanchez-Vega et al., 2018).

In 2018, it was suggested that the field was approaching saturation of identification of new driver genes, as the rate of new cancer driver genes being discovered with larger samples was declining rapidly (Hsiehchen & Hsieh, 2018). In 2020, analysis of TCGA data that included additional whole-genome sequences determined that, on average, cancer genomes contained 4–5 driver mutations, but in around 5% of cases no drivers were identified, suggesting that cancer driver discovery was still not complete (Campbell et al., 2020). In any case, the rate of identifying new driver genes is slowing and we are nearing the end of the "discovery" stage for identifying the underlying molecular alterations driving cancer. This milestone has opened the door for the next stage of cancer research – personalized treatment – which is still in its infancy.

1.2 Personalized/precision oncogenomics

In addition to providing tools to determine the landscape of cancer-driving molecular alterations through large scale studies, the introduction of advanced and relatively inexpensive "omics" techniques, primarily next-generation sequencing, has brought cancer genomics into the clinic. This is changing the way patients with cancer are managed, from a "one-size-fits-all" approach based on histological/pathological subtyping to an increasing focus on precision treatment based on the underlying molecular defects of individual tumours. In addition to complementing current histology-based classification methods to guide diagnosis, routine genome profiling is already improving prediction of prognosis of clinical outcomes and supporting treatment decisions in a variety of cancers (Hyman et al., 2017). Soon all patients will have the opportunity to have their cancer genomes sequenced; however, interpretation of this information and determination of the prognostic and therapeutically relevant cancer genome mutations remain key challenges. Despite these challenges, introduction of cancer genomics into the clinic is already making a difference in treatment of some tumours. The best example of genotype-driven therapy is the development and use of the tyrosine kinase inhibitor imatinib (Gleevec) and subsequent second generation inhibitors for the treatment of chronic myelogenous leukemias (CML) that harbor the *BCR-ABL1* balanced chromosomal translocation (Druker et al., 2006), the "Philadelphia chromosome", which leads to a fusion transcript that encodes the constitutively active BCR-ABL1 tyrosine kinase (Rowley, 1973). Chronic CML patients carrying the *BCR-ABL1* translocation can expect a normal life expectancy approaching that of the general population when treated with tyrosine kinase inhibitors (Morita & Sasaki, 2021). Other examples include Human Epidermal growth factor Receptor 2 (HER2)-targeted therapies for the treatment of women with newly diagnosed metastatic HER2-positive breast cancer

(Piccart-Gebhart et al., 2005), Rapidly Accelerated Fibrosarcoma (RAF) and Mitogen-activated protein kinase kinase (MEK) inhibitors for *BRAF* mutant melanomas (Chapman et al., 2011; Robert et al., 2015) and many more (Hyman et al., 2017; Malone et al., 2020). Individual genomic findings are also used to forgo therapies unlikely to result in clinical benefit, such as Kirsten rat sarcoma (*KRAS*), *NRAS*, and *BRAF* mutations in colorectal cancers that would otherwise receive anti-Epidermal Growth Factor (EGFR)-targeted therapies (De Roock et al., 2010). These genome-driven precision treatments are already making a difference in the clinic (Massard et al., 2017). The future of personalized oncogenomics is dependent on further linking of tumour mutations to the most effective therapies and the development of new targeted therapeutics.

1.3 Synthetic lethality

Despite the growing knowledge of specific genetic, epigenetic and other molecular alterations driving cancer development, only a small number of molecularly-targeted treatments are available. Of these, the majority directly target activated oncogenes, relying on the concept of "oncogene addiction" in which cancer cells become highly growth dependent on the activity of specific oncogenes and therefore highly growth sensitive upon their inhibition (Pagliarini et al., 2015). However, a large number of genetic alterations are not directly targetable. These include loss-of-function mutations in tumour-suppressor genes, and mutations in "undruggable" proteins that do not have catalytic activity and are therefore difficult to target with small molecules. Therefore, alternative approaches are needed to target the unique genetic vulnerabilities in such tumours.

It may be possible to target such genetic vulnerabilities using a concept from genetics called “synthetic lethality”. First described in fruit flies, synthetic lethality occurs when a combination of genetic perturbations is lethal, whereas each perturbation individually is not. In the context of a tumour, it may be possible to leverage both oncogenic and non-oncogenic mutations by identifying and exploiting second-site targets that, when disrupted in conjunction with a tumour-specific mutation, result in synthetic lethality (**Figure 1.1**; O’Neil et al., 2017). Inhibition of the protein product of a gene that is synthetic lethal with a cancer-driving mutation should provide great selectivity, since by definition healthy cells lacking the cancer cell-specific lesion will not be sensitive.

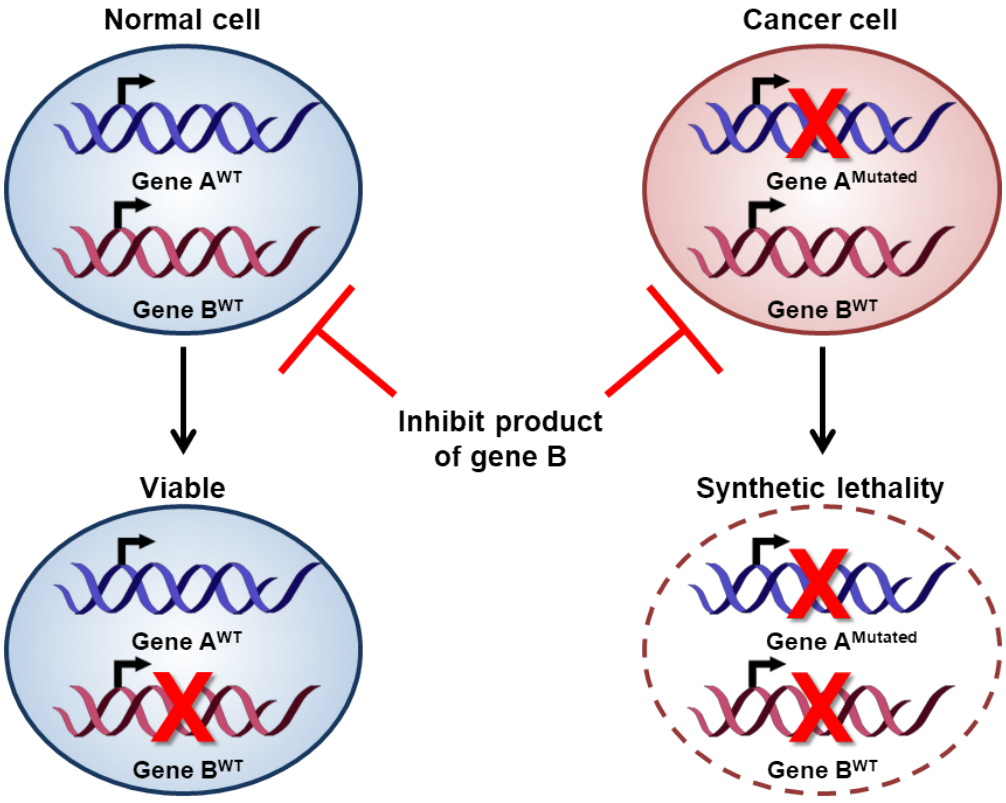

Figure 1.1 – The principle of synthetic lethality
A healthy cell carrying a wild-type version of gene A is viable upon genetic or pharmacologic perturbation of gene B, however genetic or pharmacological perturbation of gene B is lethal in a tumour cell carrying a mutant version of gene A (which is viable alone).

In a seminal 1997 paper, Hartwell et al. proposed using genetic methods to identify synthetic lethal interactions that could be used to direct development of new cancer therapeutics. Given the technological difficulties in conducting such studies in human cells, they also proposed utilizing model organisms such as *S. cerevisiae* and *C. elegans,* as many core cellular processes relevant to cancer development are highly conserved (Hartwell et al., 1997). Despite recent advances in large-scale screening in human cells developed since the publication of this idea in 1997, large-scale screening in model organisms such as yeast can still survey a much larger space than is currently feasible in human cells and identify cancer-relevant synthetic lethal interactions that can then be directly tested in human cells. While technically possible, the challenge of the scale of attempting to map all possible digenic combinations in human cells is illustrated when we look at one of the largest attempts to date. To query all pairs of 207 target genes, which represents only ~0.01% of all possible pairs in the human genome, this study generated a library of 490,000 sgRNA doublets, which is ~7x larger than the latest whole-genome single gene CRISPR/Cas9 libraries (Han et al., 2017).

High-throughput mating techniques in yeast, such as synthetic genetic array (SGA) (Tong et al., 2001), enable large-scale construction of double mutants and quantification of genetic interactions. Long-term efforts to comprehensively map all-by-all digenic interactions in *S. cerevisiae* recently resulted in an interaction map of more than 23 million double mutants covering ~90% of all *S. cerevisiae* genes, identifying over 500,000 synthetic lethal and synthetic slow growth interactions (Costanzo et al., 2016). This network can be mined for cancer-relevant synthetic lethal interactions, but can also provide the principles for elucidating synthetic lethal interactions in human cells. For example, although only ~1,000 genes in S. cerevisiae are individually essential for growth, hundreds of thousands of genetic interactions result in growth

defects and ~10,000 digenic interactions between non-essential mutations result in synthetic lethality (Costanzo et al., 2016), suggesting that the potential synthetic lethal space that can be mined for drug targets is much larger than the space that can be targeted by directly inhibiting oncogenes, increasing the probability of finding druggable targets encoded by synthetic lethal partner genes.

The success of utilizing such a cross-species approach is predicated on the conservation of genetic interactions between model organisms and human cells. Several studies utilizing query-specific screens in yeast have been successful in identifying synthetic lethal interactions that are conserved in human cells, for example between *CTF4* (*WDHD1* in human) and *MRE11A*, *CDC4*, or *BLM* (van Pel, Barrett, et al., 2013) and RAD54B-deficient cells and SOD1 or FEN1 inhibition (McManus et al., 2009; Sajesh et al., 2013). Even if a specific member of a digenic synthetic lethal interaction pair is not evolutionarily conserved, genetic interactions often display conserved interactions at the pathway level, suggesting that synthetic lethality screening in model organisms can identify interactions between biological processes from which synthetic lethal interactions in human cells can be inferred. For example, as described in section 1.4, a study utilizing *S. cerevisiae* to screen for cohesin synthetic lethal interactions identified multiple replication-fork mediators, and this was used to predict synthetic lethality between cohesin mutations and Poly (ADP-Ribose) Polymerase (PARP) inhibitors in human cell culture, even though the PARP family of genes is not conserved in yeast, a prediction which was experimentally validated (Bailey et al., 2014; McLellan et al., 2012; O'Neil et al., 2013). Recently, a systematic study to determine the degree to which synthetic lethal interactions are conserved between *S. cerevisiae* and human cancer cells found that observing a synthetic lethal interaction in yeast increased the likelihood of a synthetic lethal interaction between the

orthologous human gene pair by approximately four-fold. However, if the yeast interaction was observed in multiple environmental contexts this ratio increased to ten-fold, and for gene pairs annotated in the same biological process the likelihood of human interaction increased to ~20-fold from baseline (Srivas et al., 2016).

The direct systematic interrogation of synthetic lethal interactions in human cells is still in its infancy. As human cells cannot be manipulated through genetic mating techniques, other technologies for large-scale genetic perturbation were required before high-throughput screens became feasible. These include libraries of short hairpin RNAs (shRNAs) (Sawyers, 2009) and more recently, libraries of guide RNAs (gRNAs) for CRISPR/Cas9 genome editing (Hart et al., 2015; Shalem et al., 2014; Wang et al., 2014) that can be applied in high-throughput screening formats in isogenic cell lines or panels of cell lines to identify cancer-relevant synthetic lethal interactions (reviewed in O'Neil et al., 2017). Cost and scale improvements in screening technologies have allowed for a move away from isogenic cell line pairs to large populations of cancer cell lines (Behan et al., 2019; Cheung et al., 2011; Cowley et al., 2014; McDonald et al., 2017). By aggregating the genomic characterization of the cell lines with the functional knock-out or knock-down data, lineage and mutation-specific dependencies, including synthetic lethal interactions, can be determined (Dwane et al., 2021; Tsherniak et al., 2017).

The proof-of-concept that synthetic lethality is relevant to the clinic is the approval of PARP inhibitors for treatment of *BRCA1/2*-deficient breast and ovarian cancer (Lord & Ashworth, 2017). PARP-1 and PARP-2 are DNA damage sensors and signal transducers that operate by synthesizing negatively charged, branched poly(ADP-ribose) (PAR) chains (PARylation) on target proteins as a form of posttranslational modification (Satoh & Lindahl, 1992), and are implicated in DNA repair and genome maintenance. In 2005, two groups

described the synthetic lethal interaction between PARP inhibition and *BRCA1* or *BRCA2* mutation, suggesting a novel strategy for treating patients with *BRCA*-mutant tumors (Bryant et al., 2005; Farmer et al., 2005). Clinical trials found a clinical benefit rate of PARP inhibitor treatment of 52% in advanced refractory breast cancer and 66% in epithelial ovarian cancer in *BRCA* mutation carriers demonstrating that PARP inhibitors can be an effective therapy (Audeh et al., 2010; Tutt et al., 2010), and several PARP inhibitors have been approved for the treatment of a range of *BRCA*-mutated cancers. The initial mechanism proposed to be underlying this synthetic lethal interaction was reported to be caused by the accumulation of double strand breaks (DSBs) due to replication fork collapse when the fork encounters persistent single strand breaks (SSBs) caused by PARP inhibition (Farmer et al., 2005). However, more recently, trapping of PARP molecules at sites of DNA damage by preventing autoPARylation has been proposed as an underlying mechanism for the synthetic lethal effect (Murai et al., 2012; Murai, Huang, et al., 2014; Pommier et al., 2016).

1.4 Mutations in the cohesin complex – an emerging biomarker

The cohesin complex is a highly conserved complex mainly known for its essential role in sister-chromatid cohesion (SCC) following DNA replication until its cleavage during mitosis, thereby enabling faithful segregation of sister chromatids into two daughter cells. The complex forms a ring-like structure composed of a heterodimer of the Structural Maintenance of Chromosomes (SMC) family of ATPases, SMC1A and SMC3 (Smc1 and Smc3 in *S. cerevisiae*), the kleisin subunit RAD21 (Mcd1/Scc1 in *S. cerevisiae*), and one of two HEAT-repeat domain-containing subunits STAG1 or STAG2 (Irr1/Scc3 in *S. cerevisiae*) (reviewed in Morales & Losada, 2018). Cohesin subunit genes were originally identified in yeast in mutants that

displayed premature separation of sister chromatids (Guacci et al., 1997; Michaelis et al., 1997), and soon thereafter were found to form a complex required for sister chromatid cohesion in *X. laevis* egg extracts and mammalian cells (Losada et al., 1998, 2000). In addition to the core complex, there are several accessory proteins important for cohesin dynamics (loading and unloading from the chromosomes) and cohesin establishment following DNA replication. These include the loader heterodimer NIPBL-MAU2 (Scc2 and Scc4 in *S. cerevisiae*), the accessory proteins PDS5A/B (Pds5 in *S. cerevisiae)* which bind to the STAG subunits, WAPAL (Rad61 in *S. cerevisiae*) and Sororin (no yeast homolog), which bind to PDS5A/B and antagonize each other to maintain a balance of cohesin on the chromatin, the acetyltransferases ESCO1/ESCO2 (Eco1 in *S. cerevisiae*), which are required for acetylation of SMC3 to establish stable cohesion following DNA replication, Shugoshin 1 (Sgo1 in *S. cerevisiae*), which protects cohesin from premature cleavage, and Separase (Esp1 in *S. cerevisiae*), which cleaves the RAD21 subunit at the onset of anaphase, enabling segregation of the chromatids to the two daughter cells (reviewed in Morales & Losada, 2018). In addition to its canonical role in SCC, in mammalian cells the cohesin complex also has important roles in generating, maintaining, and regulating the DNA looping events important for the 3D genome organization and gene expression (reviewed in Waldman, 2020).

Mutations in cohesin genes and regulators are associated with several types of cancer, including bladder cancer, Ewing sarcomas, myeloid cancers, endometrial cancer and glioblastomas, with *STAG2* loss-of-function the most consistent alteration across a broad range of cancer types (Waldman, 2020). Like other pediatric cancers, Ewing sarcomas generally have very few somatic mutations (Bert Vogelstein et al., 2013); therefore the finding of frequent *STAG2* mutations is especially noteworthy. In fact, *STAG2* is considered to be a “driver” tumor

suppressor gene and recent exome sequencing of 4,742 cancer samples across 21 cancer types identified *STAG2* as one of only 12 genes that are mutated at statistically significant frequencies in at least 4 tumor types (Lawrence et al., 2014). However, the mechanism by which these mutations contribute to tumorigenesis is still unclear.

With the discovery of cohesin mutations in cancer, the initial hypothesis was that inactivation of cohesin was contributing to the aneuploidy that is a hallmark of cancer cells (Barber et al., 2008; Solomon et al., 2011). However, as genome sequencing identified more frequent cohesin mutations in a wide range of cancers, the link to aneuploidy became weaker as many tumours were euploid (for example in bladder cancer, Balbás-Martínez et al., 2013; Taylor et al., 2014). In support of this, *STAG2* mutations are most common in the early stage bladder tumours, many of which are euploid, suggesting that the contribution of *STAG2* to pathogenesis of bladder cancer is likely due to a different mechanism than aberrant sister-chromatid cohesion and aneuploidy (Hill et al., 2016). Similarly, cohesin mutations were common in myelodysplastic syndrome cancers which are mostly euploid (Kon et al., 2013), and many myeloid leukaemia tumours with cohesin mutations are euploid. Other studies demonstrated that Ewing sarcomas with cohesin mutations are often euploid (Brohl et al., 2014; Crompton et al., 2014; Tirode et al., 2014). In 2016, the Waldman group tested 50 tumour-derived *STAG2* mutant constructs in human cells and determined that, while most of the truncating mutations were poorly expressed (possibly due to nonsense mediated decay), missense tumour-derived mutations and some truncated forms of *STAG2* do not uniformly lose the ability to interact with cohesin, indicating that at least some must affect a key function of *STAG2* other than its ability to interact with cohesin. They then examined cohesion and aneuploidy and found that only one of nine tumor-derived mutations tested induced overt alterations in chromosome counts and that tumour-

derived mutations do not uniformly disrupt cohesin's enforcement of sister-chromatid cohesion (Kim et al., 2016). Alternative mechanisms proposed for the role of *STAG2* mutation in tumours are derived from the more recently studied roles of the cohesin complex in 3D genome organization and stemness/differentiation (reviewed in Waldman, 2020).

In summary, although cohesin mutations exist in a broad range of human tumours, the mechanism by which *STAG2* mutations contribute to tumour biology is still unclear, and no therapeutic approach has targeted this common genetic vulnerability. Our lab has previously utilized a cross-species approach using yeast, *C. elegans,* and human cell culture to identify and characterize synthetic lethal interactions with mutations in the cohesin complex. Synthetic Genetic Array (SGA) technology was used to screen temperature-sensitive mutants carrying mutations in either two cohesin core genes (*SMC1* and *SCC1*) or one cohesin loader gene (*SCC2*) against an array representing ~95% of all yeast genes. Filtering based on strength of the interaction, genes with a clear human homolog, and limiting the interactions only to those genes that showed a negative interaction with at least two of the three cohesin genes (under the assumption that genes interacting with more than one subunit were more likely to be true interactions) resulted in 33 interactions. These were further limited to those that showed complete synthetic lethality with at least two cohesin genes. This identified a highly connected hub of synthetic lethal partners, most of which are involved in replication fork stability (**Figure 1.2**; O'Neil et al., 2013). Even though PARP is not conserved in yeast, the identification of replication fork stability as a vulnerability in cohesin mutated cells allowed our group to predict that PARP inhibitors would be synthetic lethal in cells carrying cohesin mutations (O'Neil et al., 2013), a prediction that was validated in HCT116 and HTB-38 cells in which

SMC1 expression was depleted using siRNA (McLellan et al., 2012) as well as glioblastoma-derived cell lines carrying mutations in *STAG2* (Bailey et al., 2014).

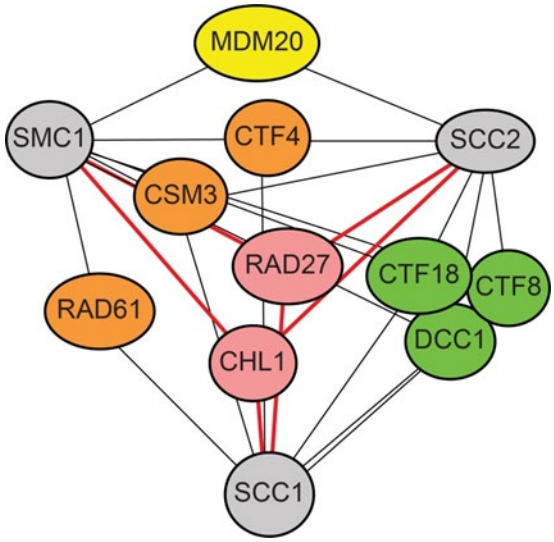

Figure 1.2 - Synthetic lethal interactions with cohesin mutations.
Hypomorphic mutations in core cohesins (*SMC1* and *SCC*1) and a cohesin loader (*SCC2*) were screened genome-wide for synthetic lethal interactions. A synthetic lethal network of the strongest synthetic lethal interactions filtered for genes with clear human homologs.
Green = Alt-RFC. Red = Genes encoding proteins with measurable enzymatic activity.
Data from (McLellan et al., 2009, 2012).

In addition to the synthetic lethality observed with PARP inhibitors, the synthetic lethal hub contains two catalytic proteins which are potentially druggable – Rad27, the yeast homolog of the human endonuclease FEN1 and Chl1, the yeast homolog of the human helicase DDX11 – the subject of this thesis.

1.5 hDDX11/yChl1

DDX11 is a superfamily 2 (SF2), ATP-dependent DEAH/DEAD-box containing helicase belonging to the XPD-like helicase family, which contains 4 members (FANCJ, XPD, RTEL1 and DDX11 (Bharti et al., 2014)), all containing a conserved iron-sulphur (Fe-S) binding

domain. These proteins play important roles in genome stability maintenance and are all implicated in rare genetic syndromes and cancer development (Brosh, 2013; Suhasini & Brosh, 2013; Wu et al., 2009). Autosomal recessive mutations in the *DDX11* gene cause a rare cohesinopathy named Warsaw Breakage Syndrome (WABS), first identified in 2010, which is characterized by a complex syndrome of clinical symptoms, including sister chromatid cohesion abnormalities at a cytological level (van der Lelij et al., 2010). To date, 23 patients have been described. Some of the mutations have been characterized biochemically (see below) and most appear to lead to significantly reduced protein stability or impaired catalytic activity (Alkhunaizi et al., 2018; Bailey et al., 2015; Bottega et al., 2019, 2021; Capo-Chichi et al., 2013; Eppley et al., 2017; van der Lelij et al., 2010; van Schie et al., 2020).The expression level of DDX11 was found to be significantly reduced in all the WABS patient-derived cell lines analyzed by immunoblots, suggesting that the pathogenic *DDX11* missense alleles are hypomorphic because they encode unstable and/or inactive (or partially active) proteins (with the exception of one mutant, R140Q, that is currently defined as a variant of unknown significance (VOUS) as it seems to behave like the wild-type protein (van Schie et al., 2020). Loss of *DDX11* in mice resulted in embryonic lethality and analysis of cells obtained from the embryos demonstrated increased frequency of chromosome missegregation, decreased chromosome cohesion, increased aneuploidy and a G2/M cell cycle delay (Inoue et al., 2007).

CHL1, the *S. cerevisiae* homolog of human DDX11, was first identified in a yeast screen for mutants that result in elevated levels of chromosome loss or missegregation (Gerring et al., 1990; Holloway, 2000). Subsequently, two human cDNAs were identified as highly similar to the yeast *CHL1* gene, one of which is *DDX11* (previously called *CHLR1*) and the other is an apparent pseudogene, *DDX12P* (previously called *CHLR2*), both located on chromosome 12

(Amann et al., 1996, 1997), likely due to a recent duplication event. It is probable that this region underwent several duplication and translocation events, as partial sequences highly similar to the C-terminus of DDX11 have been identified in the subtelomeric regions of many human chromosomes, possibly due to the appearance of an ancestral gene that originated as a rearranged portion of the primate *DDX11* gene, and propagated along many subtelomeric locations (Costa et al., 2009).

1.5.1 Biochemical properties of DDX11

Given the large number of helicases encoded by the human genome, there is great interest in analyzing the biochemical properties of each one, and in determining their roles and potential involvement in the various nucleic acid metabolism pathways. Initial biochemical analysis of DDX11 activity determined that it is an ATP-dependent DNA helicase that translocates on single-stranded DNA with a preferred 5' to 3' directionality. It is unable to unwind blunt-end duplexes, but rather requires a 5' single-strand region for loading. DDX11 does not require a free 5′-end, since it can bind and unwind from a gapped ssDNA region 10 nucleotides in length (Farina et al., 2008; Hirota & Lahti, 2000) or from a 5' flap substrate in which only a nick resides between the 5' flap and the duplex region of the DNA substrate (Wu et al., 2012). DDX11's activity is stimulated upon addition of Replication Protein A (RPA) or the Ctf18- Replication Factor C (RFC) complex, and it also interacts physically with the Ctf18-RFC complex, Proliferating Cell Nuclear Antigen (PCNA) and FEN1, suggesting a role in lagging strand DNA synthesis (Farina et al., 2008). In more recent studies, the enzymatic activity of DDX11 has been characterized on a variety of DNA substrates. DDX11 was found to resolve a three-stranded D-loop with an invading 3′-end but was not active on Holliday junctions, which suggests a role in early stage homologous recombination (HR) reactions or telomere metabolism, due to the

structural similarity between D-loops and T-loops present at the chromosomal ends (Wu et al., 2012). DDX11 is also able to unwind DNA substrates containing damaged nucleotides such as 8,5′ cyclopurine deoxynucleoside (cPu) adducts on the translocating strand, while the DNA helicase activity of the related FANCJ and RECQ1 is completely inhibited by these oxidative lesions (Khan et al., 2014), as well as DNA substrates containing alkyl phosphotriester (PTE) lesions if they are on the displaced strand but not on the translocated strand (Suhasini et al., 2012). Purified DDX11 is also able to displace proteins bound to DNA (tested by disruption of high-affinity streptavidin:biotin interaction), a property that is shared with the related FANCJ helicase, but not with other SF2 RecQ family helicases such as WRN or BLM (Sommers et al., 2009; Wu et al., 2012), although the physiological relevance of this is not clear.

Alternative DNA structures can arise at genomic loci containing repetitive sequences causing replication stress. These unconventional structures mainly consist of DNA containing triple-stranded (triplex) or G-quadruplex (G4) structures. DDX11 is able to resolve inter- and intramolecular DNA triplexes with a catalytic efficiency much higher than the one displayed by other human DNA helicases (such as WRN, BLM, and FANCJ) (Brosh et al., 2001; Guo et al., 2015). Like on duplex DNA, DDX11 helicase activity on DNA triplexes is ATP-dependent, has a 5′ to 3′ directionality and requires a 5′ single-stranded overhang on the third strand. Triplex-DNA with a 5’-overhang on the third strand represents the preferred substrate *in vitro* for DDX11 compared to forked duplex and G4 DNA structures (Guo et al., 2015). G4’s are an important source of replication stress, as they create a roadblock for the replication machinery. G4 DNA may have multiple structures being formed by four (tetra-molecular), two (bimolecular) or one (unimolecular) G-rich strand and can be parallel, anti-parallel or mixed (Hänsel-Hertsch et al., 2017). DDX11 unwinds G4 DNA with a strong preference for a two-stranded antiparallel G4

(G2'), but is only marginally active on a four-stranded parallel G4 structure (Wu et al., 2012). DDX11 is unable to unwind unimolecular G4 DNA, which distinguishes it from the sequence-related FANCJ helicase which is efficiently able to resolve all of these structures (Bharti et al., 2013). This preference of DDX11 for triplex DNA and FANCJ for G4 DNA is supported by cellular studies in which cells depleted for DDX11 or FANCJ were tested for their sensitivity to Telomestatin (a G4 DNA-binder) and benzoquinoquinoxaline (BQQ; a triplex-DNA stabilizing agent). Cells in which DDX11 was downregulated using siRNA were resistant to Telomestatin but FANCJ-depleted cells were sensitive and showed a clear increase in H2γX foci (a marker of DNA damage) compared to control cells (Bharti et al., 2013). In contrast, DDX11-depleted cells were extremely sensitive to other G4-stabilizers Quarfloxin and CX-5461, but these caused little effect in FANCJ-knock-out cells (van Schie et al., 2020). These compounds might target different G4 subsets depending on their structure/conformation and/or subcellular localization, which may explain the difference in sensitivity between DDX11 and FANCJ-depleted cells. The role of DDX11 in resolving triplex DNA is supported by the sensitivity of cells depleted for DDX11 or FANCJ to the triplex-stabilizing agent BBQ. DDX11-depleted cells demonstrate a large increase in triplex-DNA structures and H2γX foci compared to control cells, whereas in *FANCJ* knock-out cells there is no difference in triplex-DNA formation compared to control cells upon exposure to BBQ. In addition, these cells had a significantly lower level of triplex-DNA structures compared to DDX11-depleted cells, suggesting that DDX11 has a prominent role in resolving or preventing formation of triplex DNA structures as compared to FANCJ (Guo et al., 2015).

As mentioned above, the catalytic activity of several *DDX11* mutants has been characterized *in vitro.* Most of the mutated amino acid residues are located within the conserved

helicase motifs and are expected to impair the catalytic functions of DDX11. For some of the *DDX11* pathogenic missense alleles this was tested by *in vitro* enzymatic studies of the mutant proteins, which were produced in recombinant form and purified. The following amino acid substitutions were found to compromise the ability of DDX11 to unwind forked duplex DNA substrates: K897Δ (Wu et al., 2012), R263Q (Capo-Chichi et al., 2013), L836P (Bottega et al., 2021) and C705Y (van Schie et al., 2020). In addition to these patient-derived mutations, two engineered mutations have been tested. An engineered mutation in the conserved Walker A box (motif I) lysine, K50R, maintained DNA binding ability, but was unable to hydrolyse ATP or unwind a forked duplex or G4 (Wu et al., 2012). A conserved glutamine in the Q-motif of DDX11 was mutated to alanine (Q23A) and it was found that the mutant protein displayed normal ATP binding, but impaired ATPase activity, as well as reduced DNA-binding and no helicase activity (Ding et al., 2015).

1.5.2 Cellular role of DDX11

The role of *DDX11* in sister chromatid cohesion establishment is highly conserved from yeast to humans. As mentioned above, the yeast homolog, *CHL1*, was identified in genetic screens for mutants involved in chromosome loss in budding yeast (Gerring et al., 1990; Holloway, 2000) and shown to be the same gene as identified in an earlier study on mutants displaying bisexual mating behaviour due to chromosome loss (Haber, 1974; Liras et al., 1978). Subsequent studies demonstrated that deletion of *CHL1* causes premature sister chromatid separation (Skibbens, 2004), and identified a network of interactions between factors involved in the replication fork including *CHL1*, *CTF4*, *CTF18*, *CTF7/ECO1*, *CSM3*, *MRC1*, *TOF1* and *FEN1* (Borges et al., 2013; Mayer et al., 2004; Petronczki et al., 2004; Skibbens, 2004; Xu et al., 2007), which can be divided into two epistasis groups: one including *CTF4*, *CHL1*, *CSM3* and

TOF1 and the second containing *MRC1* and *CTF18-RFC* (Xu et al., 2007). The genetic evidence in yeast was recently corroborated by an elegant biochemical study demonstrating two cohesion establishment pathways – in one, Chl1, together with Ctf4 and Csm3/Tof1 convert cohesin that is associated with the unreplicated DNA into a cohesive structure during replication, and in the other, de novo cohesin is loaded at the replication fork in a manner dependent on Mrc1, Ctf18-RFC and the cohesin loader Scc2 (Srinivasan et al., 2020).

Chl1 recruits the cohesin loader, Scc2, during S-phase, suggesting that yeast Chl1 participates in the establishment of chromosomal cohesion by a mechanism proposed to take place at the replication fork along with lagging strand synthesis (Rudra & Skibbens, 2012, 2013). In a similar manner, DDX11 siRNA-mediated knock-down causes chromosome segregation anomalies and sister chromatid cohesion defects in human cells (Inoue et al., 2007; Leman et al., 2010; Parish, Rosa, et al., 2006). Human DDX11 was also reported to directly interact with FEN-1, Ctf18-RFC and RPA, stimulate the activity of FEN-1 and be stimulated by addition of RPA and Ctf18-RFC to *in vitro* activity reactions. Depletion of either DDX11 or FEN-1 resulted in sister chromatid cohesion defects in human cells (Farina et al., 2008).

More recent studies have shed light on how hDDX11/yChl1 interacts with the replisome to enhance establishment of sister chromatid cohesion in concert with replication. In yeast, Chl1 interacts with the replisome through binding to Ctf4 via a Ctf4-interacting-protein motif (CIP-box, analogous to the PCNA-binding PIP-box motif). It is this interaction (and less so the helicase activity) that is crucial for establishment of cohesion, whereas the helicase activity is required for replication fork progression under conditions of replication stress (Samora et al., 2016). In human cells a similar mechanism has been demonstrated. DDX11 helicase activity is stimulated by the presence of TIMELESS, a component of the replication fork–protection

complex, on a variety of substrates, and the two proteins physically and functionally interact to operate in the same pathway to preserve fork integrity under conditions of replication stress (Calì et al., 2015). DDX11 interaction with TIMELESS is through a conserved peptide sequence located between helicase box I and Ia that is shared only by FANCJ, but not other SF2 Fe-S DNA helicases, and this interaction is required for stable association of cohesin to the replication forks and for chromosomal cohesion. In agreement with the study in yeast, DDX11 helicase activity was not essential for sister-chromatid cohesion, as a helicase-dead mutant could partially rescue the defects in DDX11-depleted cells (Cortone et al., 2018). In contrast, DDX11 helicase activity was found to be required for cohesin establishment in chicken DT-40 cells, and the reason for this discrepancy with yeast and human cells is unclear (Abe et al., 2016). Also in DT-40 cells, it has been shown that TIMELESS contains a DNA-binding domain that exhibits specificity for G4 structures, and contributes to maintaining processive replication through G4-forming genomic sequences. This function requires interaction with and activity of DDX11, suggesting that Timeless plays a role in the detection of G4 structures at the replication fork, recruiting DDX11 to unwind them and ensure processive replication is maintained, thereby avoiding G4-induced genetic and epigenetic instability (Lerner et al., 2020). Interestingly, co-depletion of both DDX11 and FANCJ has an additive effect on the replication processivity. This is supported by a recent study demonstrating that that loss of both DDX11 and FANCJ has additive effects in DNA damage accumulation in human cells upon treatment with Pyridostatin, a G4-stabilizer, or mitomycin C, a DNA cross-linker (van Schie et al., 2020). The conservation of this role is also supported by a previous study in *C. elegans* demonstrating that CHL-1 function is required for the integrity of G4 forming DNA in the absence of DOG-1 (the worm homolog of *FANCJ*) (Chung et al., 2011). DDX11 also interacts with the replication factors DNA

polymerase δ and WDHD1, removing obstacles and generating single-stranded DNA. Depletion of DDX11 causes reduced levels of single-stranded DNA, a reduction of chromatin-bound RPA, and impaired CHK1 phosphorylation, suggesting that DDX11 plays a role in dismantling secondary structures during DNA replication, thereby promoting CHK1 activation (Simon et al., 2020).

In human cells the role played by DDX11 in cohesion might also be regulated by a long noncoding RNA, cohesion regulator non-coding RNA (CONCR). CONCR, previously annotated as *DDX11* antisense RNA 1 (*DDX11-AS1*), is a divergent non-overlapping transcript of the *DDX11* gene and was found to be upregulated in multiple tumour types. Inactivation of CONCR causes a severe defect in sister chromatid cohesion, a phenotype that can be efficiently rescued by over-expressing DDX11. CONCR depletion does not affect the DDX11 RNA and protein level, but rather appears to interact directly with DDX11 and enhance the ATPase activity (Marchese et al., 2016).

In summary, two main models have been proposed for the role of Chl1/DDX11 in coupling DNA replication and sister chromatid cohesion. In one, DDX11 is required to resolve DNA secondary structures arising at replication forks mainly on the lagging strand to enable timely maturation of Okazaki fragments and establishment of cohesion (Bharti et al., 2014; van Schie et al., 2020). In the other, Chl1 has a scaffolding role at the fork, positioning the cohesin complex in a conformation able to capture the two DNA molecules (Murayama et al., 2018; Samora et al., 2016). These two models are not mutually exclusive and identifying the molecular mechanisms by which Chl1/DDX11 promotes pairing of the newly duplicated DNA molecules together with other components of the replication machinery remains an important question in this field.

In addition to cohesion establishment, DDX11 also plays a role in replication fork stability as described above and in DNA repair, although this may be an indirect role as a cohesion establishment factor (as sister-chromatid cohesion is a prerequisite for efficient double-stranded DNA break repair, Ström et al., 2004). Yeast Chl1 is required for viability and DNA repair upon exposure to genotoxic agents such as methylmethane sulfonate (MMS) and ultraviolet (UV) rays (Laha et al., 2006). Cells cultured from WABS patients are sensitive to the DNA cross-linking agent mitomycin C (MMC) and the topoisomerase I inhibitor, camptothecin (van der Lelij et al., 2010). DDX11-depleted cells are sensitive to cisplatin, an interstrand-crosslinking agent that causes stalled replication forks, and display defects in the repair of double-strand breaks (Shah et al., 2013). In chicken DT-40 cells DDX11 is important for repair by homologous recombination (HR) of DNA bulky lesions induced by MMS, and co-operates with the 9-1-1 checkpoint clamp and its loader, RAD17, to facilitate trans-lesion synthesis through bulky lesions and abasic sites (Abe et al., 2018). A role for DDX11 in mammalian HR is supported by the finding of decreased levels of sister chromatid exchange (SCE) in DDX11-depleted cells upon exposure to the mutagen 4-nitroquinoline1-oxide in HeLa cells (Inoue et al., 2007). As mentioned above, DDX11-depleted cells are also sensitive to the G4 stabilizers Quarfloxin and CX-5461, but not Telomestatin, and to BBQ, a triplex-DNA stabilizer.

1.5.3 DDX11 and cancer

Disease-causing mutations have been described in *BLM*, *WRN*, and *RECQL4* to cause cancer predisposition syndromes: Bloom, Werner, and Rothmund-Thompson syndrome, respectively (Sharma et al., 2020). Mutations in the highly related *FANCJ* helicase have also been associated with breast cancer (Cantor & Guillemette, 2011). Given the important and conserved role *DDX11* plays in maintaining genome stability, it could be expected that *DDX11*

would act as a tumour-suppressor gene, similar to the other helicases mentioned. However, this does not seem to be the case, as WABS patients appear to lack childhood malignancies or other signs of hereditary cancer predisposition (van Schie et al., 2020) and *DDX11* does not display a mutational pattern characteristic of tumour-suppressor genes including multiple truncating mutations. In fact, a review article on DNA damage response proteins that are deregulated in various cancers included *DDX11* as a potential oncogene (Pearl et al., 2015). This is based on the "20:20 rule" proposed by Vogelstein to discriminate tumour-suppressor genes from oncogenes, according to which a gene that has >20% truncating/inactivating mutations in cancer tissues can be considered a tumour-suppressor gene, whereas if a gene has >20% missense mutations in recurrent positions, it can be considered an oncogene (Bert Vogelstein et al., 2013).

Several studies support a potential pro-tumorigenic role for *DDX11*. Human papillomavirus (HPV) causes hyper-proliferative lesions which can progress to cancer. HPV E2 protein binds DDX11 and this interaction may play a role in maintaining viral infection persistence as E2 mutants in both bovine papillomavirus (BPV) and HPV reduce binding to DDX11, and for BPV also impair maintenance of viral episomal elements (Harris et al., 2017; Parish, Bean, et al., 2006). DDX11 is also up-regulated or amplified in multiple tumour types, including hepatocellular carcinoma (HCC), lung adenocarcinomas and melanomas. In hepatocellular carcinoma, DDX11 expression is increased relative to non-tumour tissue, and this property is associated with poor prognosis. DDX11 downregulation has been found to suppress proliferation and colony formation of a number of HCC cell lines, whereas overexpression promotes proliferation, migration and invasion and prevents apoptosis of cells *in vitro*. DDX11 knock-down also inhibited tumour growth in an HCC mice-xenograft model, whereas in mice inoculated with DDX11-overexpressing cells, tumours grew faster than in mice inoculated with

control cells (Su et al., 2021; Yu et al., 2020). In lung adenocarcinoma (ADC), DDX11 mRNA is upregulated in many samples compared to healthy tissue and this is correlated with poor prognosis (Cui et al., 2021; Li et al., 2019). In melanoma, DDX11 is upregulated 8-fold in invasive melanomas compared to non-invasive melanomas. Downregulating DDX11 by siRNA in cell lines derived from metastatic melanomas caused abnormal sister chromatid cohesion, chromosome breakages, telomere shortening, apoptosis and inhibited cell proliferation (Bhattacharya et al., 2012). Collectively, these studies suggest that in addition to being an interesting synthetic lethal target for cancer therapy, development of a DDX11 inhibitor may directly target tumours that are overexpressing DDX11 or that are reliant on DDX11.

1.6 Research aims

Although its precise functions in genome homeostasis are still not well understood, the cellular and molecular/biochemical studies of yeast Chl1 and human DDX11 to date suggest that the helicase plays a critically important role in cellular replication and/or DNA repair. *DDX11/CHL1* appears to be a highly connected synthetic lethal hub with many genes involved in processes that are often defective in tumours such as cohesion, chromosome segregation, replication, DNA repair, and cell cycle progression, and as such, would make a potentially broad spectrum synthetic lethal therapeutic target. Furthermore, wild-type DDX11 appears to play a role in tumorigenesis, so DDX11 inhibition may have therapeutic benefits beyond synthetic lethality. Therefore, the overarching goal of my research is to further study h*DDX11*/y*CHL1* synthetic lethal interactions and advance development of DDX11 inhibition as an anti-cancer synthetic lethal therapeutic.

The first aim of this thesis is to directly test whether there is a synthetic lethal interaction between *DDX11* and the cohesin component *STAG2* (which is somatically mutated at high frequency in several types of cancer) in human cell lines, as well as to further study *DDX11* synthetic lethal interactions in human cells in an unbiased manner. Given the low rate of clinical success of synthetic lethal protein inhibitors, and the fact that null mutations may not fully recapitulate the effect obtained with small molecule inhibitors (discussed in Chapter 3), the second aim of this thesis is to use yeast genetic tools to test whether missense mutations can be utilized as a model for a type of protein inhibition that creates a dominant gain-of-function cytotoxicity mimicking a "trapped" protein, thus causing a cytotoxic DNA-protein or protein-protein complex. The final goal of this study is to develop a high-throughput biochemical assay suitable for screening for inhibitors, to further the development of DDX11 inhibition both as a research tool and as an anti-cancer therapeutic.

Chapter 2: Studying *DDX11* synthetic lethal interactions in mammalian cells

2.1 Introduction

As mentioned in the introduction, in 1997 Hartwell, et al. proposed using model organisms and genetic screens to identify synthetic lethal interactions that could be used to target genetic vulnerabilities (Hartwell et al., 1997). The success of utilizing a cross-species approach is predicated on the conservation of genetic interactions between model organisms and human cells. Although many cancer-relevant genes and processes are conserved between yeast and humans, it is difficult to predict which synthetic lethal interactions will be conserved (Koch et al., 2012). Therefore, synthetic lethal interactions identified in yeast that may be clinically-relevant need to be experimentally tested in human cells to determine whether they can be utilized for cancer therapeutics. As mentioned in the introduction, mutations in the cohesin complex, and in particular the cohesin core subunit gene, *STAG2*, represent a valuable cancer-relevant biomarker (Waldman, 2020), and previous studies in our lab have identified *CHL1*, the yeast homolog of human *DDX11*, as a strong synthetic lethal partner with components of the cohesin complex (McLellan et al., 2012; O'Neil et al., 2013). Therefore, one of the goals of this chapter is to directly test whether loss-of-function of *DDX11* and *STAG2* together causes synthetic lethality in human cell culture.

In addition to identifying synthetic lethal interactions, studying genetic interactions can provide functional information on a protein's role and pathways (Kim et al., 2019). DDX11 plays an important role in DNA replication, repair and sister-chromatid cohesion, and yeast *CHL1* is a highly connected synthetic lethal hub that genetically interacts with many genes involved in cancer-relevant processes (Costanzo et al., 2016), however the mammalian genetic interactions had not been studied at the time this project was initiated. Since then, a single study

of human *DDX11* genetic interactions has been published. This study utilized an arrayed whole-genome siRNA screen in Warsaw Breakage Syndrome patient-derived SV40-imortalized fibroblasts (containing an unstable hypomorphic mutation in *DDX11* that causes reduced protein levels) and isogenic cells in which the mutation was complemented by expression of wild-type *DDX11* cDNA (De Lange et al., 2015), and identified the Anaphase Promoting Complex or Cyclosome (APC/C) as a synthetic lethal partner. In light of the scarcity of information on *DDX11* genetic interactions in mammalian cells, a second goal of this chapter was to conduct an unbiased screen in *DDX11* knock-out cells to provide additional functional information, and identify genetic backgrounds sensitized to *DDX11* loss of function.

One consideration when performing genetic interaction analysis is whether or not the query gene is essential. This is not an issue for yeast screening as *CHL1* is non-essential in yeast. However, it is unclear whether *DDX11* is essential in human cell culture. On the one hand, *DDX11* is defined as a common essential gene in the Cancer Dependency Map (DepMap; Pacini et al., 2021), however it is not known whether this is due to limitations of the experimental approach. These include limitations such as determining essentiality under competitive growth conditions, and the possibility that the repetitive nature of the *DDX11* target genomic sequence results in false positive hits, as can happen when multiple loci are targeted by CRISPR/Cas9 (Aguirre et al., 2016; Munoz et al., 2016), although this phenomenon can be accounted for using computational methods (Meyers et al., 2017). On the other hand, WABS patients carry mutations in *DDX11* and fibroblasts can be immortalized and cultivated from these patients (Capo-Chichi et al., 2013; van der Lelij et al., 2010), although many may be carrying hypomorphs of *DDX11* and may retain residual activity (van Schie et al., 2020). In addition, *DDX11* knock-out lines have recently been established in HeLa uterine and U2OS osteosarcoma cancer cell lines

(Jegadesan & Branzei, 2021). Based on these studies, it is likely that *DDX11* is essential in some but not all cellular contexts. A concern for any study using a *DDX11* knock-out line is whether the cellular context that permits a viable *DDX11* knock-out cell line could alter or mask genetic interactions with *DDX11*.

In this chapter, given the high prevalence of loss-of-function mutations in the human cohesin component, *STAG2*, in several cancer types, and the strong synthetic lethal interaction between *CHL1* and cohesin component hypomorphs in yeast, we predicted that *STAG2* and *DDX11* may exhibit a synthetic lethal interaction in human cells, and set out to directly test this. To further study *DDX11* genetic interactions in human cells, we established an isogenic pair of *DDX11* wild-type and knock-out cell lines and conducted an unbiased genome-wide CRISPR/Cas9 screen to identify potential cancer biomarkers for treatment with future DDX11 inhibitors, as well as provide additional functional and therapeutic information on the role of *DDX11* in human cells.

2.2 Materials and methods

2.2.1 Cell lines

All cell lines were grown in 10 % FBS (Invitrogen) and incubated at 37°C and 5% CO2. The H4 glioblastoma-derived cell line (which contain an endogenous 25bp insertion in STAG2 that leads to protein truncation) and the H4 *STAG2* KI (in which the *STAG2* insertion was corrected by homologous recombination) have been described previously (Solomon et al., 2011). H4 and H4 *STAG2* KI cells were cultured in Dulbecco's Modified Eagle Medium (DMEM).

HAP1 cells are a near-haploid line derived from KBM-7 and have been previously described (Carette et al., 2011). HAP1 cells and HAP1 *DDX11* KO cells were cultured in Iscove's Modified Dulbecco's Medium (IMDM) maintaining confluence at <70%.

HT-29 cells are derived from a colorectal adenocarcinoma. Cells were obtained from American Type Culture Collection (ATCC) and cultured in DMEM.

2.2.2 Western blotting

Samples for western blot were lysed in Lysis buffer (50 mM Tris-HCl, pH 7.5, 150 mM NaCl, 10 % glycerol, 1 % Triton X-100 and protease inhibitors), sonicated, and debris spun down at ~18000 x g at 4°C for 15 min. Samples were normalized by protein concentration using BCA, run on SDS-PAGE gels of appropriate acrylamide concentration and transferred to PVDF membrane (Immobilon-FL; Millipore). After probing with primary and secondary antibodies, blots were then subjected to ECL (Clarity or Clarity Max Western ECL substrate, BioRad) and visualized using a BioRad ChemiDoc MP Imager in the appropriate channel. Antibodies used for Western blot were as follows: GAPDH (Abcam, ab9485), DDX11 (Abnova, H00001663-B01P), STAG2 (Santa Cruz, sc81852), α-tubulin (Abcam, ab18251).

Secondary antibodies were either Goat-anti-mouse conjugated to HRP or Goat-anti-rabbit conjugated to HRP or Cy3 (Jackson Laboratories).

2.2.3 Plasmids, primers and sgRNA

For generation of knock-out lines, sgRNAs (Appendix A) were cloned into pSpCas9-T2A-blast, which was derived from pSpCas9-T2A-puro (Addgene # 62988). Blasticidin resistance gene was amplified from lenti-dCas9-VP64-blast (Addgene #61425) using primers OPH8968 and OPH8969 and cloned into the pCR®-Blunt vector using Zero Blunt™ PCR Cloning Kit (Invitrogen) according to manufacturer's instructions. Site directed mutagenesis to

remove the BbsI site was performed using QuikChange® Site-Directed Mutagenesis Kit (Agilent) and primers OPH9364 and OPH9365 and verified by Sanger sequencing. The modified blasticidin resistance gene was then cloned into pSpCas9-T2A-puro using EcoRI (replacing the puro gene) to obtain BPH1324. Finally, gRNA's were cloned into pSpCas9-T2A-blast using BbsI.

For CRISPR inhibition (CRISPRi) experiments, the multiplex system from (Kabadi et al., 2014) was used with some modifications. KRAB was amplified from pHAGE TRE dCas9-KRAB (Addgene #50917) using OPH8228 and 8229. T2A-puro was amplified from pSpCas9n(BB)-2A-Puro (PX462) V2.0 (Addgene #62987) using OPH8227 and 8224. KRAB and T2A were cloned into pLV hUbC-dCas9 VP64-T2A-GFP (Addgene #53192) using AvrII/NheI and NheI/AgeI respectively to generate pLV hUBC-dCas9 KRAB-T2A-puro. For the sgRNA entry vectors, the system was modified to use 2 sgRNAs (instead of the original 4) by site directed mutagenesis (QuikChange® Site-Directed Mutagenesis Kit (Agilent)) of the Golden Gate site on the 5' end of phH1-gRNA (Addgene #53186) using primers OPH2818 and 2819 such that the overhang can be directly cloned into pLV hUBC-dCas9 KRAB-T2A-puro.

DDX11 CRISPRi sgRNA's (Appendix A) or a non-targeting sequence (sgNT4) were cloned into ph7SK-gRNA using BbsI and subsequently cloned, together with phH1-sgNT3, into pLV-hUBC-dCas9-KRAB-T2A-puro by Golden Gate cloning using BsmBI to generate final viral vectors.

DDX11 inducible shRNAs (Appendix A) were ordered from Sigma (MISSION pLKO_IPTG_3xLacO vectors).

2.2.4 Cell growth experiments

CRISPRi experiments: Approximately $6x10^4$ H4 and H4 KI cells were infected in 6-well plates with the pLV-hUBC-dCas9-KRAB-T2A-puro-sgRNA constructs. Approx. 24 hours after infection, cells were selected with puromycin for 2 days and then media was replaced with drug-free media for 1 day to recover from selection. Cells were collected by trypsinization and counted, and plated in 96-well plates @ 1600 cells/well with 6 technical replicates per cell line + construct. For growth analysis by confluence, cells were allowed to settle for a few hours and then placed in the Incucyte® Zoom live cell analysis system (Essen Biosciences) for 3-5 days. Images were taken every 2 hours and % confluence was calculated. For growth analysis by nuclei count, cells were plated as above and after 4-5 days, fixed in 3.7% paraformaldehyde, stained with Hoechst 33342 and nuclei were counted on a Cellomics Arrayscan VTI. Cells were also plated in 10-cm plates and harvested after 4-5 days for analysis of DDX11 protein levels by Western Blot.

Inducible shRNA experiments: H4 and H4 KI cells were infected in 6-well plates with pLKO_IPTG_3xLacO-shRNA constructs. Approx. 24 hours after infection, cells were selected with puromycin and passaged while maintaining puromycin selection. One day before plating for growth experiments, selective media was replaced with drug-free media. For growth experiments, cells were collected by trypsinization, counted and plated in 96-well plates @ 1600 cells/well with 6 technical replicates per cell line + construct in 100 µl media. The next day, shRNA was induced by the addition of 100 µl media + IPTG (final concentration 1 mM) and cells were placed in the Incucyte® Zoom live cell analysis system (Essen Biosciences) for 3-5 days. Images were taken every 2 hours and % confluence was calculated.

Drug sensitivity assays: For drug growth curves, cells were plated in 100 µl media in 96-well plates (6 wells per concentration). The next day, 100 µl media containing camptothecin, olaparib or hydroxyurea (at 2x final concentration) were added. Cells were incubated for a further 3-4 days before being fixed in 3.7% paraformaldehyde, stained with Hoechst 33342 and nuclei were counted on a Cellomics Arrayscan VTI.

2.2.5 Generation of clonal knock-out lines

HAP1 parent cells were transfected with BLA371+BLA332 (pSpCas9-T2A-Blast-DDX11 Int. 5/6.2 + pSpCas9-2A-GFP-DDX11 Intron 6/7.1) or BLA392 (pSpCas9-T2A-Blast-DDX11 gRNA exon 4) plasmids using XtremeGene 9 (Roche) according to manufacturer's instructions. HT-29 cells were transfected with BLA371+BLA332 (pSpCas9-T2A-Blast-DDX11 Int. 5/6.2 + pSpCas9-2A-GFP-DDX11 Intron 6/7.1) plasmids using Lipofectamine LTX (ThermoFisher Scientific) according to manufacturer's instructions. The following day, transfected cells were selected using Blasticidin (Sigma) for ~3 days, followed by replating at single cell density in 10 cm plates. Ten to fourteen days after plating, colonies were picked using cloning cylinders and transferred to a 96-well dish. Clones were passaged every 2-3 days until they reached 10 cm density and DDX11 protein knock-out (KO) was tested by Western blot. Parent lines and *DDX11* KO clones were checked for mycoplasma before being used. HAP1 clones were also stained with propidium iodide and compared to parent cells by Fluorescence-Activated Cell Sorting (FACS) to determine ploidy.

To sequence the clones, due to the high identity between DDX11 and other regions (DDX12P and LOC642846), genomic DNA was extracted using QuickExtract according to manufacturer's instructions and the relevant region was PCR amplified using primers OPH9318+9319 or OPH9320+9321 for HAP1 clones #1.1.5 and #2.1.5 (generated using

BLA371+BLA332) and OPH9453+9454 for HAP1 clone #3.4.9 (generated using BLA392). The PCR product was cloned into PCR_Blunt, transformed into DH5α cells and approximately 10 colonies were sequenced for each clone using M13F and M13R primers.

2.2.6 CRISPR-Cas9 knock-out screen

CRISPR-Cas9 screen was performed as previously described (Aregger et al., 2019, 2020). Briefly, cells were infected with lentiviral TKOv3 library (a sequence-optimized sgRNA library of 71,090 sgRNAs targeting 18,053 human protein-coding genes with four sgRNAs per gene) at an MOI of ~0.3 such that each sgRNA was represented in about 200–300 cells, then selected the following day with puromycin (2 µg/mL) for 48 h. Following selection, T0 samples were collected for determination of library representation at day 0, and the remaining cells were re-plated in three replicates maintaining >200-fold coverage of the library. Replicates were passaged every 3-4 days maintaining coverage of the sgRNA library and with three samples collected at T0 and all subsequent passages, until the infected population reached 16 doublings (T18). Genomic DNA was purified from T0 and endpoint samples using Promega Wizard Genomic DNA Purification kit according to manufacturer's instructions. For each sample, sgRNA inserts were amplified from ~50 µg of genomic DNA by a two-step PCR reaction using primers harboring Illumina TruSeq adaptors with i5 and i7 barcodes. The sequencing libraries were gel purified and sequenced on a Illumina HiSeq 2500. Log2-Fold-Changes (LFC) and genetic interaction (qGI) scores were processed and calculated as in Aregger et al. (Aregger et al., 2020).

2.2.7 Gene Ontology Enrichment Analysis

Genes that met the cutoff for negative or positive genetic interactions were tested for enrichment using PantherDB, release 16.0, annotation set GO-Slim Biological Processes (Mi et al., 2021).

2.3 Results

2.3.1 *DDX11* is not synthetic lethal with *STAG2* in a human glioblastoma-derived isogenic cell line pair

As mentioned in the introduction, previous work in our lab identified a synthetic lethal interaction between yeast *CHL1* and the cohesin complex (McLellan et al., 2012). Mutations in cohesin subunits, primarily *STAG2*, have been observed in multiple types of cancer, including colorectal cancer, glioblastoma, Ewing sarcoma, melanoma, acute myeloid leukemia and urothelial bladder cancer (Waldman, 2020). In fact, *STAG2* is considered to be a "driver" tumor suppressor gene (Bert Vogelstein et al., 2013) and exome sequencing of 4,742 cancer samples across 21 cancer types identified *STAG2* as one of 12 genes that are mutated at statistically significant frequencies in at least 4 tumor types (Lawrence et al., 2014). Therefore, our initial goal was to directly test whether there is a synthetic lethal interaction between *STAG2* and *DDX11* in human cell lines.

To test whether DDX11 inhibition causes synthetic lethality in cells carrying *STAG2* mutations, an isogenic pair of cell lines with and without *STAG2* mutations was used. H4 is a glioblastoma-derived cell line containing a 25-bp insertion/duplication in exon 12 of the *STAG2* gene, resulting in a frameshift and early truncation of the encoded STAG2 protein (the *STAG2* gene is located on the X-chromosome so only one mutation is required to disrupt the expression).

This mutation was corrected via homologous recombination to derive the isogenic H4 *STAG2* knock-in (KI) line (Solomon et al., 2011). DDX11 expression was knocked-down (KD) using several methods and the effect on cellular proliferation was measured via nuclei counting (Cellomics VTI) and/or confluence (Incucyte® Zoom live cell analysis system).

CRISPR-inhibition (CRISPRi) is a CRISPR/Cas9-based technique that exploits the sgRNA sequence-specific binding ability to target a catalytically-dead Cas9 fused to a Krüppel Associated Box (KRAB)-repressor domain (dCas9-KRAB) to the promotor or transcription start site of the target gene (Gilbert et al., 2013) **(Figure 2.1A)**. Ten sgRNA sequences, derived from the Weissman lab genome-wide CRISPRi library (Gilbert et al., 2014), were cloned into a single vector system expressing both dCas9-KRAB and the sgRNAs, tested for their ability to repress expression of DDX11 upon infection and selection, and 3 sgRNAs were selected for growth experiments. All three sgRNAs substantially reduced DDX11 expression **(Figure 2.1B)**, but only one sgRNA (#5) showed a significant negative effect on proliferation of the *STAG2* KO line (H4) relative to the *STAG2* KI line (H4 *STAG2* KI), measured both by nuclei count **(Figure 2.1C)** and by confluence **(Figure 2.1D)**. This result may be due to an unintended off-target effect of sgRNA #5, even though CRISPRi is considered to have minimal off-target effects (Gilbert et al., 2014). An alternative explanation may be that the expression of DDX11 needs to be reduced below a certain threshold in order to achieve the synthetic lethal effect. Despite a similar reduction when measured by western blot, it may be that only sgRNA#5 had a strong enough effect on DDX11 levels to impair the growth of both cell lines (as seen in **Figure 2.1**) with a stronger effect on the *STAG2* knock-out line.

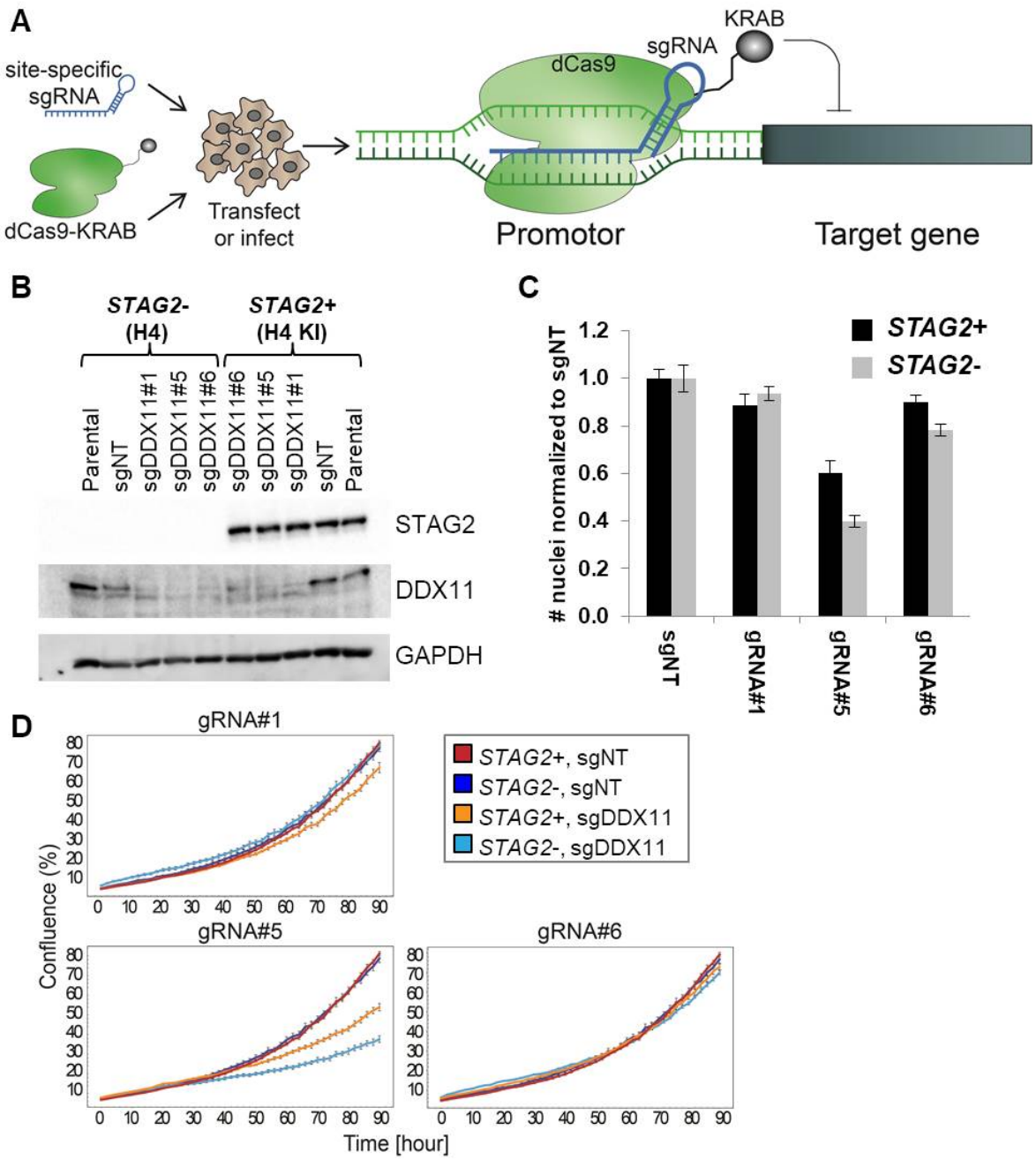

Figure 2.1 - Negative genetic interactions between *DDX11* and *STAG2* in mammalian cells (CRISPRi).

(A) A general overview of the CRISPR/dCas9 transcriptional repression system. dCas9 is linked to a KRAB domain (a transcription repressor), and binds to a specific DNA sequence (promotor or transcription start site) guided by sgRNA to repress gene expression. **(B-D)** Following the infection and selection with puromycin, cells were plated in parallel in puromycin-free media in 96-well plates for the growth experiment and in 10cm plates which were harvested for **(B)** Western blot at the last timepoint. **(C)** Endpoint assay (nuclei count by Cellomics) of growth following CRISPRi knock-down of DDX11. Cell numbers are normalized to non-targeting control gRNA in each cell line. **(D)** Incucyte growth curves of three *DDX11* gRNAs compared to non-targeting control in H4 cell line and paired cell line in which *STAG2* mutation has been repaired.

The CRISPRi growth experiments include infection and puromycin selection of infected cells, followed immediately by plating the cells for the proliferation experiments in order to minimize the effect of DDX11 knock-down on growth prior to the proliferation assay (especially in the *STAG2* KO cells in which a synthetic lethal interaction is hypothesized). These conditions may stress the cells prior to plating and have a differential effect on the subsequent proliferation measurements. Using an inducible shRNA system can decouple the infection and selection of infected cells from the expression of the shRNA and thus avoid potentially detrimental growth effects prior to plating for the proliferation experiments. We utilized a lentiviral IPTG-inducible single vector shRNA system containing a LacI (repressor) and a modified human U6 shRNA promoter with LacO (operator) sequences. In the absence of IPTG (isopropyl-ß-D-thio-galactoside), an analogue of lactose, LacI binds to LacO preventing expression of the shRNA. Upon addition of IPTG, the LacI repressor releases itself from the LacO modified human U6 promoter, and subsequently allows expression of the shRNA **(Figure 2.2A)**. Using this system, two DDX11 shRNAs were tested for inhibition of DDX11 expression and effect on growth of the *STAG2*+ (H4 KI) and *STAG2*- (H4) cell lines. DDX11 expression levels were reduced using both shRNAs upon induction with IPTG **(Figure 2.2B)**. Surprisingly, it initially appeared that depleting DDX11 had a positive effect on the proliferation of both cell lines **(Figure 2.2C+D)**.

However, when comparing the induced to the non-induced conditions, it became clear that the non-targeting control impaired growth of both lines, rather than the shDDX11 improving growth **(Figure 2.3)**. It is unclear why this is the case, and the deleterious effect of the non-targeting shRNA may warrant further investigation prior to using this system in the future. However, it appears that despite this negative effect of the control, reduction of DDX11 levels using two different shRNA sequences did not have a strong negative growth effect on either cell

line (let alone a differential synthetic lethal effect) (**Figure 2.3** – compare induced to non-induced growth curves) .

In a recent study in our lab, *DDX11* was not identified as a negative genetic interaction in CRISPR/Cas9 screens in three different *STAG2* knock-out isogenic backgrounds, one of which was the same pair of H4 and H4 *STAG2* KI lines used in this study (Bailey M. et al, in press). This result, together with the results described above, led us to conclude that DDX11 inhibition is not synthetic lethal with *STAG2* in human cells. This may be due to the fact that, unlike in yeast, in human cells *STAG2* has a highly-related paralog, *STAG1* (Losada et al., 2000), that may mask such an interaction, as either *STAG* paralogue is sufficient for viability and proliferation in cultured cells (van der Lelij et al., 2017).

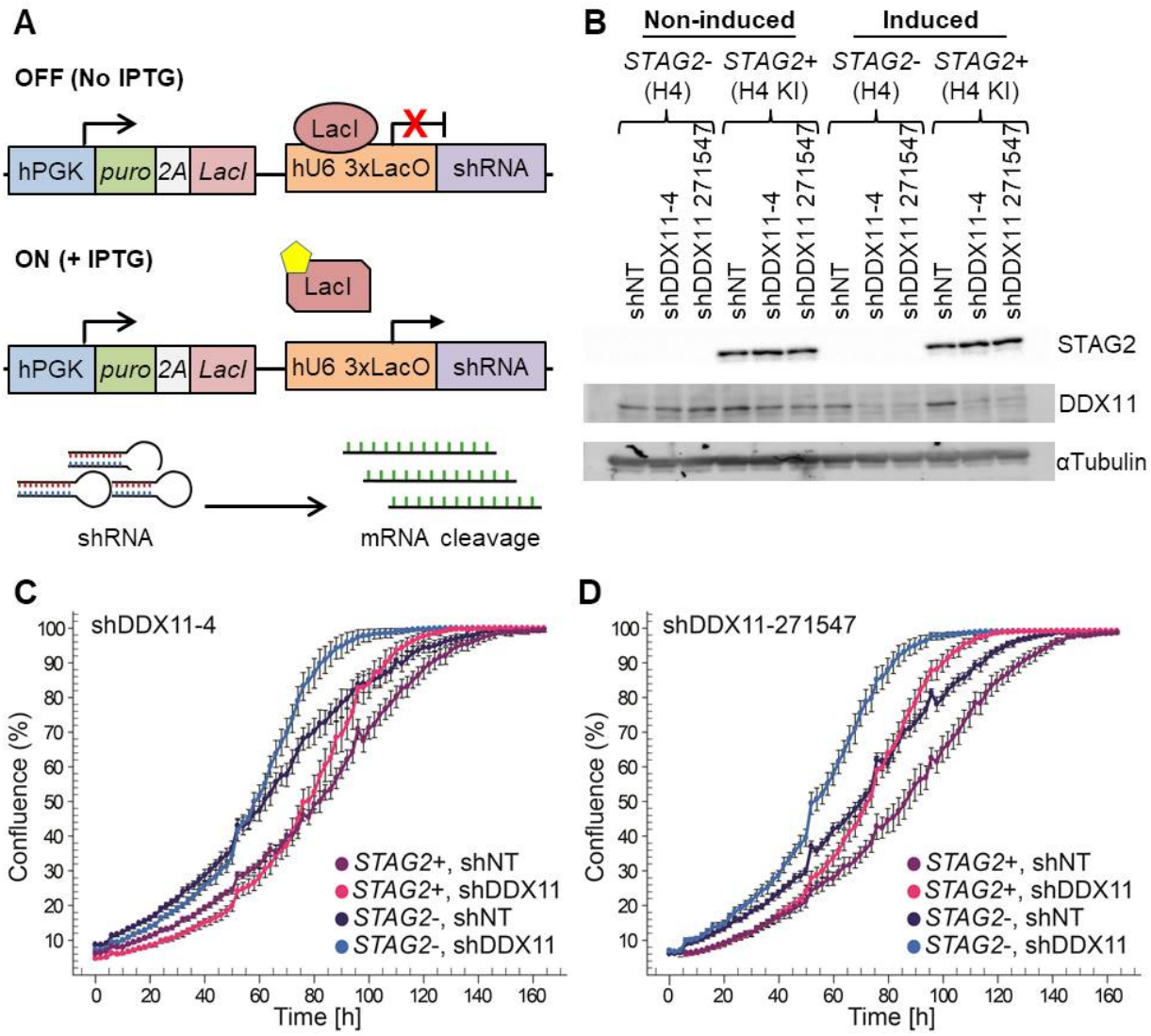

Figure 2.2 - Negative genetic interactions between *DDX11* and *STAG2* in mammalian cells (Inducible shRNA).

(A) General overview of the inducible shRNA system. In the absence of IPTG (isopropyl-ß-D-thio-galactoside), the LacI repressor is bound to the LacO operator preventing expression of the shRNA. Upon addition of IPTG, the allosteric LacI repressor changes conformation, releasing itself from LacO modified human U6 promoter, and subsequently allows expression of the shRNA. (B) Western Blot of DDX11 levels following IPTG induction of DDX11 shRNA in H4 (*STAG2-)* and H4 *STAG2* KI (*STAG2+*) cell lines. (C+D) Incucyte growth curves following induction of non-targeting shRNA (dark blue and dark purple) and DDX11 shRNA (light blue and light pink) in H4 (*STAG2-*) and H4 *STAG2* KI line (*STAG2+)* cell lines. (C) shDDX11-4 (D) shDDX11-271547

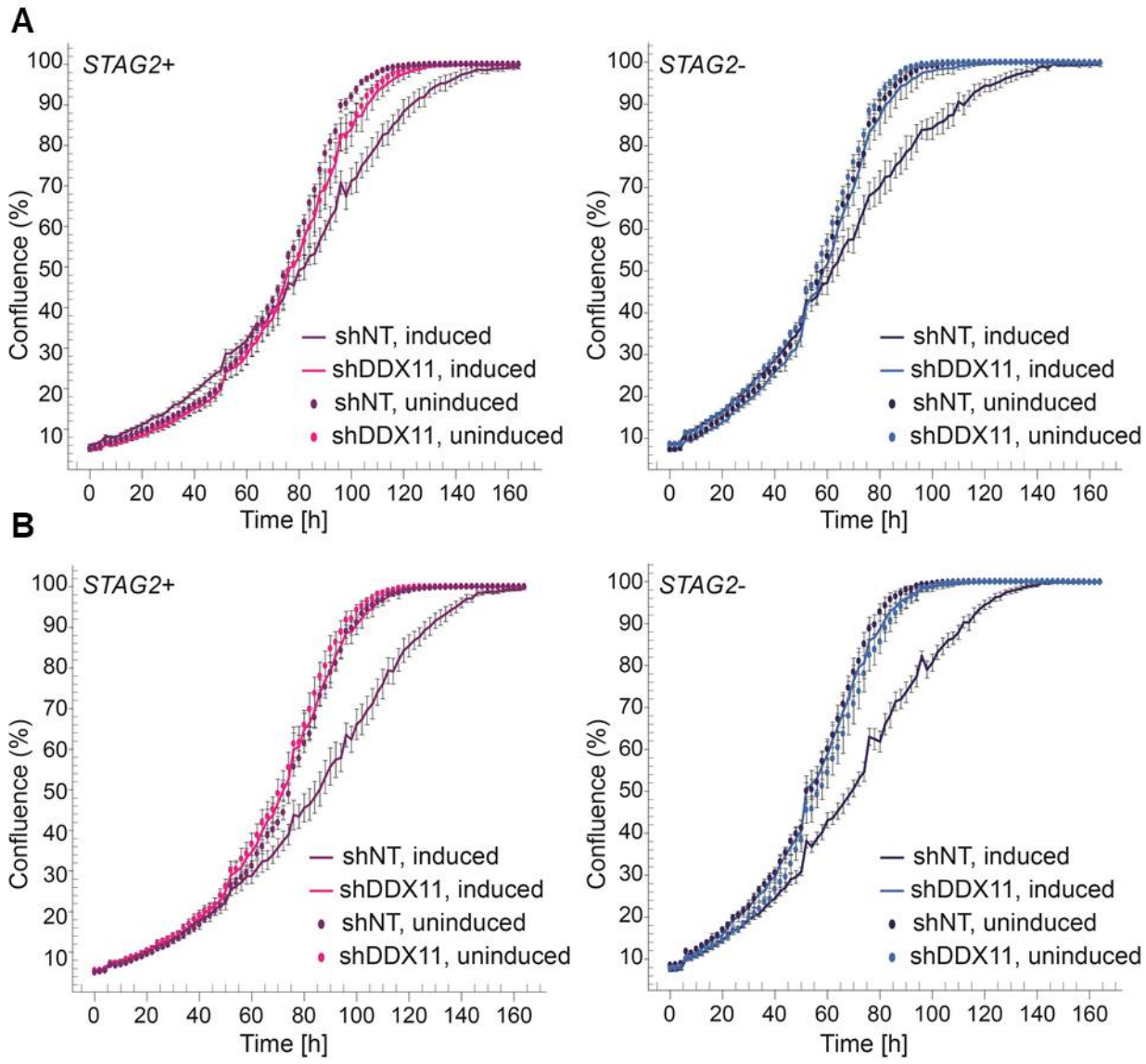

Figure 2.3 - Control (non-targeting) inducible shRNA impairs growth of both *STAG2+* and *STAG2-* cell lines.
Growth curves following IPTG-induction of non-targeting shRNA and DDX11 shRNA (solid lines) compared to non-induced cells carrying the same constructs (dotted lines) within each cell line. **(A)** shRNA DDX11-4. **(B)** shRNA shDDX11-271547. The same non-targeting shRNA was used in both experiments.

2.3.2 CRISPR/Cas9 screen for DDX11 genetic interactions in mammalian cells

As mentioned in the introduction, DDX11 plays an important role in DNA replication, repair and sister-chromatid cohesion, and yeast *CHL1* is a highly connected synthetic lethal hub with many genes involved in cancer-relevant processes, but the genetic interactions of human *DDX11* have only been studied in one paper (published after this project was initiated and using different methodology). In light of the scarcity of information on *DDX11* genetic interactions in mammalian cells, another goal of this study was to conduct an unbiased screen in *DDX11* knock-out cells to provide additional functional information and candidate genetic vulnerabilities that could be applicable to cancer therapeutics.

In recent years, several techniques have been developed for large-scale interrogation of genetic interactions in mammalian cells, including arrayed siRNA/shRNA knock-down screens, pooled shRNA knock-down screens and pooled CRISPR/Cas9 knock-out screens. CRISPR/Cas9 knock-out screens demonstrate a major advance in both sensitivity and specificity over pooled-library shRNA screens (Evers et al., 2016), and this has rapidly become the predominant method for conducting large scale genetic interaction screens in mammalian cells.

Isogenic pairs of cell lines, which differ by a single genetic modification, are powerful tools for understanding gene function through CRISPR/Cas9 knock-out screening. We chose the human near-haploid cell line HAP1 as a model system, given the relative ease of generating knock-out mutations in this background (Carette et al., 2011), to generate *DDX11* knock-out lines for a CRISPR/Cas9 screen. We also attempted to generate *DDX11* knock-out lines in the colorectal HT-29 background to obtain a second isogenic background for future follow-up studies of interactions discovered in the CRISPR/Cas9 screen.

2.3.2.1 Generating *DDX11* knock-out cell lines

Human *DDX11* is located on chromosome 12, and the genomic region is very complex, as it is repetitive with several highly-related pseudogenes, including *DDX12P* (Amann et al., 1996) and *LOC642846* (both on chromosome 12), as well as the *DDX11L* family which maps to multiple chromosomes (Costa et al., 2009) **(Figure 2.4A)**. Due to this, it is very difficult to find unique sgRNAs or PCR primers for this region. To generate *DDX11* knock-out lines, two different strategies were utilized **(Figure 2.4B)**. When aligning *DDX11* to *DDX12P* and *LOC642846*, a unique region in *DDX11* was identified between exon 6 and 7 (Appendix D). Using two sgRNAs (one targeting intron 5/6 and one targeting intron 6/7) to create two double-strand breaks may remove the entire exon 6 and create a frameshift in *DDX11* coding sequence and early termination. This strategy was expected to be specific to *DDX11* due to the ability to target one of the two sgRNAs to the unique region identified in intron 6/7. The second strategy chosen was the standard strategy of generating CRISPR/Cas9-mediated gene knock-outs in which a single sgRNA is targeted to the coding region, creating a double-strand break that is repaired by non-homologous end-joining (NHEJ) to create small indels leading to a frameshift and potentially early termination event (Cong et al., 2013; Mali et al., 2013). For this strategy, optimized sgRNA sequences derived from the TKOv3 library (Hart et al., 2017) targeting exons 3 or 4 of *DDX11* were selected. The double gRNA strategy removing exon 6 was also used to generate knock-out lines in the HT-29 background.

In the HT-29 background, 13 clones were tested and only one clone (1.1.13) appeared to be a *DDX11* knock-out upon testing by western blot. In the HAP1 background, 30 clones generated using two different combinations of intronic gRNAs were tested and only two (clones 1.1.5 and 2.1.5) appeared to contain a *DDX11* knock-out upon testing by western blot. An

additional 17 clones were generated using a single sgRNA targeting either exon 3 or 4, and only one clone (3.4.9) appeared to be a *DDX11* knock-out upon testing by western blot **(Figure 2.4C)**. The scarcity of clones containing *DDX11* knock-out supports the large-scale CRIPSR screen data that DDX11 is essential in a large number of cell lines (929 of 990 tested) when measured in pooled competitive growth conditions (Pacini et al., 2021). This suggests that (like most cell lines) there is some heterogeneity in the cells and the clones obtained may have been derived from a subpopulation able to survive the knock-out or adapt rapidly to the loss of DDX11 expression to form a viable colony.

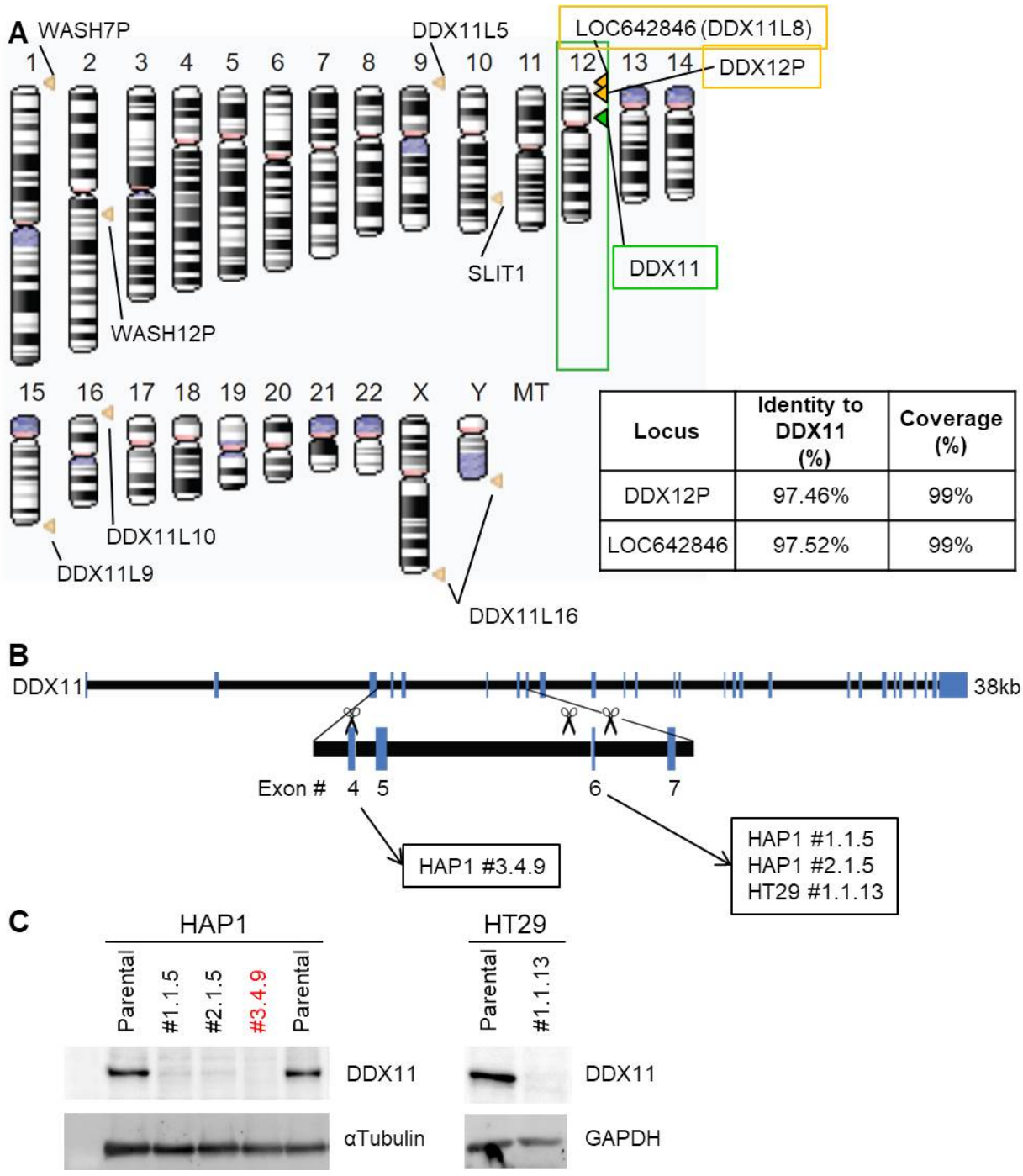

Figure 2.4 - Generating *DDX11* CRISPR/Cas9 knock-out lines.
(A) Human chromosomes ideogram illustrating alignment of *DDX11* genomic sequence to genome. Green arrow – *DDX11*. Yellow arrows – Two highly similar sequences on chromosome 12, *DDX12P* (coverage 98.12%, identity 96.34%) and *LOC642846* (coverage 98.04%, identity 96.18%). **(B)** DDX11 genomic structure and strategy for making knock-out lines. Blue boxes represent exons and black line represents intronic DNA. Scissors depict cleavage locations of gRNAs selected and boxes indicate which clones were derived from each strategy. **(C)** Western blot analysis of promising HAP1 and HT29 *DDX11* KO clones. Clone #3.4.9 highlighted in red was selected for the subsequent CRISPR/Cas9 screen.

2.3.2.2 Characterizing HAP1 *DDX11* knock-out clones

To select a HAP1 *DDX11* knock-out clone for the CRISPR/Cas9 screen, the *DDX11* knock-out clones in the HAP1 background were further characterized **(Figure 2.5)**. Human cells lacking *DDX11* are sensitive to camptothecin (CPT, a topoisomerase I inhibitor) (van der Lelij et al., 2010), and to PARP inhibitors (Stoepker et al., 2015), but *DDX11*/*CHL1* was largely dispensable for cell survival in chicken DT-40 and budding yeast cells following exposure to hydroxyurea (HU, a ribonucleotide reductase inhibitor) (Abe et al., 2018; Laha et al., 2011). To determine whether the *DDX11* knock-out caused sensitivity to these agents, we looked at the proliferation of the HAP1 clones following exposure to camptothecin, olaparib (a PARP inhibitor) and hydroxyurea. HAP1 *DDX11* KO clone #3.4.9 was sensitive to CPT and Olaparib, but not to HU. To a lesser extent, HAP1 *DDX11* KO clone #2.1.5 was also sensitive to CPT and Olaparib, while HAP1 *DDX11* KO clone #1.1.5 exhibited the same sensitivity as the parental line **(Figure 2.5)**. These results suggested that clone #3.4.9 was the most suitable for the CRISPR/Cas9 screen. One explanation for the lower sensitivity of clones #1.1.5 and #2.1.5 is that these clones were generated using the two intronic sgRNA strategy to create two breaks flanking exon 6, unlike clone #3.4.9 which was generated by targeting the coding region of *DDX11*. In western blots of clones #1.1.5 and #2.1.5, a faint band can be observed (which is not observed in clone #3.4.9), which may be a low level of residual DDX11 expression. Alternatively, this may represent a low level of protein expressed from the *DDX12P* locus, despite it being defined as a pseudogene (as the double sgRNA strategy was specifically designed not to target *DDX12P*).

HAP1 cells often contain a subpopulation of cells that spontaneously switch to a diploid state during normal cultivation, and often become fully diploid within 10-20 passages after

CRISPR/Cas9 editing (Beigl et al., 2020). To test the ploidy of the *DDX11* knock-out clones, cells were stained with propidium iodide (PI) and compared to parental cells by FACS analysis. All three knock-out clones were diploid **(Figure 2.5D)**. Although this is a small number of clones, the fact that all three are diploid suggests the possibility that diploid cells are better able to survive the *DDX11* knock-out and form a viable colony.

As mentioned above, due to the presence of highly repetitive pseudogenes, unequivocally determining one versus two edited alleles is difficult. To analyze the consequences of the CRISPR/Cas9 genome editing, genomic DNA flanking the sgRNA sites was amplified by PCR, subcloned into PCR_Blunt and multiple colonies were sequenced. Clones #1.1.5 and #2.1.5 (generated by the double sgRNA deletion strategy) were aligned to the *DDX11* region flanking exon 6 and the two sgRNA sites. HAP1 clone #1.1.5 contains two edited alleles that both align well to *DDX11*, suggesting that this clone originated in a cell that was diploid before the genome editing. One allele contains a 167bp insertion at the upstream cut site and a small 4bp deletion at the downstream cut site, and the second allele contains an inversion between the two cut sites **(Figure 2.6A)**. HAP1 clone #2.1.5 contains a single allele that aligns to *DDX11*, suggesting that this clone became diploid after genome editing. Similar to clone #1.1.5, clone #2.1.5 also contains an insertion at the upstream cut site (346bp) and a small 5bp deletion at the downstream cut site (the forward and reverse sequences did not overlap so there is missing sequence in the middle) **(Figure 2.6B)**. Interestingly, although this strategy was designed to excise exon 6, it seems that each sgRNA cut site was repaired independently as both clone #1.1.5 and clone #2.1.5 retain exon 6 coding sequence, although it appears the large insertion at the upstream cut site disrupted the expression of DDX11 as seen on the western blot **(Figure 2.4C)**. However, this

may explain the faint band observed for these clones and the lesser sensitivity to camptothecin and olaparib **(Figure 2.5)** compared to clone #3.4.9.

Clone #3.4.9 appeared to contain two editing events when aligned to *DDX11* sequence (an insertion of a single C or insertion of CT – both of which create a frameshift and early termination). However, when aligning the sequences to *DDX12P* and *LOC642846* as well as *DDX11*, the single C insertion is most likely at the *DDX11* locus, and the CT insertion is more likely to be at *DDX12P* or *LOC642846* loci **(Figure 2.6C)**. Therefore, it seems that this clone was also derived from a haploid clone that became diploid after the genome editing event. In summary, clone #3.4.9 demonstrated the cleanest knock-out by western blot and the strongest expected *DDX11* knock-out drug sensitivity, and was selected for the CRISPR/Cas9 knock-out screen.

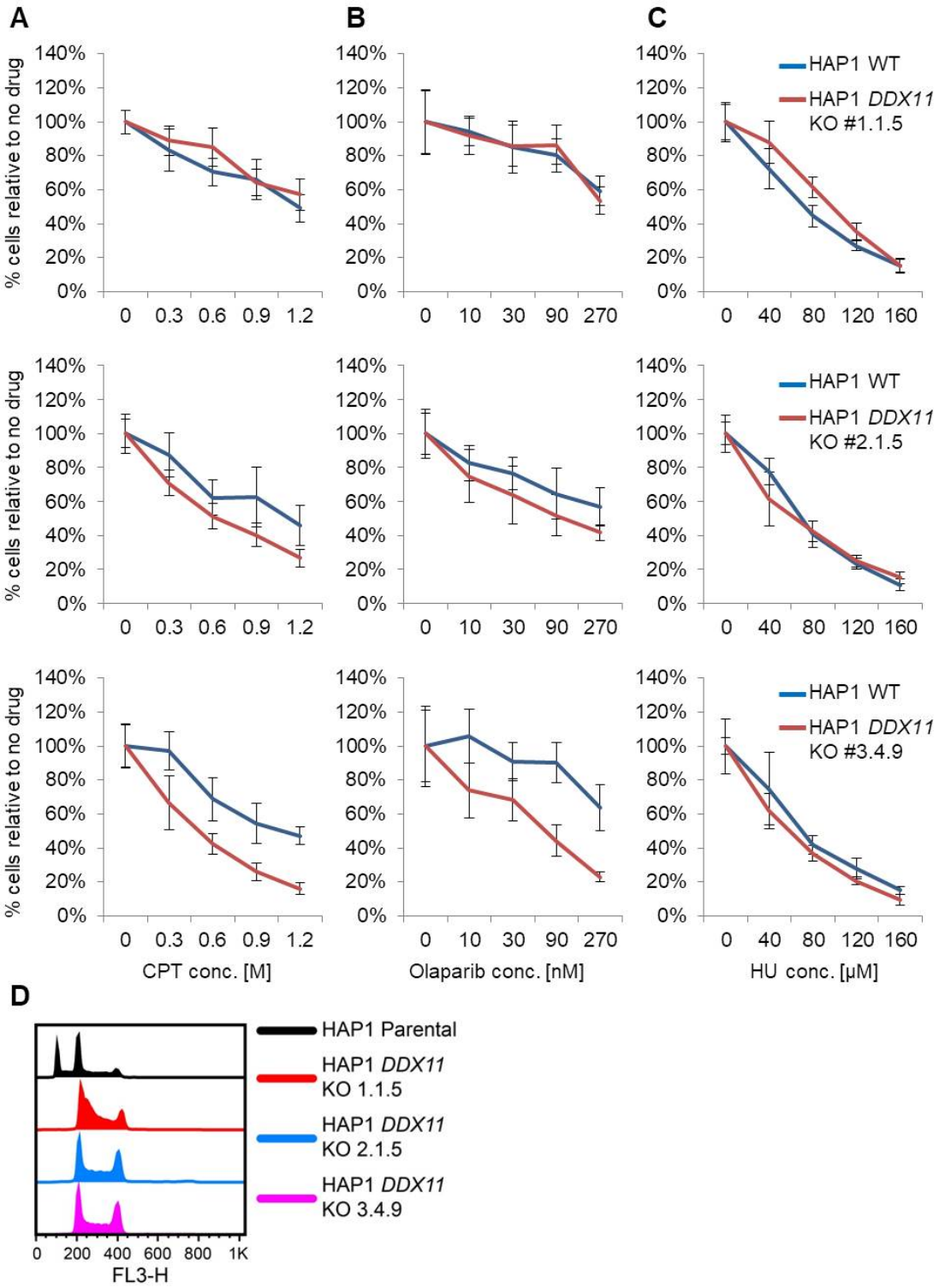

Figure 2.5 - Characterization of HAP1 *DDX11* knock-out lines.
HAP1 Parental and *DDX11* knock-out cell lines were treated with the indicated doses of **(A)** Camptothecin (CPT), **(B)** Olaparib (Ola), **(C)** Hydroxyurea (HU) or DMSO in 96-well format. After 3 days, cell numbers were quantified by nuclei counting using Cellomics Arrayscan VTI. Data are presented as mean ± SD from 6 replicates.
(D) FACS analysis of PI-stained DNA content to determine ploidy.

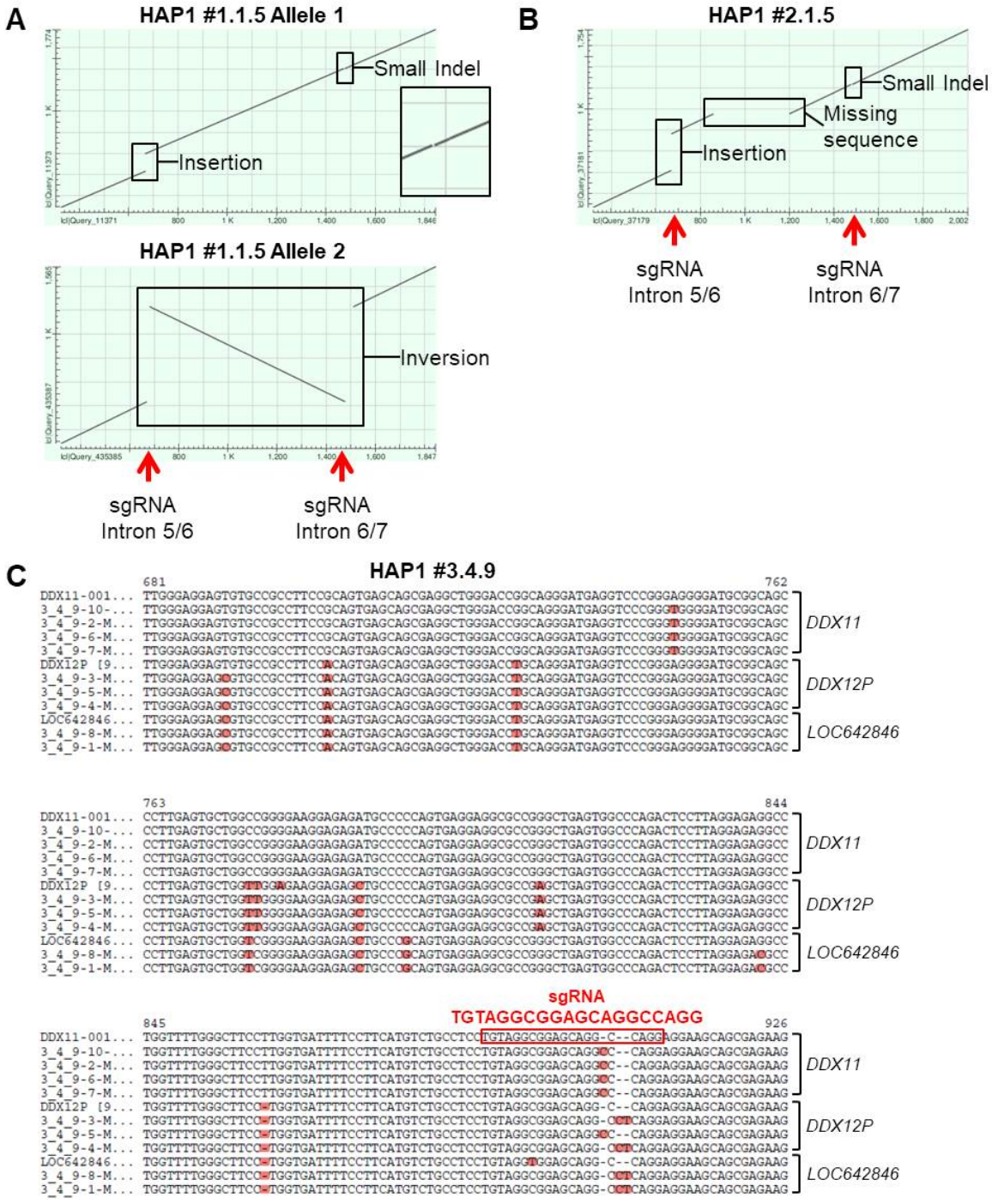

Figure 2.6 - Genomic analysis of HAP1 clones.
Genomic DNA flanking the CRISPR/Cas9 cut sites was amplified by PCR and cloned into PCR_Blunt. Approximately 10 colonies were sequenced for each clone to determine editing events. (A) HAP1 clone #1.1.5 contains 2 different alleles (both appear to be *DDX11*, but one may actually be *DDX12P* or *LOC642846*). (B) HAP1 clone #2.1.5 contains a single allele.(C) HAP1 clone #3.4.9 demonstrates two different editing events at the cut site (insertion of a single C or insertion of CT), although insertion of CT appears to be at *DDX12P* or *LOC642846*, rather than *DDX11* locus).

2.3.2.3 Genome-wide CRISPR/Cas9 knock-out screen of *DDX11*-deficient cell lines

To map *DDX11* genetic interactions, we conducted a genome-wide CRISPR/Cas9 screen using the TKOv3 guide RNA (gRNA) library, which contains ~71,090 gRNAs that target ~18,000 human protein-coding genes, most of them with four sequence-independent gRNAs (Aregger et al., 2020; Hart et al., 2017). The relative abundance of individual gRNAs was compared between the screen start (T0, following infection and selection) and end (T18, after 16 doublings) **(Figure 2.7A)**. The relative abundance of gRNAs targeting the ~18,000 genes in wild-type cells provides an estimate of single-mutant fitness, whereas the relative abundance in *DDX11* knock-out cells provides an estimate of double-mutant fitness. The genetic interactions were scored using a quantitative GI (qGI) score that measures the strength and significance of the interaction by comparing relative abundance of gRNA in the mutant cell line to the relative abundance of the same gRNA in an extensive panel of 21 wild-type HAP1 screens, after removal of frequent flyers and batch correction (Aregger et al., 2020). Negative interactions reflect genes whose gRNAs are significantly decreased in the *DDX11* knock-out line relative to the control wild-type panel, whereas positive interactions reflect genes with increased gRNA abundance in *DDX11* knock-out line compared to the control wild-type panel.

DDX11 knock-out was maintained throughout the screen and there was no reversion of the knock-out mutation to restore DDX11 levels **(Figure 2.7B)**. To evaluate screen performance, log2(fold-change) (LFC) of essential genes and nonessential genes were analyzed and compared to a reference set of core essential and non-essential genes previously described (Hart et al., 2017). The screen robustly distinguished the reference set of essential genes from non-essential genes, indicating a high-quality screen **(Figure 2.7C)**.

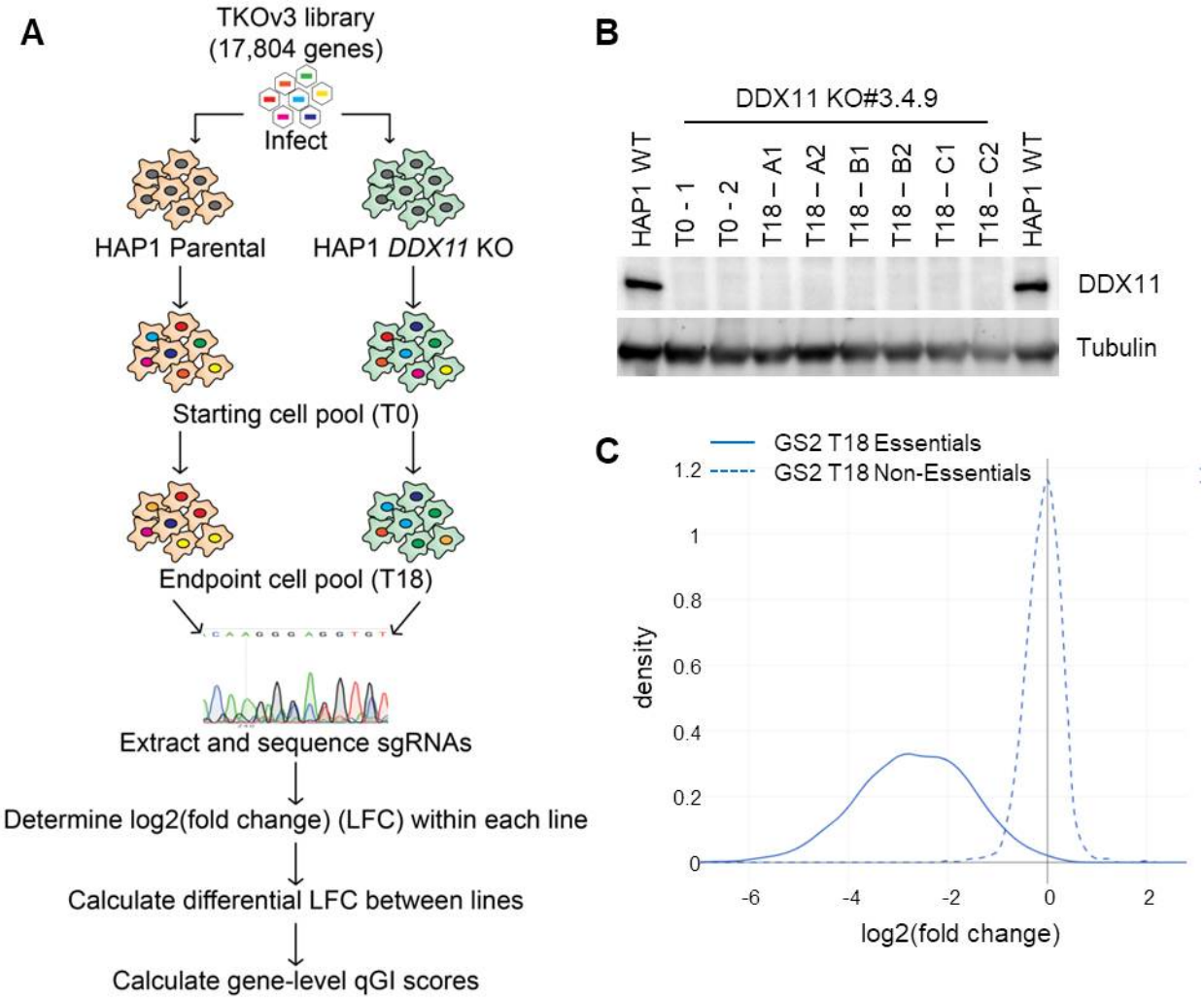

Figure 2.7 - CRISPR/Cas9 screen for identification of genetic interactions in *DDX11* knock-out HAP1 cells.
(A) Schematic of the screen. DDX11 knock-out and wild-type parental cells were infected with a lentiviral genome-wide CRISPR gene knock-out library (TKOv3), and gRNA abundance was determined. Log2(fold change) (LFC) was calculated for each gRNA within each cell line and then the differential LFC between wild-type and knock-out cells was calculated. Finally, a series of normalization steps and statistical tests were applied to these data to generate gene-level qGI scores and FDRs. **(B)** Western blot of cell lysate samples from start (T0) and end (T18) of cell growth. **(C)** Fitness effect (log2 fold-change, LFC) distributions for reference core essential (CEG2) and non-essential gene sets defined in (Hart et al., 2017).

The screen identified 226 negative genetic interactions (NGI) at a cut-off of qGI ≤-0.5, FDR≤0.2 and 147 positive genetic interactions (PGI) at a cut-off of qGI≥0.5 at FDR≤0.2. Not unsurprisingly, multiple genes associated with the cohesin complex and sister chromatid cohesion were identified as both positive and negative genetic interactions **(Figure 2.8)**.

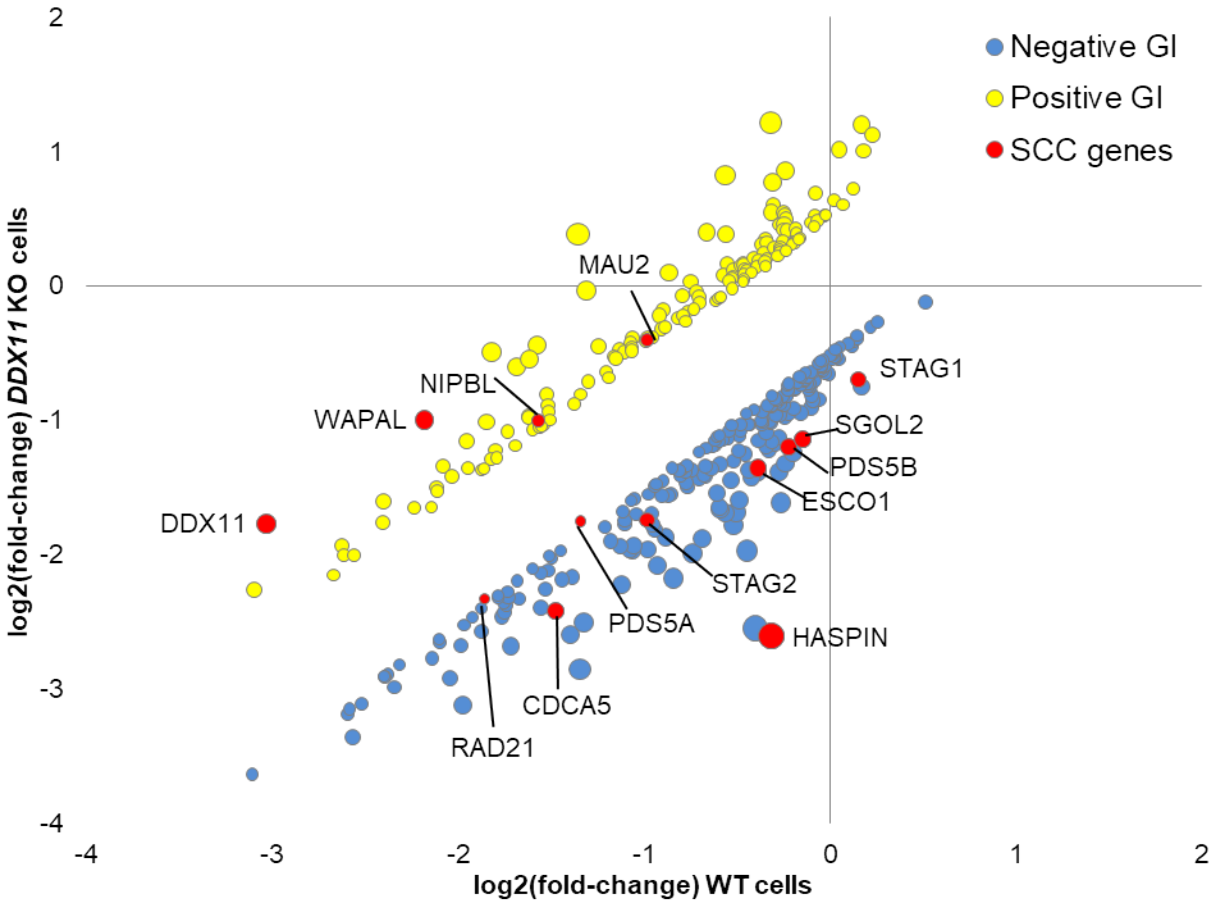

Figure 2.8 - *DDX11* negative and positive genetic interactions (GI).
A scatterplot illustrating the fitness effect (LFC) of 373 genes in *DDX11* knock-out versus wild-type parental HAP1 cell line, which exhibited a significant genetic interaction (|qGI | > 0.5, FDR < 0.2). Negative (blue) and positive (yellow) *DDX11* GIs are shown. Node size corresponds to a combined score reflecting both the qGI and the FDR. Selected genes belonging to the cohesin complex or affecting sister-chromatid cohesion are highlighted in red.

To provide further insight into the functional categories of genes identified, we performed gene ontology (GO) term (GO-Slim Biological Processes) enrichment analysis using

PantherDB PANTHER Overrepresentation Test (Mi et al., 2021). We first looked at the negative genetic interactions, which reflect genes that are synthetic lethal or synthetic sick with *DDX11* knock-out. The top 10 enriched terms for biological processes gene ontology (GO) terms are listed in **Figure 2.9A**. Consistent with the known role of DDX11, the enriched terms were associated with the cell cycle, DNA repair, and chromosome cohesion and segregation. Interestingly, the top enriched terms were associated with DNA damage response and repair, followed by cohesion-related terms, supporting the hypothesis that DDX11 inhibition may be a good therapeutic target in cancer cells, many of which carry defects in DNA repair pathways.

We next analyzed the positive genetic interactions, which represent genes whose knock-out is more detrimental to wild-type cells than to *DDX11* knock-out cells. For these interactions, the enriched terms were focused almost exclusively on sister chromatid cohesion and cell cycle GO terms, and not on other DNA-related terms **(Figure 2.9B)**. This may reflect the fact that the *DDX11* knock-out cells compensated for the cohesion-associated defects caused by the knock-out (potentially by upregulating other factors) and therefore may be less sensitive than wild-type cells to loss of other cohesion related genes. Interestingly, one of the strongest positive interactions was *DDX11* itself, which supports the quality of the screen; gRNAs in the library targeting *DDX11* cause impaired growth in the wild-type cells, but not the *DDX11* knock-out cells as the protein is not expressed, and this manifests in the screen results as a positive interaction.

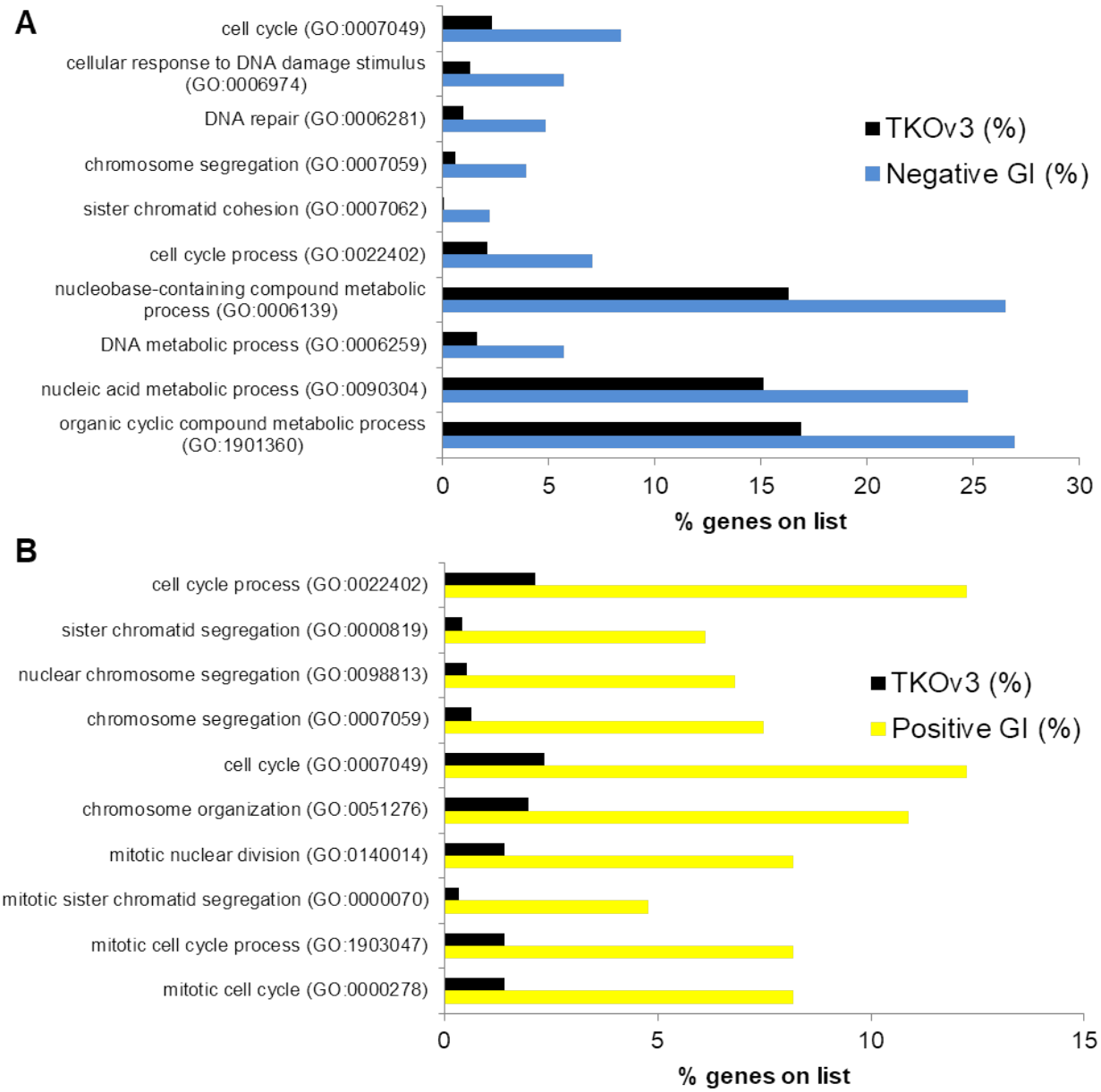

Figure 2.9 - Analyzing gene set enrichment of *DDX11* genetic interactions.
Enrichment of *DDX11* genetic interactions (|qGI|≥0.5, FDR≤20%) was analyzed using the PANTHER Overrepresentation Test (annotation set: GO-Slim Biological Processes) for **(A)** *DDX11* negative genetic interactions and **(B)** *DDX11* positive genetic interactions. The top 10 terms are presented for each analysis. Each enriched term is presented as a proportion of the total number of genes in the TKOv3 library (n=17326 genes) or *DDX11* negative genetic interactions (n=226) or positive genetic interactions (n=147).

2.4 Discussion

Studying genetic interactions of genes/proteins of interest can provide a wealth of knowledge, both for expanding our understanding of their molecular role(s) and for informing therapeutic potential. DDX11 plays an important role in DNA replication, repair and sister-chromatid cohesion, and yeast *CHL1* is a highly connected synthetic lethal hub with many genes involved in cancer-relevant processes, but the mammalian genetic interactions had not been studied at the time this project was initiated. In this chapter, we studied *DDX11* genetic interactions in human cells to provide further insight into its molecular role and the therapeutic potential of DDX11 inhibition.

2.4.1 Validating a synthetic lethal interaction between cohesin and DDX11 predicted from yeast genetics

Genetic interactions observed in model organisms (such as *Saccharomyces cerevisiae)* can be used to predict therapeutic synthetic lethal interactions in human cells (McLellan et al., 2012; O'Neil et al., 2013; Srivas et al., 2016; van Pel, Stirling, et al., 2013). Mutations in cohesin, and especially *STAG2*, have emerged in recent years as a highly cancer-relevant biomarker (Waldman, 2020), and no therapeutic has targeted this genetic vulnerability to date. Therefore, we first attempted to directly test whether the strong synthetic lethal interaction previously observed in yeast between members of the cohesin complex and *CHL1* can be recapitulated in human cells using *STAG2* and *DDX11* as the candidate synthetic lethal partner genes. We utilized an isogenic pair of *STAG2* cell lines and knocked-down DDX11 expression using several methods. However, we were unable to observe the anticipated interaction in this system. *DDX11* was not identified as a negative genetic interaction in three CRISPR/Cas9 screens conducted in our lab using three different isogenic *STAG2* backgrounds (Bailey M. et al,

in press), nor in another study (published after these results were obtained) studying *STAG2* synthetic lethal interactions (van der Lelij et al., 2017). These results, together with the results described in this chapter, led us to conclude that DDX11 inhibition is unlikely to be synthetic lethal with *STAG2* in human cell lines.

Several explanations exist for the absence of this cross-species predicted synthetic lethal interaction. The simplest one is that in human cells, unlike in yeast, *STAG2* has a highly related paralog, *STAG1* (Losada et al., 2000), that may mask such an interaction, as either cohesin variant appears to be able to support viability and proliferation in cultured cells (van der Lelij et al., 2017). It is not feasible to test if the *DDX11*/cohesin interaction would be conserved in the absence of both *STAG1* and *STAG2*, as knocking-out both STAG proteins is synthetic lethal across multiple cell types (Benedetti et al., 2017; Liu et al., 2018; van der Lelij et al., 2017, 2020).

Another explanation could lie in the differences in the roles of the cohesin complex between yeast and humans. In recent years, there is a growing understanding that the role of cohesin, and especially of STAG2, is more complex in human cells compared to yeast. In addition to its role in sister-chromatid cohesion, in human cells the cohesin complex plays a significant role in generating, maintaining and regulating the intra-chromosomal DNA looping events that modulate 3D genome organization and gene expression (Waldman, 2020). Human cohesin binds DNA at discreet regulated sites in different cell types, through association with CCCTC-Binding Factor (CTCF) (Parelho et al., 2008; Rubio et al., 2008), which does not have a yeast orthologue, supporting the fact that it plays a role in mammalian cellular biology other than enforcing sister-chromatid cohesion. This difference in roles and the relative importance of each

role in yeast versus human cells may also explain the lack of synthetic lethal interaction with *DDX11* observed in these experiments.

2.4.2 Unbiased screen for DDX11 genetic interactions

High-throughput identification of genetic interactions originated in yeast model organisms, as technologies that facilitate the high-throughput generation and analysis of double mutants under defined laboratory conditions are readily available (for example the Synthetic Genetic Array (SGA) technique (Tong et al., 2001)). Advances in RNA interference (RNAi) and, more recently, CRISPR technology have now made it possible to carry out large-scale unbiased synthetic lethality screening directly in human cell culture. In light of the scarcity of information on *DDX11* genetic interactions in human cells, a second goal of this chapter was to conduct an unbiased screen in *DDX11* knock-out cells to provide additional functional and therapeutic information.

For our screen, we chose to use isogenic paired HAP1 lines with/without *DDX11* knock-out. In a previous study, *DDX11* was defined as an essential gene in HAP1 cells using a gene-trap method to systematically inactivate genes (Blomen et al., 2015). This essentiality is supported by data from the DepMap project (a large-scale project aiming to systematically identify genetic and pharmacologic dependencies in a large panel of cancer lines) (Pacini et al., 2021), in which *DDX11* is defined as a "common essential" gene. Despite this, we were able to obtain *DDX11* knock-out lines, albeit not many. This discrepancy may be due to the fact that the conditions under which *DDX11* was deemed essential were pooled competitive growth conditions (both the gene trap and the genome-wide CRISPR screens), whereas in the case of our generated clones – cells were edited and plated at single cell density until formation of a colony. Under these conditions, even cells with fitness defects may be able to survive and form colonies.

In support of this, other groups have also managed to knock-out *DDX11* in human cells, as evidenced by a recently published study in which *DDX11* knock-out lines were generated in both HeLa and U2OS cells using CRISPR/Cas9 genome editing (Jegadesan & Branzei, 2021).

Our screen identified multiple genetic interactions (both positive and negative) with genes involved in sister-chromatid cohesion or cohesion establishment and maintenance (**Figure 2.8**). In addition to overall supporting the conservation of *DDX11/CHL1*'s role between yeast and humans, a number of the identified interactions provide additional assurance that even though the knock-out cells may have adapted to DDX11 loss, the genetic interactions observed reflect the underlying molecular roles of DDX11. For example, Sororin (CDCA5), WAPAL and PDS5 form a cohesin-regulator complex in vertebrates, in which Sororin and WAPAL antagonize each other by competing for binding to a specific site on PDS5 to regulate association of cohesin on chromatin. This complex positively or negatively regulates the association of cohesin with chromosomes, depending on which protein binds PDS5. PDS5-Sororin complex maintains sister-chromatid cohesion, whereas PDS5-WAPAL dislodges cohesin from chromatin (reviewed in N. Zhang et al., 2021). In our screen, both *CDCA5* and *PDS5A/B* were identified as negative genetic interactions, whereas *WAPAL* was identified as a positive genetic interaction. This is consistent with the known role of DDX11 in establishing and maintaining sister-chromatid cohesion. In the absence of DDX11, cohesion is less robust and further dissociation through the loss of PDS5 or Sororin may be detrimental to the knock-out cells. On the other hand, in wild-type cells loss of WAPAL is detrimental as it leads to increased cohesin on the DNA, whereas in the knock-out cells this effect is counteracted by the loss of cohesion due to the loss of DDX11 activity. Another protein that ties into the regulation of cohesin maintenance versus removal is the kinase HASPIN (GSG2). *HASPIN* was the strongest negative genetic

interaction identified in the screen. HASPIN binds and phosphorylates WAPAL, directly inhibiting the interaction of WAPAL with PDS5B. Cells expressing a WAPAL-binding-deficient mutant of HASPIN or treated with HASPIN inhibitors show centromeric cohesion defects (Liang et al., 2018). In contrast, HASPIN also binds to PDS5B, and knock-out of *HASPIN* or disruption of HASPIN-PDS5B interaction causes weakened centromeric cohesion and premature chromatid separation, which can be reverted by centromeric targeting of a short fragment of HASPIN containing the PDS5B-binding motif or by prevention of WAPAL-dependent cohesin removal (Zhou et al., 2017). Together, the interactions identified support a central role for DDX11 in regulation of cohesin establishment/protection versus removal.

One of the goals of this screen was to identify potential biomarkers for tumours that would benefit from DDX11 inhibition. While no single cancer-relevant genetic biomarker was identified, the pattern of interactions identified suggests DDX11 inhibition may be therapeutic for tumours inhibiting a cohesin-dysregulation/premature separation phenotype. This builds upon the concept of expanding the definition of clinically-relevant synthetic lethality from a gene/gene (or inhibitor) negative interaction to a phenotype or pathway + inhibitor interaction, similar to the recent evidence for expansion of PARP inhibitors from treatment of tumours carrying *BRCA1/2* mutations to tumours displaying a "BRCAness" phenotype (reviewed in Lord and Ashworth 2016).

2.4.3 Comparing results obtained in *DDX11* screen to literature

As mentioned in the introduction, at the time of this project initiation, human *DDX11* genetic interactions had not been studied. Since then, a genome-wide siRNA screen has been conducted in WABS patient-derived, SV40-immortalized fibroblasts and a paired isogenic line expressing wild-type *DDX11* following stable transfection of *DDX11* cDNA (not at the

endogenous location). Of the top negative genetic interactions, multiple subunits of the anaphase promoting complex or cyclosome (APC/C) were identified (De Lange et al., 2015). The APC/C was not identified in our screen, possibly because a complete abolishment of APC/C activity is lethal (J. Zhang et al., 2014). The negative genetic interactions that met the cutoff in our screen (n=226) were compared with the 98 negative interactions selected for further validation in the siRNA screen and only one gene overlapped - CDCA5 (Sororin). This is not unexpected, as large scale comparisons of siRNA and CRISPR screens for detection of essential genes have demonstrated little correlation in previous studies (for example Evers et al., 2016; Morgens et al., 2016), and many genetic interactions are highly context dependent (Henkel et al., 2019).

Several differences between the CRISPR/Cas9 knock-out screen described in this chapter and the published siRNA screen may explain the lack of overlap in the obtained results. The first is the choice of cell lines used for the screen. As described above, the siRNA screen was conducted in SV-40 immortalized fibroblasts obtained from a WABS patient. This patient carries biallelic mutations in *DDX11* – a splice site mutation in intron 22 of the maternal allele that leads to the deletion of the last 10 bp of exon 22, and an in-frame 3 bp deletion in exon 26 of the paternal allele that leads to deletion of a highly conserved lysine near the C-terminus of the protein (van der Lelij et al., 2010). The resulting protein is likely unstable as it is barely detectable by western blot; however, it is possible that the derived protein is a hypomorph and some residual activity remains. In addition, the isogenic complemented line was constructed by stably transfecting *DDX11* cDNA, which rescued the cohesion defect of the cells, but is not under control of its endogenous promotor. In comparison, the screen described in this chapter was conducted in the tumor-derived HAP1 cell line containing endogenously regulated DDX11 and its isogenic pair in which DDX11 expression was knocked-out.

Another difference between the two screens is the choice of technology for generating the genome-wide loss-of-function (siRNA knock-down versus CRISPR/Cas9 knock-outs). A systematic study targeting 93 genes previously identified as essential genes concluded that CRISPR knock-out technology was superior to RNAi or CRISPRi, both in terms of sensitivity and specificity (Evers et al., 2016). However, a similar study concluded that both shRNA and CRISPR had high precision, but that the CRISPR/Cas9 library identified more essential genes. The essential genes identified by the two methods also differed in GO enrichment terms, suggesting that the screens identified different aspects of biological processes and may therefore be complementary (Morgens et al., 2016). One possibility suggested for the difference in the two technologies is that RNAi is less able to perturb genes expressed at low levels (Hart et al., 2015). Alternatively, this may imply that identification of many cellular dependencies may require full gene inactivation. If this is the case, it suggests that many dependencies may not translate upon use of chemical inhibition, as 100% inhibition is rarely achieved, and residual activity may be sufficient to rescue the synthetic lethal effect from a therapeutic perspective.

Another recent study of *DDX11* genetic interactions in human cells used a candidate gene approach studying the relationship between *DDX11* and *ESCO1/2* (the human homologs of the yeast acetyltransferase *ECO1* that plays an essential role in cohesin acetylation and establishment of sister chromatid cohesion). This study demonstrated that *DDX11*-deficient cells rely on ESCO2, but not ESCO1, for sister-chromatid cohesion and survival (Faramarz et al., 2020). In the genome-wide siRNA screen mentioned above, *ESCO2* was one of the strongest synthetic lethal hits (De Lange et al., 2015). *ECO1* and *CHL1* genetically interact in yeast (Borges et al., 2013; Skibbens, 2004) and synthetic lethality between *DDX11* and *ESCO2* was also reported in chicken DT40 cells (Abe et al., 2016). Interestingly, in our data set, *ESCO1*, but not *ESCO2*, is a

strong negative genetic interaction with *DDX11*. This may reflect the fact that *ESCO2* was defined as essential in HAP1 cells (Blomen et al., 2015) and therefore there is little differential in log2 (fold change) between wild-type and *DDX11* knock-out cells for gRNAs targeting *ESCO2*. This difference may also reflect context dependency of synthetic lethal interactions, in which different genes in the same pathway are identified as synthetic lethal partners of the same query gene in different genetic backgrounds (Ku et al., 2020).

Finally, we compared the *DDX11* screen results to *S. cerevisiae chl1*Δ genetic interactions. Genetic interaction networks highlight mechanistic connections between genes and their corresponding pathways, and the pattern of genetic interactions of a given gene can be used to functionally annotate the genome by clustering genes with highly correlated genetic interaction profiles together (Costanzo et al., 2010). *S. cerevisiae* orthologues of the positive and negative genetic interacting genes identified in the screen were derived from YeastMine (Balakrishnan et al., 2012), mapped onto the global genetic interaction map (Costanzo et al., 2016) and compared to the map generated by *S. cerevisiae chl1*Δ genetic interactions **(Figure 2.10)**. The maps are remarkably similar, again supporting the highly conserved role of DDX11 in human cells. For genes involved in mitosis, the yeast data shows a predominantly negative interaction pattern, whereas the yeast orthologs of human genes contain both negative and positive interactions. *CHL1* is a non-essential gene in yeast (unlike *DDX11* in humans). Like the human GO term enrichment of positive genetic interactions, this may reflect a compensation by *DDX11* knock-out cells for the cohesion-associated defects caused by the knock-out (potentially by upregulating other factors) and therefore less sensitivity than wild-type cells to loss of other cohesion related genes which manifests as positive interactions. Other minor differences are in genes involved in protein turnover, which are highly linked to *CHL1* in yeast

but not to *DDX11* - the meaning of which is unclear, although it may reflect a lack of orthologous genes.

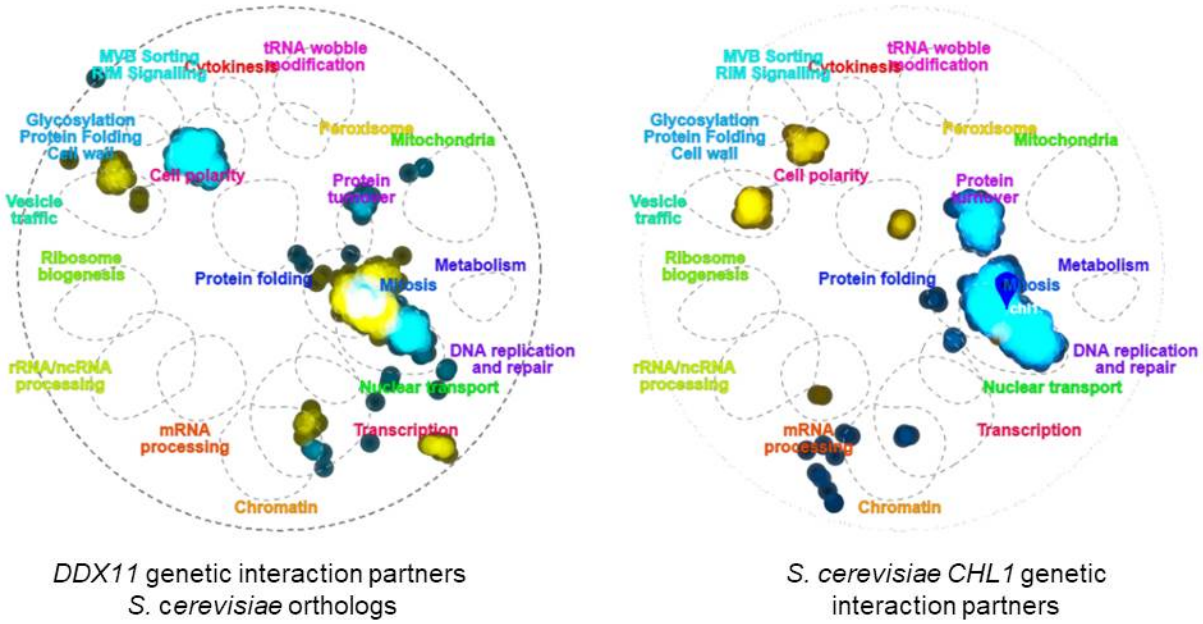

Figure 2.10 - Comparison of human *DDX11* genetic interactions to *S. cerevisiae CHL1* genetic interactions.
Left: *S. cerevisiae* orthologues of the positive and negative genetic interacting genes identified in the human DDX11 CRISPR/Cas9 screen were derived from YeastMine (Balakrishnan et al., 2012) and mapped onto the yeast global genetic interaction map (Costanzo et al., 2016). The generated map is illustrated compared to the map generated by the genetic interactions of *DDX11 S. cerevisiae* homolog, *chl1*Δ (Right, cutoff NGI < -0.12, PGI > 0.16).
Blue = negative genetic interaction partners. Yellow = positive genetic interaction partners.

Patterns of genetic interaction are deeply informative. In large scale, systematic screens across multiple query backgrounds, genes that operate in the same biological process tend to interact genetically with the same sets of other genes in discrete, related pathways, culminating in highly correlated genetic interaction profiles. This has been demonstrated both in yeast (Costanzo et al., 2016), and on a smaller scale in human cells (for example Bassik et al., 2013; Kampmann et al., 2013; Roguev et al., 2013). This suggests that beyond the specific interactions identified, a gene's pattern of fitness phenotypes across a diverse set of backgrounds can inform

our knowledge of that gene's function. Translating this into human cells has been complicated both by the scale of the genome, as well as by technological considerations such as the size of the libraries required and the multitude of genetic backgrounds available (Kim et al., 2019). However, the Hart lab has developed an indirect method of deriving functional interactions using fitness data following knock-out in more than 400 cancer and immortalized cell lines in the Cancer Dependency Map (Pacini et al., 2021). They demonstrated that genes having correlated knock-out fitness profiles across diverse, non-isogenic cell lines are analogous to genes having correlated genetic interaction profiles across isogenic query strains and similarly imply shared biological function (Kim et al., 2019). This suggests that analyzing *DDX11's* top co-dependencies (genes that show a similar pattern of fitness phenotypes upon knock-out across multiple cell lines) can provide additional functional information on the role of DDX11 and corroborate genetic interaction screens in individual, isogenic backgrounds. We performed gene ontology (GO) term (GO-Slim Biological Processes) enrichment analysis using PantherDB PANTHER Overrepresentation Test (Mi et al., 2021) on the top 100 co-dependencies for *DDX11* identified in DepMap. The top 10 enriched terms for biological processes gene ontology (GO) terms are listed in **Figure 2.11**. Not surprisingly, in line with the known role of *DDX11* and the genetic interactions identified in our screen, the top enriched terms were associated with the cell cycle, replication and mitosis – further strengthening the role that DDX11 may play in these processes.

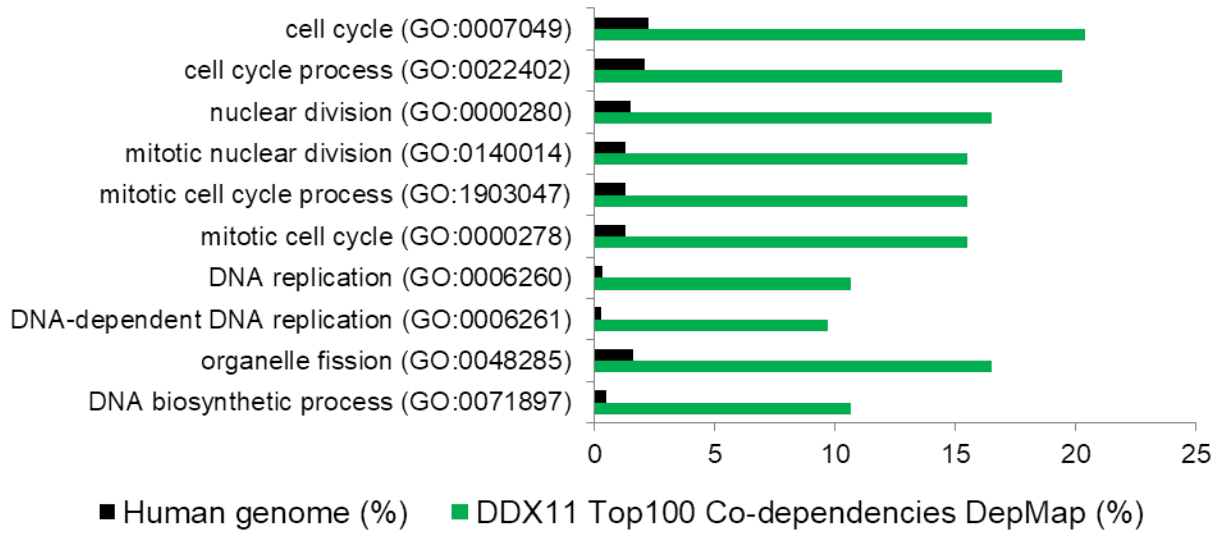

Figure 2.11 - *DDX11* top 100 co-dependencies from DepMap (Pacini et al., 2021).
Enrichment of *DDX11* top 100 co-dependencies (genes that show a similar pattern of fitness phenotypes upon knockout across a diverse set of 400 cellular backgrounds) was analyzed using the PANTHER Overrepresentation Test (annotation set: GO-Slim Biological Processes).

In summary, in this chapter we studied the genetic interactions of *DDX11* in human cells. We attempted to validate a potentially clinically-relevant interaction identified in yeast between the cohesin complex and Chl1. We also conducted an unbiased screen for genetic interactions in a pair of isogenic cell lines with/without *DDX11* knock-out. While the specific genetic interaction between the *STAG2* subunit and *DDX11* did not validate in our hands, the pattern of genetic interactions identified in the screen confirms the conserved role of *DDX11* and supports DDX11 inhibition as a potential synthetic lethal therapy for tumours with a phenotype displaying defects in sister-chromatid cohesion. The lack of conservation of the predicted interaction led us to reconsider the utility of using null mutations or depletion through RNAi to mimic inhibitors, and to develop a new paradigm for genetic screening using missense mutations to mimic desired properties of clinically-relevant synthetic lethal inhibitors as described in the next chapter.

Chapter 3: Modeling DNA- or protein-protein trapping of yeast *CHL1* using catalytically-inactive missense mutations identifies dominant synthetic lethal interactions in yeast

3.1 Introduction

The idea of utilizing tumour-specific genetic vulnerabilities to selectively target tumour cells with therapeutics, and specifically the idea of utilizing synthetic lethality, was proposed over 20 years ago (Hartwell et al., 1997). Large scale genetic screens using null alleles have been the bedrock of synthetic lethality discovery, first in model organisms such as *S. cerevisiae* resulting in a global genetic interaction network (Costanzo et al., 2016), and more recently in mammalian cells with the introduction of suitable techniques such as si/shRNA and CRISPR (Mair et al., 2019). While such screening has produced a wealth of functional and biological information, the yield from a therapeutic perspective has been low. Only one synthetic lethal-based therapeutic has reached the clinic – PARP inhibitors for tumours carrying *BRCA1/2* mutations (O'Neil et al., 2017). The success rate of synthetic lethal based therapies could conceivably be improved by analyzing the properties of PARP inhibitors and of topoisomerase inhibitors that, while not specifically developed as synthetic lethal drugs, exert their effect in part due to synthetic lethal interactions with tumour-specific mutations affecting replication, checkpoints or repair (Delgado et al., 2018).

PARP1 and PARP2 are DNA damage sensors and signal transducers that operate by synthesizing negatively charged, branched poly(ADP-ribose) (PAR) chains (PARylation) on target proteins as a form of posttranslational modification (Satoh & Lindahl, 1992), and are implicated in DNA repair and genome maintenance. PARP inhibitors were specifically developed as synthetic lethal-based therapeutics for the treatment of homologous recombination

(HR) repair-deficient tumors (Bryant et al., 2005; Farmer et al., 2005). Research into the mechanism of synthetic lethality caused by PARP inhibitors has found that the cytotoxicity of PARP inhibitors derives not from the loss of PARP activity, per se, but rather from the trapping of PARP protein on DNA, thereby generating a PARP–DNA cytotoxic lesion. PARP inhibitors with equivalent *in vitro* potency have very different cytotoxicities, and this is correlated with their ability to trap PARP on the DNA (Murai et al., 2012; Murai, Huang, et al., 2014). PARP inhibitors are also more cytotoxic than genetic depletion of PARP (Murai et al., 2012). Losing PARP expression is one of the mechanisms of resistance to PARP inhibitors in both *BRCA* wild-type and *BRCA* mutated cells (Pettitt et al., 2018), supporting the fact that it is the trapped PARP protein, and not the loss of PARylation, that is the basis for the toxicity and synthetic lethal targeting of PARP inhibitors. The trapped PARP-DNA complex not only creates a cytotoxic lesion, it can also block access of other proteins to the DNA (Pommier et al., 2016). PARP inhibition is also synergistic with other anti-cancer drugs such as temozolomide (a DNA alkylating agent) and this is dependent on PARP trapping, as talazoparib and olaparib (which are strong PARP trappers) are more efficient at killing temozolamide-treated cells than veliparib (a weak PARP trapper) or *PARP1/2* genetic inactivation (Murai, Zhang, et al., 2014).

Topoisomerases are enzymes that relieve supercoiling-associated tension in double stranded DNA. They do this by transiently cutting one strand (type I topoisomerases) or both DNA strands (type II topoisomerases). As part of their catalytic cycle, covalent bonds are formed between the enzyme and DNA (Buzun et al., 2020). Similar to PARP inhibitors, studying the mechanism of action of topoisomerase inhibitors revealed an important principle of drug action - creating a poisonous enzyme-drug complex, rather than simply inhibiting the catalytic activity, can drive the drug's toxicity (reviewed in Pommier 2013). Topoisomerase inhibitors such as

camptothecin (Top1 inhibitor) and etoposide (Top2 inhibitor) specifically bind at the interface of the topoisomerase-DNA complex, and trap the enzyme on the DNA. This was elegantly demonstrated for camptothecin and Top1 in both yeast and human cells. Yeast cells carrying a *top1* null mutation cells are resistant to camptothecin (Eng et al., 1988; Nitiss & Wang, 1988). Similarly, human cancer cells depleted for Top1 become resistant to camptothecin, implying that Top1 is required for the cytotoxicity of camptothecin, whereas reduction of Top1 by siRNA is tolerated, albeit with genomic instability and replication defects (Miao et al., 2007). The requirement of Top1 for the cytotoxicity of camptothecins and other Top1 inhibitors is supported by biochemical evidence demonstrating the formation of Top1-DNA complexes in cells treated with Top1 inhibitors (Covey et al., 1989; Padget et al., 2000; Subramanian et al., 1995).

It is possible that other DNA repair enzymes, such as helicases and nucleases, could be candidates for DNA trapping-mediated synthetic lethal cytotoxicity. Helicases are an extremely attractive therapeutic target. Inhibitors have been identified for several human helicases that play an important role in maintaining genome stability. The effect of inhibitors of the WRN, BLM helicases and the DNA2 helicase-nuclease is dependent on the presence of the DNA helicase, suggesting that pharmacological inactivation of helicase function interferes with genome maintenance in a way which is distinct from the effect imposed by the absence of the helicase altogether (Aggarwal et al., 2011; Aggarwal, Banerjee, Sommers, Iannascoli, et al., 2013; Liu et al., 2016). Other inhibitors of human helicases have been shown to trap their target protein on the DNA/RNA. Some examples include inhibitors of the RNA helicase E1F4A, which were found to stabilize eIF4A on RNA, decrease the off-rate of polypurine RNA-bound eIF4A and sequester eIF4A, causing depletion from eIF4F (L. Shen & Pelletier, 2020) and a recently identified inhibitor of the BLM helicase, compound 2, which exhibits allosteric trapping of a DNA-bound

translocation intermediate and “locks” the helicase into a conformational state where DNA substrates remain bound but cannot be unwound (Chen et al., 2021).

A major challenge for the development of trapping mediated synthetic lethality is screening. One of the limitations of current screening methods for discovery of synthetic lethal interactions is that most methods rely on null mutants under the assumption that ablation of the protein product of a gene of interest is akin to chemical inhibition. In model organisms, such mutations are often full deletions of the gene of interest, and more recently methods such as RNAi knock-down and CRISPR/Cas9 knock-out have been used in mammalian cells. Common to all these methods is the removal of the target protein from the cells, as opposed to chemical inhibition in which the target protein is still present and potentially able to bind the DNA and/or form a poisonous protein complex – essentially converting the target protein into a dominant cytotoxic lesion. Another limitation of synthetic lethal screening using null alleles is that this method does not allow for screening of essential genes, even though a large number of them may play key roles in cancer-relevant processes such as DNA replication or repair. Furthermore, essential genes may display synthetic lethal interactions upon partial inhibition, trapping or inhibiting one function of a multi-functional protein. Some synthetic lethal interactions identified using null mutations may not reproduce upon chemical inhibition, as residual activity of uninhibited protein may be sufficient to prevent the synthetic lethal interaction, causing potentially promising synthetic lethal interactions to be less translatable therapeutically as full inhibition is rarely achieved using small molecule inhibition.

We hypothesized that small molecule-induced trapping may represent a generalized mechanism for clinically relevant synthetic lethal interactions and that missense mutations that mimic such inhibitors can be utilized as an alternative to knock-out/knock-down based screens.

Missense-derived synthetic lethal genetic interactions may be more clinically relevant than interactions that are based on complete knock-outs, as they are assessed when the target protein is present and retains DNA and/or protein interactions, but is inactivated. In both DNA- and protein-trapping scenarios, the trapped inactivated protein would be predicted to elicit a dominant phenotype, as the trapped protein would compete with wild-type protein for substrate or binding partners **(Figure 3.1)**.

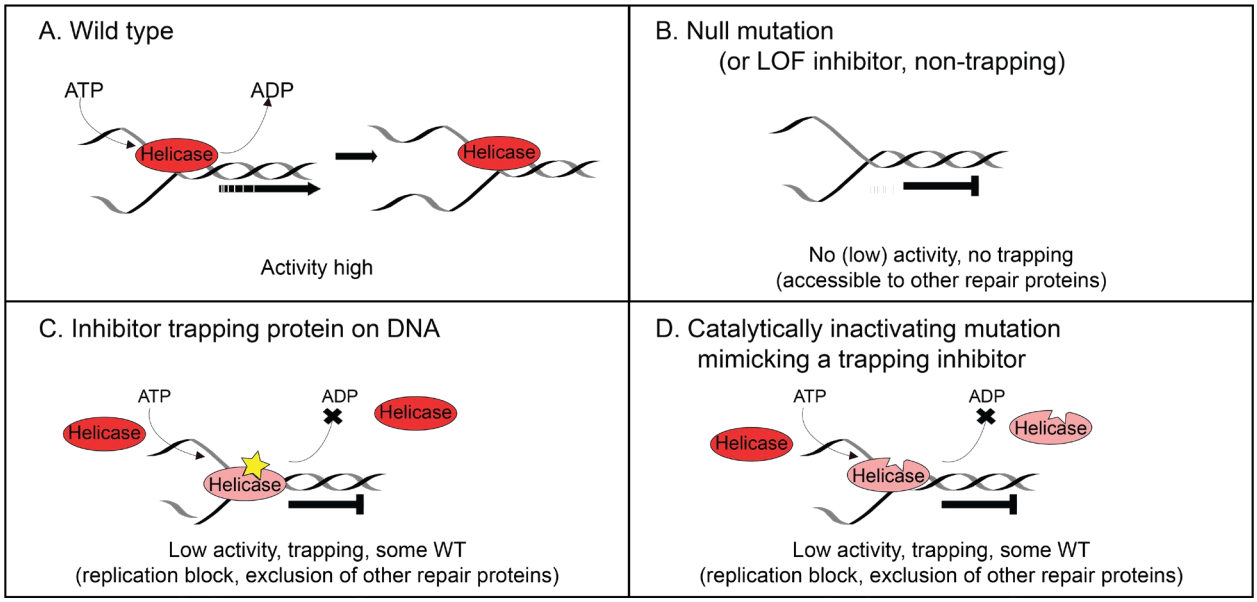

Figure 3.1 - Model for dominant synthetic lethality or trapping inhibitor versus a null mutation. **(A)** In the absence of an inhibitor, wild-type helicase binds to DNA, hydrolysis ATP, translocates along DNA and unwinds. **(B)** In the case of a null mutation (or loss-of-function inhibitor/mutation), DDX11 activity is absent, however other helicases or DNA-repair proteins can access the DNA and compensate (partially or fully) for the absence of DDX11. **(C)** A chemical inhibitor (yellow star) that prevents activity but allows (or requires) DNA-binding may trap the enzyme on the DNA, where it forms a potentially cytotoxic protein-DNA complex (for example a replication block), or blocks access by alternative helicases or DNA repair enzymes. **(D)** Dominant synthetic lethal catalytically-inactive mutant binds to DNA but is unable to translocate and is trapped on the DNA, mimicking the inhibitor in C.
LOF = Loss-of-function, WT = wild-type

In this way, dominant synthetic lethal interactions can capture genetic interactions that occur in the presence of the wild-type or residual non-inhibited protein, thus mimicking both a trapped enzyme and residual activity from uninhibited protein. Screening for trapping-based

dominant synthetic lethal interactions may also enable exploitation of inhibition of essential proteins, where a full knock-out would be inviable and therefore not amenable to screening. Trapping even a subset of the target protein pool, or inhibiting only one function of a multi-function essential protein, may create a dominant synthetic lethal interaction that could then guide development of an appropriate therapeutic.

In addition to the known trapping of PARP and topoisomerase inhibitors, utilizing missense mutations instead of nulls to model trapping and guide development of inhibitors is supported by several lines of evidence. Specific missense mutations in *S. cerevisiae* Top1 enhance the stability of the covalent topoisomerase–DNA intermediate and phenocopy the effect of the topoisomerase inhibitor camptothecin (Megonigal et al., 1997). These camptothecin mimetic mutations cause a dominant phenotype and have been used to screen for mutations that sensitize cells to topoisomerase trapping (Reid et al., 2011). ATPase-defective missense mutants of *S. cerevisiae* Prp16 and Prp22 (RNA-dependent ATPases required for pre-mRNA splicing) bind to spliceosomes *in vitro* but are defective in mRNA release, and block the function of the respective wild-type proteins in a dominant manner (Schneider et al., 2002; Schwer & Meszaros, 2000). Examples of missense mutations causing dominant negative phenotypes also exist in mammalian systems. One relevant example is observed in *FANCJ*, a DEAD-box helicase highly related to *DDX11*. A patient-derived pathogenic missense mutant (A349P, immediately adjacent to a highly conserved cysteine in the iron-sulfur domain) binds DNA but is defective in coupling adenosine triphosphate (ATP) hydrolysis and translocase activity to unwinding forked duplex or G-quadruplex DNA substrates or disrupting protein-DNA complexes. Expression of this mutant in a wild-type background exerts a dominant negative effect, suggesting that it interferes with normal DNA metabolism (Wu et al., 2010). The phenomenon of missense mutations causing a

more severe phenotype than loss of the protein is not restricted to DNA metabolizing enzymes. Mouse models expressing kinase-dead mutants of three PI3-kinases instrumental in the DNA-damage response (ATM, ATR and DNA-PK) revealed an unexpected structural function causing more genomic instability than a null, with each kinase displaying a unique spectrum of genomic instability and physiological consequences, suggesting a model in which catalytic inhibition leads to the persistence of the kinases at the DNA lesion, which in turn affects repair pathway choice and outcomes (Menolfi & Zha, 2020).

In this chapter, we utilize yeast high-throughput genetic techniques to conduct proof-of-principle experiments using a missense mutation in yeast *CHL1* to model a specific form of inhibition in which catalytic activity is inhibited, but binding to the DNA is unaffected. We conduct a screen for dominant synthetic lethal interactions with a panel of knock-out mutants involved in DNA- and cell cycle-associated processes. We also study the impact of replisome- and DNA-binding on the dominant synthetic lethal effect by use of additional missense mutations in *CHL1*.

3.2 Materials and methods

3.2.1 Expression vectors

Yeast *CHL1* from the Gateway-compatible FLEX array (Hu et al., 2007) was shuttled to a donor vector to generate entry clones using BP Clonase II (Invitrogen). Missense mutations were introduced in the entry clone using the QuikChange Site-Directed Mutagenesis Kit (Agilent) and verified by Sanger sequencing. Wild-type and mutant *CHL1* entry clones were shuttled into the yeast destination vector pAG415GAL-ccdB (LEU2, CEN, inducible GAL promoter) (Alberti et al., 2007).

Gateway-compatible *URA3*-integration vectors (two versions) were constructed by modifying pWS1291 (containing homology upstream and downstream to the *URA3* locus and flanked by NotI digestion sites) (gift from Tom Ellis, Imperial College London, London, United Kingdom). The yeast *LEU2* cassette was PCR amplified from pRS415 (Sikorski & Hieter, 1989) using primers (OPH9725 and 9726) and cloned between PstI and SpeI sites to create a yeast selectable version of pWS1291. To convert pWS1291 and pWS1291_LEU2 to Gateway-compatible plasmids, the origins of replication and bacterial selection markers were replaced with those from pAG415GAL-ccdB (Alberti et al., 2007) using a PCR-amplified fragment (primers OPH9834 and 9835) that was cloned between the NotI sites in pWS1291 and pWS1291_LEU2. Another PCR product containing the *GAL1* promotor, ccdB cassette, and C-terminal 3xHA tag was amplified using primers (OPH9727 and 9728) and cloned between the BmgBI sites. Correct orientation of inserts was verified by PCR and sequencing. The resultant vector, pLA581 (ura3_int_GAL-ccdB-HA_LEU2) was used to integrate ORFs into the *ura3* locus.

3.2.2 Yeast strains

Yeast strains used in this chapter are listed in Appendix A .

The miniarray was constructed by repinning 332 nonessential yeast knock-out strains from the Deletion Mutant Array (DMA) collection (Giaever et al., 2002). Each *MAT*a haploid yeast knock-out, marked by kanMX, was verified by PCR. The corresponding yeast proteins function in DNA-related pathways and mostly have conserved human homolog(s). Fifty *MAT*a wild-type (*his3Δ1::kanMX*) spots were pinned randomly in the array as control strains.

For experiments using hetero-allelic haploids, wild-type and mutant *CHL1* ORFs (containing stop codons) were shuttled from entry clones to pLA581 using LR Clonase II.

Following NotI digestion, the galactose-inducible ORFs were integrated into the *ura3Δ0* locus by transformation of the linearized vectors into the SGA starter strain Y7092 *(MAT*α *can1Δ::STE2pr-his5 lyp1Δ ura3Δ0 leu2Δ0 his3Δ1 met15Δ0*) and selection of transformants on SD−Leu medium to obtain YPH2742-YPH2749. Correct integration was confirmed by PCR. These hetero-allelic haploids were then mated to *MAT*a *kanMX*-marked deletion strains (from the miniarray) and *URA3*-marked temperature-sensitive (McLellan et al., 2012) strains. Diploids were selected and sporulated using the same methods described for the screen. Following sporulation, hetero-allelic haploids containing deletions or temperature-sensitive mutations were obtained by streaking to single colonies on haploid selection media SD−HRLK (−His −Arg −Leu −Lys + 50 µg/mL canavanine + 50 µg/mL thialysine + 2% dextrose) containing either 200 µg/mL G418 (for deletion strains) or lacking uracil (for temperature-sensitive strains).

For the cohesion assays, the galactose-inducible ORFs were integrated into the *ura3* locus of YPH2655 (Guacci et al., 2015) by transformation of the linearized vectors and selection on SD-Leu media to obtain YLM49-YLM56. Correct integration was confirmed by PCR.

Hemagglutinin (HA)-tagged strains were constructed using the hetero-allelic haploids by removing the stop codons and bringing the 3xHA tag in-frame with the ORFs. The CRISPR/Cas9 protocol utilized a guide RNA (gRNA) targeted to the linker region between the ORF and the 3xHA tag (guide: AATTCGATATCAAGCTTAGG). Donor DNA was constructed by annealing two complimentary oligos composed of flanking homology to the left and right of the integration site (primers OPH9879 and 9880) to obtain YPH2750-YPH2757. Correct sequence was verified by PCR and sequencing.

3.2.3 Dominant synthetic lethal screen

Galactose-inducible expression vectors and the vector control pRS415 (LEU2, CEN) were transformed into the SGA-starter strain (Y7092), and transformants were selected on SD−Leu medium. Query strains (Y7092) containing LEU2-marked vectors were crossed to the miniarray using SGA technology (Tong et al., 2001). A series of replica-pinning steps using a Singer RoToR robot generated an array of deletion mutants on dextrose media containing either a vector control or the expression plasmids, which were induced by pinning onto media containing galactose. Initially, query strains were grown to saturation in triplicates in SD−Leu before plating on the same media to generate lawns of cells. Query strains were mated to the miniarray on yeast extract, peptone, and dextrose (YPD), and diploids were selected on SD−Leu+G418 (200 μg/mL) by two rounds of pinning. Diploids were pinned on sporulation medium (+ 50 μg/mL G418) and incubated for 7 days at 25°C. Haploids were selected on SD−HRLK + drugs (−His −Arg −Leu −Lys + 50 μg/mL canavanine + 50 μg/mL thialysine + 200 μg/mL G418 + 2% dextrose) for two rounds before pinning on the same haploid selection plates containing either 2% dextrose or 2% galactose (two rounds of pinning on galactose). After the final plates were scanned, the area of each pinned spot was measured by Balony software (Young & Loewen, 2013) where the area of each deletion strain was normalized to the average area of all wild-type spots (n = 50) on the same plate. Interactions with a cutoff of >20% change in growth differential compared to the vector control plate were chosen for validation (experimental-control values <−0.2).

3.2.4 Yeast assays

For **liquid growth assays**, plasmid-bearing cultures were grown to midlog phase in −Leu selective medium containing either 2% dextrose or 2% galactose before diluting to optical

density at 600 nm (OD_{600}) = 0.1 in 200 µL of the same medium. The 200-µL yeast cultures prepared in 96-well plates were loaded in a TECAN M200 plate reader, and OD_{600} readings were measured every 30 min over a period of 24h. Before each reading, plates were shaken for 10 min. Each strain was tested in three replicates per plate per condition, and area under the curve (AUC) was calculated for each replicate. "Relative strain fitness" was defined as the AUC of each yeast strain curve relative to the AUC of the control strain curve grown on the same plate in the same medium condition.

For **spot assays**, an overnight culture was diluted and grown to mid-log phase. Cells were then diluted to OD_{600}=0.1 and then serially diluted in 10-fold increments and plated (5 µL each spot) onto indicated media. Spotting on SG (synthetic medium containing 2% galactose) induced expression of ORFs. Growth assays involving temperature-sensitive strains were carried out at 25°C while all remaining assays were conducted at 30°C.

A-Like-Faker assay was conducted as previously described (Duffy et al., 2016). In brief, expression of wild-type or mutant *CHL1* was induced for 2 days by patching the *MATα* hetero-allelic strains on galactose for 2 days. Each strain was then patched out on galactose in 1 cm^2 patches and mated to a *MATα his1* tester lawn by replica plating on galactose containing media. His+ prototrophs were selected on minimal media.

Cohesion assays: Cohesion was monitored using the *LacO*-LacI system, in which cells contained a GFP-LacI fusion and tandem *LacO* repeats integrated at the *LYS4* chromosomal locus (located 470 kb from CEN4) as previously described (Guacci & Koshland, 2012; Straight et al., 1996), with modifications for galactose-inducible expression of the integrated *CHL1* constructs. Briefly, cells were grown to mid-log phase at 30°C in YP media +2% raffinose (YPR). Cells were then re-diluted in YPR to OD_{600}=0.2, α-factor was added to 10^{-8} M final

concentration and cells were incubated for an additional 2 h to induce arrest in G1. The cells were then washed three times with fresh YPRG (YP+2% raffinose+2% galactose) plus Pronase (final concentration 0.1 mg/ml), resuspended in fresh YPRG plus Nocodazole (final concentration 15 μg/ml) and incubated at 30°C for an additional 3 h to arrest at G2/M. Cells were fixed with 80% ethanol, kept at 4°C overnight and imaged the next day. Between 150 and 400 cells were counted for each strain and % of cells with premature chromatid separation (cells with two GFP signals) was calculated. DNA content was measured by FACS on samples obtained at the end of the α-factor arrest (G1) and fixed cells (G2/M) prior to imaging.

3.2.5 Whole cell extract and western blotting

Yeast cells were grown in inducing (2% galactose) or noninducing (2% dextrose) medium at 30°C to mid-log phase and harvested before resuspension of cell pellets in equal volume of Tackett Extraction Buffer [20 mM 4-(2-hydroxyethyl)-1-piperazineethanesulfonic acid (Hepes), pH 7.4, 0.1% Tween 20, 2 mM MgCl2, 200 mM NaCl, protease inhibitors] (Hamza & Baetz, 2012). To lyse the cells, glass beads were added to the samples and the mixture was vortexed in five 1-min blasts with 1-min incubation on ice between each vortex round. A 21-gauge needle (Becton Dickinson) was used to separate the crude whole cell extract from the beads into a new Eppendorf by poking a hole in the bottom of the tube and centrifuging at 1,000 rpm for 1 min. Lysates were cleared via centrifugation at 13,000 rpm for 15 min at 4 °C and normalized by protein concentration using the Bradford assay (Bio-Rad). Protein samples were subjected to sodium dodecyl sulfate polyacrylamide gel electrophoresis (SDS/PAGE) and Western blotting. Primary antibodies used included mouse anti-HA (catalog no. ab18181, 1:1,000; Abcam), and mouse anti-PGK1 (Invitrogen, catalog no. 459250, 1:5,000). Secondary antibodies used were goat anti-mouse horseradish peroxidase (HRP) (1:10,000).

3.3 Results

3.3.1 Helicase-deficient Chl1^{K48R*} is dominant synthetic lethal with spindle-associated and *CTF18-RFC* mutants

A conserved lysine to arginine substitution has previously been described in both yeast Chl1 (K48R) and human DDX11 (K50R). This mutation abolishes helicase activity of both yeast Chl1 (Samora et al., 2016) and human DDX11 proteins (Hirota & Lahti, 2000; Wu et al., 2012) but retains human DDX11 binding to DNA *in vitro* (Wu et al., 2012) and recruitment to the replication fork in yeast (Samora et al., 2016). In proof-of-principle experiments, we expressed galactose-inducible *CHL1*^{WT} or helicase-deficient *CHL1*^{K48R} (in the presence of endogenous wild-type Chl1 protein) to mimic a specific case of chemical inhibition (in which protein activity was inhibited but substrate binding was unaffected) to screen for dominant synthetic lethal interactions with a panel of DNA-associated knock-out mutants. We utilized synthetic genetic array (SGA) technology to introduce plasmid-borne, open reading frames (ORFs) into an arrayed library of yeast deletion strains. The result is an output array of plasmid-bearing haploid single mutants whose relative fitness can be assessed following induction by measuring colony size **(Figure 3.2A)**. We constructed a miniarray comprising 332 yeast deletion mutants that affect various DNA transactions (Appendix C). The plasmid-borne ORFs were under the control of a galactose-inducible promotor allowing induction of wild-type Chl1 protein or the catalytically inactive Chl1^{K48R} mutant form. Unlike yeast Rad27, where induced ectopic expression of either

* A note about the nomenclature used in this chapter: We used standard *S. cerevisiae* nomenclature (gene names upper case italics, dominant alleles uppercase italics, recessive alleles lower case italics with an allele identifier, proteins capitalized first letter) and added the words "protein" or "mutant form" to improve clarity when discussing expression of mutant Chl1 protein.

wild-type Rad27 or the Rad27^{D179A} mutant form caused profound growth defects in yeast (Hamza et al., 2021), expression of either the wild-type or the K48R catalytically-inactive form of Chl1 does not cause a significant growth defect in wild-type yeast cells **(Figure 3.2B)**; the plasmids were therefore considered suitable for a dominant synthetic lethality screen.

Twenty-five of the 332 mutants on the SGA miniarray exhibited reduced growth (>20% growth defects) upon induced ectopic expression of wild-type Chl1 protein in the initial screen, but none of the strains selected for subsequent validation testing confirmed the reduced growth, suggesting that elevated levels of the wild-type protein are tolerated in all of the 332 yeast deletion strains tested (Table C.1). We identified 59 putative dominant synthetic lethal interactions that displayed >20% growth defects upon ectopic expression of Chl1^{K48R} mutant protein (Table C.2). We selected the top negative interactions for testing by liquid growth assays and validated the Chl1^{K48R} dominant synthetic lethal interaction with four mutants in the array: *bub1Δ* and *bim1Δ*, which are spindle-associated genes, and *dcc1Δ* and *ctf8Δ*, which are part of the Ctf18-RFC complex (**Figure 3.2C** and **Appendix Figure C.1**).

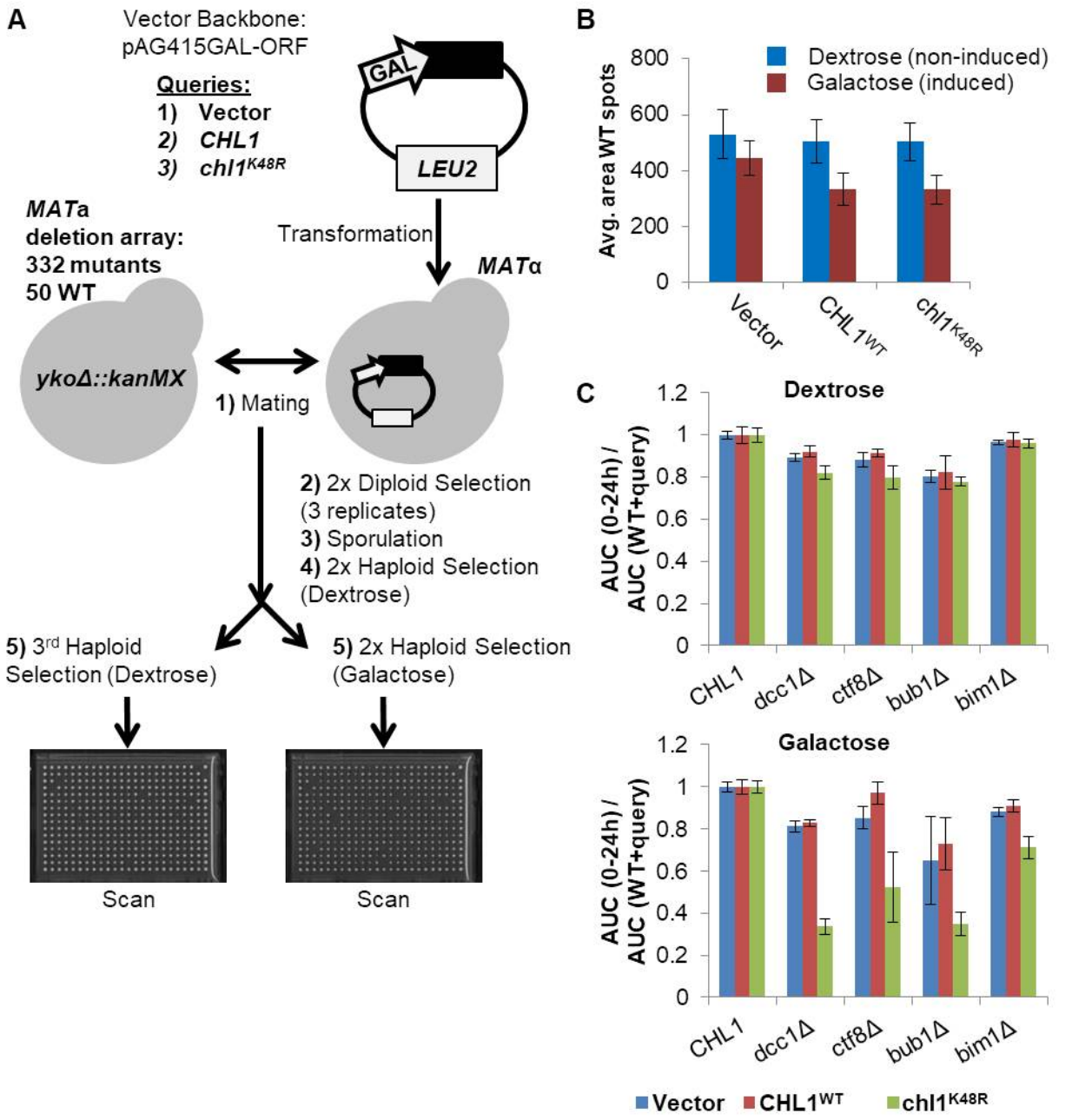

Figure 3.2 - Catalytically-inactive CHL1 causes dominant synthetic lethality with spindle-associated and Ctf18-RFC complex mutants.
(A) Inducible yeast expression vectors, or a vector control were transformed to generate query strains. Using synthetic genetic array technology, each query strain was mated to a pinned mini-array comprising 332 haploid yeast knockouts and 50 wild-type strains to generate diploids. A series of replica-pinning steps generated a haploid array where each knockout mutant was combined with the expression vector. After haploid selection, strains were pinned onto galactose media to induce expression of the open reading frame (ORF). The final plates were scanned, and area of each pinned spot was determined to detect dominant synthetic lethal interactions. **(B)** Quantification of the fitness defects that result from

ectopic expression of Chl1^{WT} or Chl1^{K48R} protein in wild-type cells. The average area of wild-type (WT) spots (n=50) on each haploid array (n=3) demonstrate that expression of both wild-type Chl1 and the catalytically-inactive Chl1^{K48R} proteins cause minimal growth defects in wild-type cells relative to vector control. **(C)** Quantification of Chl1^{K48R} dominant synthetic lethal interactions using liquid growth curve assays following expression of catalytically-inactive Chl1^{K48R}. For each validation, three isolates of each yeast strain (wild-type or knock-out mutants) containing a vector control or indicated *CHL1* ORF cloned in a yeast expression vector were grown in dextrose (non-inducing) or galactose (inducing) media. Each represented curve is the average of three replicates. Fitness of each strain was quantified by calculating area under the curve (AUC) of each replicate independently and normalized to the AUC of the wild-type strain containing the vector control and grown in the same media condition (mean +/- SD). Growth curves for each individual strain are shown in Figure C.1.

Given that both *CHL1* and the identified interacting genes are required for chromosome maintenance, which could affect plasmid segregation and stability, we constructed hetero-allelic haploids by integrating galactose-inducible gene cassettes expressing either yeast Chl1 or the Chl1^{K48R} mutant forms at the *URA3* locus, in a strain expressing wild-type Chl1 protein at the endogenous locus. We retested the effects of induced expression in the previously validated mutants (*bub1Δ*, *bim1Δ*, *dcc1Δ*, and *ctf8Δ*), as well as additional mutants of interest using spot assays, and confirmed the dominant synthetic lethality that occurs upon induction of Chl1^{K48R} mutant protein **(Figure 3.3)**. The Ctf18–RFC is a multimeric complex comprised of *RFC2-5* (common to all RFC complexes) as well as three unique genes (*DCC1*, *CTF8*, and *CTF18*) (Mayer et al., 2001). As we identified two of three unique *CTF18-RFC* genes in our screen, we directly tested *ctf18Δ* and confirmed that expression of Chl1^{K48R} mutant form also causes a dominant synthetic lethal effect in this mutant **(Figure 3.3)**.

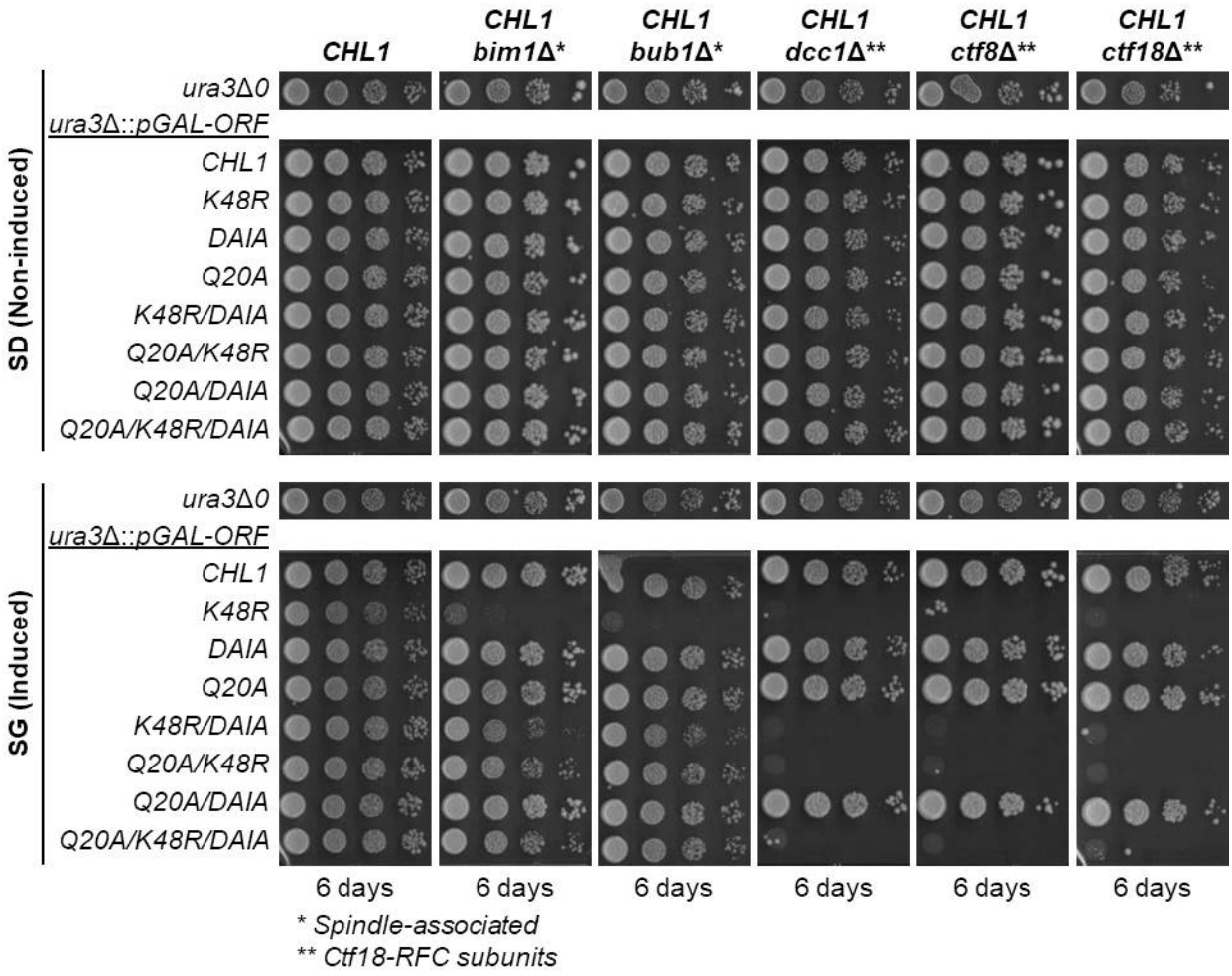

Figure 3.3 - DNA- and replisome-binding mutations have different effects on rescue of Chl1^{K48R} dominant synthetic lethality, depending on pathway.
Yeast heteroallelic haploids, containing a genomic copy of endogenously-regulated *CHL1*, were generated by integrating galactose-inducible ORFs at the *URA3* locus. Yeast strains were spotted in 10-fold dilution on indicated media containing either dextrose (non-inducing) or galactose (inducing) and imaged after 6 days. Inducible expression of the catalytically-inactive Chl1 mutant form, K48R, causes dominant synthetic lethality in spindle-associated *bim1*Δ and *bub1*Δ mutant strains, and in Ctf18-RFC subunit *dcc1*Δ, *ctf8*Δ and *ctf18*Δ mutant strains. The replisome binding mutant (DAIA) and putative DNA binding mutant (Q20A) can suppress (separate or together) the dominant synthetic lethality observed in the spindle-associated mutant strains (*bim1*Δ and *bub1*Δ). The same mutants (separate or together) are unable to suppress the dominant synthetic lethality observed in the Ctf18-RFC subunit mutant strains (*dcc1*Δ, *ctf8*Δ and *ctf18*Δ).

A similar screen with the human *FEN1^{D181A}* catalytically-inactive mutant identified dominant synthetic lethal interactions primarily with proteins involved in the Homologous Recombination (HR) pathway (Hamza et al., 2021). In contrast, expression of the yeast Chl1^{K48R}

mutant protein caused a very mild growth defect in a *rad52*Δ mutated strain **(Figure 3.4)**, suggesting that the mechanism underlying dominant synthetic lethality is different between *hFEN1* and *yCHL1* and that catalytically-inactive Chl1^{K48R} protein is not dominant synthetic lethal in HR mutants. Furthermore, and in agreement with previous studies (Samora et al., 2016), expression of Chl1^{K48R} mutant protein did not confer growth defects in a *chl1Δ* mutant **(Figure 3.4)**. This is in contrast to the severe growth defects observed for a *rad27Δ* mutant that expressed the catalytically-inactive hFEN1^{D181A} protein (Hamza et al., 2021).

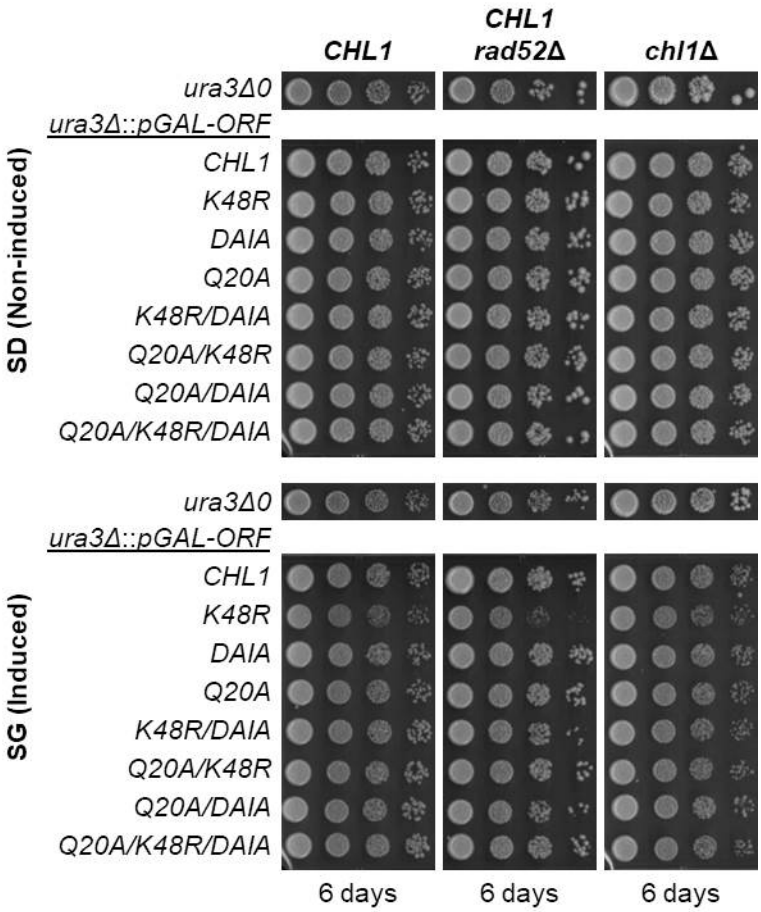

Figure 3.4 - Analysis of dominant synthetic lethality in additional mutant strains.
As in Figure 3.3, yeast heteroallelic haploids, containing a genomic copy of endogenously-regulated *CHL1*, were generated by integrating galactose-inducible ORFs at the *URA3* locus. Strains were spotted in 10-fold dilution on indicated media containing either dextrose (non-inducing) or galactose (inducing) and imaged after 6 days. Inducible expression of the catalytically-inactive Chl1 mutant form, K48R, causes only a mild growth defect in an HR-mutated strain (*rad52Δ)* and has no effect on a *chl1Δ* mutated strain. The replisome-binding (DAIA) and/or putative DNA-binding (Q20A) mutations have no effect on

growth, either alone or in combination with the catalytically-inactive K48R mutation. *CHL1* panels are the same as **Figure 3.3** as they are derived from the same experiment.

3.3.2 The effect of DNA- or replisome-binding mutations on the Chl1^{K48R} dominant synthetic lethality is dependent on the synthetic lethal partner mutation.

To test whether DNA or replisome binding was required for the observed Chl1^{K48R} dominant synthetic lethal effect, we tested several mutations previously identified as disrupting the replisome- or DNA-binding of yChl1/hDDX11. Yeast Chl1 binds the replisome through a protein–protein interaction with Ctf4, and it has been shown that a DDIL-to-DAIA mutation in Chl1, which disrupts the Ctf4-interacting-peptide (CIP-box) motif, abrogates this binding (Samora et al., 2016). A glutamine-to-alanine mutation at a conserved residue in the Q-motif of hDDX11 (hQ23A or yQ20A) abolished the DNA-binding ability of the purified human protein *in vitro* (Ding et al., 2015) **(Figure 3.5A)**.

We used the same inducible hetero-allelic system (in which various *CHL1* constructs are integrated at the *URA3* locus, in the presence of endogenously regulated wild-type Chl1 protein), to express the replisome-binding (Chl1^{DAIA}) and putative DNA-binding (Chl1^{Q20A}) mutant proteins alone, in combination with the K48R catalytically-inactive mutation (Chl1$^{K48R/DAIA}$ or Chl1$^{Q20A/K48R}$), or as a triple mutant (Chl1$^{Q20A/K48R/DAIA}$) in the genetic backgrounds in which the dominant synthetic lethal effect was observed. Introduction of these mutations in different combinations did not affect the stability of the Chl1 protein **(Figure 3.5C)**. Expression of the two binding mutations alone (Chl1^{Q20A} or Chl1^{DAIA}), or together (Chl1$^{Q20A/DAIA}$), did not result in a dominant effect on growth. The dominant synthetic lethality caused by Chl1^{K48R} protein expression in the spindle-associated mutants was suppressed by introduction of both the replisome-binding and DNA-binding mutations (separate or together). In contrast, in the CTF18-

RFC mutated strains, the Chl1^{K48R} dominant synthetic lethality was not suppressed by introduction of either or both of the binding mutations, suggesting that the mechanism of dominant synthetic lethality varies between these two pathways **(Figure 3.3)**.

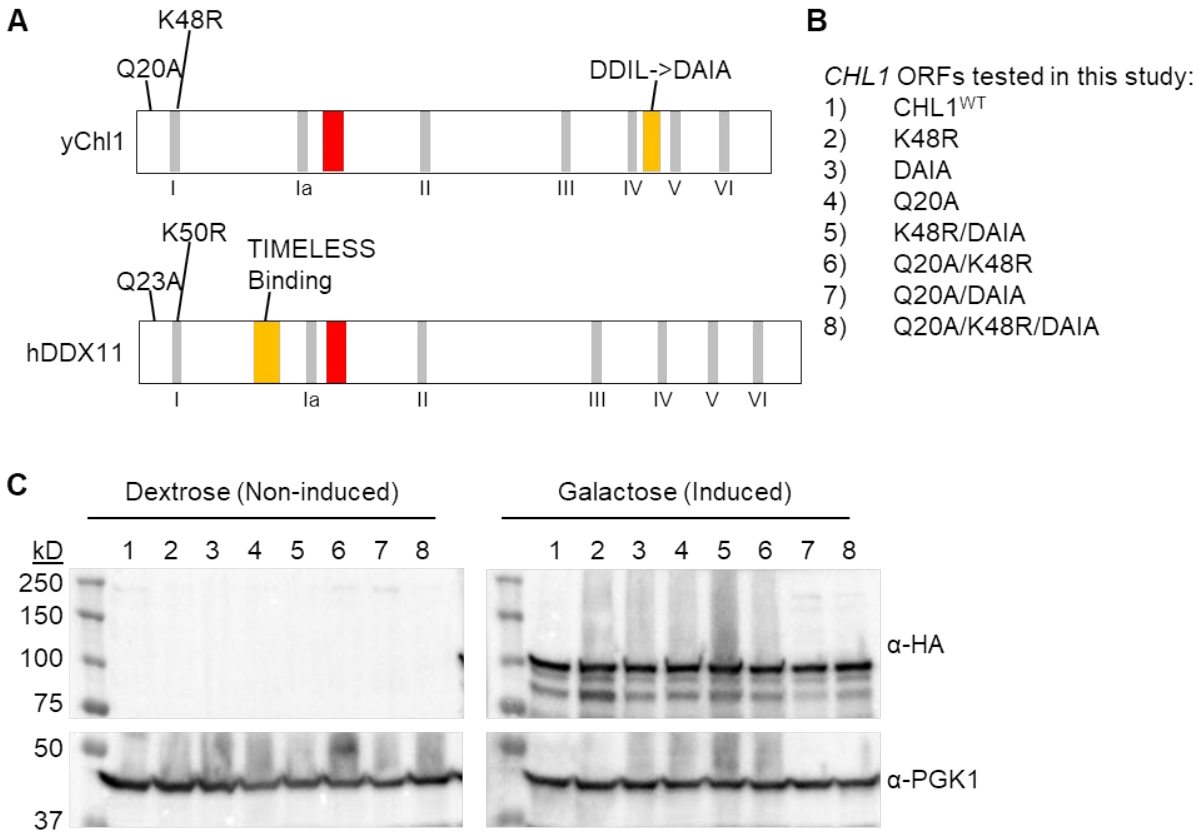

Figure 3.5 - Yeast *CHL1* mutants tested in this study.
(A) Schematic of yChl1 aligned to hDDX11 protein indicating mutations tested in this study. Grey domains: Helicase motifs. Red domains: Fe-S binding region. Yellow domains: replisome-binding region (yeast through CIP box, human through binding to Timeless). **(B)** List of mutants tested in the study. K48R: catalytically inactive, DAIA: Ctf4-binding defective, Q20A: putative DNA binding mutation. **(C)** Western blot analysis of HA-tagged *CHL1* ORFs. Yeast cultures were grown in non-inducing (dextrose) or inducing (galactose) media to mid-log phase before cell lysis. Lanes are indicated in panel B. Introduction of mutations does not impact Chl1 protein stability.

3.3.3 Helicase-deficient Chl1^{K48R} is dominant synthetic lethal with cohesin mutants.

Yeast *chl1Δ* mutant cells exhibit increased rates of chromosome instability (Gerring et al., 1990), as well as sister chromatid cohesion defects (Mayer et al., 2004; Samora et al., 2016; Skibbens, 2004). The deletion mutants identified in the screen as synthetic lethal with dominant Chl1^{K48R} also display defects in chromosome stability or sister chromatid cohesion (Fernius & Hardwick, 2007; Mayer et al., 2001, 2004). CTF assays, which measure loss of artificial chromosomes, revealed a dominant effect of Chl1^{K48R} mutant protein on chromosome stability (Holloway, 2000).

Knock-out mutants of *CHL1*, spindle-associated genes, and *CTF18-RFC* complex genes are also synthetic lethal with mutations in cohesin genes (McLellan et al., 2012; O'Neil et al., 2013). We tested whether expression of the Chl1^{K48R} mutant protein was dominant synthetic lethal with mutations affecting the cohesion pathway. The cohesin complex is comprised of four essential core proteins (Smc1, Smc3, Scc1, Irr1) that are loaded onto DNA by a separate complex composed of Scc2 and Scc4 (Uhlmann, 2016). As these are essential genes, we selected temperature-sensitive mutants of core (*smc1-259* and *scc1-73*) and loader (*scc2-4*) subunits and examined the effect of inducible expression of wild-type Chl1 or Chl1^{K48R} protein on growth. Expression of Chl1^{K48R}, in the presence of wild-type Chl1, caused severe growth defects in all three cohesin mutants **(Figure 3.6A)**, indicating a dominant synthetic lethal interaction with mutations in the cohesion pathway. However, Chl1^{K48R} does not exhibit dominant synthetic lethality with all cohesion mutants. For example, the nonessential cohesin accessory subunit, Rad61, also functions in the cohesion pathway. The *rad61Δ* mutant did not meet the cutoff in our Chl1^{K48R} dominant synthetic lethal screen (Table C.2). To determine if this was a false-negative hit, we directly tested the effect of expression of the Chl1^{K48R} mutant protein on fitness of a

rad61Δ mutant strain and determined that expression of this allele was not dominant synthetic lethal in this mutant background **(Figure 3.6B)**.

To examine the requirement for replisome- or DNA-binding for the dominant synthetic lethal effect of Chl1^{K48R} on growth of cohesin-mutated strains, we combined the K48R mutant with the replisome-binding (DAIA) and/or DNA-binding (Q20A) mutations. In the strains bearing mutations in the cohesin core subunits (*smc1-259* and *scc1-73*), the Chl1^{K48R} dominant synthetic lethal interaction was suppressed by both the Q20A and DAIA mutants. In contrast, the Chl1^{K48R} dominant synthetic lethality with the cohesin loader mutation (*scc2-4*) was not suppressed by either the Q20A or the DAIA mutants. Instead, expression of the Chl1$^{Q20A/DAIA}$ mutant protein caused dominant growth defects in the *scc2-4* mutant **(Figure 3.6A)**. Together, these results suggest that dominant synthetic lethality may be able to separate the functional differences between members of the same biological pathway.

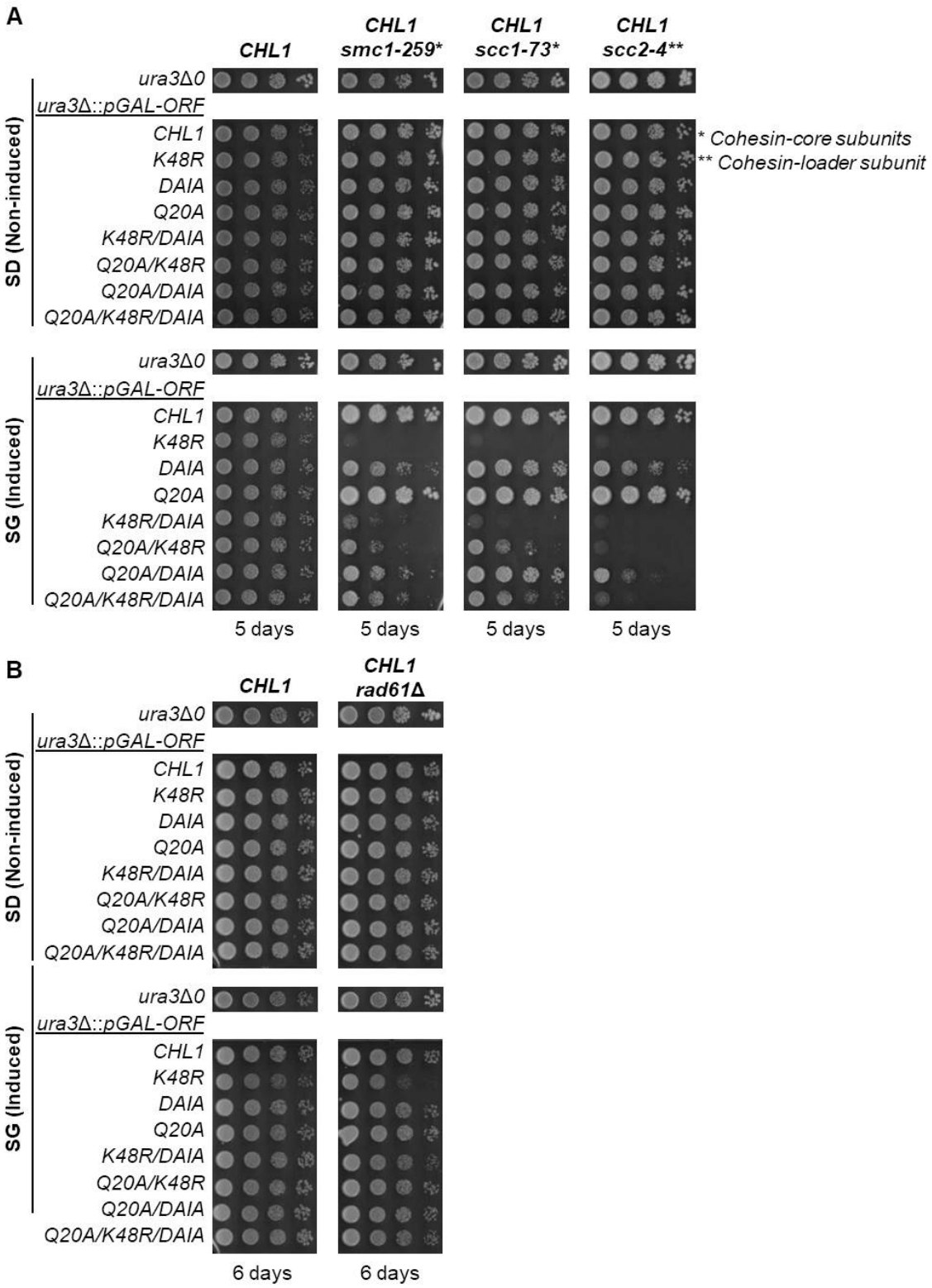

Figure 3.6 - Helicase-deficient *CHL1* is dominant SL with cohesin mutants.
(A) Yeast heteroallelic haploids, containing a genomic copy of endogenously-regulated *CHL1*, were generated by integrating galactose-inducible ORFs at the *URA3* locus. Yeast strains were spotted in 10-fold dilution on indicated media containing either dextrose (non-inducing) or galactose (inducing) and

imaged after 5 or 6 days. Inducible expression of the helicase-deficient *CHL1* mutant, Chl1^{K48R}, causes dominant SL in the cohesin core (*smc1-259 and scc1-73)*, and cohesin loader (*scc2-4)*, temperature-sensitive mutant strains. The replisome-binding mutant (DAIA) and putative DNA-binding mutant (Q20A) can suppress (separate or together) the dominant SL observed in the cohesin core mutant strains, but not the loader mutant strain. (B) Inducible expression of the helicase-deficient *CHL1* mutant, Chl1^{K48R}, does not cause dominant SL in another cohesin-related mutant, *rad61Δ. CHL1* panels are the same as Figure 3.3 as they are derived from the same experiment.

3.3.4 Expression of Chl1^{K48R} mutant protein causes increased genome instability, but not sister-chromatid cohesion defects

To further understand the dominant synthetic lethal effect of Chl1^{K48R} protein expression, we utilized assays for genome stability and sister-chromatid cohesion. A previous study using the Chromosome Transmission Fidelity (CTF) assay revealed a dominant effect of Chl1^{K48R} expression on chromosome stability (Holloway, 2000). The CTF assay monitors inheritance of an artificial chromosome fragment, and whole chromosome loss is the predominant mechanism observed (Yuen et al., 2007).

To confirm the dominant genome instability phenotype caused by expression of the Chl1^{K48R} mutant protein, we used the A-Like-Faker (ALF) assay, which measures loss of an endogenous genomic locus (the mating type locus *MAT* on chromosome III) through identification of spurious mating events (Novoa et al., 2018). Loss of the *MATα* locus leads to the default mating type in yeast, which is the a-type differentiation state. Thus, haploid MATα cells that lose the *MAT* locus will mate as a-type cells and are called "a-like fakers" (ALFs). These *MATnull* cells lead to growth of diploid progeny on minimal media when mated to a *MATα his1* tester strain **(Figure 3.7A)**. Mechanisms causing an ALF phenotype include whole chromosome loss similar to the CTF assay, but also *MAT* allele disruption by chromosomal rearrangement, and gene conversion from the silent mating type locus *HMRa* (Yuen et al., 2007). Using the ALF assay, galactose-inducible expression of the Chl1^{K48R} mutant protein significantly

increased genome instability compared to expression of wild-type Chl1 protein **(Figure 3.7B)**, confirming that the increase in genome instability is a dominant effect and not due to increased expression levels.

Chl1/DDX11 plays an important role in both DNA replication and sister-chromatid cohesion in yeast and mammalian cells (Bharti et al., 2014; Pisani et al., 2018). Interestingly, in both yeast and mammalian cells, separation of function mutants have recently been described that suggest that binding to the replisome, and not the helicase function, is crucial for the cohesion function of Chl1/DDX11, whereas the helicase activity is more important for the replicative role (Cortone et al., 2018; Samora et al., 2016). To assess whether dominant expression of $Chl1^{K48R}$ mutant protein impairs cohesion, we integrated the galactose-inducible *CHL1* ORFs at the *URA3* locus (in the presence of endogenous *CHL1*) in a cohesion assay strain (Guacci & Koshland, 2012). Cohesion was scored at the *LYS4* locus, located 470 kb from *CEN4*, using a LacO/LacI system in which a LacO array is integrated at the *LYS4* locus and visualized via binding of a LacI-GFP fusion protein (Straight et al., 1996) **(Figure 3.7C)**. Cells are synchronized by arresting in G1 (using α-factor) and then synchronously released in the presence of nocodazole to rearrest at the G2/M transition (Michaelis et al., 1997). Successful establishment and maintenance of cohesion leads to the presence of a single GFP spot in cells, whereas a failure to establish or maintain cohesion is visible as premature separation between the two sister-chromatid labelled regions that leads to the presence of two GFP foci (spots) in cells **(Figure 3.7D)**.

Parental cells (YPH2655) containing wild-type *CHL1* at the endogenous location were found to have tightly paired sister chromatids such that few (2.8%) sister-chromatids were dissociated. In contrast, *chl1Δ* mutant cells contained a significant increase in the number of

separated sisters (22.5%), consistent with previous studies (Mayer et al., 2004; Samora et al., 2016; Skibbens, 2004). Galactose-inducible expression of wild-type *CHL1* integrated at the *URA3* locus (in the presence of Chl1 protein expressed from the endogenous location) caused a slight increase of separated sister chromatids (about 3-fold over the parental strain). Surprisingly, expression of $Chl1^{K48R}$ mutant protein expression demonstrated a low level of prematurely dissociated sister chromatids (6.6%), similar to the parental strain and the one expressing wild-type Chl1 protein. Expression of the other *CHL1* mutated constructs containing either the Ctf4-binding DAIA mutation or the DNA-binding Q20A mutation alone or in various combinations with the K48R mutation also demonstrated low levels of prematurely dissociated chromatids **(Figure 3.7E)**. This result indicates that despite the fact that the DAIA mutation causes premature separation in the absence of wild-type Chl1 (Samora et al., 2016), in our system the endogenous wild-type is able to bind the replisome and is sufficient to prevent premature dissociation, even in the presence of the dominant catalytically-inactive K48R mutation. This suggests that the dominant effect of the $Chl1^{K48R}$ mutant form is not derived from increased premature sister-chromatid cohesion, but may be derived from its role in replication or from an ability of the bound but inactive protein to block a different function essential for viability in the absence of the synthetic lethal interacting proteins.

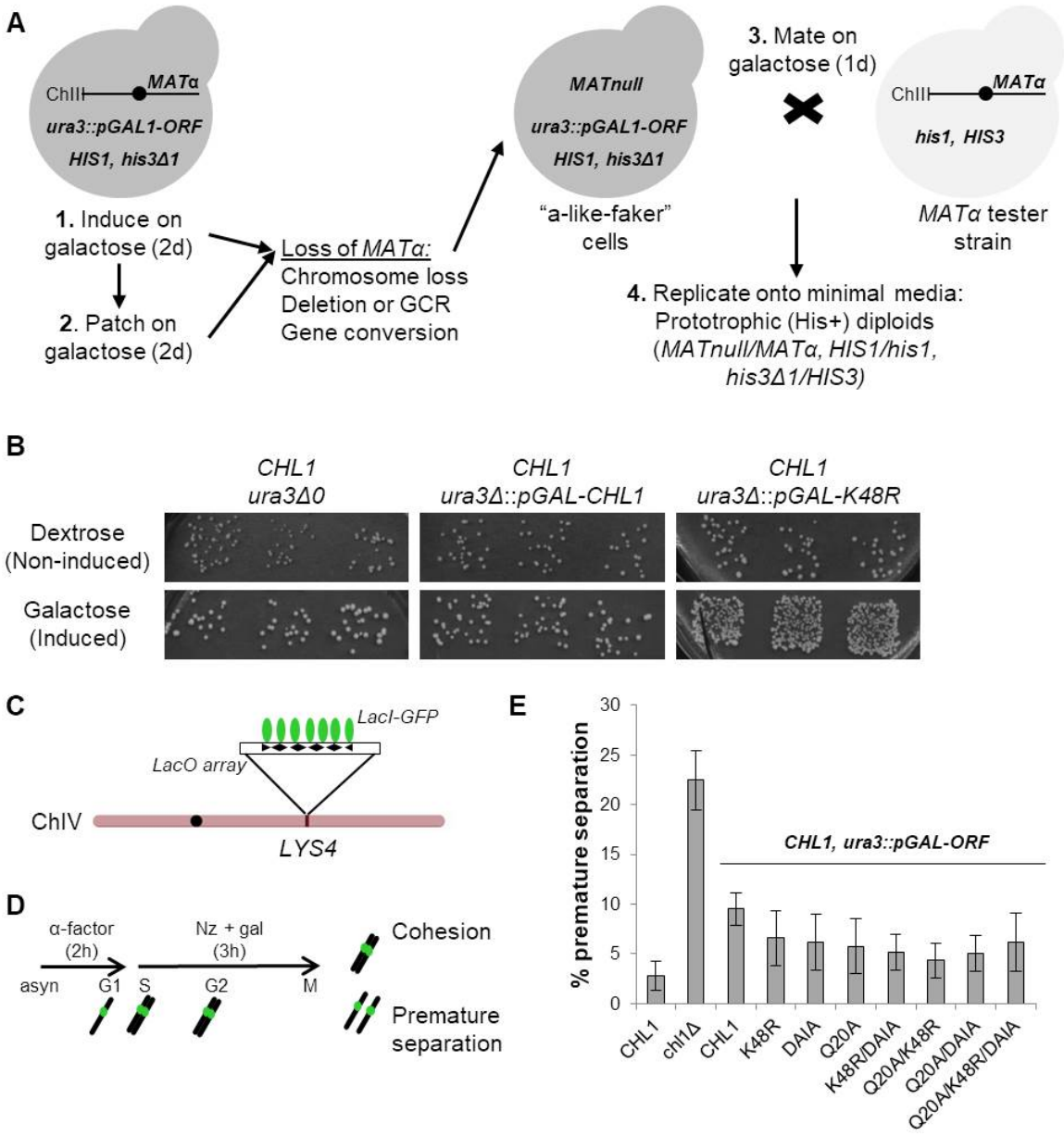

Figure 3.7 - Dominant expression of Chl1^{K48R} causes increased genome instability, but not sister-chromatid cohesion defects.
(A) Schematic of the a-like-faker (ALF) assay. *MAT*α hetero-allelic haploids containing galactose-inducible *CHL1* or *CHL1^{K48R}* integrated at the *ura3* locus were patched twice on galactose to induce expression and then mated to a *MAT*α tester strain, and growth of diploid progeny was assessed on selective media. Loss, deletion, or inactivation of the *MAT*α locus allows *MAT*α cells to mate as a-type cells. **(B)** Expression of dominant-negative Chl1^{K48R} causes elevated frequency of ALF cells. **(C-E)** Measuring cohesion loss at a *CEN*-distal *LYS4* locus (ch. IV). **(C)** Schematic of the tagged *LYS4* locus containing the LacO repeats and the binding of the LacI-GFP. **(D)** Assay used to assess cohesion. Cells were arrested in G1 using α-factor and then released and rearrested in G2/M using nocodazole. Cells were then fixed and imaged and the percentage of cells with two GFP dots (premature separation) was counted. **(E)** Galactose-inducible *CHL1* constructs integrated at the *ura3* locus were assessed for premature sister chromatid cohesion. Expression of dominant chl1^{K48R} mutant does not cause premature sister-chromatid cohesion.

3.4 Discussion

Inducing DNA damage in rapidly replicating cancer cells has been a mainstay of cancer therapy for decades, as emphasized by the fact that two of the main therapies existing today (chemotherapy and radiotherapy) work by causing direct or indirect DNA damage (Reuvers et al., 2020). However, these are blunt tools that also target healthy cells, and the therapeutic window is derived from the fact that many tumours are more sensitive to these agents due to rapid replication and/or defects in DNA damage response. Synthetic lethality holds the promise of a much more targeted approach, although to date most synthetic lethal screens have been conducted with null mutations in yeast and mammalian cells (O'Neil et al., 2017). Unlike the absence of protein in a null mutant, small-molecule inhibition can trap the target protein on the DNA or sequester other proteins through protein-protein interactions, and create a cytotoxic lesion that will require processing or trigger a checkpoint response, even without full inhibition of activity. In this way, the phenotypic consequences of proteins inhibited by small molecules can differ substantially from null mutations by virtue of the fact that the protein is present and trapped and may be more toxic than simple loss of activity (Pommier et al., 2016).

In this chapter, we expressed a catalytically inactive (but DNA-binding) form of yeast Chl1 to model the expected effect of a small molecule inhibitor that inhibits activity but does not abrogate the DNA-binding. This approach utilizes the power of missense mutations and yeast genetics to screen for dominant synthetic lethal interactions in the presence of the endogenous protein, modeling both incomplete inhibition and potential trapping. Expression of this mutant had little effect in wild-type cells, but caused severe growth defects in strains carrying mutations in spindle-associated, Ctf18-RFC and cohesin genes. **Table 3.1** contains a summary of the dominant synthetic lethal interactions identified in this study, as well as the effect of replisome

and DNA-binding mutations on the dominant synthetic lethality in the various genetic backgrounds.

Table 3.1 – Summary of Chl1^{K48R} dominant SL interactions identified in this study

	Yeast mutant strains sensitive to chl1^{K48R}*	**Dominant SL suppressed by DAIA (replisome binding mutation)?**	**Dominant SL suppressed by *Q20A* (DNA binding mutation)?**
Spindle-associated	*bim1*Δ	Yes	Yes
	*bub1*Δ	Yes	Yes
Ctf18-RFC complex	*dcc1*Δ	No	No
	*ctf8*Δ	No	No
	*ctf18*Δ	No	No
Cohesin core	*smc1-259***	Yes	Yes
	*scc1-73***	Yes	Yes
Cohesin loader	*scc2-4****	No	No

** Strains contain endogenous CHL1*

Both null synthetic lethal and dominant synthetic lethal interactions identify candidate drug targets and genetic backgrounds that can potentially be selectively targeted by inhibitors. In the case of both *rad27Δ* (the yeast homolog of human FEN1) and *chl1Δ*, knock-out-based synthetic lethal screens identify a much larger and broader genetic interaction network than the dominant synthetic lethal network identified in this study (**Figure 3.8** and Hamza et al. 2021), demonstrating that genetic interaction networks generated with null mutations differ from those of dominant inhibited proteins. While in this study the dominant synthetic lethal screens did not identify additional interactions compared to the null screens (for the list of mutants screened in this study), they identified a smaller and more specialized subset of interactions. Thus, dominant synthetic lethal screens may provide a way to prioritize potentially more clinically relevant interactions that occur when the protein is present but potentially trapped and in the presence of residual wild-type activity.

Yeast systematic name	Yeast standard name
YCL016C	DCC1
YCL061C	MRC1
YDL003W *	SCC1 *
YDR180W *	SCC2 *
YER016W	BIM1
YFL008W *	SMC1 *
YGL086W	MAD1
YGL240W	DOC1
YGR184C	UBR1
YGR188C	BUB1
YHR191C	CTF8
YJL030W **	MAD2
YKL113C **	RAD27
YMR078C	CTF18
YNL068C	FKH2
YOR014W	RTS1
YOR026W	BUB3
YOR144C	ELG1

** Chl1^{K48R} dominant SL with cohesin temperature-sensitive mutants were identified by direct testing.*
*** Putative dominant SL with Chl1^{K48R} that met the cutoff of (experimental-control <-0.2) but were not validated.*

Figure 3.8 - Comparing c*hl1*Δ synthetic lethal interactions to Chl1^{K48R} dominant synthetic lethal interactions.
Genetic interaction data was obtained from TheCellMap.org (PubMed PMID: 27708008). Mutants that met a genetic interaction cutoff of <-0.2 with the *chl1*Δ deletion mutation were extracted from TheCellMap.org and filtered for genes in the list of 332 mutants screened in this study (and three cohesin temperature-sensitive mutants directly tested). Mutants that were identified by the same cutoff and validated (in this study) to have dominant synthetic lethal interactions with helicase-deficient Chl1^{K48R} are highlighted.

The Chl1^{K48R} dominant synthetic lethal screen also identified a very different genetic dependency pattern compared to human FEN1^{D181A}. In the case of human FEN1^{D181A}, while the *rad27Δ* screen identified many interactions, the dominant screen only identified the HR pathway (Hamza et al., 2021), which is consistent with the formation of a toxic DNA-protein lesion. In contrast, yeast Chl1^{K48R} mutant protein did not have a dominant synthetic lethal effect in HR mutants, even though some of the effect was dependent on binding. Chl1 is a hub of replication,

repair and sister chromatid cohesion and has many genetic and physical interactions (Bharti et al., 2014; Mayer et al., 2004; Pisani et al., 2018; Rudra & Skibbens, 2013; Skibbens, 2004). The complex pattern of dominant synthetic lethal interactions observed in the screen reflects this complexity, as do the suppressive effects of the replisome and DNA binding mutations. The mutations affecting the DNA- and Ctf4-binding domains suppressed the dominant synthetic lethality with the spindle-associated mutations but not the Ctf18-RFC mutations **(Figure 3.3)**, and suppressed the dominant synthetic lethality with the core cohesin mutations but not the cohesin loader mutations **(Figure 3.6)**. This suggests that at least some of the dominant synthetic lethal interactions are not dependent on DNA binding. It is possible that the dominant synthetic lethal interaction with the Ctf18-RFC and the cohesin loader is due to direct physical interactions between Chl1 and these proteins. This is supported by the fact that human DDX11 interacts physically with the Ctf18-RFC (Farina et al., 2008) and yeast Chl1 regulates the deposition of the Scc2 loader on DNA during S-phase (Rudra & Skibbens, 2013).

It has been proposed that catalytically inactive helicases can bind DNA or other proteins and block access to replication and other repair factors (Wu & Brosh, 2010). Some previously identified helicase inhibitors are dependent on the presence of the helicase target. For example, HeLa cells in which the Werner syndrome (WRN) helicase was depleted using siRNA were resistant to the anti-proliferative effect of a WRN inhibitor, suggesting that the inhibited form is more toxic than a simple loss of WRN activity (Aggarwal et al., 2011). This suggests that inhibition of helicase function by small molecules may cause interference with a genome maintenance pathway which is distinct from the effect imposed by the absence of the helicase altogether. Backup mechanisms may come into play upon removal of a specific helicase, whereas an inhibitor bound to its target helicase will cause a unique defect, similar to the protein-

trapping mechanism observed with PARP and topoisomerase inhibitors. The catalytically inactive form of Chl1 could affect replication through binding to the Ctf18-RFC or cohesin loaders, without binding to the DNA or replisome, providing one possible explanation for the difference in suppression of the dominant synthetic lethal effect in the various mutants.

This chapter demonstrates the ability to generate dominant genetic interaction networks using missense mutations instead of gene knock-outs. These dominant synthetic lethal interactions can identify more robust therapeutic targets, suggest mechanisms underlying the synthetic lethal interactions and direct small molecule screening efforts to identify drugs that phenocopy the dominant synthetic lethal effect. This approach can increase the chance that synthetic lethal targets translate into clinically relevant, effective therapies.

Chapter 4: Developing a high-throughput, fluorescent *in vitro* assay for DDX11 activity to facilitate screening for inhibitors

4.1 Introduction

In recent years, there has been an increased interest in developing helicase inhibitors as cancer therapies, in light of the prominent and ubiquitous role these proteins play in maintaining the genome (Datta & Brosh, 2018). In order to further the development of DDX11 as a synthetic lethal anti-cancer therapeutic, there is a need to identify small molecules capable of inhibiting and/or modifying its activity. Identification of an inhibitor can also serve as a research tool to further study the role of DDX11 in human cells through inhibition of its activity, rather than removal of the protein (via knock-out or knock-down). Like other helicases, DDX11 catalyzes the separation of two complementary strands of a duplex nucleic acid in an enzymatic reaction dependent on energy derived from nucleoside 5′-triphosphate (NTP) hydrolysis (Hirota & Lahti, 2000). Therefore, potential inhibitors could target the DNA-binding, ATP-binding or hydrolysis, or DNA unwinding of DDX11. In addition, as discussed in the previous chapter, an inhibitor may trap DDX11 – thus converting it into a poisonous protein complex whose toxicity results from more than simple inhibition of activity.

To facilitate the discovery and development of DDX11 inhibitors, a robust and sensitive method for monitoring the catalytic activity is needed. Multiple methods exist for measuring helicase activity – most are based on assaying either the unwinding activity or the ATPase activity of the enzyme (reviewed in Mojumdar and Deka 2019). The main difference between the methods is in the read-out, as they all require a suitable substrate, purified protein, appropriate salt buffer, and source of energy. The assays can be divided into end-point assays or continuous assays. In end-point assays, the reaction can only be detected following a series of steps and are

therefore less suitable for continuous measurement (although some may be suitable for high-throughput studies), whereas continuous assays provide a real-time measurement of activity, usually using fluorescent or colorimetric methods, and are more amenable to high-throughput measurements.

The first human DNA helicase inhibitor discovered was NSC19630, an inhibitor that specifically inhibited the Werner-syndrome helicase-nuclease, WRN. NSC19630 was identified from a National Cancer Institute (NCI) library of compounds by a gel-based, radioactive assay (Aggarwal et al., 2011). A subsequent study identified a structurally-related compound, NSC617145 (Aggarwal, Banerjee, Sommers, Iannascoli, et al., 2013), and both compounds were determined to be active in human cell cultures and have been used to study the role of WRN in response to DNA damage and replication stress (Aggarwal, Banerjee, Sommers, & Robert M Brosh, 2013). An additional helicase inhibitor that inhibits the related Bloom-syndrome helicase, BLM, was identified through a large-scale screen using a high-throughput fluorescent method (Nguyen et al., 2013) and more recently, the WRN helicase assay has been adapted to a high-throughput format using fluorescence and used to identify additional potential inhibitors (Sommers et al., 2019).

Several biochemical studies have been performed to date to characterize DDX11's enzymatic activity, nucleotide preference, and ability to unwind a variety of substrates, including duplex DNA, recombination intermediates, triplex DNA and G-quadraplexes (Capo-Chichi et al., 2013; Ding et al., 2015; Farina et al., 2008; Guo et al., 2015; Hirota & Lahti, 2000; Wu et al., 2012). Common to all these studies is the use of a low-throughput, radioactive, gel-based assay – a method not suitable for large-scale testing of potential inhibitors. In order to screen for an inhibitor, it is useful to develop an expedient, easily measured, high-throughput *in vitro* activity

assay. Therefore, the goal of this chapter is to develop such an assay for future inhibitor screening.

4.2 Materials and methods

4.2.1 Expression vectors

All plasmids and primers are listed in Appendix A .

Human *DDX11* in a gateway-compatible entry clone was obtained from hORFeome V8.1 (clone 56187). The open reading frame without the stop codon was PCR amplified using primers OPH8961 (including an extra N-terminal 6xHis-tag and a HindIII restriction site) and OPH8962 (containing a C-terminal 3xFLAG tag and a XhoI restriction site), and cloned into the HindIII and XhoI sites of pcDNA3.1(+) to obtain BLA223.

For the DDX11^{K50R} mutation, attB sites were added by PCR amplification to the 6xHis-DDX11-3xFLAG construct using primers OPH9269 and OPH9270 and the resulting PCR product was cloned by gateway cloning into the pDONR221 plasmid to obtain BLA313. Site directed mutagenesis was performed using QuikChange® Site-Directed Mutagenesis Kit (Agilent) with primers OPH8963 and OPH8964, and verified by Sanger sequencing to obtain BLA320. 6xHis-DDX11^{K50R}-3xFlag construct was amplified by PCR using primers OPH8961 and OPH8962 and cloned into the HindIII and XhoI sites of pcDNA3.1(+).

All constructs were sequenced to verify that no undesired mutations were introduced during PCR and cloning.

4.2.2 Expression and purification of DDX11 and DDX11^{K50R}

Expression and purification of human 6xHis-DDX11-3xFlag proteins (wild-type and K50R mutant) were based on a previously described protocol (Ding et al., 2015; Guo et al.,

2015). Briefly, six 10-cm plates (0.7-1x10^7 cells/plate) of HEK293T cells were transfected with plasmids expressing either wild-type or the K50R DDX11 mutant using Lipofectamine 2000 (Invitrogen) according to manufacturer's instructions. The next day, transfection reagent was washed off gently using PBS and replaced with fresh media. Three days after transfection, cells were harvested by trypsinization and centrifugation. Pelleted cells were washed with cold PBS and cold PBS with Protease Inhibitor Cocktail (Sigma Aldrich), resuspended in 6 ml of buffer A [10 mM Tris HCl (pH 7.4), 10 mM KCl, 1.5 mM MgCl2, 1 mM DTT, protease inhibitor cocktail], lysed for 30 min at 4°C with mild agitation and centrifuged at 43,500 g for 30 min at 4°C. Anti-FLAG M2 affinity gel resin (Sigma) (50µl resin suspension per ml of supernatant) was prepped according to manufacturer's instructions and incubated with supernatant for 2 h at 4°C with mild agitation. The resin was then washed twice with at least 5 volumes (0.5 ml/tube) buffer B [20 mM Tris HCl (pH 7.4), 500 mM NaCl, 10% glycerol, 0.5% Nonidet P-40, 1.5 mM MgCl2, 0.2 mM EDTA]. DDX11 was eluted with 4 µg/mL of 3 × FLAG peptide (Sigma) in buffer C [25 mM Tris HCl (pH 7.4), 100 mM NaCl, 10% glycerol, 0.1% Tween 20, 5 mM Tris (2-carboxyethyl) phosphine hydrochloride;TCEP] for 1 h at 4°C. To remove the 3xFLAG peptide, the eluent was dialyzed against buffer C for 2 h at 4°C using a dialysis tube with a 50-kDa molecular weight cutoff (Tube-O-Dialyzer^{TM}). Aliquots were flash frozen in liquid nitrogen and stored at -80°C. Protein concentration was determined by the Bradford assay using BSA as a standard.

4.2.3 DNA substrates

HPLC-purified labelled oligonucleotides based on the forked duplex substrate described previously for measuring DDX11 activity (Wu et al., 2012) were purchased from Integrated DNA Technologies and are listed in Appendix A . Oligonucleotides were resuspended to stock

concentration of 100µM in nuclease-free water. One µl of each oligo was added to a 50 µl annealing reaction (final conc. 2µM) in annealing buffer (50 mM Tris-HCl pH8.0, 50 mM NaCl, 1 mM Dithiothreitol (DTT)). The oligos were annealed by heating to 90°C for 5 min, cooling to 70°C for 5 min and then gradually cooling to room temperature (5°C\min).

Desalted unlabelled 44-mer and 19-mer capture oligonucleotides were purchased from Thermo Fisher and resuspended to stock concentration of 100µM in nuclease-free water.

4.2.4 Helicase assay

Helicase assays were conducted in 96-well clear-bottom black plates covered with a black seal. Wild-type or K50R mutant DDX11 protein was incubated at 2x the indicated concentration in 25µl reaction buffer containing 25mM HEPES-NaOH pH7.5, 25 mM potassium acetate (KOAc), 1mM magnesium acetate (MgOAc), 1mM DTT and 100 µg/ml bovine serum albumin (BSA). Helicase reaction was initiated by addition of 25µl reaction buffer containing 40nM substrate concentration, 400nM unlabelled capture strand (10x) + 2mM ATP (final concentration 20nM duplex substrate, 200nM capture strand and 1 mM ATP). The plate was transferred into a TECAN Infinite® 200 plate reader where the reaction progress was measured in fluorescence mode at multiple timepoints at 37°C using fluorescence optics (excitation filter 490 nm, emission filter 525 nm).

4.3 Results

4.3.1 Design of the DDX11 fluorescent helicase assay

To further develop DDX11 inhibition as a cancer therapy target, we aimed to develop a method for measuring activity in a high-throughput manner that would be suitable for a small-molecule screen. Helicase assays require a DNA substrate that is relevant for measuring helicase

activity, purified helicase protein devoid of contaminating nuclease activity, reaction salts optimal for helicase activity, a source of energy (typically ATP) and a technique to read out the activity. Fluorescence is a sensitive technique that has the clear advantage of monitoring a reaction process in real time, at low concentration, and at high throughput. The simplest structure unwound by DDX11 is a forked duplex (Wu et al., 2012) and we adapted this substrate to utilize a 3' fluorophore-labelled (6-FAM) strand partially hybridized to a 5' quencher (Iowa Dark® FQ), in a manner similar to previous work in our lab on FEN1 activity (van Pel, Barrett, et al., 2013). The main difference between this assay and the FEN1 assay, apart from the substrate structure, is the placement of the fluorophore and the quencher. In the FEN1 assay, the fluorophore and quencher are on the 5' and 3' ends of a single oligo that is hybridized to two unlabeled oligos to form a flap containing substrate. When FEN1 cleaves the DNA flap the fluorophore is released and can diffuse away from the quencher. In the helicase assay, the fluorophore and quencher are two separate complementary strands that are dissociated by helicase activity.

As in previous studies utilizing radioactive labelling, in our fluorescence-based assay the helicase substrate contains two partially complementary oligonucleotides that anneal to create a forked duplex. The strands are labelled such that one strand contains a 3' 6-FAM fluorophore and the other contains a 5' Iowa Dark® FQ quencher molecule. Both the fluorophore and the quencher are located on the annealed part of the forked duplex so that the quencher molecule is located in close proximity to the 6-FAM fluorophore and quenches the fluorescence. After unwinding, the strands are separated and the fluorophore can diffuse away from the quencher resulting in a measurable increase in fluorescence. We also included an excess of unlabeled capture oligonucleotide to prevent duplex reannealing of the fluorophore and quencher strands.

In the presence of an inactive form of DDX11 or an inhibitor, the unwinding activity will be inhibited resulting in a low level of fluorescence **(Figure 4.1)**.

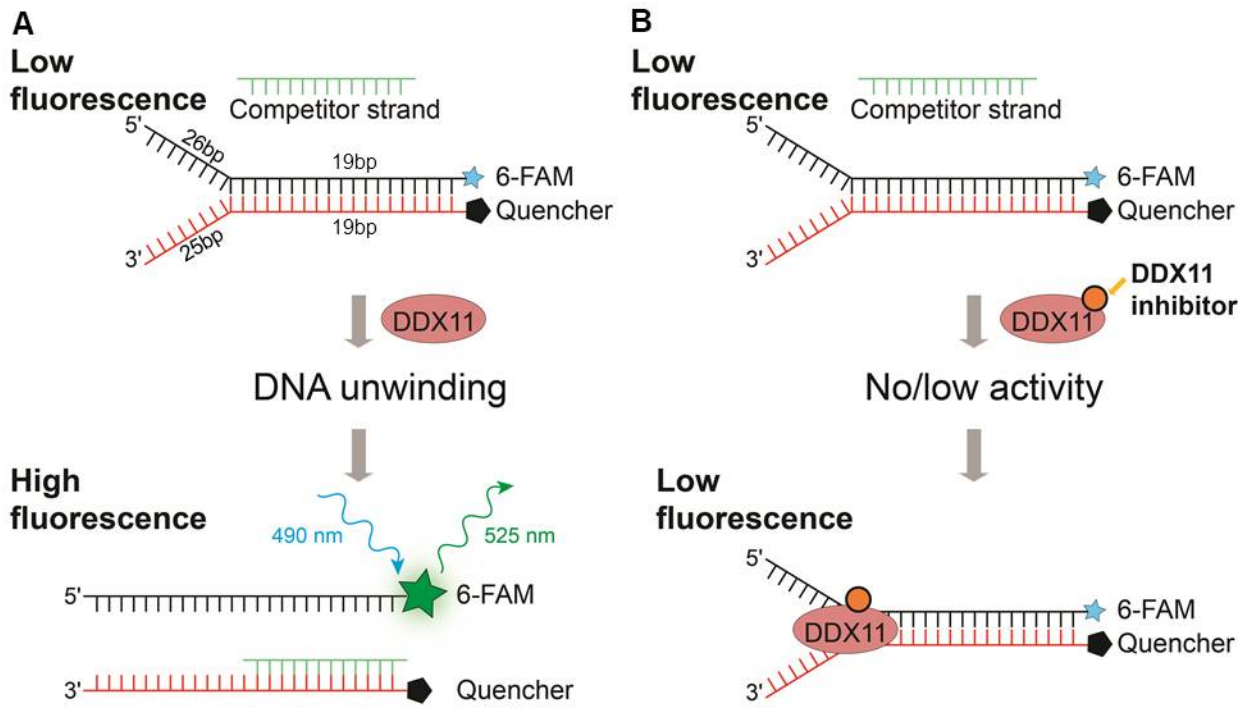

Figure 4.1 - Schematic of the DDX11 fluorescence-based biochemical assay.
(A) A 45-mer reporter strand with a fluorophore (6-FAM) at the 3' end is annealed to a complementary 44-mer strand with an Iowa Dark® FQ quencher. DDX11 unwinds the two strands and the quencher strand anneals to a capture strand, preventing re-annealing with the strand containing the fluorophore. The unwound partial duplex results in increased fluorescence. **(B)** In the presence of an inactive form of DDX11, a DDX11 inhibitor or lack of ATP, the partial duplex is not unwound and fluorescence remains low.

4.3.2 Testing the fluorophore-labeled forked duplex substrate

The reaction conditions (pH, cation, nucleoside triphosphate, etc.) for DDX11 activity on a forked duplex substrate have been previously characterized (Farina et al., 2008; Hirota & Lahti, 2000; Wu et al., 2012). The most significant difference between our devised assay and previous studies is the substrate labeling and detection. Therefore, we first wanted to test these in the absence of DDX11 protein. Fluorescence measurement (Relative Fluorescent Units RFU) was

linear with the concentration of the 6-FAM labeled single-strand DNA molecule and upon annealing at an equimolar ratio to the Iowa Dark® FQ-labelled strand, the fluorescence was quenched to a near-zero level, as expected **(Figure 4.2A)**.

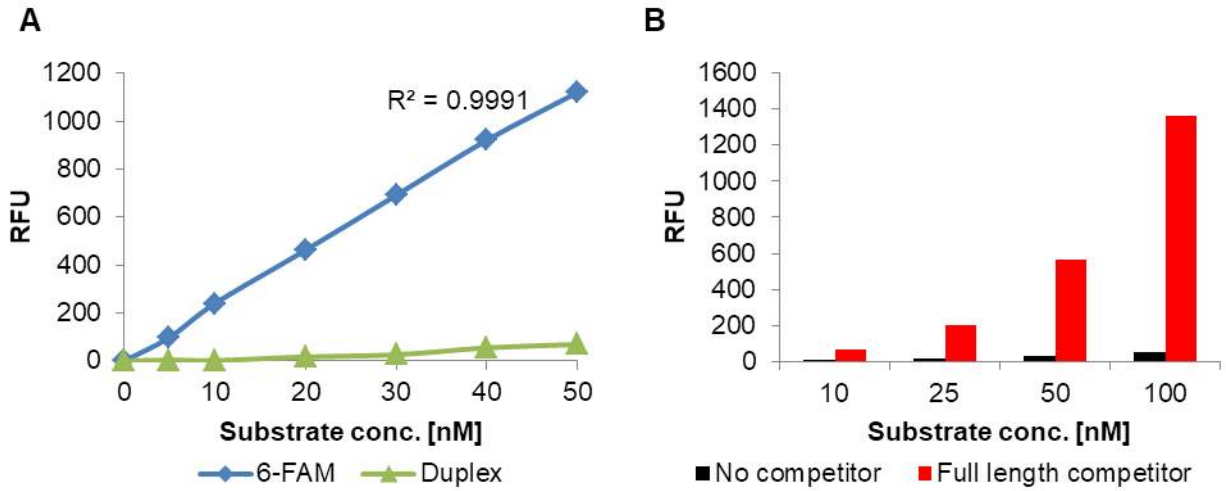

Figure 4.2 - Testing fluorescent substrate for a high-throughput DDX11 helicase assay.
(A) Concentration dependent fluorescence of 6-FAM labelled reporter strand. Increasing concentrations of 6-FAM labelled ssDNA were incubated in a 96-well plate and fluorescence was measured at excitation and emission wavelengths of 490 and 525 nm respectively. Fluorescent measurements are linear with labelled singe-strand DNA concentration. Testing quenching of fluorescence by Iowa Dark® FQ quencher. 6-FAM reporter strand was annealed in an equimolar reaction to the partially complementary Iowa Dark® FQ quencher strand. **(B)** Fluorescence of increasing concentrations of the duplex DNA with and without a 10x concentration of an unlabeled capture strand fully complementary to the Iowa Dark® FQ labelled strand.

We then tested the addition of the unlabeled capture strand to the reaction. Addition of a 10x concentration of a 44-mer capture strand that is fully complementary to the quencher strand resulted in an increase in fluorescence in the absence of DDX11 protein **(Figure 4.2B)**, suggesting that the partial duplex may be "breathing" (dissociating and reannealing) and/or that the fully complementary capture strand can bind the free flap and outcompete the partially complementary 6-FAM labeled strand to cause dissociation of the quencher strand from the 6-FAM labeled strand. This result may be due to the fact that the fully annealed capture strand-quencher strand duplex will be more stable than the partially annealed 6-FAM-quencher duplex,

as the annealed region is longer; the predicted melting temperature (T_m) of the partially annealed duplex (19 bp duplex) is approximately 53°C and the Tm of the fully complimentary duplex (44 bp) is approximately 75°C.

To circumvent this issue, we tested two shorter capture strands that are complementary only to the 19 bp annealed duplex portion of the 6-FAM or Iowa Dark® FQ-labelled strand **(Figure 4.3A)**. Neither of the shorter capture strands demonstrated the increase in fluorescence observed with the longer, fully complementary capture strand **(Figure 4.3B)**. To test the effect of the two 19-mer capture strands on the unwound duplex, we incubated a higher concentration (200nM) of the duplex alone or in the presence of a 10x concentration of a capture strand complimentary to either the 6-FAM or the Iowa Dark® FQ at 95°C to simulate the unwinding reaction and then placed on ice and transferred to a plate to measure fluorescence. The 19-mer that binds to the 6-FAM labeled strand reduced the fluorescence significantly compared to the 19-mer that binds to the Iowa Dark® FQ labeled strand **(Figure 4.3C)**, possibly due to the 5' guanine that anneals near the 6-FAM fluorophore (Crockett & Wittwer, 2001). The duplex alone also demonstrated reduced fluorescence after boiling and placing on ice, suggesting that the addition of the 19-mer capture strand may prevent reannealing of the unwound substrate and improve the performance of the assay. A previous study using a fluorescent duplex substrate to study activity of RNA helicases also concluded that adding an excess of a DNA capture strand was found to prevent reannealing and resulted in the maximum rate of unwinding (Özeş et al., 2011).

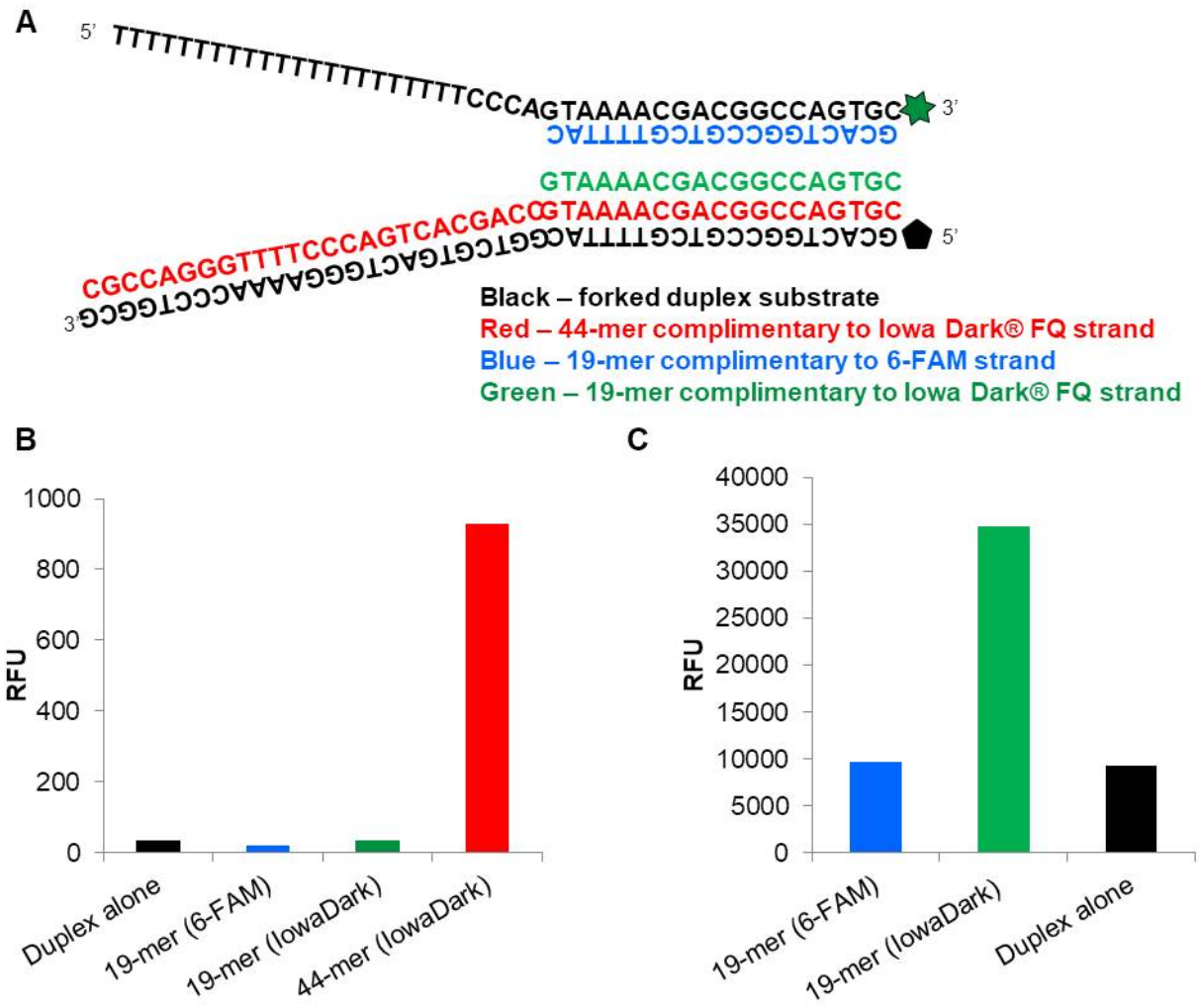

Figure 4.3 - Testing alternative unlabeled capture strands.
(A) Schematic of the duplex substrate and the unlabeled trapping strands tested (green star = 6-FAM, black pentagon = Iowa Dark® FQ). **(B)** 20nM quenched duplex substrate was incubated alone or in the presence of 10x short capture strands complimentary to the 19bp duplex portion of the 6-FAM or Iowa Dark® FQ labeled strand or the longer fully complementary capture strand. **(C)** 200nM quenched duplex substrate was boiled and placed on ice alone or in the presence of 10x short capture strands complimentary to the 19bp duplex portion of the 6-FAM or Iowa Dark® FQ labeled strand.

4.3.3 Testing DDX11 helicase activity

To test the activity of DDX11 in the fluorescence assay, we purified recombinant wild-type DDX11 protein (tagged with a 3xFLAG epitope, see *Materials and Methods*) expressed in human HEK293T cells according to a previously described protocol (Ding et al., 2015). We also

purified an inactive form of DDX11, the K50R mutant, in which the conserved lysine residue in Walker box A was replaced with an arginine. The recombinant proteins were purified from mammalian cells using a hypotonic lysis buffer followed by incubation with anti-FLAG resin and then eluted from the resin using 3xFLAG peptide and dialysed against the final buffer to remove the peptide **(Figure 4.4A)**. The purified proteins had a molecular mass of ~120 kDa, a size expected for the His-DDX11-FLAG fusion protein **(Figure 4.4B)**.

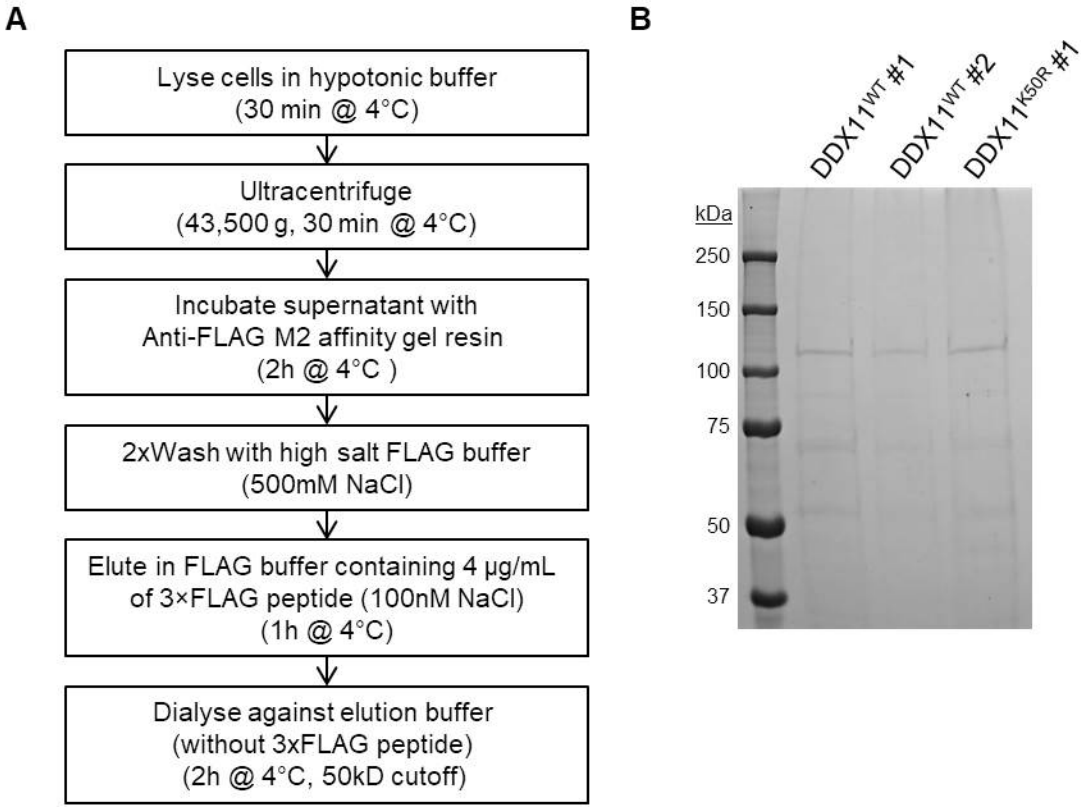

Figure 4.4 - Purification of recombinant DDX11 proteins.
(A) Main purification steps of recombinant DDX11 proteins. **(B)** The purity of the $DDX11^{WT}$ (two purification runs) and $DDX11^{K50R}$ proteins was evaluated by their detected migration after SDS-PAGE on Coomassie-stained gels according to their predicted sizes. Expected DDX11 molecular weight: ~120 kDa.

We examined DDX11 activity on the forked duplex substrate as a function of DDX11 concentration. Increasing concentrations of DDX11 were incubated in reaction buffer and the reaction was initiated by the addition of substrate and ATP. Fluorescence was measured upon reaction initiation and at various time points after initiation. As shown in **Figure 4.5A**, unwinding of the forked duplex substrate as measured at various time points ranging from 10 to 20 minutes post-reaction initiation was correlated with the DDX11 concentration. However, DDX11 failed to unwind the substrate in the absence of ATP **(Figure 4.5A)**, indicating that the unwinding is dependent on the hydrolysis of ATP and supporting the observation that the increase in fluorescence observed in the presence of ATP is due to intrinsic DDX11 activity.

In preparation for a large-scale screen, we also tested the freeze-thaw stability of the purified DDX11 protein. The activity of increasing concentrations of freshly thawed DDX11 protein was compared to that of DDX11 that had previously been thawed and refrozen. The activity curve of the previously thawed protein was indistinguishable from the freshly thawed protein **(Figure 4.5B)**.

A mutant form of DDX11 (K50R), which has significantly reduced ATPase activity (Farina et al., 2008) has been used in previous studies to demonstrate that the unwinding activity of the radioactively-labeled substrate is intrinsic to DDX11, and not due to a contaminant in the helicase preparation (Wu et al., 2012). In this study, the K50R mutant was expressed and purified using the same purification process as the wild-type protein and the unwinding activity was tested using the fluorescently labeled substrate **(Figure 4.5C)**. As expected, the K50R mutant was unable to unwind this type of substrate under conditions in which wild-type DDX11 showed high activity, confirming that the activity observed with the wild-type protein is intrinsic to DDX11 and not an increase in fluorescence due to a contaminant in the protein preparation.

The lack of activity observed with this mutant also suggests that the assay will be able to detect inhibition of DDX11 by a small molecule inhibitor.

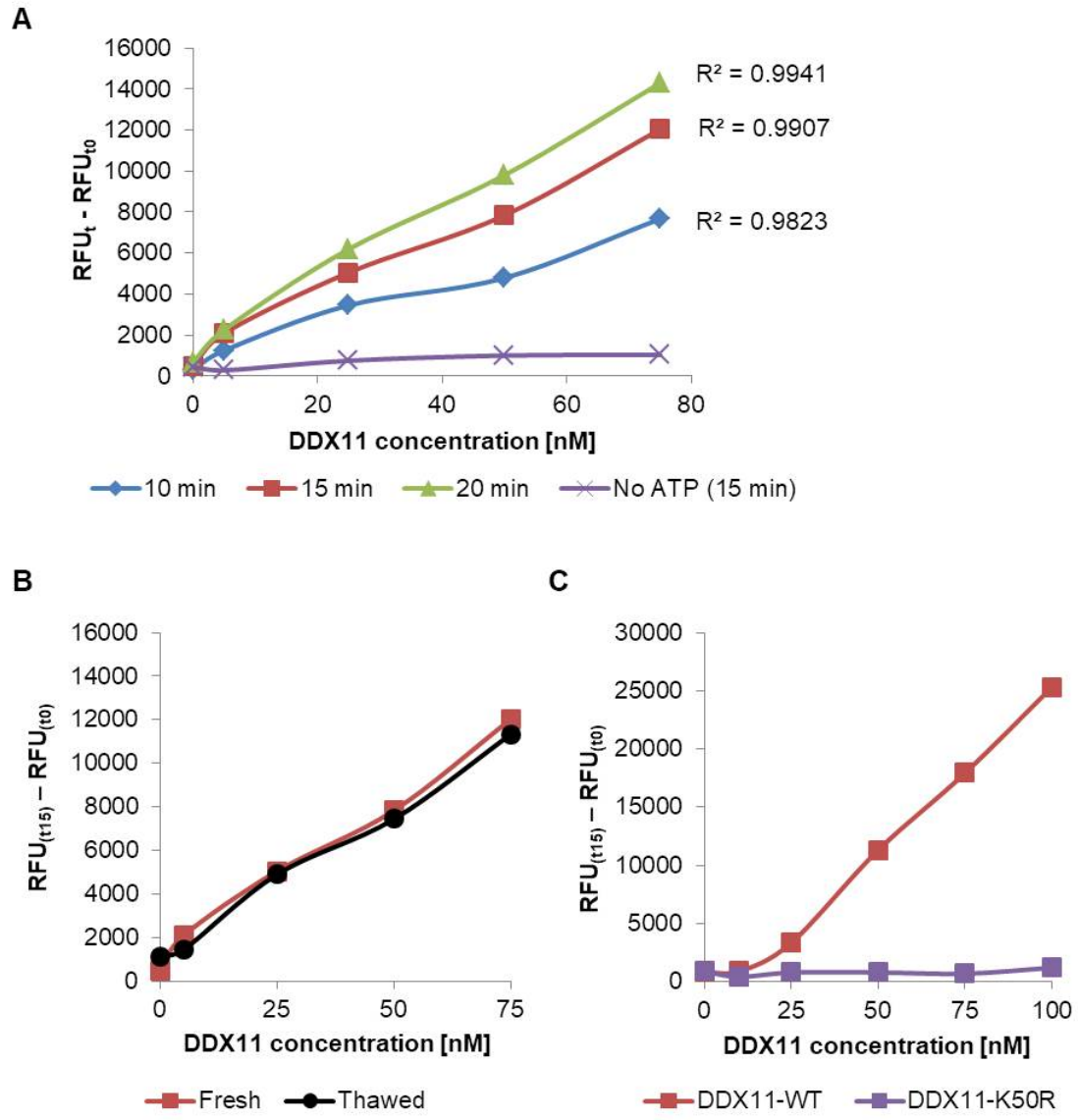

Figure 4.5 - Testing DDX11 activity in fluorescence-based assay.
Helicase reactions were carried out using conditions described in materials and methods. All reactions contain 20nM quenched substrate and 200nM capture strand, unless specified. **(A)** Increasing concentrations of purified recombinant DDX11 protein were incubated with duplex substrate in reaction buffer containing ATP. Fluorescence was measured at multiple timepoints and ΔRFU was plotted as a function of DDX11 concentration at each time point. ATP-dependence was tested by conducting the reaction in buffer with/without addition of ATP. **(B)** Freeze-thaw stability was assessed by comparing freshly thawed protein to protein from the same lot that had been previously thawed and refrozen at -80°C. **(C)** An ATPase-deficient form of DDX11, DDX11^{K50R}, was purified and tested using the same assay.
RFU=Relative Fluorescent Units.

4.4 Discussion

DNA helicases are ubiquitous enzymes found in all domains of life and involved in all aspects of nucleic acid metabolism. In light of their important roles in cellular DNA replication, transcription, DNA repair, and other genome stability processes, there is considerable interest in identifying small molecule inhibitors of helicases, both as research tools and as potential therapeutic drugs.

To date, DDX11 biochemical activity has been studied *in vitro* using a variety of radiometric, gel electrophoresis-based assays. While it is possible to use such assays to search for small molecule inhibitors, as demonstrated by identification of WRN helicase inhibitors (Aggarwal et al., 2011), these assays are low-throughput and generate radioactive waste and are therefore less suitable for high-throughput screening. The development of easy, fast and robust biochemical assays to measure helicase activity, overcoming the limitations of the current methods, is important for the discovery of helicase inhibitors through high-throughput screens. In this chapter, we have adapted the radiometric assay to a fluorescence-based assay that is one more suitable for future inhibitor screening. The basic premise of the assay is the same as the existing radiometric one in which purified DDX11 protein unwinds a labeled forked-duplex substrate in the presence of ATP, however the substrate has been labeled with a fluorophore annealed in close proximity to a quencher molecule. Upon dissociation, the fluorophore can diffuse away from the quencher molecule and this can be detected as an increase in fluorescence. Our results demonstrate the suitability of the labeling and detection method and the correlation of activity with DDX11 protein concentration. In addition, consistent with previous radiometric studies, the measured activity is dependent on the presence of ATP and an inactive mutant shows no activity in the assay (Hirota & Lahti, 2000; Wu et al., 2012).

One important aspect in designing a screening assay is the choice of substrate. In this study, we selected a simple forked duplex substrate previously shown to be unwound by DDX11. However, DDX11 also unwinds additional DNA structures that may be relevant to its role in replication, maintaining genomic stability or linking replication and sister chromatid cohesion. These structures include three-stranded D-loops, bi-molecular anti-parallel G-quadruplex (G4) and DNA molecules containing triple-stranded (triplex) structures (Guo et al., 2015; Wu et al., 2012). The existing assay is most likely amenable to testing DDX11 activity on these structures with the appropriate positioning of fluorophore and quencher labeling, in a manner similar to a previous study utilizing fluorescence-based techniques to monitor the effect of G4 structures on the activity of the Pif1 helicase (Mendoza et al., 2015). It is important to consider how the selection of substrate may influence identification of inhibitors. For example, IC50 for BLM inhibitor ML216 was 3μM for a forked duplex substrate, but inhibition of branch-migration activity on a mobile D-loop substrate or a Holiday junction was significantly more modest, requiring a concentration of 50μM. This suggests that a small molecule may differentially affect helicase vs branch-migration activity of those helicase proteins that have multiple functions. Once an initial screen has been conducted, it will be useful to assay the effect of potential inhibitors on DDX11 activity on other, more complex substrates (using either existing radioactive assays or a fluorescence gel- or plate-based assay).

One existing limitation of the developed method is the quantity of purified DDX11 protein obtained from each purification batch. The current process results in approximately 130 μg of purified DDX11, which is sufficient to run the assay in about 500 wells at a reaction volume of 50 μl and a DDX11 concentration of 50 nM (or 1000 wells at a DDX11 concentration of 25 nM). The assay can potentially be scaled down to use lower volumes (for example by using

half-well plates) or by moving to a 1536-well format similar to a high-throughput screen for inhibitors of WRN helicase (Sommers et al., 2019), in which initial assay development was conducted in 96-well volume and then scaled down to 1536-well, low volume format with the appropriate instrumentation. At the current scale, multiple purification batches will be required to obtain enough protein for testing even a small library of inhibitors. As DDX11 belongs to a family of Fe-S binding proteins, there is a need to express the protein in a system that can support the incorporation of the Fe-S cofactor during protein expression. The majority of previous studies on DDX11 biochemical activity used protein purified from HEK293 cells using transient transfection and a purification process similar to the one used in this study. One previous study expressed and purified human DDX11 using a recombinant baculovirus transformed into High Five insect cells (Hirota & Lahti, 2000), however a subsequent study stated that DDX11 was purified from mammalian cells as initial attempts to purify from bacteria or insect cells were unsuccessful (Farina et al., 2008). The same group established a stable clone of HEK293 cells expressing DDX11 by transfection and selection for two weeks. They then propagated this clone in 4L media and purified DDX11 using a purification process similar to the one described in this chapter but using columns rather than beads. For future studies, a similar process could be used to increase the scale and therefore the yield of purified DDX11 from each purification batch.

High throughput screens have been conducted for two RecQ family helicases, WRN and BLM, which are also SF2 family helicases (Estep & Brosh, 2018), although not in the Fe-S family to which DDX11 belongs. In these screens, truncated forms of the helicase containing only the helicase domain in the case of the WRN helicase (Sommers et al., 2019) or only the helicase, RecQ C-terminal (RQC), and Helicase RNase D-like C-terminal (HRDC) domains in

the case of the BLM helicase (Nguyen et al., 2013) were used in order to scale up the purification to quantities required for large-scale screens. However, a similar strategy of identifying a truncated form maintaining helicase activity is unlikely to be successful for DDX11, as the helicase motifs are spread out across almost the entire length of the protein (essentially creating an almost full-length helicase domain), unlike the RecQ helicases where the helicase motifs are tightly located in the helicase domain and the full-length protein contains multiple additional domains **(Figure 4.6)**.

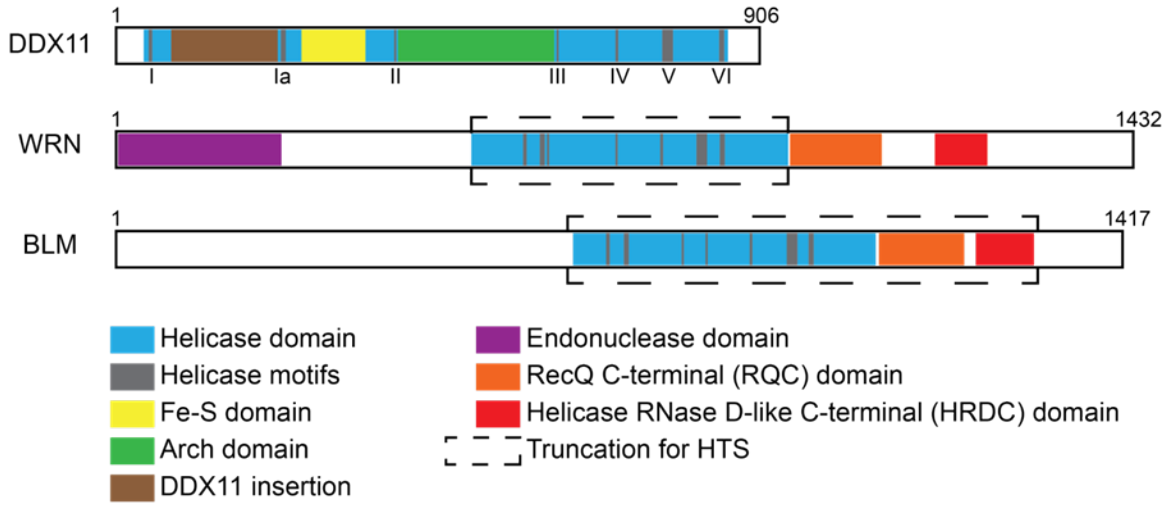

Figure 4.6 - Structure of human DDX11 (Fe-S), WRN and BLM (RecQ) helicases.
Shown is a sequence schematic of DDX11 and two RecQ helicases previously used in high throughout screens (HTS) for inhibitors using truncated versions. Important domains in each helicase are shown, and the truncated portion of WRN and BLM used in previous screens (containing the helicase domain) is depicted in the dashed squares.
RQC = RecQ C-terminal, HDRC = Helicase Rnase D-like C-terminal.

Another potential strategy to effectively reduce the number of compounds to be screened using this assay is to conduct an initial structure-based virtual (*in-silico*) screen, followed by biochemical testing of the promising candidates only. Such a screen has been conducted to identify inhibitors of the human RNA-helicase, DDX3, which is an important host factor for the replication of multiple viruses. In this study, the three-dimensional crystal structure of the RNA-

free open conformation of DDX3, together with homology modeling of the RNA-bound closed conformation based on a close homolog, led to a structural model of DDX3 bound to RNA. This structural model was subsequently used to screen *in-silico* for potential inhibitors that were then tested using a biochemical assay. As a result, an impressive hit rate of 40% (10 active compounds of 25 tested using a biochemical assay) was obtained (Fazi et al., 2015), suggesting that this is a viable strategy for reducing the scale of an *in vitro* biochemical screen. A similar strategy was used to identify inhibitors of the West Nile virus NS3 proteinase. In this study, a ~275,000 compound library was first subjected to a virtual screen, followed by *in-silico* optimization of the hits and eventually 50 compounds were tested using an *in vitro* cleavage assay (Shiryaev et al., 2011).

To enable structure-based-virtual-screening (SBVS), a 3D structure of the protein of interest is required. In the absence of such a structure, homology-based modeling can help predict the structure from the amino acid sequence and a known structure of a homologous protein. While the structure of DDX11 has not yet been determined, several known structures of related proteins have been used to build a homology-based model that may be used for SBVS. DDX11 shares sequence homology with the XPD/Rad3 family of proteins present in Archaea and Eukarya, all containing a Fe-S cluster. The structure of related proteins contains a four-domain organization, including two canonical RecA folds (Helicase Domain (HD) 1 and 2) which form the helicase catalytic core and two accessory domains (the Fe-S and Arch domains) which are unique to this family. When DDX11 sequence is compared to other XPD-family members, a long insertion of about 150 amino acids is found in the HD1 domain, between motifs I and Ia **(Figure 4.6)**. This insertion is less conserved than the rest of the protein and the amino acid composition suggests it is likely to be a partially unstructured region (Pisani et al., 2018).

An initial screen should be conducted at a drug concentration high enough to ensure potential hits are not missed but low enough to avoid detecting a large number of false positives (for example 50 μM as recommended in Banerjee et al. 2016). Once potential hits have been identified, there are several important counter screens that should be conducted. False positives identified in the screen may be due to compounds that quench fluorescence in the 525 nm range. Identification of such compounds can be achieved by incubating the drugs with the 6-FAM labelled ssDNA (or with a duplex substrate containing 6-FAM but no quencher) and detecting a reduction in fluorescence even in the absence of DDX11. Alternatively, a gel-based assay that allows direct visualization of the conversion of a forked DNA-duplex into its component single-stranded oligonucleotides via the helicase activity of DDX11 (or lack thereof in the presence of an inhibitor) can be used.

It is generally desirable for a small molecule to be specific in its mechanism of inhibition. Compounds that directly bind the DNA substrate are less likely to be specific as they may affect the catalytic function of other DNA helicases as well as other DNA metabolizing proteins such as polymerases and nucleases. It is therefore useful to test if a potential inhibitor compound directly binds DNA and a convenient assay for this purpose is an intercalator dye displacement assay. Intercalation of the duplex DNA by the dye enhances the fluorescence of the dye and subsequent displacement of the intercalator by a DNA binding compound results in a decrease in fluorescence directly related to the extent of binding. A preferred dye is Thiazole Orange (TO) as an increase in its fluorescence upon intercalation far exceeds that of other commonly used dyes (such as Ethidium Bromide) and it also displays less sequence-dependent DNA binding and minimal fluorescence in solution or when bound to ssDNA (Banerjee et al., 2016). Additional specificity can be determined by studying the effect of potential inhibitors on the activity of

related helicases such as FANCJ, as well as more distantly related DNA metabolizing enzymes. It is generally desirable that a small molecule compound demonstrate *in vitro* specificity for its intended target, but this may not always apply. For example, in the case of the BLM helicase inhibitor ML216, the drug also inhibited the closely related WRN helicase *in vitro.* However, ML216 acted specifically towards BLM *in vivo* as demonstrated in cell-based proliferation assays in WRN mutated and wild-type cells (Nguyen et al., 2013).

Once potential hits have been identified, their *in vitro* potency can be determined by testing for inhibition as a function of drug concentration and the most potent molecules can be studied further. It can also be useful to test compounds structurally related to the ones that test positive for helicase inhibition, as these may be better candidates to pursue for subsequent studies based on their potency or drug-like properties. For example, in the case of the WRN helicase, NSC617145 (a close structural analog of the initially identified inhibitor NSC19630) was found to be ~80-fold more potent than NSC19630 (Aggarwal, Banerjee, Sommers, Iannascoli, et al., 2013).

This chapter describes development of a method suitable for high-throughput screening for DDX11 inhibitors, both as a potential research tool and for identifying potential therapeutics. High-throughput screening has become a mainstay of pharmaceutical drug discovery, and has led to the development of inhibitors for other helicases (reviewed in Datta and Brosh 2018). These inhibitors may interfere with the catalytic activity of DNA helicases by a variety of mechanisms including disrupting DNA binding or competing with ATP binding. Inhibitors may also alter the helicase interactions with DNA or other proteins by orthosteric (binding at the active site) or allosteric (binding outside of the active site) mechanisms, causing the protein to become trapped

on DNA or in a DNA-adjacent complex through enhanced protein-protein interactions, resulting in a toxic complex.

Chapter 5: Conclusions and future directions

DDX11 is a relatively unexplored human helicase, despite the fact that it plays an important role in sister-chromatid cohesion and in linking DNA replication to cohesion. Since this project was initiated, several studies have been published shedding more light on the details of DDX11 physical interaction with the replisome, as well as analyzing separation of function mutants identified in both yeast and human cells that impact its role in replication versus sister-chromatid cohesion, providing further support for the central role DDX11 may play in coupling DNA replication and sister-chromatid cohesion (Cortone et al., 2018; Samora et al., 2016). In light of its central role in core processes important for cellular division, and the extensive synthetic lethal interactions of the yeast homolog, Chl1, with genes involved in DNA replication, repair and cohesion, DDX11 is likely to be a good target for cancer therapeutics. Therefore, the overarching goal of this thesis was to advance the study of DDX11 inhibition as a synthetic lethal cancer therapeutic.

5.1 Exploring the genetic interactions of DDX11 in human cell lines

CHL1 was previously identified in our lab as a strong synthetic lethal partner in yeast with the cohesin complex, which is highly mutated in several cancer types. In Chapter 2 of this thesis, we directly tested the genetic interaction of *DDX11* with the commonly cancer-mutated cohesin gene *STAG2* in human cell lines and found that it did not result in synthetic lethality (at least in the cellular context we used to study this question). The lack of negative genetic interaction is most likely due to the fact that in human cells, *STAG2* has a highly related paralog, *STAG1*, which may mask the interaction. In addition, as discussed in Chapter 2, the role of cohesin, and especially of STAG2, is more complex in human cells than in yeast cells, which

may also contribute to the lack of conservation observed for this proposed synthetic lethal interaction. While we didn't directly test this, DDX11 inhibition may be synthetic lethal with other cohesin genes (such as *RAD21* or *SMC3*) in tumours carrying hypomorphs of these genes and these would not be identified in the CRISPR/Cas9 knock-out screen as full knock-out of cohesin genes is expected to be lethal both in the wild-type and the DDX11 knock-out lines.

In additional to potential therapeutic potential, studying genetic interactions can provide information on the biological role of a gene of interest. Therefore, we also conducted an unbiased forward genetics screen using a whole genome CRISPR/Cas9 knock-out library in isogenic HAP1 cell lines in which *DDX11* had been knocked-out. The screen identified multiple genes important for sister-chromatid cohesion, as well as genes involved in DNA repair, providing further support for the conservation of DDX11's role from yeast to human, and strengthening the idea of DDX11 inhibition as a therapeutic for cancer with cohesion defects. Of course, such cancers would need to be identified by the presence of a biomarker (similar to *BRCA1/2* mutations as an indication for treatment with PARP inhibitors). Even in the absence of a defined genotypic vulnerability, such tumours could potentially be identified by a phenotypic assay of cohesion defects (for example, by observing chromosomes in cells arrested in metaphase; van der Lelij et al., 2010).

Our studies described here provide information on the role of DDX11 in human cells, and will add to construction of a large-scale genetic interaction map in HAP1 cells. However, one limitation of the study is that genetic interactions were studied in a single cell line, HAP1. Studies of essential genes have revealed that the essentiality of many genes is context dependent, both in model organisms and in human cells, and this is dependent on both the genetic background and the environment in which they are studied (reviewed in Rancati et al. 2017). For

example, in two widely-used laboratory strains of *S. cerevisiae*, 44 genes are uniquely essential in the Sigma1278b strain, whereas 13 are essential only in the S288c strain (Dowell et al., 2010). The same is true for genetic interactions where a specific synthetic lethal interaction may only be identified in certain cellular lineages or environmental conditions. For example, a recent study utilized three human cancer cell lines of variable lineages to study pairwise gene knock-out combinations of 73 cancer genes with dual-guide RNAs. Interestingly, only 10.5% of identified interactions were common to given cell-line pairs, and no shared interactions were seen in all three cell lines (J. P. Shen et al., 2017). This suggests a high degree of diversity in genetic interactions between different human cell lines may be a common feature. An additional example is a recent study conducted in our lab to identify *STAG2* synthetic lethal interactions. In this study, CRISPR/Cas9 knock-out screens were conducted in three different isogenic pairs of *STAG2* wild-type and knock-out cell lines, and only one synthetic lethal interaction, *STAG1*, was identified in all three lines (Bailey M. et al., in press). Such studies imply that ideally, any clinically-relevant interactions should be validated in additional cell lines and tumour models in the future.

For this study, we chose to use isogenic lines differing only in the presence/absence of *DDX11*. These are an attractive model as it is much easier to infer synthetic lethal relationships from screens (as the primary difference between the lines is the mutational status of the query gene), and they can be used to test any gene of interest. However, as mentioned, their limitation is that they represent only one genetic background. An alternative approach is to use a panel of genetically diverse lines divided into two groups depending on the status of the gene of interest. The advantage of this approach is that it represents multiple different genetic backgrounds and cell types. However, this approach has limitations as well. Available panels often lack a

corresponding “control” cell line, and only have a small number of cell lines carrying the mutation of interest. Synthetic lethal interactions are determined by comparing the growth of cells with/without the mutation of interest, but this can be difficult to establish when the statistical power is low due to the underrepresentation of most specific genetic alterations in the cell line panel. In addition, some clinically-relevant synthetic lethal interactions may not occur in all backgrounds and would be missed using such an approach.

5.2 Utilizing missense mutations to identify dominant synthetic lethality and mimic trapping inhibition by small molecules

The lack of synthetic lethality in human cells between *STAG2* and *DDX11* led us to reassess synthetic lethality as a therapeutic paradigm. Although synthetic lethality was first proposed as an approach to anti-cancer therapeutics over 20 years ago (Hartwell et al., 1997), and screening in both model organisms and human cell lines has produced a wealth of functional and biological information, the yield from a therapeutic perspective has been low (O’Neil et al., 2017). Large scale genetic screens using null alleles have been the bedrock of synthetic lethality discovery, first in model organisms such as *S. cerevisiae* and more recently in mammalian cells with the introduction of suitable techniques. It may be the case that we have been looking at the problem through an inaccurate lens. A reductionist view encourages us to view genetic ablation (null mutations/knock-down/knock-out) as akin to small molecule inhibition; however, this is not always the case. Absence of a target may not phenocopy a chemically-inhibited protein, in which the inhibited protein is still present in the cell, as described in Chapter 3**.** The phenotype of protein loss may reflect the loss of catalytic activity, loss of protein-protein scaffolding activity or both. In addition, protein elimination may allow forms of compensation (by other

proteins/enzymes present in the cell) that are prevented when the target protein is present but inhibited with a drug.

Examining the properties of clinically successful synthetic lethal drugs (such as PARP and Topoisomerase inhibitors) may improve the success rate of future synthetic lethal drug development. For both of the above, a significant part of their toxicity can be attributed to their ability to trap the target protein on DNA, converting it into a poisonous complex (Pommier, 2013; Pommier et al., 2016). In Chapter 3, we start with the premise that small molecules that cause trapping are desirable, and hypothesize that using missense mutations that inhibit activity, but not DNA binding, may better mimic chemical inhibition, and enable identification of dominant synthetic lethal interactions in the presence of the wild-type protein – thus modeling both a trapped protein and incomplete inhibition, as is often the case with chemical inhibition.

The model organism *S. cerevisiae* is a genetically tractable model organism and work by the yeast genetics community has provided a wealth of tools for generating and screening alleles in various genetic backgrounds, including the construction of an arrayed collection of yeast strains each carrying a deletion of a single gene (Giaever et al., 2002), and high throughput mating and selection technology such as the Synthetic Genetic Array (Tong et al., 2001).

As a proof-of-principle, we utilized a known catalytic mutant of *CHL1* to test the hypothesis that a missense mutation can mimic the predicted effect of inhibitors that induce dominant cytotoxic complexes by inhibiting protein activity without affecting binding to DNA substrates. Subsequently, we used additional missense mutations to disrupt DNA- and protein-binding domains in conjunction with the inactivating mutations to determine whether DNA or protein binding were required for the dominant effects observed for catalytically inactive Chl1.

We identified that a catalytically-inactive mutant of *CHL1* has a dominant synthetic lethal interaction with spindle-associated, Ctf18-RFC and cohesin genes. In addition, the effects of replisome and/or DNA binding mutants on the dominant synthetic lethal effect is varied between the different pathways, suggesting that studying the interactions of various alleles (alone or in the presence of wild-type protein) can provide functional and structural information that may help guide inhibitor development.

In this study, we restricted our dominant synthetic lethal screens to testing a mini-array of 332 yeast deletion mutants that function in various DNA transactions. A potential future study is to expand to yeast genome-wide screens to generate a larger dominant synthetic lethal interaction network. Genome-wide screens using catalytically inactive Chl1 as a query may identify cancer-relevant targets other than those identified in our study where DDX11 inhibitors may be applied. Similar to our study screening a library of deletion mutants, yeast can also be utilized to screen a query gene mutation against the whole-genome overexpression library (Hu et al., 2007). In this case, we can identify yeast homologs of cancer-relevant genes that sensitize to the presence of dominant synthetic lethal Chl1 when overexpressed. These results may be applicable for human DDX11 inhibitors to selectively target cancer cells that overexpress the conserved human genes.

The Chl1^{K48R} dominant negative effects have significant ramifications given the large number of different DNA/RNA helicases encoded in the genome, as the K48 reside is an invariant lysine in the Walker box A motif and is conserved in all helicases (Bhattacharyya & Keck, 2014; Walker et al., 1982). This suggests that this approach can be applied to additional helicases and ATPase proteins to identify dominant synthetic lethal interactions. In addition, the K48R mutation is conserved in human DDX11 (K50R). One future avenue of study would be to express DDX11^{K50R} in human cell lines and screen for genetic backgrounds that are sensitive to

the presence of this presumably dominant synthetic lethal allele (in an analogous manner to our study in yeast). The catalytic mutant can be expressed in one or more of the backgrounds identified in Chapter 2 (which would be expected to be sensitive to expression of $DDX11^{K50R}$) as a proof-of-concept to identify the optimal cell line and expression methods prior to embarking on a genome-wide screen. Alternatively, in light of the synthetic lethal interactions identified in Chapter 2, the synthetic lethal effect of the catalytic mutant can be tested on panels of cells with or without a defective sister-chromatid cohesion phenotype. If this dominant synthetic lethality effect is conserved in human cells, additional missense mutations can be explored to identify residues or allosteric changes that can be targeted by development of small molecule inhibitors. Such inhibitors can then be tested in cells to phenocopy the interactions observed with the missense mutations, as support for their specificity.

In our study, we utilized missense mutations in two proteins of interest, human FEN1 and yeast CHL1. This approach can be expanded to other proteins with or without known dominant mutations. For example, FANCJ is also an important DEAD-box helicase, closely related to DDX11 (Brosh & Cantor, 2014). In addition to the conserved Walker box A lysine, a dominant-negative patient-derived mutation has been identified in FANCJ, A349P (Wu et al., 2010). This residue is not conserved in DDX11, but is immediately adjacent to a conserved cysteine in the iron-sulfur domain. Unlike K50R (K52R in FANCJ), which in DDX11 retains DNA binding but not ATP hydrolysis (Wu et al., 2012), A349P retains both DNA binding and ATPase activity, but cannot translocate on DNA, suggesting that the mechanisms of inhibition is more specific than the general ATPase-dead K50R. In addition to the biochemical impact of the mutations, in this study exogenous wild-type and A349P FANCJ were expressed in cells at a level approximately 3-fold lower than endogenous FANCJ, yet the mutant had a dominant-negative effect (Wu et al.,

2010). This suggests that if this mutation is indeed "trapping" FANCJ, even a small amount of poisonous DNA-protein (or protein-protein) complex is sufficient for the effect. Elucidation of the effects of this mutation on protein structure may reveal features that can be modelled for DDX11 to further inhibitor development as discussed below.

As mentioned, most large-scale screens to date have used null mutations. In this study, we utilized known missense mutations that inhibit activity but do not affect protein stability or DNA binding to demonstrate the principle of dominant synthetic lethality. This concept can be expanded to find additional novel missense mutations that may cause a dominant synthetic lethal effect through unbiased mutational screening of proteins of interest. Once we have identified genetic backgrounds that exhibit dominant synthetic lethality with a specific target (as achieved in this study), technologies such as deep mutational scanning (Fowler & Fields, 2014) can be used to screen for residues that are mutable to a dominant synthetic lethal phenotype. These residues can then be mapped onto the protein structure to inform development of inhibitors that mimic the structural changes and elicit target trapping. For example, Zandarashvili et al. recently demonstrated the feasibility of this approach by converting a non-trapping PARP inhibitor to a trapping PARP inhibitor using a combination of structural data and mutational analysis (Zandarashvili et al., 2020). Dominant synthetic lethal mutations may identify protein regions for targeting with small molecules to induce trapping, even if it is not possible to directly mimic the structural changes caused by a missense mutation using a small molecule inhibitor. A deeper structural understanding of DDX11, through structural studies and/or mutational mapping studies, can assist in identifying allosteric inhibitors. For example, a recent study utilizing crystallographic analysis of the BLM-DNA-drug complex identified a novel allosteric binding site and revealed a distinctive conformational step in the helicase mechanism, that can be trapped

by small-molecules (Chen et al., 2021). Of course, trapped protein-DNA adducts is only one form of cytotoxic lesion that could be induced by a small molecule binding to its protein target. Other forms could be generated by enhancing protein-protein interactions, sequestering peripheral proteins required for function or blocking post-translational modifications required for removal of the protein (such as ubiquitination, sumoylation, and others; Psakhye & Branzei, 2021).

Model organisms such as *S. cerevisiae* are easy to work with, inexpensive and genetically tractable. Recent and classic work by the yeast genetics community has led to the development of a complete platform to generate and screen alleles of human disease-relevant genes. One such tool is the use of "humanized" yeast, in which a human gene is expressed in yeast. For this approach to be utilized, a relevant phenotype of the human protein needs to be detected. For some genes, such as FEN1, the human gene complements a null allele of the yeast homolog (Rad27 in this case; Hamza et al., 2020). The resulting humanized yeast can then be used in a myriad of assays to analyze the function of the human gene, including screening small molecules for activity against human protein targets (for example FEN1; Hamza et al., 2020) or using deep mutational screening as described above to generate a site-saturated mutagenesis library to annotate human variants of unknown significance (for example as was recently performed for the human CYP2C9 protein; Amorosi et al., 2021).

Unlike human *FEN1* and yeast *RAD27*, human *DDX11* does not complement the chemical sensitivity and/or CIN defects of a null mutant of yeast *CHL1* (Hamza et al., 2020). This may be due to the lack of conservation of the Ctf4-binding site (CIP-box) required for yeast Chl1 protein to bind to the replisome (Samora et al., 2016). However, it may be possible to identify a phenotype of human DDX11 expression in yeast, or alternatively to improve the

complementation, possibly by adding a CIP-box to the human protein, analogous to replacing the human PCNA-interacting domain in human FEN1 with the corresponding yeast segment (Greene et al., 1999). If a phenotype can be identified or complementation improved, humanized yeast expressing human DDX11 can be used to screen missense mutations or potential inhibitors.

5.3 Identifying a DDX11 inhibitor

In order to further the development of DDX11 as an anti-cancer therapeutic, there is a need to identify small molecules capable of inhibiting or modifying its activity. Identification of an inhibitor can also serve as a research tool to further study the role of DDX11 in human cells through inhibition or modification of its activity, rather than removal of the protein as was done in Chapter 2 (via knock-out or knock-down). In Chapter 4 we adapted a low throughput, gel-based assay to a high throughout fluorescence-based assay suitable for screening small molecule libraries for compounds that inhibit the activity of DDX11. As mentioned in that chapter, following identification of lead compounds that potentially inhibit DDX11, a number of assays would be required to test the mechanism of action and the specificity of potential inhibitors. These include testing whether the molecules inhibit by binding DNA directly (in which case they are less likely to be specific), as well as testing inhibition of other related proteins.

One intriguing point observed from studying BLM is that the inhibitor ML216 potently inhibited BLM unwinding of a forked duplex *in vitro*, but only modestly affected unwinding of other DNA substrates such as G4, Holliday junction or plasmid-based D-loops at much higher drug concentrations (Nguyen et al., 2013). Identifying inhibitors such as this, that may also demonstrate specific activity *in vivo* against one function/substrate of the protein, can serve as a tool for more refined cellular studies than those that can be conducted using full ablation (knock-

out or knock-down) (Banerjee et al., 2013). Of course, it is possible that missense mutations may also abrogate one function while maintaining another and are a complimentary tool for such studies.

As described in Chapter 3, inhibitors that trap the target protein may make better synthetic lethal drug therapies than inhibitors that prevent DNA binding or inhibit activity without creating a toxic protein complex. The screening method described in Chapter 4 is unable to differentiate between inhibitors that trap DDX11 and those that do not. The assay will identify competitive inhibitors that prevent binding to DNA, molecules that inhibit ATP hydrolysis (that may or may not also trap the protein on the DNA) and allosteric inhibitors that may prevent a conformation change required for DDX11 translocation along the DNA. One way to test whether an inhibitor creates a dominant-negative form of DDX11 would be to test the sensitivity of cells to the inhibitor in which DDX11 expression has been depleted (through knock-out or siRNA). If the inhibitor indeed creates a toxic form of DDX11, it can be expected that the inhibitor will be significantly more toxic than an absence of DDX11 activity (in normal cells and/or in specific genetic backgrounds), and that this toxicity would be dependent on the presence of DDX11. There already exist helicase inhibitors that trap the helicase on the substrate or are proposed to work in a trapping/dominant manner. For example, E1F4A inhibitors have been identified that trap the helicase on the RNA substrate (L. Shen & Pelletier, 2020). Also, as mentioned above, a BLM inhibitor has been identified that binds allosterically and prevents the conformational change required to translocate and release DNA (Chen et al., 2021). Also, the fact that a WRN inhibitor is more toxic than a knock-down and enriches WRN's association with chromatin (Aggarwal, Banerjee, Sommers, Iannascoli, et al., 2013) suggests that the inhibitor is creating a

toxic complex. These examples suggest that identifying a trapping inhibitor for additional helicases, such as DDX11, is a worthwhile approach.

Of course, while this relatively conventional activity-based screening method can identify molecules that inhibit DDX11 activity directly, it may miss an entire class of potentially therapeutically relevant molecules in light of the extensive genetic and protein-protein interactions described for human DDX11/yeast Chl1. Conceivably, a molecule that does not impact the unwinding activity in a simplified *in vitro* assay, but is able to bind and trap DDX11 in the full context of the replisome may be highly therapeutically relevant, but missed by this assay. This notion is strengthened by the separation of function between the various hDDX11/yChl1 mutants in which the catalytic activity seems to play a role in the replicative function of the helicase, whereas the binding to the replisome (but less so the catalytic activity) is important for the role in sister chromatid cohesion (Cortone et al., 2018; Samora et al., 2016).

5.4 Concluding remarks

DDX11 is a relatively unexplored helicase that appears to be a key player in the link between DNA replication and cohesion establishment to ensure proper mitosis. In recent years, interest has grown in studying these mechanisms as evidenced by the publication of several important papers studying the role of DDX11; however, the molecular mechanisms behind DDX11's role in sister-chromatid cohesion, replication fork stability and linking replication to cohesion establishment are still not well understood. The overarching goal of this thesis was to further advance inhibition of DDX11 as a synthetic lethal cancer drug target. In order to develop inhibitors that target helicases successfully *in vitro* and *in vivo* with optimal characteristics, a deep molecular knowledge of helicase conformational states, substrate specificities, genetic and

protein interactions, pathways, etc. is required. Key to this approach is the development of both *in vitro* tools (such as biochemical assays, trapping assays, and others) and *in vivo* experimental platforms in human cells and model organisms as described in this thesis.

Bibliography

Abdellah, Z., Ahmadi, A., Ahmed, S., Aimable, M., Ainscough, R., Almeida, J., Almond, C., Ambler, A., Ambrose, K., Ambrose, K., Andrew, R., Andrews, D., Andrews, N., Andrews, D., Apweiler, E., Arbery, H., Archer, B., Ash, G., Ashcroft, K., … Kamholz, S. (2004). Finishing the euchromatic sequence of the human genome. *Nature 2004 431:7011*, *431*(7011), 931–945. https://doi.org/10.1038/nature03001

Abe, T., Kawasumi, R., Arakawa, H., Hori, T., Shirahige, K., Losada, A., Fukagawa, T., & Branzei, D. (2016). Chromatin determinants of the inner-centromere rely on replication factors with functions that impart cohesion. *Oncotarget*, *7*(42). https://doi.org/10.1039/j39690001537

Abe, T., Ooka, M., Kawasumi, R., Miyata, K., Takata, M., Hirota, K., & Branzei, D. (2018). Warsaw breakage syndrome DDX11 helicase acts jointly with RAD17 in the repair of bulky lesions and replication through abasic sites. *Proceedings of the National Academy of Sciences of the United States of America*, *115*(33), 8412–8417. https://doi.org/10.1073/pnas.1803110115

Aggarwal, M., Banerjee, T., Sommers, J. A., Iannascoli, C., Pichierri, P., Shoemaker, R. H., & Brosh, R. M. (2013). Werner syndrome helicase has a critical role in DNA damage responses in the absence of a functional Fanconi Anemia pathway. *Cancer Research*, *73*(17), 5497–5507. https://doi.org/10.1158/0008-5472.CAN-12-2975

Aggarwal, M., Banerjee, T., Sommers, J. A., & Robert M Brosh, J. (2013). Targeting an Achilles' heel of cancer with a WRN helicase inhibitor. *Http://Dx.Doi.Org/10.4161/Cc.26320*, *12*(20), 3329–3335. https://doi.org/10.4161/CC.26320

Aggarwal, M., Sommers, J. A., Shoemaker, R. H., & Brosh, R. M. (2011). Inhibition of helicase activity by a small molecule impairs Werner syndrome helicase (WRN) function in the cellular response to DNA damage or replication stress. *Proceedings of the National Academy of Sciences*, *108*(4), 1525–1530. https://doi.org/10.1073/pnas.1006423108

Aguirre, A. J., Meyers, R. M., Weir, B. A., Vazquez, F., Zhang, C.-Z., Ben-David, U., Cook, A., Ha, G., Harrington, W. F., Doshi, M. B., Kost-Alimova, M., Gill, S., Xu, H., Ali, L. D., Jiang, G., Pantel, S., Lee, Y., Goodale, A., Cherniack, A. D., … Hahn, W. C. (2016). Genomic Copy Number Dictates a Gene-Independent Cell Response to CRISPR/Cas9 Targeting. *Cancer Discovery*, *6*(8), 914–929. https://doi.org/10.1158/2159-8290.CD-16-0154

Alberti, S., Gitler, A. D., & Lindquist, S. (2007). A suite of Gateway® cloning vectors for high-throughput genetic analysis in Saccharomyces cerevisiae. *Yeast*, *24*(10), 913–919. https://doi.org/10.1002/yea.1502

Alkhunaizi, E., Shaheen, R., Bharti, S. K., Joseph-George, A. M., Chong, K., Abdel-Salam, G. M. H., Alowain, M., Blaser, S. I., Papsin, B. C., Butt, M., Hashem, M., Martin, N., Godoy, R., Brosh, R. M., Alkuraya, F. S., & Chitayat, D. (2018). Warsaw breakage syndrome: Further clinical and genetic delineation. *American Journal of Medical Genetics, Part A*, *176*(11), 2404–2418. https://doi.org/10.1002/ajmg.a.40482

Amann, J., Kidd, V. J., & Lahti, J. M. (1997). Characterization of putative human homologues of the yeast chromosome transmission fidelity gene, CHL1. *Journal of Biological Chemistry*,

272(6), 3823–3832. https://doi.org/10.1074/jbc.272.6.3823

Amann, J., Valentine, M., Kidd, V. J., & Lahti, J. M. (1996). Localization of Chl1-related helicase genes to human chromosome regions 12p11 and 12p13: Similarity between parts of these genes and conserved human telomeric-associated DNA. *Genomics*, *32*(2), 260–265. https://doi.org/10.1006/geno.1996.0113

Amorosi, C. J., Chiasson, M. A., McDonald, M. G., Wong, L. H., Sitko, K. A., Boyle, G., Kowalski, J. P., Rettie, A. E., Fowler, D. M., & Dunham, M. J. (2021). Massively parallel characterization of CYP2C9 variant enzyme activity and abundance. *The American Journal of Human Genetics*. https://doi.org/10.1016/J.AJHG.2021.07.001

Aregger, M., Chandrashekhar, M., Tong, A. H. Y., Chan, K., & Moffat, J. (2019). Pooled Lentiviral CRISPR-Cas9 Screens for Functional Genomics in Mammalian Cells. In *Methods in Molecular Biology* (Vol. 1869). https://doi.org/10.1007/978-1-4939-8805-1_15

Aregger, M., Lawson, K. A., Billmann, M., Costanzo, M., Tong, A. H. Y., Chan, K., Rahman, M., Brown, K. R., Ross, C., Usaj, M., Nedyalkova, L., Sizova, O., Habsid, A., Pawling, J., Lin, Z. Y., Abdouni, H., Wong, C. J., Weiss, A., Mero, P., … Moffat, J. (2020). Systematic mapping of genetic interactions for de novo fatty acid synthesis identifies C12orf49 as a regulator of lipid metabolism. *Nature Metabolism*, *2*(6), 499–513. https://doi.org/10.1038/s42255-020-0211-z

Audeh, M. W., Carmichael, J., Penson, R. T., Friedlander, M., Powell, B., Bell-McGuinn, K. M., Scott, C., Weitzel, J. N., Oaknin, A., Loman, N., Lu, K., Schmutzler, R. K., Matulonis, U., Wickens, M., & Tutt, A. (2010). Oral poly(ADP-ribose) polymerase inhibitor olaparib in patients with BRCA1 or BRCA2 mutations and recurrent ovarian cancer: a proof-of-concept trial. *The Lancet*, *376*(9737), 245–251. https://doi.org/10.1016/S0140-6736(10)60893-8

Bailey, C., Fryer, A. E., & Greenslade, M. (2015). Warsaw breakage syndrome - A further report, emphasising cutaneous findings. *European Journal of Medical Genetics*, *58*(4), 235–237. https://doi.org/10.1016/j.ejmg.2015.02.001

Bailey, M. L., O'Neil, N. J., van Pel, D. M., Solomon, D. A., Waldman, T., & Hieter, P. (2014). Glioblastoma Cells Containing Mutations in the Cohesin Component STAG2 Are Sensitive to PARP Inhibition. *Molecular Cancer Therapeutics*, *13*(3), 724–732. https://doi.org/10.1158/1535-7163.MCT-13-0749

Balakrishnan, R., Park, J., Karra, K., Hitz, B. C., Binkley, G., Hong, E. L., Sullivan, J., Micklem, G., & Michael Cherry, J. (2012). YeastMine—an integrated data warehouse for Saccharomyces cerevisiae data as a multipurpose tool-kit. *Database*, *2012*. https://doi.org/10.1093/DATABASE/BAR062

Balbás-Martínez, C., Sagrera, A., Carrillo-De-Santa-Pau, E., Earl, J., Márquez, M., Vazquez, M., Lapi, E., Castro-Giner, F., Beltran, S., Bayés, M., Carrato, A., Cigudosa, J. C., Domínguez, O., Gut, M., Herranz, J., Juanpere, N., Kogevinas, M., Langa, X., López-Knowles, E., … Real, F. X. (2013). Recurrent inactivation of STAG2 in bladder cancer is not associated with aneuploidy. *Nature Genetics*, *45*(12), 1464–1469. https://doi.org/10.1038/ng.2799

Banerjee, T., Aggarwal, M., & Robert M. Brosh, J. (2013). A new development in DNA repair modulation. *Http://Dx.Doi.Org/10.4161/Cc.23953*, *12*(5), 713–714. https://doi.org/10.4161/CC.23953

Banerjee, T., Aggarwal, M., Sommers, J. A., & Brosh, R. M. (2016). Biochemical and cell

biological assays to identify and characterize DNA helicase inhibitors. *Methods*, *108*, 130–141. https://doi.org/10.1016/j.ymeth.2016.04.007

Barber, T. D., McManus, K., Yuen, K. W. Y., Reis, M., Parmigiani, G., Shen, D., Barrett, I., Nouhi, Y., Spencer, F., Markowitz, S., Velculescu, V. E., Kinzler, K. W., Vogelstein, B., Lengauer, C., & Hieter, P. (2008). Chromatid cohesion defects may underlie chromosome instability in human colorectal cancers. *Proceedings of the National Academy of Sciences of the United States of America*, *105*(9), 3443. https://doi.org/10.1073/PNAS.0712384105

Bass, A. J., Thorsson, V., Shmulevich, I., Reynolds, S. M., Miller, M., Bernard, B., Hinoue, T., Laird, P. W., Curtis, C., Shen, H., Weisenberger, D. J., Schultz, N., Shen, R., Weinhold, N., Kelsen, D. P., Bowlby, R., Chu, A., Kasaian, K., Mungall, A. J., … Liu, J. (2014). Comprehensive molecular characterization of gastric adenocarcinoma. *Nature 2014 513:7517*, *513*(7517), 202–209. https://doi.org/10.1038/nature13480

Bassik, M. C., Kampmann, M., Lebbink, R. J., Wang, S., Hein, M. Y., Poser, I., Weibezahn, J., Horlbeck, M. A., Chen, S., Mann, M., Hyman, A. A., LeProust, E. M., McManus, M. T., & Weissman, J. S. (2013). A Systematic Mammalian Genetic Interaction Map Reveals Pathways Underlying Ricin Susceptibility. *Cell*, *152*(4), 909–922. https://doi.org/10.1016/J.CELL.2013.01.030

Behan, F. M., Iorio, F., Picco, G., Gonçalves, E., Beaver, C. M., Migliardi, G., Santos, R., Rao, Y., Sassi, F., Pinnelli, M., Ansari, R., Harper, S., Jackson, D. A., McRae, R., Pooley, R., Wilkinson, P., van der Meer, D., Dow, D., Buser-Doepner, C., … Garnett, M. J. (2019). Prioritization of cancer therapeutic targets using CRISPR–Cas9 screens. *Nature*, *568*(7753), 511–516. https://doi.org/10.1038/s41586-019-1103-9

Beigl, T. B., Kjosås, I., Seljeseth, E., Glomnes, N., & Aksnes, H. (2020). Efficient and crucial quality control of HAP1 cell ploidy status. *Biology Open*, *9*(11). https://doi.org/10.1242/BIO.057174

Bell, D., Berchuck, A., Birrer, M., Chien, J., Cramer, D. W., Dao, F., Dhir, R., Disaia, P., Gabra, H., Glenn, P., Godwin, A. K., Gross, J., Hartmann, L., Huang, M., Huntsman, D. G., Iacocca, M., Imielinski, M., Kalloger, S., Karlan, B. Y., … Thomson, E. (2011). Integrated genomic analyses of ovarian carcinoma. *Nature 2011 474:7353*, *474*(7353), 609–615. https://doi.org/10.1038/nature10166

Benedetti, L., Cereda, M., Monteverde, L., Desai, N., Ciccarelli, F. D., Benedetti, L., Cereda, M., Monteverde, L., Desai, N., & Ciccarelli, F. D. (2017). Synthetic lethal interaction between the tumour suppressor STAG2 and its paralog STAG1. *Oncotarget*, *8*(23), 37619–37632. https://doi.org/10.18632/ONCOTARGET.16838

Bharti, S. K., Khan, I., Banerjee, T., Sommers, J. A., Wu, Y., & Brosh, R. M. (2014). Molecular functions and cellular roles of the ChlR1 (DDX11) helicase defective in the rare cohesinopathy Warsaw breakage syndrome. *Cellular and Molecular Life Sciences*, *71*(14), 2625–2639. https://doi.org/10.1007/s00018-014-1569-4

Bharti, S. K., Sommers, J. A., George, F., Kuper, J., Hamon, F., Shin-Ya, K., Teulade-Fichou, M. P., Kisker, C., & Brosh, R. M. (2013). Specialization among iron-sulfur cluster helicases to resolve G-quadruplex DNA structures that threaten genomic stability. *Journal of Biological Chemistry*, *288*(39), 28217–28229. https://doi.org/10.1074/jbc.M113.496463

Bhattacharya, C., Wang, X., & Becker, D. (2012). The DEAD/DEAH box helicase, DDX11, is essential for the survival of advanced melanomas. *Molecular Cancer*, *11*(1), 1.

https://doi.org/10.1186/1476-4598-11-82

Bhattacharyya, B., & Keck, J. L. (2014). Grip it and rip it: Structural mechanisms of DNA helicase substrate binding and unwinding. *Protein Science*, *23*(11), 1498–1507. https://doi.org/10.1002/PRO.2533

Blomen, V. A., Májek, P., Jae, L. T., Bigenzahn, J. W., Nieuwenhuis, J., Staring, J., Sacco, R., Van Diemen, F. R., Olk, N., Stukalov, A., Marceau, C., Janssen, H., Carette, J. E., Bennett, K. L., Colinge, J., Superti-Furga, G., & Brummelkamp, T. R. (2015). Gene essentiality and synthetic lethality in haploid human cells. *Science*, *350*(6264), 1092–1096. https://doi.org/10.1126/science.aac7557

Borges, V., Smith, D. J., Whitehouse, I., & Uhlmann, F. (2013). An Eco1-independent sister chromatid cohesion establishment pathway in S. cerevisiae. *Chromosoma*, *122*(1–2), 121–134. https://doi.org/10.1007/s00412-013-0396-y

Bottega, R., Napolitano, L. M. R., Carbone, A., Cappelli, E., Corsolini, F., Onesti, S., Savoia, A., Gasparini, P., & Faletra, F. (2019). Two further patients with Warsaw breakage syndrome. Is a mild phenotype possible? *Molecular Genetics and Genomic Medicine*, *7*(5), 1–6. https://doi.org/10.1002/mgg3.639

Bottega, R., Ravera, S., Napolitano, L. M. R., Chiappetta, V., Zini, N., Crescenzi, B., Arniani, S., Faleschini, M., Cortone, G., Faletra, F., Medagli, B., Sirchia, F., Moretti, M., Lange, J. de, Cappelli, E., Mecucci, C., Onesti, S., Pisani, F. M., & Savoia, A. (2021). Genomic integrity and mitochondrial metabolism defects in Warsaw syndrome cells: a comparison with Fanconi anemia. *Journal of Cellular Physiology*, *236*(8), 5664–5675. https://doi.org/10.1002/JCP.30265

Brohl, A. S., Solomon, D. A., Chang, W., Wang, J., Song, Y., Sindiri, S., Patidar, R., Hurd, L., Chen, L., Shern, J. F., Liao, H., Wen, X., Gerard, J., Kim, J.-S. S., Lopez Guerrero, J. A., Machado, I., Wai, D. H., Picci, P., Triche, T., … Khan, J. (2014). The Genomic Landscape of the Ewing Sarcoma Family of Tumors Reveals Recurrent STAG2 Mutation. *PLoS Genetics*, *10*(7), e1004475. https://doi.org/10.1371/journal.pgen.1004475

Brosh, R. M. (2013). DNA helicases involved in DNA repair and their roles in cancer. *Nature Reviews. Cancer*, *13*(8), 542–558. https://doi.org/10.1038/nrc3560

Brosh, R. M., & Cantor, S. B. (2014). Molecular and cellular functions of the FANCJ DNA helicase defective in cancer and in Fanconi anemia. *Frontiers in Genetics*, *5*(OCT), 1–14. https://doi.org/10.3389/fgene.2014.00372

Brosh, R. M., Majumdar, A., Desai, S., Hickson, I. D., Bohr, V. A., & Seidman, M. M. (2001). Unwinding of a DNA Triple Helix by the Werner and Bloom Syndrome Helicases. *Journal of Biological Chemistry*, *276*(5), 3024–3030. https://doi.org/10.1074/JBC.M006784200

Brown, A.-L., Li, M., Goncearenco, A., & Panchenko, A. R. (2019). Finding driver mutations in cancer: Elucidating the role of background mutational processes. *PLOS Computational Biology*, *15*(4), e1006981. https://doi.org/10.1371/JOURNAL.PCBI.1006981

Bryant, H. E., Schultz, N., Thomas, H. D., Parker, K. M., Flower, D., Lopez, E., Kyle, S., Meuth, M., Curtin, N. J., & Helleday, T. (2005). Specific killing of BRCA2-deficient tumours with inhibitors of poly(ADP-ribose) polymerase. *Nature*, *434*(7035), 913–917. https://doi.org/10.1038/nature03443

Buzun, K., Bielawska, A., Bielawski, K., & Gornowicz, A. (2020). DNA topoisomerases as molecular targets for anticancer drugs. *Journal of Enzyme Inhibition and Medicinal*

Chemistry, *35*(1), 1781–1799. https://doi.org/10.1080/14756366.2020.1821676

Calì, F., Bharti, S. K., Perna, R. Di, Brosh, R. M., & Pisani, F. M. (2015). Tim/Timeless, a member of the replication fork protection complex, operates with the Warsaw breakage syndrome DNA helicase DDX11 in the same fork recovery pathway. *Nucleic Acids Research*, *44*(2), 705–717. https://doi.org/10.1093/nar/gkv1112

Campbell, P. J., Getz, G., Korbel, J. O., Stuart, J. M., Jennings, J. L., Stein, L. D., Perry, M. D., Nahal-Bose, H. K., Ouellette, B. F. F., Li, C. H., Rheinbay, E., Nielsen, G. P., Sgroi, D. C., Wu, C. L., Faquin, W. C., Deshpande, V., Boutros, P. C., Lazar, A. J., Hoadley, K. A., … Zhang, J. (2020). Pan-cancer analysis of whole genomes. *Nature*, *578*(7793), 82–93. https://doi.org/10.1038/s41586-020-1969-6

Cantor, S. B., & Guillemette, S. (2011). Hereditary breast cancer and the BRCA1-associated FANCJ/BACH1/BRIP1. *Future Oncology (London, England)*, *7*(2), 253–261. https://doi.org/10.2217/FON.10.191

Capo-Chichi, J. M., Bharti, S. K., Sommers, J. A., Yammine, T., Chouery, E., Patry, L., Rouleau, G. A., Samuels, M. E., Hamdan, F. F., Michaud, J. L., Brosh, R. M., Mégarbane, A., & Kibar, Z. (2013). Identification and Biochemical Characterization of a Novel Mutation in DDX11 Causing Warsaw Breakage Syndrome. *Human Mutation*, *34*(1), 103–107. https://doi.org/10.1002/humu.22226

Carette, J. E., Raaben, M., Wong, A. C., Herbert, A. S., Obernosterer, G., Mulherkar, N., Kuehne, A. I., Kranzusch, P. J., Griffin, A. M., Ruthel, G., Cin, P. D., Dye, J. M., Whelan, S. P., Chandran, K., & Brummelkamp, T. R. (2011). Ebola virus entry requires the cholesterol transporter Niemann-Pick C1. *Nature*, *477*(7364), 340–343. https://doi.org/10.1038/nature10348

Chapman, P. B., Hauschild, A., Robert, C., Haanen, J. B., Ascierto, P., Larkin, J., Dummer, R., Garbe, C., Testori, A., Maio, M., Hogg, D., Lorigan, P., Lebbe, C., Jouary, T., Schadendorf, D., Ribas, A., O'Day, S. J., Sosman, J. A., Kirkwood, J. M., … McArthur, G. A. (2011). Improved Survival with Vemurafenib in Melanoma with BRAF V600E Mutation. *The New England Journal of Medicine*, *364*(26), 2507–2516. https://doi.org/10.1056/NEJMOA1103782

Chen, X., Ali, Y. I., Fisher, C. E. L., Arribas-Bosacoma, R., Rajasekaran, M. B., Williams, G., Walker, S., Booth, J. R., Hudson, J. J. R., Mark Roe, S., Pearl, L. H., Ward, S. E., Pearl, F. M. G., & Oliver, A. W. (2021). Uncovering an allosteric mode of action for a selective inhibitor of human bloom syndrome protein. *ELife*, *10*. https://doi.org/10.7554/eLife.65339

Cheung, H. W., Cowley, G. S., Weir, B. A., Boehm, J. S., Rusin, S., Scott, J. A., East, A., Ali, L. D., Lizotte, P. H., Wong, T. C., Jiang, G., Hsiao, J., Mermel, C. H., Getz, G., Barretina, J., Gopal, S., Tamayo, P., Gould, J., Tsherniak, A., … Hahn, W. C. (2011). Systematic investigation of genetic vulnerabilities across cancer cell lines reveals lineage-specific dependencies in ovarian cancer. *Proceedings of the National Academy of Sciences*, *108*(30), 12372–12377. https://doi.org/10.1073/PNAS.1109363108

Chung, G., O'Neil, N. J., & Rose, A. M. (2011). CHL-1 provides an essential function affecting cell proliferation and chromosome stability in Caenorhabditis elegans. *DNA Repair*, *10*(11), 1174–1182. https://doi.org/10.1016/j.dnarep.2011.09.011

Collisson, E. A., Campbell, J. D., Brooks, A. N., Berger, A. H., Lee, W., Chmielecki, J., Beer, D. G., Cope, L., Creighton, C. J., Danilova, L., Ding, L., Getz, G., Hammerman, P. S., Hayes,

D. N., Hernandez, B., Herman, J. G., Heymach, J. V., Jurisica, I., Kucherlapati, R., … Cheney, R. (2014). Comprehensive molecular profiling of lung adenocarcinoma. *Nature 2014 511:7511*, *511*(7511), 543–550. https://doi.org/10.1038/nature13385

Cong, L., Ran, F. A., Cox, D., Lin, S., Barretto, R., Habib, N., Hsu, P. D., Wu, X., Jiang, W., Marraffini, L. A., & Zhang, F. (2013). Multiplex genome engineering using CRISPR/Cas systems. *Science*, *339*(6121), 819–823. https://doi.org/10.1126/science.1231143

Cortone, G., Zheng, G., Pensieri, P., Chiappetta, V., Tatè, R., Malacaria, E., Pichierri, P., Yu, H., & Pisani, F. M. (2018). Interaction of the Warsaw breakage syndrome DNA helicase DDX11 with the replication fork-protection factor Timeless promotes sister chromatid cohesion. *PLoS Genetics*, *14*(10), 1–22. https://doi.org/10.1371/journal.pgen.1007622

Costa, V., Casamassimi, A., Roberto, R., Gianfrancesco, F., Matarazzo, M. R., D'Urso, M., D'Esposito, M., Rocchi, M., & Ciccodicola, A. (2009). DDX11L: A novel transcript family emerging from human subtelomeric regions. *BMC Genomics*, *10*, 1–11. https://doi.org/10.1186/1471-2164-10-250

Costanzo, M., Baryshnikova, A., Bellay, J., Kim, Y., Spear, E. D., Sevier, C. S., Ding, H., Koh, J. L. Y., Toufighi, K., Mostafavi, S., Prinz, J., Onge, R. P. St., VanderSluis, B., Makhnevych, T., Vizeacoumar, F. J., Alizadeh, S., Bahr, S., Brost, R. L., Chen, Y., … Boone, C. (2010). The Genetic Landscape of a Cell. *Science*, *327*(5964), 425–431. https://doi.org/10.1126/SCIENCE.1180823

Costanzo, M., VanderSluis, B., Koch, E. N., Baryshnikova, A., Pons, C., Tan, G., Wang, W., Usaj, M., Hanchard, J., Lee, S. D., Pelechano, V., Styles, E. B., Billmann, M., Leeuwen, J. van, Dyk, N. van, Lin, Z.-Y., Kuzmin, E., Nelson, J., Piotrowski, J. S., … Boone, C. (2016). A global genetic interaction network maps a wiring diagram of cellular function. *Science*, *353*(6306). https://doi.org/10.1126/SCIENCE.AAF1420

Covey, J. M., Jaxel, C., Kohn, K. W., & Pommier, Y. (1989). Protein-linked DNA Strand Breaks Induced in Mammalian Cells by Camptothecin, an Inhibitor of Topoisomerase I. *Cancer Research*, *49*(18).

Cowley, G. S., Weir, B. A., Vazquez, F., Tamayo, P., Scott, J. A., Rusin, S., East-Seletsky, A., Ali, L. D., Gerath, W. F., Pantel, S. E., Lizotte, P. H., Jiang, G., Hsiao, J., Tsherniak, A., Dwinell, E., Aoyama, S., Okamoto, M., Harrington, W., Gelfand, E., … Hahn, W. C. (2014). Parallel genome-scale loss of function screens in 216 cancer cell lines for the identification of context-specific genetic dependencies. *Scientific Data 2014 1:1*, *1*(1), 1–12. https://doi.org/10.1038/sdata.2014.35

Crockett, A. O., & Wittwer, C. T. (2001). Fluorescein-Labeled Oligonucleotides for Real-Time PCR: Using the Inherent Quenching of Deoxyguanosine Nucleotides. *Analytical Biochemistry*, *290*(1), 89–97. https://doi.org/10.1006/ABIO.2000.4957

Crompton, B. D., Stewart, C., Taylor-Weiner, A., Alexe, G., Kurek, K. C., Calicchio, M. L., Kiezun, A., Carter, S. L., Shukla, S. A., Mehta, S. S., Thorner, A. R., de Torres, C., Lavarino, C., Suñol, M., McKenna, A., Sivachenko, A., Cibulskis, K., Lawrence, M. S., Stojanov, P., … Stegmaier, K. (2014). The genomic landscape of pediatric Ewing sarcoma. *Cancer Discovery*, *4*(11), 1326–1341. https://doi.org/10.1158/2159-8290.CD-13-1037

Cui, Y., Hunt, A., Li, Z., Birkin, E., Lane, J., Ruge, F., & Jiang, W. G. (2021). Lead DEAD/H box helicase biomarkers with the therapeutic potential identified by integrated bioinformatic approaches in lung cancer. *Computational and Structural Biotechnology Journal*, *19*, 261.

https://doi.org/10.1016/J.CSBJ.2020.12.007

Datta, A., & Brosh, R. M. (2018). New Insights Into DNA Helicases as Druggable Targets for Cancer Therapy. *Frontiers in Molecular Biosciences*, *5*(June), 1–21. https://doi.org/10.3389/fmolb.2018.00059

De Lange, J., Faramarz, A., Oostra, A. B., De Menezes, R. X., Van Der Meulen, I. H., Rooimans, M. A., Rockx, D. A., Brakenhoff, R. H., Van Beusechem, V. W., King, R. W., De Winter, J. P., & Wolthuis, R. M. F. (2015). Defective sister chromatid cohesion is synthetically lethal with impaired APC/C function. *Nature Communications*, *6*, 1–12. https://doi.org/10.1038/ncomms9399

De Roock, W., Claes, B., Bernasconi, D., De Schutter, J., Biesmans, B., Fountzilas, G., Kalogeras, K. T., Kotoula, V., Papamichael, D., Laurent-Puig, P., Penault-Llorca, F., Rougier, P., Vincenzi, B., Santini, D., Tonini, G., Cappuzzo, F., Frattini, M., Molinari, F., Saletti, P., … Tejpar, S. (2010). Effects of KRAS, BRAF, NRAS, and PIK3CA mutations on the efficacy of cetuximab plus chemotherapy in chemotherapy-refractory metastatic colorectal cancer: a retrospective consortium analysis. *The Lancet Oncology*, *11*(8), 753–762. https://doi.org/10.1016/S1470-2045(10)70130-3

Delgado, J. L., Hsieh, C.-M., Chan, N.-L., & Hiasa, H. (2018). Topoisomerases as anticancer targets. *The Biochemical Journal*, *475*(2), 373–398. https://doi.org/10.1042/BCJ20160583

Ding, H., Guo, M., Vidhyasagar, V., Talwar, T., & Wu, Y. (2015). The Q motif is involved in DNA binding but not ATP binding in ChlR1 helicase. *PLoS ONE*, *10*(10), 1–22. https://doi.org/10.1371/journal.pone.0140755

Ding, L., Bailey, M. H., Porta-Pardo, E., Thorsson, V., Colaprico, A., Bertrand, D., Gibbs, D. L., Weerasinghe, A., Huang, K., Tokheim, C., Cortés-Ciriano, I., Jayasinghe, R., Chen, F., Yu, L., Sun, S., Olsen, C., Kim, J., Taylor, A. M., Cherniack, A. D., … Mariamidze, A. (2018). Perspective on Oncogenic Processes at the End of the Beginning of Cancer Genomics. *Cell*, *173*(2), 305-320.e10. https://doi.org/10.1016/J.CELL.2018.03.033

Dowell, R. D., Ryan, O., Jansen, A., Cheung, D., Agarwala, S., Danford, T., Bernstein, D. A., Rolfe, P. A., Heisler, L. E., Chin, B., Nislow, C., Giaever, G., Phillips, P. C., Fink, G. R., Gifford, D. K., & Boone, C. (2010). Genotype to Phenotype: A Complex Problem. *Science*, *328*(5977), 469–469. https://doi.org/10.1126/SCIENCE.1189015

Druker, B. J., Guilhot, F., O'Brien, S. G., Gathmann, I., Kantarjian, H., Gattermann, N., Deininger, M. W. N., Silver, R. T., Goldman, J. M., Stone, R. M., Cervantes, F., Hochhaus, A., Powell, B. L., Gabrilove, J. L., Rousselot, P., Reiffers, J., Cornelissen, J. J., Hughes, T., Agis, H., … Larson, R. A. (2006). Five-Year Follow-up of Patients Receiving Imatinib for Chronic Myeloid Leukemia. *The New England Journal of Medicine*, *355*(23), 2408–2417. https://doi.org/10.1056/NEJMOA062867

Duffy, S., Fam, H. K., Wang, Y. K., Styles, E. B., Kim, J.-H., Ang, J. S., Singh, T., Larionov, V., Shah, S. P., Andrews, B., Boerkoel, C. F., & Hieter, P. (2016). Overexpression screens identify conserved dosage chromosome instability genes in yeast and human cancer. *Proceedings of the National Academy of Sciences*, *113*(36), 9967–9976. https://doi.org/10.1073/pnas.1611839113

Dwane, L., Behan, F. M., Gonçalves, E., Lightfoot, H., Yang, W., van der Meer, D., Shepherd, R., Pignatelli, M., Iorio, F., & Garnett, M. J. (2021). Project Score database: a resource for investigating cancer cell dependencies and prioritizing therapeutic targets. *Nucleic Acids*

Research, *49*(D1), D1365–D1372. https://doi.org/10.1093/NAR/GKAA882

Eng, W.-K., Faucette, L., Johnson, R. K., Sternglanz, R., Kilne, S., & Laboratories, F. (1988). Evidence that DNA Topoisomerase I Is Necessary for the Cytotoxic Effects of Camptothecin. *Molecular Pharmacology*, *34*, 755–760.

Eppley, S., Hopkin, R. J., Mendelsohn, B., & Slavotinek, A. M. (2017). Clinical Report: Warsaw Breakage Syndrome with small radii and fibulae. *American Journal of Medical Genetics Part A*, *173*(11), 3075–3081. https://doi.org/10.1002/AJMG.A.38382

Estep, K. N., & Brosh, R. M. (2018). RecQ and Fe – S helicases have unique roles in DNA metabolism dictated by their unwinding directionality , substrate specificity , and protein interactions. *Biochemical Society Transactions*, *46*(December 2017), 77–95. https://doi.org/10.1042/BST20170044

Evers, B., Jastrzebski, K., Heijmans, J. P. M., Grernrum, W., Beijersbergen, R. L., & Bernards, R. (2016). CRISPR knockout screening outperforms shRNA and CRISPRi in identifying essential genes. *Nature Biotechnology*, *34*(6), 631–633. https://doi.org/10.1038/nbt.3536

Faramarz, A., Balk, J. A., Schie, J. J. M. van, Oostra, A. B., Ghandour, C. A., Rooimans, M. A., Wolthuis, R. M. F. F., Lange, J. de, van Schie, J. J. M., Oostra, A. B., Ghandour, C. A., Rooimans, M. A., Wolthuis, R. M. F. F., & de Lange, J. (2020). Non-redundant roles in sister chromatid cohesion of the DNA helicase DDX11 and the SMC3 acetyl transferases ESCO1 and ESCO2. *PLoS ONE*, *15*(1), e0220348. https://doi.org/10.1371/journal.pone.0220348

Farina, A., Shin, J. H., Kim, D. H., Bermudez, V. P., Kelman, Z., Seo, Y. S., & Hurwitz, J. (2008). Studies with the human cohesin establishment factor, ChlR1: Association of ChlR1 with Ctf18-RFC and Fen1. *Journal of Biological Chemistry*, *283*(30), 20925–20936. https://doi.org/10.1074/jbc.M802696200

Farmer, H., McCabe, N., Lord, C. J., Tutt, A. N. J. H. J., Johnson, D. A., Richardson, T. B., Santarosa, M., Dillon, K. J., Hickson, I., Knights, C., Martin, N. M. B., Jackson, S. P., Smith, G. C. M., Ashworth, A., McCabe, H., Lord, C. J., Tutt, A. N. J. H. J., Johnson, D. A., Richardson, T. B., … TB, R. (2005). Targeting the DNA repair defect in BRCA mutant cells as a therapeutic strategy. *Nature*, *14*(7035), 917–921. https://doi.org/10.1038/nature03445

Fazi, R., Tintori, C., Brai, A., Botta, L., Selvaraj, M., Garbelli, A., Maga, G., & Botta, M. (2015). Homology Model-Based Virtual Screening for the Identification of Human Helicase DDX3 Inhibitors. *Journal of Chemical Information and Modeling*, *55*(11), 2443–2454. https://doi.org/10.1021/acs.jcim.5b00419

Fernius, J., & Hardwick, K. G. (2007). Bub1 Kinase Targets Sgo1 to Ensure Efficient Chromosome Biorientation in Budding Yeast Mitosis. *PLoS Genetics*, *3*(11), e213. https://doi.org/10.1371/journal.pgen.0030213

Fowler, D. M., & Fields, S. (2014). Deep mutational scanning: A new style of protein science. In *Nature Methods* (Vol. 11, Issue 8, pp. 801–807). Nature Publishing Group. https://doi.org/10.1038/nmeth.3027

Futreal, P. A., Coin, L., Marshall, M., Down, T., Hubbard, T., Wooster, R., Rahman, N., & Stratton, M. R. (2004). A census of human cancer genes. *Nature Reviews Cancer 2004 4:3*, *4*(3), 177–183. https://doi.org/10.1038/nrc1299

Gerring, S. L., Spencer, F., & Hieter, P. (1990). The CHL 1 (CTF 1) gene product of

Saccharomyces cerevisiae is important for chromosome transmission and normal cell cycle progression in G2/M. *The EMBO Journal*, *9*(13), 4347–4358.

Giaever, G., Chu, A. M., Ni, L., Connelly, C., Riles, L., Véronneau, S., Dow, S., Lucau-Danila, A., Anderson, K., André, B., Arkin, A. P., Astromoff, A., Bakkoury, M. El, Bangham, R., Benito, R., Brachat, S., Campanaro, S., Curtiss, M., Davis, K., … Johnston, M. (2002). Functional profiling of the Saccharomyces cerevisiae genome. *Nature*, *418*(6896), 387–391. https://doi.org/10.1038/nature00935

Gilbert, L. A., Horlbeck, M. A., Adamson, B., Villalta, J. E., Chen, Y., Whitehead, E. H., Guimaraes, C., Panning, B., Ploegh, H. L., Bassik, M. C., Qi, L. S., Kampmann, M., & Weissman, J. S. (2014). Genome-Scale CRISPR-Mediated Control of Gene Repression and Activation. *Cell*, *159*(3), 647–661. https://doi.org/10.1016/j.cell.2014.09.029

Gilbert, L. A., Larson, M. H., Morsut, L., Liu, Z., Brar, G. A., Torres, S. E., Stern-Ginossar, N., Brandman, O., Whitehead, E. H., Doudna, J. A., Lim, W. A., Weissman, J. S., & Qi, L. S. (2013). CRISPR-mediated modular RNA-guided regulation of transcription in eukaryotes. *Cell*, *154*(2), 442–451. https://doi.org/10.1016/j.cell.2013.06.044

Greene, A. L., Snipe, J. R., Gordenin, D. A., & Resnick, M. A. (1999). Functional Analysis of Human FEN1 in Saccharomyces Cerevisiae and Its Role in Genome Stability. *Human Molecular Genetics*, *8*(12), 2263–2273. https://doi.org/10.1093/HMG/8.12.2263

Guacci, V., & Koshland, D. (2012). Cohesin-independent segregation of sister chromatids in budding yeast. *Molecular Biology of the Cell*, *23*(4), 729–739. https://doi.org/10.1091/mbc.E11-08-0696

Guacci, V., Koshland, D., & Strunnikov, A. (1997). A Direct Link between Sister Chromatid Cohesion and Chromosome Condensation Revealed through the Analysis of MCD1 in S. cerevisiae. *Cell*, *91*(1), 47–57. https://doi.org/10.1016/S0092-8674(01)80008-8

Guacci, V., Stricklin, J., Bloom, M. S., Guo, X., Bhatter, M., & Koshland, D. (2015). A novel mechanism for the establishment of sister chromatid cohesion by the ECO1 acetyltransferase. *Molecular Biology of the Cell*, *26*(1), 117–133. https://doi.org/10.1091/mbc.E14-08-1268

Guo, M., Hundseth, K., Ding, H., Vidhyasagar, V., Inoue, A., Nguyen, C. H., Zain, R., Lee, J. S., & Wu, Y. (2015). A distinct triplex DNA unwinding activity of ChlR1 helicase. *Journal of Biological Chemistry*, *290*(8), 5174–5189. https://doi.org/10.1074/jbc.M114.634923

Haber, J. E. (1974). Bisexual mating behavior in a diploid of Saccharomyces cerevisiae: evidence for genetically controlled non random chromosome loss during vegetative growth. *Genetics*, *78*(3), 843–858.

Hammerman, P. S., Voet, D., Lawrence, M. S., Voet, D., Jing, R., Cibulskis, K., Sivachenko, A., Stojanov, P., McKenna, A., Lander, E. S., Gabriel, S., Getz, G., Imielinski, M., Helman, E., Hernandez, B., Pho, N. H., Meyerson, M., Chu, A., Hye-Chun, J. E., … Shen, R. (2012). Comprehensive genomic characterization of squamous cell lung cancers. *Nature 2012 489:7417*, *489*(7417), 519–525. https://doi.org/10.1038/nature11404

Hamza, A., Amitzi, L., Ma, L., Driessen, M. R. M., O'Neil, N. J., & Hieter, P. (2021). Modeling DNA trapping of anticancer therapeutic targets using missense mutations identifies dominant synthetic lethal interactions. *Proceedings of the National Academy of Sciences*, *118*(14), e2100240118. https://doi.org/10.1073/pnas.2100240118

Hamza, A., & Baetz, K. (2012). Iron-responsive transcription factor Aft1 interacts with

kinetochore protein Iml3 and promotes pericentromeric cohesin. *Journal of Biological Chemistry*, *287*(6), 4139–4147. https://doi.org/10.1074/jbc.M111.319319

Hamza, A., Driessen, M. R. M., Tammpere, E., O'Neil, N. J., & Hieter, P. (2020). Cross-species complementation of nonessential yeast genes establishes platforms for testing inhibitors of human proteins. *Genetics*, *214*(3), 735–747. https://doi.org/10.1534/genetics.119.302971

Han, K., Jeng, E. E., Hess, G. T., Morgens, D. W., Li, A., & Bassik, M. C. (2017). Synergistic drug combinations for cancer identified in a CRISPR screen for pairwise genetic interactions. *Nature Biotechnology 2017 35:5*, *35*(5), 463–474. https://doi.org/10.1038/nbt.3834

Hanahan, D., & Weinberg, R. A. (2000). The Hallmarks of Cancer. *Cell*, *100*(1), 57–70. https://doi.org/10.1016/S0092-8674(00)81683-9

Hanahan, D., & Weinberg, R. A. (2011). Hallmarks of Cancer: The Next Generation. *Cell*, *144*(5), 646–674. https://doi.org/10.1016/J.CELL.2011.02.013

Hänsel-Hertsch, R., Di Antonio, M., & Balasubramanian, S. (2017). DNA G-quadruplexes in the human genome: detection, functions and therapeutic potential. *Nature Reviews Molecular Cell Biology 2017 18:5*, *18*(5), 279–284. https://doi.org/10.1038/nrm.2017.3

Harris, L., McFarlane-Majeed, L., Campos-León, K., Roberts, S., & Parish, J. L. (2017). The Cellular DNA Helicase ChlR1 Regulates Chromatin and Nuclear Matrix Attachment of the Human Papillomavirus 16 E2 Protein and High-Copy-Number Viral Genome Establishment. *Journal of Virology*, *91*(1), 1853–1869. https://doi.org/10.1128/JVI.01853-16

Hart, T., Chandrashekhar, M., Aregger, M., Steinhart, Z., Brown, K. R., MacLeod, G., Mis, M., Zimmermann, M., Fradet-Turcotte, A., Sun, S., Mero, P., Dirks, P., Sidhu, S., Roth, F. P., Rissland, O. S., Durocher, D., Angers, S., & Moffat, J. (2015). High-Resolution CRISPR Screens Reveal Fitness Genes and Genotype-Specific Cancer Liabilities. *Cell*, *163*(6), 1515–1526. https://doi.org/10.1016/j.cell.2015.11.015

Hart, T., Tong, A. H. Y., Chan, K., Van Leeuwen, J., Seetharaman, A., Aregger, M., Chandrashekhar, M., Hustedt, N., Seth, S., Noonan, A., Habsid, A., Sizova, O., Nedyalkova, L., Climie, R., Tworzyanski, L., Lawson, K., Sartori, M. A., Alibeh, S., Tieu, D., … Moffat, J. (2017). Evaluation and Design of Genome-Wide CRISPR/SpCas9 Knockout Screens. *G3 Genes, Genomes, Genet.*, *7*(8), 2719–2727. https://doi.org/10.1534/g3.117.041277

Hartwell, L. H., Szankasi, P., Roberts, C. J., Murray, A. W., & Friend, S. H. (1997). Integrating genetic approaches into the discovery of anticancer drugs. *Science*, *278*(5340), 1064–1068. https://doi.org/10.1126/science.278.5340.1064

Henkel, L., Rauscher, B., & Boutros, M. (2019). Context-dependent genetic interactions in cancer. *Current Opinion in Genetics & Development*, *54*, 73–82. https://doi.org/10.1016/J.GDE.2019.03.004

Hill, V. K., Kim, J. S., & Waldman, T. (2016). Cohesin mutations in human cancer. *Biochimica et Biophysica Acta - Reviews on Cancer*, *1866*(1), 1–11. https://doi.org/10.1016/j.bbcan.2016.05.002

Hirota, Y., & Lahti, J. M. (2000). Characterization of the enzymatic activity of hChlR1, a novel human DNA helicase. *Nucleic Acids Research*, *28*(4), 917–924. http://www.ncbi.nlm.nih.gov/pubmed/10648783

Hoadley, K. A., Yau, C., Hinoue, T., Wolf, D. M., Lazar, A. J., Drill, E., Shen, R., Taylor, A. M., Cherniack, A. D., Thorsson, V., Akbani, R., Bowlby, R., Wong, C. K., Wiznerowicz, M., Sanchez-Vega, F., Robertson, A. G., Schneider, B. G., Lawrence, M. S., Noushmehr, H., … Laird, P. W. (2018). Cell-of-Origin Patterns Dominate the Molecular Classification of 10,000 Tumors from 33 Types of Cancer. *Cell*, *173*(2), 291-304.e6. https://doi.org/10.1016/J.CELL.2018.03.022

Hoadley, K. A., Yau, C., Wolf, D. M., Cherniack, A. D., Tamborero, D., Ng, S., Leiserson, M. D. M., Niu, B., McLellan, M. D., Uzunangelov, V., Zhang, J., Kandoth, C., Akbani, R., Shen, H., Omberg, L., Chu, A., Margolin, A. A., Veer, L. J. van't, Lopez-Bigas, N., … Stuart, J. M. (2014). Multiplatform Analysis of 12 Cancer Types Reveals Molecular Classification within and across Tissues of Origin. *Cell*, *158*(4), 929–944. https://doi.org/10.1016/J.CELL.2014.06.049

Holloway, S. L. (2000). CHL1 is a nuclear protein with an essential ATP binding site that exhibits a size-dependent effect on chromosome segregation. *Nucleic Acids Research*, *28*(16), 3056–3064. https://doi.org/10.1093/nar/28.16.3056

Hsiehchen, D., & Hsieh, A. (2018). Nearing saturation of cancer driver gene discovery. *Journal of Human Genetics 2018 63:9*, *63*(9), 941–943. https://doi.org/10.1038/s10038-018-0481-4

Hu, Y., Rolfs, A., Bhullar, B., Murthy, T. V. S., Zhu, C., Berger, M. F., Camargo, A. A., Kelley, F., McCarron, S., Jepson, D., Richardson, A., Raphael, J., Moreira, D., Taycher, E., Zuo, D., Mohr, S., Kane, M. F., Williamson, J., Simpson, A., … LaBaer, J. (2007). Approaching a complete repository of sequence-verified protein-encoding clones for Saccharomyces cerevisiae. *Genome Research*, *17*(4), 536–543. https://doi.org/10.1101/gr.6037607

Hyman, D. M., Taylor, B. S., & Baselga, J. (2017). Implementing Genome-Driven Oncology. *Cell*, *168*(4), 584–599. https://doi.org/10.1016/j.cell.2016.12.015

Inoue, A., Li, T., Roby, S. K., Valentine, M. B., Inoue, M., Boyd, K., Kidd, V. J., & Lahti, J. M. (2007). Loss of ChlR1 helicase in mouse causes lethality due to the accumulation of aneuploid cells generated by cohesion defects and placental malformation. *Cell Cycle*, *6*(13), 1646–1654. https://doi.org/10.4161/cc.6.13.4411

Jegadesan, N. K., & Branzei, D. (2021). DDX11 loss causes replication stress and pharmacologically exploitable DNA repair defects. *Proceedings of the National Academy of Sciences*, *118*(17). https://doi.org/10.1073/PNAS.2024258118

Kabadi, A. M., Ousterout, D. G., Hilton, I. B., & Gersbach, C. A. (2014). Multiplex CRISPR/Cas9-based genome engineering from a single lentiviral vector. *Nucleic Acids Research*, *42*(19), e147–e147. https://doi.org/10.1093/nar/gku749

Kampmann, M., Bassik, M. C., & Weissman, J. S. (2013). Integrated platform for genome-wide screening and construction of high-density genetic interaction maps in mammalian cells. *Proceedings of the National Academy of Sciences*, *110*(25), E2317–E2326. https://doi.org/10.1073/PNAS.1307002110

Khan, I., Suhasini, A. N., Banerjee, T., Sommers, J. A., Kaplan, D. L., Kuper, J., Kisker, C., & Brosh, R. M. (2014). Impact of age-associated cyclopurine lesions on DNA repair helicases. *PLoS ONE*, *9*(11), 1–13. https://doi.org/10.1371/journal.pone.0113293

Kim, E., Dede, M., Lenoir, W. F., Wang, G., Srinivasan, S., Colic, M., & Hart, T. (2019). A network of human functional gene interactions from knockout fitness screens in cancer cells. *Life Science Alliance*, *2*(2), e201800278. https://doi.org/10.26508/LSA.201800278

Kim, J. S., He, X., Orr, B., Wutz, G., Hill, V., Peters, J. M., Compton, D. A., & Waldman, T. (2016). Intact Cohesion, Anaphase, and Chromosome Segregation in Human Cells Harboring Tumor-Derived Mutations in STAG2. *PLoS Genetics*, *12*(2), 1–18. https://doi.org/10.1371/journal.pgen.1005865

Koboldt, D. C., Fulton, R. S., McLellan, M. D., Schmidt, H., Kalicki-Veizer, J., McMichael, J. F., Fulton, L. L., Dooling, D. J., Ding, L., Mardis, E. R., Wilson, R. K., Ally, A., Balasundaram, M., Butterfield, Y. S. N., Carlsen, R., Carter, C., Chu, A., Chuah, E., Chun, H. J. E., … Palchik, J. D. (2012). Comprehensive molecular portraits of human breast tumours. *Nature 2012 490:7418*, *490*(7418), 61–70. https://doi.org/10.1038/nature11412

Koch, E. N., Costanzo, M., Bellay, J., Deshpande, R., Chatfield-Reed, K., Chua, G., D'Urso, G., Andrews, B. J., Boone, C., & Myers, C. L. (2012). Conserved rules govern genetic interaction degree across species. *Genome Biology 2012 13:7*, *13*(7), 1–15. https://doi.org/10.1186/GB-2012-13-7-R57

Kon, A., Shih, L.-Y., Minamino, M., Sanada, M., Shiraishi, Y., Nagata, Y., Yoshida, K., Okuno, Y., Bando, M., Nakato, R., Ishikawa, S., Sato-Otsubo, A., Nagae, G., Nishimoto, A., Haferlach, C., Nowak, D., Sato, Y., Alpermann, T., Nagasaki, M., … Ogawa, S. (2013). Recurrent mutations in multiple components of the cohesin complex in myeloid neoplasms. *Nature Genetics 2013 45:10*, *45*(10), 1232–1237. https://doi.org/10.1038/ng.2731

Ku, A. A., Hu, H.-M., Zhao, X., Shah, K. N., Kongara, S., Wu, D., McCormick, F., Balmain, A., & Bandyopadhyay, S. (2020). Integration of multiple biological contexts reveals principles of synthetic lethality that affect reproducibility. *Nature Communications 2020 11:1*, *11*(1), 1–12. https://doi.org/10.1038/s41467-020-16078-y

Laha, S. S., Das, S. P., Hajra, S., Sanyal, K., & Sinha, P. (2011). Functional characterization of the Saccharomyces cerevisiae protein Chl1 reveals the role of sister chromatid cohesion in the maintenance of spindle length during S-phase arrest. *BMC Genetics*, *12*. https://doi.org/10.1186/1471-2156-12-83

Laha, S. S., Das, S. P., Hajra, S., Sau, S., & Sinha, P. (2006). The budding yeast protein Chl1p is required to preserve genome integrity upon DNA damage in S-phase. *Nucleic Acids Research*, *34*(20), 5880–5891. https://doi.org/10.1093/nar/gkl749

Lander, E. S., Linton, L. M., Birren, B., Nusbaum, C., Zody, M. C., Baldwin, J., Devon, K., Dewar, K., Doyle, M., Fitzhugh, W., Funke, R., Gage, D., Harris, K., Heaford, A., Howland, J., Kann, L., Lehoczky, J., Levine, R., McEwan, P., … Morgan, M. J. (2001). Initial sequencing and analysis of the human genome. *Nature 2001 409:6822*, *409*(6822), 860–921. https://doi.org/10.1038/35057062

Lawrence, M. S., Stojanov, P., Mermel, C. H., Robinson, J. T., Garraway, L. A., Golub, T. R., Meyerson, M., Gabriel, S. B., Lander, E. S., & Getz, G. (2014). Discovery and saturation analysis of cancer genes across 21 tumour types. *Nature*, *505*(7484), 495–501. https://doi.org/10.1038/nature12912

Leman, A. R., Noguchi, C., Lee, C. Y., & Noguchi, E. (2010). Human Timeless and Tipin stabilize replication forks and facilitate sister-chromatid cohesion. *Journal of Cell Science*, *123*(5), 660–670. https://doi.org/10.1242/jcs.057984

Lerner, L. K., Holzer, S., Kilkenny, M. L., Šviković, S., Murat, P., Schiavone, D., Eldridge, C. B., Bittleston, A., Maman, J. D., Branzei, D., Stott, K., Pellegrini, L., & Sale, J. E. (2020). Timeless couples G-quadruplex detection with processing by DDX11 helicase during DNA

replication. *The EMBO Journal*, *39*(18), e104185. https://doi.org/10.15252/embj.2019104185

Li, J., Liu, L., Liu, X., Xu, P., Hu, Q., & Yu, Y. (2019). The Role of Upregulated DDX11 as A Potential Prognostic and Diagnostic Biomarker in Lung Adenocarcinoma. *Journal of Cancer*, *10*(18), 4208. https://doi.org/10.7150/JCA.33457

Liang, C., Chen, Q., Yi, Q., Zhang, M., Yan, H., Zhang, B., Zhou, L., Zhang, Z., Qi, F., Ye, S., & Wang, F. (2018). A kinase-dependent role for Haspin in antagonizing Wapl and protecting mitotic centromere cohesion. *EMBO Reports*, *19*(1), 43–56. https://doi.org/10.15252/embr.201744737

Liras, P., McCusker, J., Mascioli, S., & Haber, J. E. (1978). Characterization of a mutation in yeast causing nonrandom chromosome loss during mitosis. *Genetics*, *88*(4 Pt 1), 651–671.

Liu, W., Zhou, M., Li, Z., Li, H., Polaczek, P., Dai, H., Wu, Q., Liu, C., Karanja, K. K., Popuri, V., Shan, S. O., Schlacher, K., Zheng, L., Campbell, J. L., & Shen, B. (2016). A Selective Small Molecule DNA2 Inhibitor for Sensitization of Human Cancer Cells to Chemotherapy. *EBioMedicine*, *6*, 73–86. https://doi.org/10.1016/j.ebiom.2016.02.043

Liu, Y., Xu, H., Van Der Jeught, K., Li, Y., Liu, S., Zhang, L., Fang, Y., Zhang, X., Radovich, M., Schneider, B. P., He, X., Huang, C., Zhang, C., Wan, J., Ji, G., & Lu, X. (2018). Somatic mutation of the cohesin complex subunit confers therapeutic vulnerabilities in cancer. *The Journal of Clinical Investigation*, *128*(7), 2951–2965. https://doi.org/10.1172/JCI98727

Lord, C. J., & Ashworth, A. (2016). BRCAness revisited. *Nature Reviews Cancer 2016 16:2*, *16*(2), 110–120. https://doi.org/10.1038/nrc.2015.21

Lord, C. J., & Ashworth, A. (2017). PARP inhibitors: Synthetic lethality in the clinic. *Science*, *355*(6330), 1152–1158. https://doi.org/10.1126/SCIENCE.AAM7344

Losada, A., Hirano, M., & Hirano, T. (1998). Identification of Xenopus SMC protein complexes required for sister chromatid cohesion. *Genes & Development*, *12*(13), 1986. https://doi.org/10.1101/GAD.12.13.1986

Losada, A., Yokochi, T., Kobayashi, R., & Hirano, T. (2000). Identification and characterization of SA/Scc3p subunits in the Xenopus and human cohesin complexes. *Journal of Cell Biology*, *150*(3), 405–416. https://doi.org/10.1083/jcb.150.3.405

MacConaill, L. E., & Garraway, L. A. (2010). Clinical Implications of the Cancer Genome. *Journal of Clinical Oncology*, *28*(35), 5219. https://doi.org/10.1200/JCO.2009.27.4944

Mair, B., Moffat, J., Boone, C., & Andrews, B. J. (2019). Genetic interaction networks in cancer cells. *Current Opinion in Genetics and Development*, *54*, 64–72. https://doi.org/10.1016/j.gde.2019.03.002

Mali, P., Yang, L., Esvelt, K. M., Aach, J., Guell, M., DiCarlo, J. E., Norville, J. E., & Church, G. M. (2013). RNA-guided human genome engineering via Cas9. *Science*, *339*(6121), 823–826. https://doi.org/10.1126/science.1232033

Malone, E. R., Oliva, M., Sabatini, P. J. B., Stockley, T. L., & Siu, L. L. (2020). Molecular profiling for precision cancer therapies. *Genome Medicine 2020 12:1*, *12*(1), 1–19. https://doi.org/10.1186/S13073-019-0703-1

Marchese, F. P., Grossi, E., Marín-Béjar, O., Bharti, S. K., Raimondi, I., González, J., Martínez-Herrera, D. J., Athie, A., Amadoz, A., Brosh, R. M., & Huarte, M. (2016). A Long

Noncoding RNA Regulates Sister Chromatid Cohesion. *Molecular Cell*, *63*(3), 397–407. https://doi.org/10.1016/j.molcel.2016.06.031

Martínez-Jiménez, F., Muiños, F., Sentís, I., Deu-Pons, J., Reyes-Salazar, I., Arnedo-Pac, C., Mularoni, L., Pich, O., Bonet, J., Kranas, H., Gonzalez-Perez, A., & Lopez-Bigas, N. (2020). A compendium of mutational cancer driver genes. *Nature Reviews Cancer 2020 20:10*, *20*(10), 555–572. https://doi.org/10.1038/s41568-020-0290-x

Massard, C., Michiels, S., Ferté, C., Deley, M.-C. Le, Lacroix, L., Hollebecque, A., Verlingue, L., Ileana, E., Rosellini, S., Ammari, S., Ngo-Camus, M., Bahleda, R., Gazzah, A., Varga, A., Postel-Vinay, S., Loriot, Y., Even, C., Breuskin, I., Auger, N., … Soria, J.-C. (2017). High-Throughput Genomics and Clinical Outcome in Hard-to-Treat Advanced Cancers: Results of the MOSCATO 01 Trial. *Cancer Discovery*, *7*(6), 586–595. https://doi.org/10.1158/2159-8290.CD-16-1396

Mayer, M. L., Gygi, S. P., Aebersold, R., & Hieter, P. (2001). Identification of RFC(Ctf18p, Ctf8p, Dcc1p): An alternative RFC complex required for sister chromatid cohesion in S. cerevisiae. *Molecular Cell*, *7*(5), 959–970. https://doi.org/10.1016/S1097-2765(01)00254-4

Mayer, M. L., Pot, I., Chang, M., Xu, H., Aneliunas, V., Kwok, T., Newitt, R., Aebersold, R., Boone, C., Brown, G. W., & Hieter, P. (2004). Identification of protein complexes required for efficient sister chromatid cohesion. *Molecular Biology of the Cell*, *15*(4), 1736–1745. https://doi.org/10.1091/mbc.E03-08-0619

McDonald, E. R., Weck, A. de, Schlabach, M. R., Billy, E., Mavrakis, K. J., Hoffman, G. R., Belur, D., Castelletti, D., Frias, E., Gampa, K., Golji, J., Kao, I., Li, L., Megel, P., Perkins, T. A., Ramadan, N., Ruddy, D. A., Silver, S. J., Sovath, S., … Sellers, W. R. (2017). Project DRIVE: A Compendium of Cancer Dependencies and Synthetic Lethal Relationships Uncovered by Large-Scale, Deep RNAi Screening. *Cell*, *170*(3), 577-592.e10. https://doi.org/10.1016/J.CELL.2017.07.005

McLellan, J., O'Neil, N. J., Barrett, I., Ferree, E., van Pel, D. M., Ushey, K., Sipahimalani, P., Bryan, J., Rose, A. M., & Hieter, P. (2012). Synthetic lethality of cohesins with PARPs and replication fork mediators. *PLoS Genetics*, *8*(3). https://doi.org/10.1371/journal.pgen.1002574

McLellan, J., O'Neil, N., Tarailo, S., Stoepel, J., Bryan, J., Rose, A., & Hieter, P. (2009). Synthetic lethal genetic interactions that decrease somatic cell proliferation in Caenorhabditis elegans identify the alternative RFC CTF18 as a candidate cancer drug target. *Molecular Biology of the Cell*, *20*(24), 5306–5313. https://doi.org/10.1091/mbc.E09-08-0699

McLendon, R., Friedman, A., Bigner, D., Van Meir, E. G., Brat, D. J., Mastrogianakis, G. M., Olson, J. J., Mikkelsen, T., Lehman, N., Aldape, K., Yung, W. K. A., Bogler, O., Weinstein, J. N., VandenBerg, S., Berger, M., Prados, M., Muzny, D., Morgan, M., Scherer, S., … Thomson, E. (2008). Comprehensive genomic characterization defines human glioblastoma genes and core pathways. *Nature 2008 455:7216*, *455*(7216), 1061–1068. https://doi.org/10.1038/nature07385

McManus, K. J., Barrett, I. J., Nouhi, Y., & Hieter, P. (2009). Specific synthetic lethal killing of RAD54B-deficient human colorectal cancer cells by FEN1 silencing. *Proceedings of the National Academy of Sciences*, *106*(9), 3276–3281. https://doi.org/10.1073/pnas.0813414106

Megonigal, M. D., Fertala, J., & Bjornsti, M.-A. (1997). Alterations in the Catalytic Activity of Yeast DNA Topoisomerase I Result in Cell Cycle Arrest and Cell Death. *Journal of Biological Chemistry*, *272*(19), 12801–12808. https://doi.org/10.1074/JBC.272.19.12801

Mendoza, O., Gueddouda, N. M., Boulé, J.-B., Bourdoncle, A., & Mergny, J.-L. (2015). A fluorescence-based helicase assay: application to the screening of G-quadruplex ligands. *Nucleic Acids Research*, *43*(11), 1–10. https://doi.org/10.1093/nar/gkv193

Menolfi, D., & Zha, S. (2020). ATM, ATR and DNA-PKcs kinases—the lessons from the mouse models: inhibition ≠ deletion. *Cell & Bioscience 2020 10:1*, *10*(1), 1–15. https://doi.org/10.1186/S13578-020-0376-X

Meyers, R. M., Bryan, J. G., McFarland, J. M., Weir, B. A., Sizemore, A. E., Xu, H., Dharia, N. V, Montgomery, P. G., Cowley, G. S., Pantel, S., Goodale, A., Lee, Y., Ali, L. D., Jiang, G., Lubonja, R., Harrington, W. F., Strickland, M., Wu, T., Hawes, D. C., … Tsherniak, A. (2017). Computational correction of copy number effect improves specificity of CRISPR–Cas9 essentiality screens in cancer cells. *Nature Genetics 2017 49:12*, *49*(12), 1779–1784. https://doi.org/10.1038/ng.3984

Mi, H., Ebert, D., Muruganujan, A., Mills, C., Albou, L.-P., Mushayamaha, T., & Thomas, P. D. (2021). PANTHER version 16: a revised family classification, tree-based classification tool, enhancer regions and extensive API. *Nucleic Acids Research*, *49*(D1), D394–D403. https://doi.org/10.1093/NAR/GKAA1106

Miao, Z.-H., Player, A., Shankavaram, U., Wang, Y.-H., Zimonjic, D. B., Lorenzi, P. L., Liao, Z.-Y., Liu, H., Shimura, T., Zhang, H.-L., Meng, L.-H., Zhang, Y.-W., Kawasaki, E. S., Popescu, N. C., Aladjem, M. I., Goldstein, D. J., Weinstein, J. N., & Pommier, Y. (2007). Nonclassic Functions of Human Topoisomerase I: Genome-Wide and Pharmacologic Analyses. *Cancer Research*, *67*(18), 8752–8761. https://doi.org/10.1158/0008-5472.CAN-06-4554

Michaelis, C., Ciosk, R., & Nasmyth, K. (1997). Cohesins: Chromosomal proteins that prevent premature separation of sister chromatids. *Cell*, *91*(1), 35–45. https://doi.org/10.1016/S0092-8674(01)80007-6

Mojumdar, A., & Deka, J. (2019). Assaying the Activity of Helicases: An Overview. *Helicases from All Domains of Life*, 235–246. https://doi.org/10.1016/B978-0-12-814685-9.00014-2

Morales, C., & Losada, A. (2018). Establishing and dissolving cohesion during the vertebrate cell cycle. *Current Opinion in Cell Biology*, *52*, 51–57. https://doi.org/10.1016/J.CEB.2018.01.010

Morgens, D. W., Deans, R. M., Li, A., & Bassik, M. C. (2016). Systematic comparison of CRISPR/Cas9 and RNAi screens for essential genes. *Nature Biotechnology 2016 34:6*, *34*(6), 634–636. https://doi.org/10.1038/nbt.3567

Morita, K., & Sasaki, K. (2021). Current status and novel strategy of CML. *International Journal of Hematology 2021 113:5*, *113*(5), 624–631. https://doi.org/10.1007/S12185-021-03127-5

Munoz, D. M., Cassiani, P. J., Li, L., Billy, E., Korn, J. M., Jones, M. D., Golji, J., Ruddy, D. A., Yu, K., McAllister, G., DeWeck, A., Abramowski, D., Wan, J., Shirley, M. D., Neshat, S. Y., Rakiec, D., Beaumont, R. de, Weber, O., Kauffmann, A., … Schlabach, M. R. (2016). CRISPR Screens Provide a Comprehensive Assessment of Cancer Vulnerabilities but Generate False-Positive Hits for Highly Amplified Genomic Regions. *Cancer Discovery*,

6(8), 900–913. https://doi.org/10.1158/2159-8290.CD-16-0178

Murai, J., Huang, S.-Y. N., Renaud, A., Zhang, Y., Ji, J., Takeda, S., Morris, J., Teicher, B., Doroshow, J. H., & Pommier, Y. (2014). Stereospecific PARP trapping by BMN 673 and comparison with olaparib and rucaparib. *Molecular Cancer Therapeutics*, *13*(2), 433–443. https://doi.org/10.1158/1535-7163.MCT-13-0803

Murai, J., Huang, S. -y. N., Das, B. B., Renaud, A., Zhang, Y., Doroshow, J. H., Ji, J., Takeda, S., & Pommier, Y. (2012). Trapping of PARP1 and PARP2 by Clinical PARP Inhibitors. *Cancer Research*, *72*(21), 5588–5599. https://doi.org/10.1158/0008-5472.CAN-12-2753

Murai, J., Zhang, Y., Morris, J., Ji, J., Takeda, S., Doroshow, J. H., & Pommier, Y. (2014). Rationale for Poly(ADP-ribose) Polymerase (PARP) Inhibitors in Combination Therapy with Camptothecins or Temozolomide Based on PARP Trapping versus Catalytic Inhibition. *The Journal of Pharmacology and Experimental Therapeutics*, *349*(3), 408. https://doi.org/10.1124/JPET.113.210146

Murayama, Y., Samora, C. P., Kurokawa, Y., Iwasaki, H., & Uhlmann, F. (2018). Establishment of DNA-DNA Interactions by the Cohesin Ring. *Cell*, *172*(3), 465-477.e15. https://doi.org/10.1016/J.CELL.2017.12.021

Muzny, D. M., Bainbridge, M. N., Chang, K., Dinh, H. H., Drummond, J. A., Fowler, G., Kovar, C. L., Lewis, L. R., Morgan, M. B., Newsham, I. F., Reid, J. G., Santibanez, J., Shinbrot, E., Trevino, L. R., Wu, Y. Q., Wang, M., Gunaratne, P., Donehower, L. A., Creighton, C. J., … Thomson., E. (2012). Comprehensive molecular characterization of human colon and rectal cancer. *Nature 2012 487:7407*, *487*(7407), 330–337. https://doi.org/10.1038/nature11252

Nguyen, G. H., Dexheimer, T. S., Rosenthal, A. S., Chu, W. K., Singh, D. K., Mosedale, G., Bachrati, C. Z., Schultz, L., Sakurai, M., Savitsky, P., Abu, M., McHugh, P. J., Bohr, V. A., Harris, C. C., Jadhav, A., Gileadi, O., Maloney, D. J., Simeonov, A., & Hickson, I. D. (2013). A small molecule inhibitor of the BLM helicase modulates chromosome stability in human cells. *Chemistry and Biology*, *20*(1), 55–62. https://doi.org/10.1016/j.chembiol.2012.10.016

Nitiss, J., & Wang, J. C. (1988). DNA topoisomerase-targeting antitumor drugs can be studied in yeast. *Proceedings of the National Academy of Sciences*, *85*(20), 7501–7505. https://doi.org/10.1073/PNAS.85.20.7501

Novoa, C. A., Ang, J. S., & Stirling, P. C. (2018). The A-like faker assay for measuring yeast chromosome III stability. In *Methods in Molecular Biology* (Vol. 1672, pp. 1–9). Humana Press Inc. https://doi.org/10.1007/978-1-4939-7306-4_1

O'Neil, N. J., Bailey, M. L., & Hieter, P. (2017). Synthetic lethality and cancer. *Nature Reviews Genetics*, *18*(10), 613–623. https://doi.org/10.1038/nrg.2017.47

O'Neil, N. J., van Pel, D. M., & Hieter, P. (2013). Synthetic lethality and cancer: Cohesin and PARP at the replication fork. *Trends in Genetics*, *29*(5), 290–297. https://doi.org/10.1016/j.tig.2012.12.004

Özeş, A. R., Feoktistova, K., Avanzino, B. C., & Fraser, C. S. (2011). Duplex Unwinding and ATPase Activities of the DEAD-Box Helicase eIF4A Are Coupled by eIF4G and eIF4B. *Journal of Molecular Biology*, *412*(4), 674–687. https://doi.org/10.1016/J.JMB.2011.08.004

Pacini, C., Dempster, J. M., Boyle, I., Gonçalves, E., Najgebauer, H., Karakoc, E., Meer, D. van der, Barthorpe, A., Lightfoot, H., Jaaks, P., McFarland, J. M., Garnett, M. J., Tsherniak, A., & Iorio, F. (2021). Integrated cross-study datasets of genetic dependencies in cancer. *Nature*

Communications 2021 12:1, *12*(1), 1–14. https://doi.org/10.1038/s41467-021-21898-7

Padget, K., Carr, R., Pearson, A. D. J., Tilby, M. J., & Austin, C. A. (2000). Camptothecin-stabilised topoisomerase I–DNA complexes in leukaemia cells visualised and quantified in situ by the TARDIS assay (trapped in agarose DNA immunostaining). *Biochemical Pharmacology*, *59*(6), 629–638. https://doi.org/10.1016/S0006-2952(99)00372-X

Pagliarini, R., Shao, W., & Sellers, W. R. (2015). Oncogene addiction: pathways of therapeutic response, resistance, and road maps toward a cure. *EMBO Reports*, *16*(3), 280–296. https://doi.org/10.15252/EMBR.201439949

Parelho, V., Hadjur, S., Spivakov, M., Leleu, M., Sauer, S., Gregson, H. C., Jarmuz, A., Canzonetta, C., Webster, Z., Nesterova, T., Cobb, B. S., Yokomori, K., Dillon, N., Aragon, L., Fisher, A. G., & Merkenschlager, M. (2008). Cohesins Functionally Associate with CTCF on Mammalian Chromosome Arms. *Cell*, *132*(3), 422–433. https://doi.org/10.1016/J.CELL.2008.01.011

Parish, J. L., Bean, A. M., Park, R. B., & Androphy, E. J. (2006). ChlR1 Is Required for Loading Papillomavirus E2 onto Mitotic Chromosomes and Viral Genome Maintenance. *Molecular Cell*, *24*(6), 867–876. https://doi.org/10.1016/J.MOLCEL.2006.11.005

Parish, J. L., Rosa, J., Wang, X., Lahti, J. M., Doxsey, S. J., & Androphy, E. J. (2006). The DNA helicase ChlR1 is required for sister chromatid cohesion in mammalian cells. *Journal of Cell Science*, *119*(23), 4857–4865. https://doi.org/10.1242/jcs.03262

Pearl, L. H., Schierz, A. C., Ward, S. E., Al-Lazikani, B., & Pearl, F. M. G. G. (2015). Therapeutic opportunities within the DNA damage response. *Nature Reviews Cancer*, *15*(3), 166–180. https://doi.org/10.1038/nrc3891

Petronczki, M., Chwalla, B., Siomos, M. F., Yokobayashi, S., Helmhart, W., Deutschbauer, A. M., Davis, R. W., Watanabe, Y., & Nasmyth, K. (2004). Sister-chromatid cohesion mediated by the alternative RFC-Ctf18/Dcc1/Ctf8, the helicase Chl1 and the polymerase-alpha-associated protein Ctf4 is essential for chromatid disjunction during meiosis II. *Journal of Cell Science*, *117*(16), 3547–3559. https://doi.org/10.1242/jcs.01231

Pettitt, S. J., Krastev, D. B., Brandsma, I., Dréan, A., Song, F., Aleksandrov, R., Harrell, M. I., Menon, M., Brough, R., Campbell, J., Frankum, J., Ranes, M., Pemberton, H. N., Rafiq, R., Fenwick, K., Swain, A., Guettler, S., Lee, J.-M., Swisher, E. M., … Lord, C. J. (2018). Genome-wide and high-density CRISPR-Cas9 screens identify point mutations in PARP1 causing PARP inhibitor resistance. *Nature Communications 2018 9:1*, *9*(1), 1–14. https://doi.org/10.1038/s41467-018-03917-2

Piccart-Gebhart, M. J., Procter, M., Leyland-Jones, B., Goldhirsch, A., Untch, M., Smith, I., Gianni, L., Baselga, J., Bell, R., Jackisch, C., Cameron, D., Dowsett, M., Barrios, C. H., Steger, G., Huang, C.-S., Andersson, M., Inbar, M., Lichinitser, M., Láng, I., … Gelber, R. D. (2005). Trastuzumab after adjuvant chemotherapy in HER2-positive breast cancer. *The New England Journal of Medicine*, *353*(16), 1659–1672. https://doi.org/10.1056/NEJMOA052306

Pisani, F. M., Napolitano, E., Napolitano, L. M. R. R., & Onesti, S. (2018). Molecular and cellular functions of the warsaw breakage syndrome DNA helicase DDX11. *Genes*, *9*(11), 564. https://doi.org/10.3390/genes9110564

Pommier, Y. (2013). Drugging Topoisomerases: Lessons and Challenges. *ACS Chemical Biology*, *8*(1), 82–95. https://doi.org/10.1021/CB300648V

Pommier, Y., O'Connor, M. J., & De Bono, J. (2016). Laying a trap to kill cancer cells: PARP inhibitors and their mechanisms of action. *Science Translational Medicine*, *8*(362), 1–8. https://doi.org/10.1126/scitranslmed.aaf9246

Psakhye, I., & Branzei, D. (2021). SMC complexes are guarded by the SUMO protease Ulp2 against SUMO-chain-mediated turnover. *Cell Reports*, *36*(5), 109485. https://doi.org/10.1016/J.CELREP.2021.109485

Rancati, G., Moffat, J., Typas, A., & Pavelka, N. (2017). Emerging and evolving concepts in gene essentiality. *Nature Reviews Genetics 2017 19:1*, *19*(1), 34–49. https://doi.org/10.1038/nrg.2017.74

Reid, R. J. D., González-Barrera, S., Sunjevaric, I., Alvaro, D., Ciccone, S., Wagner, M., & Rothstein, R. (2011). Selective ploidy ablation, a high-throughput plasmid transfer protocol, identifies new genes affecting topoisomerase I–induced DNA damage. *Genome Research*, *21*(3), 477–486. https://doi.org/10.1101/GR.109033.110

Reuvers, T. G. A., Kanaar, R., & Nonnekens, J. (2020). DNA Damage-Inducing Anticancer Therapies: From Global to Precision Damage. *Cancers*, *12*(8), 2098. https://doi.org/10.3390/cancers12082098

Robert, C., Karaszewska, B., Schachter, J., Rutkowski, P., Mackiewicz, A., Stroiakovski, D., Lichinitser, M., Dummer, R., Grange, F., Mortier, L., Chiarion-Sileni, V., Drucis, K., Krajsova, I., Hauschild, A., Lorigan, P., Wolter, P., Long, G. V., Flaherty, K., Nathan, P., … Schadendorf, D. (2015). Improved Overall Survival in Melanoma with Combined Dabrafenib and Trametinib. *The New England Journal of Medicine*, *372*(1), 30–39. https://doi.org/10.1056/NEJMOA1412690

Roguev, A., Talbot, D., Negri, G. L., Shales, M., Cagney, G., Bandyopadhyay, S., Panning, B., & Krogan, N. J. (2013). Quantitative genetic-interaction mapping in mammalian cells. *Nature Methods 2013 10:5*, *10*(5), 432–437. https://doi.org/10.1038/nmeth.2398

Rowley, J. D. (1973). A New Consistent Chromosomal Abnormality in Chronic Myelogenous Leukaemia identified by Quinacrine Fluorescence and Giemsa Staining. *Nature 1973 243:5405*, *243*(5405), 290–293. https://doi.org/10.1038/243290a0

Rubio, E. D., Reiss, D. J., Welcsh, P. L., Disteche, C. M., Filippova, G. N., Baliga, N. S., Aebersold, R., Ranish, J. A., & Krumm, A. (2008). CTCF physically links cohesin to chromatin. *Proceedings of the National Academy of Sciences*, *105*(24), 8309–8314. https://doi.org/10.1073/PNAS.0801273105

Rudra, S., & Skibbens, R. V. (2012). Sister chromatid cohesion establishment occurs in concert with lagging strand synthesis. *Cell Cycle*, *11*(11), 2114–2121. https://doi.org/10.4161/cc.20547

Rudra, S., & Skibbens, R. V. (2013). Chl1 DNA Helicase Regulates Scc2 Deposition Specifically during DNA-Replication in Saccharomyces cerevisiae. *PLoS ONE*, *8*(9), 1–17. https://doi.org/10.1371/journal.pone.0075435

Sajesh, B. V., Bailey, M., Lichtensztejn, Z., Hieter, P., & McManus, K. J. (2013). Synthetic lethal targeting of superoxide dismutase 1 selectively kills RAD54B-deficient colorectal cancer cells. *Genetics*, *195*(3), 757–767. https://doi.org/10.1534/genetics.113.156836

Samora, C. P., Saksouk, J., Goswami, P., Wade, B. O., Singleton, M. R., Bates, P. A., Lengronne, A., Costa, A., & Uhlmann, F. (2016). Ctf4 Links DNA Replication with Sister Chromatid Cohesion Establishment by Recruiting the Chl1 Helicase to the Replisome.

Molecular Cell, *63*(3), 371–384. https://doi.org/10.1016/j.molcel.2016.05.036

Sanchez-Vega, F., Mina, M., Armenia, J., Chatila, W. K., Luna, A., La, K. C., Dimitriadoy, S., Liu, D. L., Kantheti, H. S., Saghafinia, S., Chakravarty, D., Daian, F., Gao, Q., Bailey, M. H., Liang, W.-W., Foltz, S. M., Shmulevich, I., Ding, L., Heins, Z., … Schultz, N. (2018). Oncogenic Signaling Pathways in The Cancer Genome Atlas. *Cell*, *173*(2), 321-337.e10. https://doi.org/10.1016/J.CELL.2018.03.035

Satoh, M. S., & Lindahl, T. (1992). Role of poly(ADP-ribose) formation in DNA repair. *Nature 1992 356:6367*, *356*(6367), 356–358. https://doi.org/10.1038/356356a0

Sawyers, C. L. (2009). Finding and Drugging the Vulnerabilities of RAS-Dependent Cancers. *Cell*, *137*(5), 796–798. https://doi.org/10.1016/J.CELL.2009.05.011

Schneider, S., Hotz, H.-R., & Schwer, B. (2002). Characterization of Dominant-negative Mutants of the DEAH-box Splicing Factors Prp22 and Prp16. *Journal of Biological Chemistry*, *277*(18), 15452–15458. https://doi.org/10.1074/JBC.M112473200

Schwer, B., & Meszaros, T. (2000). RNA helicase dynamics in pre-mRNA splicing. *The EMBO Journal*, *19*(23), 6582. https://doi.org/10.1093/EMBOJ/19.23.6582

Shah, N., Inoue, A., Woo Lee, S., Beishline, K., Lahti, J. M., & Noguchi, E. (2013). Roles of ChlR1 DNA helicase in replication recovery from DNA damage. *Experimental Cell Research*, *319*(14), 2244–2253. https://doi.org/10.1016/j.yexcr.2013.06.005

Shalem, O., Sanjana, N. E., Hartenian, E., Shi, X., Scott, D. A., Mikkelson, T., Heckl, D., Ebert, B. L., Root, D. E., Doench, J. G., & Zhang, F. (2014). Genome-Scale CRISPR-Cas9 Knockout Screening in Human Cells. *Science (New York, N.Y.)*, *343*(6166), 84. https://doi.org/10.1126/SCIENCE.1247005

Sharma, R., Lewis, S., & Wlodarski, M. W. (2020). DNA Repair Syndromes and Cancer: Insights Into Genetics and Phenotype Patterns. *Frontiers in Pediatrics*, *0*, 683. https://doi.org/10.3389/FPED.2020.570084

Shen, J. P., Zhao, D., Sasik, R., Luebeck, J., Birmingham, A., Bojorquez-Gomez, A., Licon, K., Klepper, K., Pekin, D., Beckett, A. N., Sanchez, K. S., Thomas, A., Kuo, C. C., Du, D., Roguev, A., Lewis, N. E., Chang, A. N., Kreisberg, J. F., Krogan, N., … Mali, P. (2017). Combinatorial CRISPR-Cas9 screens for de novo mapping of genetic interactions. *Nature Methods*, *14*(6), 573–576. https://doi.org/10.1038/nmeth.4225

Shen, L., & Pelletier, J. (2020). Selective targeting of the DEAD-box RNA helicase eukaryotic initiation factor (eIF) 4A by natural products. *Natural Product Reports*, *37*(5), 609–616. https://doi.org/10.1039/C9NP00052F

Shiryaev, S. A., Cheltsov, A. V., Gawlik, K., Ratnikov, B. I., & Strongin, A. Y. (2011). Virtual ligand screening of the National Cancer Institute (NCI) compound library leads to the allosteric inhibitory scaffolds of the West Nile virus NS3 proteinase. *Assay and Drug Development Technologies*, *9*(1), 69–79. https://doi.org/10.1089/ADT.2010.0309

Sikorski, R. S., & Hieter, P. (1989). A system of shuttle vectors and yeast host strains designed for efficient manipulation of DNA in Saccharomyces cerevisiae. *Genetics*, *122*(1).

Simon, A. K., Kummer, S., Wild, S., Lezaja, A., Teloni, F., Jozwiakowski, S. K., Altmeyer, M., & Gari, K. (2020). The iron–sulfur helicase DDX11 promotes the generation of single-stranded DNA for CHK1 activation. *Life Science Alliance*, *3*(3). https://doi.org/10.26508/LSA.201900547

Skibbens, R. V. (2004). Ch11p, a DNA Helicase-Like Protein in Budding Yeast, Functions in Sister-Chromatid Cohesion. *Genetics*, *166*(1), 33–42. https://doi.org/10.1534/genetics.166.1.33

Solomon, D. A., Kim, T., Diaz-Martinez, L. A., Fair, J., Elkahloun, A. G., Harris, B. T., Toretsky, J. A., Rosenberg, S. A., Shukla, N., Ladanyi, M., Samuels, Y., James, C. D., Yu, H., Kim, J.-S., & Waldman, T. (2011). Mutational Inactivation of STAG2 Causes Aneuploidy in Human Cancer. *Science*, *333*(6045), 1039–1043. https://doi.org/10.1126/science.1203619.Mutational

Sommers, J. A., Kulikowicz, T., Croteau, D. L., Dexheimer, T., Dorjsuren, D., Jadhav, A., Maloney, D. J., Simeonov, A., Bohr, V. A., & Brosh, R. M. (2019). A high-throughput screen to identify novel small molecule inhibitors of the Werner Syndrome Helicase-Nuclease (WRN). *PLOS ONE*, *14*(4), 1–23. https://doi.org/10.1371/journal.pone.0210525

Sommers, J. A., Rawtani, N., Gupta, R., Bugreev, D. V., Mazin, A. V., Cantor, S. B., & Brosh, R. M. (2009). FANCJ Uses Its Motor ATPase to Destabilize Protein-DNA Complexes, Unwind Triplexes, and Inhibit RAD51 Strand Exchange. *Journal of Biological Chemistry*, *284*(12), 7505–7517. https://doi.org/10.1074/JBC.M809019200

Sondka, Z., Bamford, S., Cole, C. G., Ward, S. A., Dunham, I., & Forbes, S. A. (2018). The COSMIC Cancer Gene Census: describing genetic dysfunction across all human cancers. *Nature Reviews Cancer 2018 18:11*, *18*(11), 696–705. https://doi.org/10.1038/s41568-018-0060-1

Srinivasan, M., Fumasoni, M., Petela, N. J., Murray, A., & Nasmyth, K. A. (2020). Cohesion is established during DNA replication utilising chromosome associated cohesin rings as well as those loaded de novo onto nascent DNAs. *ELife*, *9*, 1–27. https://doi.org/10.7554/ELIFE.56611

Srivas, R., Shen, J. P., Yang, C. C., Sun, S. M., Li, J., Gross, A. M., Jensen, J., Licon, K., Bojorquez-Gomez, A., Klepper, K., Huang, J., Pekin, D., Xu, J. L., Yeerna, H., Sivaganesh, V., Kollenstart, L., van Attikum, H., Aza-Blanc, P., Sobol, R. W., & Ideker, T. (2016). A Network of Conserved Synthetic Lethal Interactions for Exploration of Precision Cancer Therapy. *Molecular Cell*, *63*(3), 514–525. https://doi.org/10.1016/j.molcel.2016.06.022

Stoepker, C., Faramarz, A., Rooimans, M. A., van Mil, S. E., Balk, J. A., Velleuer, E., Ameziane, N., te Riele, H., & de Winter, J. P. (2015). DNA helicases FANCM and DDX11 are determinants of PARP inhibitor sensitivity. *DNA Repair*, *26*, 54–64. https://doi.org/10.1016/j.dnarep.2014.12.003

Straight, A. F., Belmont, A. S., Robinett, C. C., & Murray, A. W. (1996). GFP tagging of budding yeast chromosomes reveals that protein-protein interactions can mediate sister chromatid cohesion. *Current Biology*, *6*(12), 1599–1608. https://doi.org/10.1016/S0960-9822(02)70783-5

Ström, L., Lindroos, H. B., Shirahige, K., & Sjögren, C. (2004). Postreplicative Recruitment of Cohesin to Double-Strand Breaks Is Required for DNA Repair. *Molecular Cell*, *16*(6), 1003–1015. https://doi.org/10.1016/J.MOLCEL.2004.11.026

Su, S.-G., Li, Q.-L., Zhang, M.-F., Zhang, P.-W., Shen, H., & Zhang, C. Z. (2021). An E2F1/DDX11/EZH2 Positive Feedback Loop Promotes Cell Proliferation in Hepatocellular Carcinoma. *Frontiers in Oncology*, *10*, 3289. https://doi.org/10.3389/FONC.2020.593293

Subramanian, D., Kraut, E., Staubus, A., Young, D. C., & Muller, M. T. (1995). Analysis of

Topoisomerase I/DNA Complexes in Patients Administered Topotecan. *Cancer Research*, *55*(10).

Suhasini, A. N., & Brosh, R. M. (2013). Disease-causing missense mutations in human DNA helicase disorders. *Mutation Research - Reviews in Mutation Research*, *752*(2), 138–152. https://doi.org/10.1016/j.mrrev.2012.12.004

Suhasini, A. N., Sommers, J. A., Yu, S., Wu, Y., Xu, T., Kelman, Z., Kaplan, D. L., & Brosh, R. M. (2012). DNA Repair and Replication Fork Helicases Are Differentially Affected by Alkyl Phosphotriester Lesion. *Journal of Biological Chemistry*, *287*(23), 19188–19198. https://doi.org/10.1074/JBC.M112.352757

Tate, J. G., Bamford, S., Jubb, H. C., Sondka, Z., Beare, D. M., Bindal, N., Boutselakis, H., Cole, C. G., Creatore, C., Dawson, E., Fish, P., Harsha, B., Hathaway, C., Jupe, S. C., Kok, C. Y., Noble, K., Ponting, L., Ramshaw, C. C., Rye, C. E., … Forbes, S. A. (2019). COSMIC: the Catalogue Of Somatic Mutations In Cancer. *Nucleic Acids Research*, *47*(D1), D941–D947. https://doi.org/10.1093/NAR/GKY1015

Taylor, C. F., Platt, F. M., Hurst, C. D., Thygesen, H. H., & Knowles, M. A. (2014). Frequent inactivating mutations of STAG2 in bladder cancer are associated with low tumour grade and stage and inversely related to chromosomal copy number changes. *Human Molecular Genetics*, *23*(8), 1964. https://doi.org/10.1093/HMG/DDT589

Tirode, F., Surdez, D., Ma, X., Parker, M., Le Deley, M. C., Bahrami, A., Zhang, Z., Lapouble, E., Grossetete-Lalami, S., Rusch, M., Reynaud, S., Rio-Frio, T., Hedlund, E., Wu, G., Chen, X., Pierron, G., Oberlin, O., Zaidi, S., Lemmon, G., … Delattre, O. (2014). Genomic landscape of ewing sarcoma defines an aggressive subtype with co-association of STAG2 and TP53 mutations. *Cancer Discovery*, *4*(11), 1342–1353. https://doi.org/10.1158/2159-8290.CD-14-0622

Tong, A. H. Y., Evangelista, M., Parsons, A. B., Xu, H., Bader, G. D., Pagé, N., Robinson, M., Raghibizadeh, S., Hogue, C. W. V., Bussey, H., Andrews, B., Tyers, M., & Boone, C. (2001). Systematic genetic analysis with ordered arrays of yeast deletion mutants. *Science*, *294*(5550), 2364–2368. https://doi.org/10.1126/science.1065810

Tsherniak, A., Vazquez, F., Montgomery, P. G., Weir, B. A., Kryukov, G., Cowley, G. S., Gill, S., Harrington, W. F., Pantel, S., Krill-Burger, J. M., Meyers, R. M., Ali, L., Goodale, A., Lee, Y., Jiang, G., Hsiao, J., Gerath, W. F. J., Howell, S., Merkel, E., … Hahn, W. C. (2017). Defining a Cancer Dependency Map. *Cell*, *170*(3). http://www.cell.com/article/S0092867417306517/fulltext

Tutt, A., Robson, M., Garber, J. E., Domchek, S. M., Audeh, M. W., Weitzel, J. N., Friedlander, M., Arun, B., Loman, N., Schmutzler, R. K., Wardley, A., Mitchell, G., Earl, H., Wickens, M., & Carmichael, J. (2010). Oral poly(ADP-ribose) polymerase inhibitor olaparib in patients with BRCA1 or BRCA2 mutations and advanced breast cancer: a proof-of-concept trial. *The Lancet*, *376*(9737), 235–244. https://doi.org/10.1016/S0140-6736(10)60892-6

Uhlmann, F. (2016). SMC complexes: From DNA to chromosomes. *Nature Reviews Molecular Cell Biology*, *17*(7), 399–412. https://doi.org/10.1038/nrm.2016.30

van der Lelij, P., Chrzanowska, K. H., Godthelp, B. C., Rooimans, M. A., Oostra, A. B., Stumm, M., Zdzienicka, M. Z., Joenje, H., & de Winter, J. P. (2010). Warsaw Breakage Syndrome, a Cohesinopathy Associated with Mutations in the XPD Helicase Family Member DDX11/ChlR1. *American Journal of Human Genetics*, *86*(2), 262–266.

https://doi.org/10.1016/j.ajhg.2010.01.008

van der Lelij, P., Lieb, S., Jude, J., Wutz, G., Santos, C. P., Falkenberg, K., Schlattl, A., Ban, J., Schwentner, R., Hoffmann, T., Kovar, H., Real, F. X., Waldman, T., Pearson, M. A., Kraut, N., Peters, J. M., Zuber, J., & Petronczki, M. (2017). Synthetic lethality between the cohesin subunits STAG1 and STAG2 in diverse cancer contexts. *ELife*, *6*, e26980. https://doi.org/10.7554/eLife.26980

van der Lelij, P., Newman, J. A., Lieb, S., Jude, J., Katis, V., Hoffmann, T., Hinterndorfer, M., Bader, G., Kraut, N., Pearson, M. A., Peters, J. M., Zuber, J., Gileadi, O., & Petronczki, M. (2020). STAG1 vulnerabilities for exploiting cohesin synthetic lethality in STAG2-deficient cancers. *Life Science Alliance*, *3*(7), e202000725. https://doi.org/10.26508/lsa.202000725

van Pel, D. M., Barrett, I. J., Shimizu, Y., Sajesh, B. V., Guppy, B. J., Pfeifer, T., McManus, K. J., & Hieter, P. (2013). An Evolutionarily Conserved Synthetic Lethal Interaction Network Identifies FEN1 as a Broad-Spectrum Target for Anticancer Therapeutic Development. *PLoS Genetics*, *9*(1). https://doi.org/10.1371/journal.pgen.1003254

van Pel, D. M., Stirling, P. C., Minaker, S. W., Sipahimalani, P., & Hieter, P. (2013). *Saccharomyces cerevisiae* Genetics Predicts Candidate Therapeutic Genetic Interactions at the Mammalian Replication Fork. *G3: Genes|Genomes|Genetics*, *3*(2), 273–282. https://doi.org/10.1534/g3.112.004754

van Schie, J. J. M., Faramarz, A., Balk, J. A., Stewart, G. S., Cantelli, E., Oostra, A. B., Rooimans, M. A., Parish, J. L., de Almeida Estéves, C., Dumic, K., Barisic, I., Diderich, K. E. M., van Slegtenhorst, M. A., Mahtab, M., Pisani, F. M., te Riele, H., Ameziane, N., Wolthuis, R. M. F., & de Lange, J. (2020). Warsaw Breakage Syndrome associated DDX11 helicase resolves G-quadruplex structures to support sister chromatid cohesion. *Nature Communications 2020 11:1*, *11*(1), 1–18. https://doi.org/10.1038/s41467-020-18066-8

Venter, J. C., Adams, M. D., Myers, E. W., Li, P. W., Mural, R. J., Sutton, G. G., Smith, H. O., Yandell, M., Evans, C. A., Holt, R. A., Gocayne, J. D., Amanatides, P., Ballew, R. M., Huson, D. H., Wortman, J. R., Zhang, Q., Kodira, C. D., Zheng, X. H., Chen, L., … Zhu, X. (2001). The Sequence of the Human Genome. *Science*, *291*(5507), 1304–1351. https://doi.org/10.1126/SCIENCE.1058040

Vogelstein, B, Fearon, E. R., Hamilton, S. R., Kern, S. E., Preisinger, A. C., Leppert, M., Nakamura, Y., White, R., Smits, A. M., Bos, J. L., B, V., ER, F., SR, H., SE, K., AC, P., M, L., Y, N., R, W., AM, S., & JL, B. (1988). Genetic alterations during colorectal-tumor development. *The New England Journal of Medicine*, *319*(9), 525–532. https://doi.org/10.1056/NEJM198809013190901

Vogelstein, Bert, Papadopoulos, N., Velculescu, V. E., Zhou, S., Diaz, L. A., & Kinzler, K. W. (2013). Cancer genome landscapes. *Science (New York, N.Y.)*, *339*(6127), 1546–1558. https://doi.org/10.1126/science.1235122

Waldman, T. (2020). Emerging themes in cohesin cancer biology. *Nature Reviews Cancer*, *20*(9), 504–515. https://doi.org/10.1038/s41568-020-0270-1

Walker, J. E., Saraste, M., Runswick, M. J., & Gay, N. J. (1982). Distantly related sequences in the alpha- and beta-subunits of ATP synthase, myosin, kinases and other ATP-requiring enzymes and a common nucleotide binding fold. *The EMBO Journal*, *1*(8), 945–951. https://doi.org/10.1002/J.1460-2075.1982.TB01276.X

Wang, T., Wei, J. J., Sabatini, D. M., & Lander, E. S. (2014). Genetic screens in human cells

using the CRISPR/Cas9 system. *Science (New York, N.Y.)*, *343*(6166), 80. https://doi.org/10.1126/SCIENCE.1246981

Weinstein, J. N., Akbani, R., Broom, B. M., Wang, W., Verhaak, R. G. W., McConkey, D., Lerner, S., Morgan, M., Creighton, C. J., Smith, C., Cherniack, A. D., Kim, J., Pedamallu, C. S., Noble, M. S., Al-Ahmadie, H. A., Reuter, V. E., Rosenberg, J. E., F.Bajorin, D., Bochner, B. H., … Eley, G. (2014). Comprehensive molecular characterization of urothelial bladder carcinoma. *Nature 2014 507:7492*, *507*(7492), 315–322. https://doi.org/10.1038/nature12965

Wu, Y., & Brosh, R. M. (2010). Helicase-inactivating mutations as a basis for dominant negative phenotypes. *Cell Cycle*, *9*(20), 4080–4090. https://doi.org/10.4161/cc.9.20.13667

Wu, Y., Sommers, J. A., Khan, I., De Winter, J. P., & Brosh, R. M. (2012). Biochemical characterization of Warsaw breakage syndrome helicase. *Journal of Biological Chemistry*, *287*(2), 1007–1021. https://doi.org/10.1074/jbc.M111.276022

Wu, Y., Sommers, J. A., Suhasini, A. N., Leonard, T., Deakyne, J. S., Mazin, A. V., Shin-ya, K., Kitao, H., Jr, R. M. B., Brosh, R. M., Jr, R. M. B., & Jr. (2010). Fanconi anemia group J mutation abolishes its DNA repair function by uncoupling DNA translocation from helicase activity or disruption of protein-DNA complexes. *Blood*, *116*(19), 3780–3791. https://doi.org/10.1182/blood-2009-11-256016

Wu, Y., Suhasini, A. N., & Brosh, R. M. (2009). Welcome the Family of FANCJ-like Helicases to the Block of Genome Stability Maintenance Proteins. *Cellular and Molecular Life Sciences*, *66*(7), 1209–1222. https://doi.org/10.1007/s00018-008-8580-6

Xu, H., Boone, C., & Brown, G. W. (2007). Genetic Dissection of Parallel Sister-Chromatid Cohesion Pathways. *Genetics*, *176*(3), 1417–1429. https://doi.org/10.1534/GENETICS.107.072876

Young, B. P., & Loewen, C. J. R. (2013). Balony: A software package for analysis of data generated by synthetic genetic array experiments. *BMC Bioinformatics*, *14*(1), 354. https://doi.org/10.1186/1471-2105-14-354

Yu, Y., Zhao, D., Li, K., Cai, Y., Xu, P., Li, R., Li, J., Chen, X., Chen, P., & Cui, G. (2020). E2F1 mediated DDX11 transcriptional activation promotes hepatocellular carcinoma progression through PI3K/AKT/mTOR pathway. *Cell Death & Disease 2020 11:4*, *11*(4), 1–16. https://doi.org/10.1038/s41419-020-2478-0

Yuen, K. W. Y., Warren, C. D., Chen, O., Kwok, T., Hieter, P., & Spencer, F. A. (2007). Systematic genome instability screens in yeast and their potential relevance to cancer. *Proceedings of the National Academy of Sciences of the United States of America*, *104*(10), 3925–3930. https://doi.org/10.1073/pnas.0610642104

Zandarashvili, L., Langelier, M. F., Velagapudi, U. K., Hancock, M. A., Steffen, J. D., Billur, R., Hannan, Z. M., Wicks, A. J., Krastev, D. B., Pettitt, S. J., Lord, C. J., Talele, T. T., Pascal, J. M., & Black, B. E. (2020). Structural basis for allosteric PARP-1 retention on DNA breaks. *Science*, *368*(6486). https://doi.org/10.1126/science.aax6367

Zhang, J., Wan, L., Dai, X., Sun, Y., & Wei, W. (2014). Functional characterization of Anaphase Promoting Complex/Cyclosome (APC/C) E3 ubiquitin ligases in tumorigenesis. *Biochimica et Biophysica Acta (BBA) - Reviews on Cancer*, *1845*(2), 277–293. https://doi.org/10.1016/J.BBCAN.2014.02.001

Zhang, N., Coutinho, L. E., & Pati, D. (2021). PDS5A and PDS5B in Cohesin Function and

Human Disease. *International Journal of Molecular Sciences 2021, Vol. 22, Page 5868*, *22*(11), 5868. https://doi.org/10.3390/IJMS22115868

Zhong, L., Li, Y., Xiong, L., Wang, W., Wu, M., Yuan, T., Yang, W., Tian, C., Miao, Z., Wang, T., & Yang, S. (2021). Small molecules in targeted cancer therapy: advances, challenges, and future perspectives. *Signal Transduction and Targeted Therapy 2021 6:1*, *6*(1), 1–48. https://doi.org/10.1038/s41392-021-00572-w

Zhou, L., Liang, C., Chen, Q., Zhang, Z., Zhang, B., Yan, H., Qi, F., Zhang, M., Yi, Q., Guan, Y., Xiang, X., Zhang, X., Ye, S., & Wang, F. (2017). The N-Terminal Non-Kinase-Domain-Mediated Binding of Haspin to Pds5B Protects Centromeric Cohesion in Mitosis. *Current Biology*, *27*(7), 992–1004. https://doi.org/10.1016/J.CUB.2017.02.019

Appendices

Appendix A - List of oligonucleotides, plasmids and yeast strains

Table A.1 – List of cloning primers

Ch.	Cloning primers	Sequence	Description
2	OPH8968	CTGGACATGCTGATTAACgaattcGGCAGTGGAGAGGGCAGAG	to amplify BLAST from 61425 and insert into 62988 using EcoRI
2	OPH8969	cgataagcttgatatcgaattcttagccctcccacacataac	to amplify BLAST from 61425 and insert into 62988 using EcoRI
2	OPH9364	gctggcgacgctgtaAtcCtcagagatggggatg	SDM to remove Bbs1 (in blast gene)
2	OPH9365	catccccatctctgaGgaTtacagcgtcgccagc	SDM to remove Bbs1 (in blast gene)
2	OPH8224	GCGAGCTCTAGTTAGACCGGTCAGGCACCGGGCTT	to move puro from addgene 62987 to 53190
2	OPH8227	Caaaaaagaaaaaggctagcggcagtggagaggg	to amplify T2A-puro from 62987 with NheI and AgeI sites
2	OPH8228	Ccagattacgctcctaggatggacgcgaaatcac	to amplify KRAB from 50917 with AvrII and NheI sites
2	OPH2889	GCCGCTTATCCGGATTCGCTAGCTACCAGCCAAGGTTC	to amplify KRAB from 50917 with AvrII and NheI sites
3	OPH9725	TAAGCACTGCAGttcgtgtcgtttctattatg	F Primer to add LEU2 cassette from pRS415 to pWS1291 with PstI site
3	OPH9726	TAAGCAACTAGTgaaatatcttgaccgcag	R Primer to add LEU2 cassette from pRS415 to pWS1291 with SpeI site
3	OPH9834	TAAGCAGCGGCCGCGTGGCACTTTTCGGGGAAATGTG	Fwd primer for amplifying ColE1 origin and Amp resistance from pAG415GAL1 with NotI site
3	OPH9835	TAAGCAGCGGCCGCTGTGAGCAAAAGGCCAGCAAAAG	Rev primer for amplifying ColE1 origin and Amp resistance from pAG415GAL1 with NotI site
3	OPH9727	cacaccaCGTCTCaCTGAcaggaaacagctatgaccatg	Upstream primer for cloning GAL1/GPD+gene from Lindquist plasmids from M13R with BsmBI site
3	OPH9728	cacaccaCGTCTCaTGCTtgtaaaacgacggccagt	Downstream primer for cloning GAL1/GPD+gene from Lindquist plasmids from M13F with BsmBI site
3	OPH9879	ACACATCAGGTCATTTCTTCAACACGGAAGTTTTTTTCAATGCGCAGCCTGAATTCACGCtacccatacgatgttcctgactatgcgggctatccctatgacgtcccggactatgcagga	sense donor DNA for removing linker and expressing HA tag in GAL-CHL1 integrated mutants
3	OPH9880	tcctgcatagtccgggacgtcatagggatagcccgcatagtcaggaacatcgtatgggtaGCGTGAATTCAGGCTGCGCATTGAAAAAAACTTCCGTGTTGAAGAAATGACCTGATGTGT	antisense donor DNA for removing linker and expressing HA tag in GAL-CHL1 integrated mutants
4	OPH8961	GCATAAGCTTATGCATCATCACCATCACCACATGGCTAATGAAACACAGAAG	human DDX11 Fwd-HindIII for cloning into pCDNA3.1
4	OPH8962	GCATCTCGAGTCACTTGTCATCGTCATCCTTGTAATCGATGTCATGATCTTTATAATCACCGTCATGGTCTTTGTAGTCGGAAGAGGCCGACTTCTCCCG	human DDX11 Rev XhoI for cloning into pCDNA3.1+
4	OPH8963	CCAACTGGCACTGGGAGGTCCTTAAGTCTTATTTG	human DDX11 K50R fwd primer for site directed mutagenesis

Ch.	Cloning primers	Sequence	Description
4	OPH8964	CAAATAAGACTTAAGGACCTCCCAGTG CCAGTTGG	human DDX11 K50R rev primer for site directed mutagenesis
4	OPH9269	GGGGacaagtttgtacaaaaaagcaggctACCATGGc taatgaaacacagaaggttg	Forward primer for PCR DDX11-flag from pcDNA3.1 with attB for cloning into pDONR221
4	OPH9270	GGGGaccactttgtacaagaaagctgggtTCACTTGT CATCGTCATCCTTG	Reverse primer for PCR DDX11-flag from pcDNA3.1 with attB for cloning into pDONR221

Table A.2 – CRISPRi sgRNA sequences

Ch.	Oligos	Sequence	Description
2	OPH8537	cctcgGACCCCTATTTGCAAAGGT	DDX11 sgRNA#1 for ph7SK-gRNA sense
2	OPH8538	aaacACCTTTGCAAATAGGGGTCc	DDX11 sgRNA#1 for ph7SK-gRNA antisense
2	OPH8539	cctcgCGCCGGACCCCTATTTGCAA	DDX11 sgRNA#2 for ph7SK-gRNA sense
2	OPH8540	aaacTTGCAAATAGGGGTCCGGCGc	DDX11 sgRNA#2 for ph7SK-gRNA antisense
2	OPH8541	cctcgTTGTTCCGGCTGCCTTTCACTG	DDX11 sgRNA#3 for ph7SK-gRNA sense
2	OPH8542	aaacCAGTGAAAGGCAGCCGGAACAAc	DDX11 sgRNA#3 for ph7SK-gRNA antisense
2	OPH8543	cctcgGGCCACCCACCTTTGCAAAT	DDX11 sgRNA#4 for ph7SK-gRNA sense
2	OPH8544	aaacATTTGCAAAGGTGGGTGGCCc	DDX11 sgRNA#4 for ph7SK-gRNA antisense
2	OPH8545	cctcgCCACTGAGTTAGAAACTGG	DDX11 sgRNA#5 for ph7SK-gRNA sense
2	OPH8546	aaacCCAGTTTCTAACTCAGTGGc	DDX11 sgRNA#5 for ph7SK-gRNA antisense
2	OPH8547	cctcgGTCCCCTCAGTGAAAGGCAGC	DDX11 sgRNA#6 for ph7SK-gRNA sense
2	OPH8548	aaacGCTGCCTTTCACTGAGGGGAc	DDX11 sgRNA#6 for ph7SK-gRNA antisense
2	OPH8549	cctcgCAGAGCTCCTTAGGACG	DDX11 sgRNA#7 for ph7SK-gRNA sense
2	OPH8550	aaacCGTCCTAAGGAGCTCTGc	DDX11 sgRNA#7 for ph7SK-gRNA antisense
2	OPH8551	cctcgTGTGGCAGCAGAGCTCCTT	DDX11 sgRNA#8 for ph7SK-gRNA sense
2	OPH8552	aaacAAGGAGCTCTGCTGCCACAc	DDX11 sgRNA#8 for ph7SK-gRNA antisense
2	OPH8553	cctcgGACCCGCCAGTTTCTAACTCAG	DDX11 sgRNA#9 for ph7SK-gRNA sense
2	OPH8554	aaacCTGAGTTAGAAACTGGCGGGTCc	DDX11 sgRNA#9 for ph7SK-gRNA antisense
2	OPH8555	cctcgCAGCAGCGAGAATCTACA	DDX11 sgRNA#10 for ph7SK-gRNA sense
2	OPH8556	aaacTGTAGATTCTCGCTGCTGc	DDX11 sgRNA#10 for ph7SK-gRNA antisense
2	OPH8431	cctcgAATGCCTAGACCTGTTGGGA	sgNT4 for ph7SK-gRNA sense
2	OPH8432	aaacTCCCAACAGGTCTAGGCATTc	sgNT4 for ph7SK-gRNA antisense
2	OPH8429	tcccaTCCCCCCCTCCGGGGTCTAT	sgNT3 for phH1-gRNA sense
2	OPH8430	aaacATAGACCCCGGAGGGGGGGAt	sgNT3 for phH1-gRNA antisense

Table A.3 – DDX11 shRNA sequences

Ch.	Oligos	Sequence
2	shDDX11-4	GCAGGCACGAGAAGAAGAATT
2	shDDX11-271547	CACTCTCTGGTCTCAATTTAA

Table A.4 – DDX11 CRISPR/Cas9 knock-out sgRNA sequences

Ch.	Oligos	Sequence	Description
2	OPH9445	caccgTGTAGGCGGAGCAGGCCAGG	CRISPR KO gRNA DDX11 exon 4 sense
2	OPH9446	aaacCCTGGCCTGCTCCGCCTACAc	CRISPR KO gRNA DDX11 exon 4 antisense
2	OPH9313	caccgCCACAGACCTGAGCGGCCAT	DDX11 CRISPR KO Intron 5/6 gRNA 2 sense
2	OPH9312	aaacATGGCCGCTCAGGTCTGTGGC	DDX11 CRISPR KO Intron 5/6 gRNA 2 antisense
2	OPH9305	caccgACTTGTTTTCTGTCGGAAGT	DDX11 CRISPR KO Intron 6/7 gRNA 1 sense
2	OPH9304	aaacACTTCCGACAGAAAACAAGTC	DDX11 CRISPR KO Intron 6/7 gRNA 1 antisense
2	OPH9318	AATGAGATGGGTGTGAAGAGCAGG	forward primer for detecting exon 6 deletion PCR
2	OPH9319	TCCCAATGCACAAAGCCGAG	reverse primer for detecting exon 6 deletion PCR
2	OPH9320	AATGAGATGGGTGTGAAGAGCAGGG	forward primer for detecting exon 6 deletion PCR
2	OPH9321	GGAGACCAGCCGAACATCCT	reverse primer for detecting exon 6 deletion PCR
2	OPH9453	ATTGTTCTGGGGCGATTCCG	DDX11 exon 4 forward PCR primer for detecting editing
2	OPH9454	GCACATAGCCAGTGAGGGTC	DDX11 exon 4 reverse PCR primer for detecting editing

Table A.5 – DDX11 *in vitro* assay oligonucleotides

Ch.	Oligos	Sequence	Description
4	OPH9503	TTTTTTTTTTTTTTTTTTTTTTCCCAgtaaaacgacggccagtgc-6FAM	DT26 - oligo for DDX11 helicase reaction labelled on 3' with 6-FAM. Lowercase is part that anneals to Tstem25 oligo
4	OPH9504	IowaDarkFQ - gcactggccgtcgttttacGGTCGTGACTGGGAAAACCCTGGCG	Tstem25 - oligo for DDX11 helicase reaction labelled on 5' with Iowa Dark FQ (quencher). Lowercase is part that anneals to DT26
4	OPH9505	CGCCAGGGTTTTCCCAGTCACGACCgtaaacgacggccagtgc	Reverse complement to Tstem25 - full length
4	OPH9602	GCACTGGCCGTCGTTTTAC	reverse complement to OPH9503 duplex sequence (6-FAM for DDX11 assay)
4	OPH9603	gtaaaacgacggccagtgc	reverse complement to OPH9504 duplex sequence (quencher for DDX11 assay)

Table A.6 – Plasmids

Ch.	BLA/BPH#	Description
2	BPH1324	pSp-Cas9-T2A-blast
2	BLA371	spCas9-T2A-Blast-DDX11 Int. 5/6-2
2	BLA332	spCas9-2A-GFP-DDX11 Intron 6/7-1
2	BLA334	spCas9-2A-GFP-DDX11 Intron 6/7-2
2	BLA371	pSpCas9-T2A-Blast-DDX11 Int. 5/6.2
2	BLA332	pSpCas9-2A-GFP-DDX11 Intron 6/7.1
2	BLA392	pSpCas9-T2A-BLAST-DDX11 gRNA Exon 4
3	BPH1430	pAG415GAL-CHL1
3	BPH1431	pAG415GAL-chl1K48R
3	BPH1438	pLA581 (ura3_int_GAL-ccdB-HA_LEU2)
3	BPH1439	pLA575 (ura3_int_GAL-ccdB-HA)
4	BLA223	pcDNA3.1(+)-6xHis-DDX11(906AA)WT-3xFlag
4	BLA409	pcDNA3.1(+)-6xHis-DDX11(906AA)K50R-3xFlag
4	BLA313	pDONR221-6xHis-DDX11(906AA)WT-3xFlag
4	BLA320	pDONR221-6xHis-DDX11(906AA)K50R-3xFlag

Table A.7 – Yeast strains

Ch.	Yeast (YPH#)	Yeast strains	Source
3	YPH1920	MATα can1Δ::STE2pr-his5 lyp1Δ leu2Δ0 his3Δ1 met15Δ0 ura3Δ0	Y7092
3	YPH2742	MATα can1Δ::STE2pr-his5 lyp1Δ leu2Δ0 his3Δ1 met15Δ0 ura3Δ::pGAL-CHL1[LEU2]	This study
3	YPH2743	MATα can1Δ::STE2pr-his5 lyp1Δ leu2Δ0 his3Δ1 met15Δ0 ura3Δ::pGAL-chl1K48R[LEU2]	This study
3	YPH2744	MATα can1Δ::STE2pr-his5 lyp1Δ leu2Δ0 his3Δ1 met15Δ0 ura3Δ::pGAL-chl1DAIA[LEU2]	This study
3	YPH2745	MATα can1Δ::STE2pr-his5 lyp1Δ leu2Δ0 his3Δ1 met15Δ0 ura3Δ::pGAL-chl1Q20A[LEU2]	This study
3	YPH2746	MATα can1Δ::STE2pr-his5 lyp1Δ leu2Δ0 his3Δ1 met15Δ0 ura3Δ::pGAL-chl1K48R/DAIA[LEU2]	This study
3	YPH2747	MATα can1Δ::STE2pr-his5 lyp1Δ leu2Δ0 his3Δ1 met15Δ0 ura3Δ::pGAL-chl1Q20A/K48R[LEU2]	This study
3	YPH2748	MATα can1Δ::STE2pr-his5 lyp1Δ leu2Δ0 his3Δ1 met15Δ0 ura3Δ::pGAL-chl1Q20A/DAIA[LEU2]	This study
3	YPH2749	MATα can1Δ::STE2pr-his5 lyp1Δ leu2Δ0 his3Δ1 met15Δ0 ura3Δ::pGAL-chl1Q20A/K48R/DAIA[LEU2]	This study
3	YPH2750	MATα can1Δ::STE2pr-his5 lyp1Δ leu2Δ0 his3Δ1 met15Δ0 ura3Δ::pGAL-CHL1-3HA[LEU2]	This study
3	YPH2751	MATα can1Δ::STE2pr-his5 lyp1Δ leu2Δ0 his3Δ1 met15Δ0 ura3Δ::pGAL-chl1K48R-3HA[LEU2]	This study
3	YPH2752	MATα can1Δ::STE2pr-his5 lyp1Δ leu2Δ0 his3Δ1 met15Δ0 ura3Δ::pGAL-chl1DAIA-3HA[LEU2]	This study
3	YPH2753	MATα can1Δ::STE2pr-his5 lyp1Δ leu2Δ0 his3Δ1 met15Δ0 ura3Δ::pGAL-chl1Q20A-3HA[LEU2]	This study
3	YPH2754	MATα can1Δ::STE2pr-his5 lyp1Δ leu2Δ0 his3Δ1 met15Δ0 ura3Δ::pGAL-chl1K48R/DAIA-3HA[LEU2]	This study
3	YPH2755	MATα can1Δ::STE2pr-his5 lyp1Δ leu2Δ0 his3Δ1 met15Δ0 ura3Δ::pGAL-chl1Q20A/K48R-3HA[LEU2]	This study
3	YPH2756	MATα can1Δ::STE2pr-his5 lyp1Δ leu2Δ0 his3Δ1 met15Δ0 ura3Δ::pGAL-chl1Q20A/DAIA-3HA[LEU2]	This study
3	YPH2757	MATα can1Δ::STE2pr-his5 lyp1Δ leu2Δ0 his3Δ1 met15Δ0 ura3Δ::pGAL-chl1Q20A/K48R/DAIA-3HA[LEU2]	This study
3	YPH316	MATα his1 HIS3	PMID: 2407610
3	YPH2655	MATa trp1Δ::pGPD1-TIR1-CaTRP1 lys4::LacO(DK)-NAT leu2-3,112 pHIS3-GFPLacI-HIS3:his3-11,15 ura3-52 bar1	PMID: 25378582
3	YLM49	MATa trp1Δ::pGPD1-TIR1-CaTRP1 lys4::LacO(DK)-NAT leu2-3,112 pHIS3-GFPLacI-HIS3:his3-11,15 ura3Δ::pGAL-CHL1[LEU2] bar1	This study
3	YLM50	MATa trp1Δ::pGPD1-TIR1-CaTRP1 lys4::LacO(DK)-NAT leu2-3,112 pHIS3-GFPLacI-HIS3:his3-11,15 ura3Δ::pGAL-chl1K48R[LEU2] bar1	This study
3	YLM51	MATa trp1Δ::pGPD1-TIR1-CaTRP1 lys4::LacO(DK)-NAT leu2-3,112 pHIS3-GFPLacI-HIS3:his3-11,15 ura3Δ::pGAL-chl1DAIA[LEU2] bar1	This study
3	YLM52	MATa trp1Δ::pGPD1-TIR1-CaTRP1 lys4::LacO(DK)-NAT leu2-3,112 pHIS3-GFPLacI-HIS3:his3-11,15 ura3Δ::pGAL-chl1Q20A[LEU2] bar1	This study
3	YLM53	MATa trp1Δ::pGPD1-TIR1-CaTRP1 lys4::LacO(DK)-NAT leu2-3,112 pHIS3-GFPLacI-HIS3:his3-11,15 ura3Δ::pGAL-chl1K48R/DAIA[LEU2] bar1	This study

Ch.	Yeast (YPH#)	Yeast strains	Source
3	YLM54	MATa trp1Δ::pGPD1-TIR1-CaTRP1 lys4::LacO(DK)-NAT leu2-3,112 pHIS3-GFPLacI-HIS3:his3-11,15 ura3Δ::pGAL-chl1Q20A/K48R[LEU2] bar1	This study
3	YLM55	MATa trp1Δ::pGPD1-TIR1-CaTRP1 lys4::LacO(DK)-NAT leu2-3,112 pHIS3-GFPLacI-HIS3:his3-11,15 ura3Δ::pGAL-chl1Q20A/DAIA[LEU2] bar1	This study
3	YLM56	MATa trp1Δ::pGPD1-TIR1-CaTRP1 lys4::LacO(DK)-NAT leu2-3,112 pHIS3-GFPLacI-HIS3:his3-11,15 ura3Δ::pGAL-chl1Q20A/K48R/DAIA[LEU2] bar1	This study

Appendix B - DDX11 CRISPR/Cas9 screen results

Negative Genetic Interactions:

Gene	qGI score	FDR	Gene	qGI score	FDR	Gene	qGI score	FDR	Gene	qGI score	FDR
GSG2	-2.287	0	HUWE1	-0.885	0.001	ZNF598	-0.717	0.006	FBXL5	-0.609	0.089
LRWD1	-2.143	0	SMARCA5	-0.876	0.001	PODXL2	-0.711	0.016	SATB2	-0.609	0.089
TGIF2	-1.524	0	GRSF1	-0.875	0.001	CHTF18	-0.697	0.003	FOXM1	-0.606	0.102
NXT1	-1.508	0	LINS	-0.874	0.039	AIFM1	-0.697	0.007	FBXO11	-0.604	0.048
CENPQ	-1.346	0	SSH2	-0.872	0.042	NDUFA13	-0.696	0.009	TBCD	-0.6	0.032
GPBP1	-1.33	0	CCDC77	-0.849	0	KPNA2	-0.695	0.002	RNF126	-0.6	0.145
BAZ1B	-1.257	0	STAG1	-0.847	0	TRIM50	-0.695	0.02	ACTR1A	-0.598	0.001
PAXIP1	-1.257	0	ATXN7	-0.847	0.001	CCNA2	-0.692	0.004	SIRT5	-0.593	0.06
CLPP	-1.197	0	CCAR2	-0.847	0.14	CTDSPL2	-0.689	0.026	MBTD1	-0.592	0.004
MPV17L2	-1.192	0.006	MED12	-0.84	0.049	SMEK1	-0.687	0	POLR3K	-0.592	0.016
CLASP2	-1.182	0	TADA2B	-0.814	0.017	SMAD4	-0.687	0.089	MCM5	-0.592	0.067
CAB39	-1.18	0.006	NARG2	-0.809	0	SKA2	-0.674	0.012	SBNO2	-0.591	0.006
TXNDC17	-1.148	0	IDO2	-0.803	0	PFDN5	-0.673	0.005	C17orf70	-0.59	0
TADA1	-1.147	0.002	MED13	-0.795	0.05	NACC2	-0.669	0.02	DEK	-0.587	0.042
CENPO	-1.123	0	CCNF	-0.792	0.003	TIMM8B	-0.668	0.076	HNRNPH3	-0.585	0.001
EIF4E2	-1.11	0	FZD3	-0.788	0.001	RECQL5	-0.659	0.009	PLCL2	-0.585	0.097
SRSF10	-1.107	0	SORBS3	-0.786	0	PUM1	-0.658	0.013	POLE3	-0.584	0
BABAM1	-1.097	0	GMEB1	-0.78	0.074	SLC20A1	-0.657	0.028	SEC61B	-0.583	0.087
LIN37	-1.08	0	RAD51B	-0.779	0.004	IPO9	-0.651	0.101	C10orf25	-0.582	0.074
CENPP	-1.072	0	HMG20B	-0.766	0.027	KIAA0513	-0.65	0.005	GIGYF2	-0.58	0.002
BRE	-1.049	0	LARP4B	-0.761	0	FBXO7	-0.65	0.04	CDK13	-0.58	0.022
TMCO6	-1.045	0	STAG2	-0.756	0.002	E2F6	-0.646	0.109	LGI3	-0.579	0.073
NCAPH2	-1	0	PGM2	-0.755	0	MRPL41	-0.645	0.096	VCPIP1	-0.578	0.007
FZR1	-0.999	0	TM2D2	-0.748	0.001	C19orf40	-0.643	0.038	PRR24	-0.573	0.003
SGOL2	-0.997	0	MCM3	-0.746	0.023	EDC4	-0.641	0.004	KCNH3	-0.573	0.012
TIMM8A	-0.984	0.001	RHOA	-0.74	0.005	CNR1	-0.637	0.002	COL6A2	-0.572	0.013
PPP1CC	-0.977	0.016	CSTF2	-0.737	0.057	CDCA2	-0.635	0.044	ECSIT	-0.571	0.103
PDS5B	-0.971	0	MPP6	-0.736	0.075	USE1	-0.635	0.052	ZNF584	-0.571	0.115
ESCO1	-0.969	0	HEXIM1	-0.734	0	DOT1L	-0.634	0	PUS1	-0.57	0.191
ORC2	-0.963	0	CEBPD	-0.734	0.002	KEAP1	-0.634	0.043	E2F4	-0.568	0
CDCA5	-0.94	0	MRPL23	-0.731	0.053	KLF5	-0.63	0.011	MED16	-0.568	0.115
KIF22	-0.933	0	NDUFA9	-0.728	0.073	CHTF8	-0.629	0.046	LARP1	-0.567	0.03
NFRKB	-0.929	0.001	TFPT	-0.727	0	VBP1	-0.626	0.062	PDCD1	-0.567	0.049
RIC8A	-0.914	0	NDUFA6	-0.726	0.012	CLUH	-0.625	0	STRAP	-0.566	0.148
SIVA1	-0.914	0.007	HECTD1	-0.724	0	RBM26	-0.625	0.081	FANCG	-0.565	0.007
MEAF6	-0.908	0	STK11	-0.719	0.001	AP1G1	-0.619	0.032	CXorf56	-0.565	0.141
UBE3A	-0.889	0	HK2	-0.717	0.001	LYPD2	-0.614	0.007	SLC22A3	-0.564	0.001

Gene	qGI score	FDR	Gene	qGI score	FDR	Gene	qGI score	FDR
FAP	-0.563	0.019	NDUFB11	-0.53	0.169	ARPC2	-0.501	0.056
SCNM1	-0.563	0.03	ALG11	-0.529	0.05	ATP8A1	-0.5	0.017
ACOT7	-0.562	0.002	CSNK1A1L	-0.529	0.084	KAT8	-0.5	0.19
PPP2R5D	-0.562	0.004	RNF4	-0.528	0.108			
DAZAP1	-0.562	0.113	ITPK1	-0.527	0.145			
CHD6	-0.561	0.009	SRPX	-0.526	0.01			
UVSSA	-0.56	0.012	CSMD3	-0.526	0.044			
CCDC90B	-0.559	0.014	LSM2	-0.525	0.042			
TRIM71	-0.558	0.19	TMEM229A	-0.523	0.009			
ZHX1-C8ORF76	-0.557	0.115	SLC2A1	-0.522	0.149			
TFAP2C	-0.555	0.002	DIS3L2	-0.521	0			
SLC22A12	-0.555	0.008	WDR12	-0.521	0.049			
PSMB5	-0.555	0.023	PDYN	-0.521	0.101			
FTSJ2	-0.554	0.037	TMEM179	-0.518	0.019			
APOA4	-0.554	0.2	XRCC1	-0.517	0.048			
SFR1	-0.553	0.009	NAMPT	-0.515	0.015			
TGM5	-0.553	0.052	PSPC1	-0.515	0.016			
RRP1B	-0.551	0.067	FAM169B	-0.515	0.017			
NSUN3	-0.551	0.113	PNPT1	-0.515	0.049			
PLXDC2	-0.548	0.004	SLC24A4	-0.512	0.007			
HMG20A	-0.548	0.004	STK35	-0.511	0.006			
SLC52A3	-0.548	0.009	LRCH3	-0.511	0.053			
RNF167	-0.547	0.013	TIMM17A	-0.511	0.08			
TMEFF1	-0.543	0.002	PRMT2	-0.51	0.018			
ATG9A	-0.542	0.056	DDX23	-0.508	0.005			
DHX35	-0.541	0.003	MTMR12	-0.508	0.085			
DCP2	-0.541	0.006	TM2D1	-0.507	0.051			
BHLHA9	-0.54	0.029	PRMT10	-0.507	0.154			
RNASEH2C	-0.54	0.13	GPI	-0.506	0.013			
NR2F2	-0.539	0.039	KIAA1524	-0.505	0.002			
CETN1	-0.537	0.004	GDPD4	-0.504	0.019			
USP14	-0.536	0	CEP57L1	-0.504	0.102			
CDS2	-0.535	0.004	SLC1A2	-0.503	0.027			
NDE1	-0.534	0.062	CSPP1	-0.502	0.041			
IPMK	-0.533	0.088	COQ9	-0.502	0.058			
OTUB1	-0.53	0.008	XRCC2	-0.502	0.112			
MCM6	-0.53	0.154	KCND3	-0.502	0.181			

Positive genetic interactions:

Gene	qGI score	FDR	Gene	qGI score	FDR	Gene	qGI score	FDR	Gene	qGI score	FDR
TACC3	1.741	0	ANAPC7	0.711	0.001	ITGA7	0.593	0.018	POR	0.538	0.003
DCAF15	1.535	0	EIF4H	0.698	0	TAF8	0.592	0	MKI67	0.537	0.044
FUS	1.39	0	CARM1	0.698	0.029	EIF4E	0.592	0	MCL1	0.537	0.049
TMED2	1.328	0	WRB	0.692	0	LEMD2	0.589	0.002	INTS10	0.535	0.052
MED26	1.273	0	KAT2A	0.678	0.002	MYH7B	0.589	0.026	GTF2E2	0.533	0.005
DDX11	1.266	0	THRAP3	0.675	0.001	MAU2	0.588	0	SLC25A48	0.532	0.048
WAPAL	1.187	0	WIBG	0.674	0	GINS4	0.588	0.001	LRRC9	0.525	0.083
EIF4G1	1.14	0	CPSF7	0.671	0.073	MON2	0.587	0.007	RNF7	0.525	0.188
HDAC8	1.098	0.001	SLC25A33	0.663	0.012	CDK11A	0.587	0.043	HR	0.522	0.121
DONSON	1.087	0	PMF1	0.662	0	PTPN9	0.584	0.066	NDC80	0.517	0.002
ZWINT	1.082	0	MED4	0.657	0	GINS3	0.583	0	MTA3	0.517	0.025
NAA30	1.071	0	ODC1	0.656	0.011	SMARCB1	0.583	0.003	CUEDC2	0.517	0.078
KNTC1	1.064	0	ACACA	0.651	0	SEC11A	0.582	0.005	MMP28	0.517	0.122
ZNF638	1.032	0.042	PPP3R2	0.651	0.103	GAK	0.582	0.016	RASL12	0.516	0.021
YBX1	0.97	0	MED7	0.649	0.001	CHP1	0.581	0.025	HTT	0.516	0.178
DGUOK	0.966	0.09	ATP6V1B2	0.646	0	ALX3	0.58	0.01	DCTN6	0.514	0
DLGAP5	0.942	0	VAMP8	0.646	0	CCNT1	0.58	0.029	HNRNPL	0.513	0
ZFAT	0.91	0.197	GTF3C4	0.64	0	NUP98	0.579	0	VASN	0.513	0.049
CUL4B	0.895	0.084	UBE2J2	0.639	0.052	CKAP5	0.578	0.006	RARG	0.513	0.068
CNBP	0.866	0.001	WDR48	0.638	0.004	ARID4B	0.577	0.084	NCAPD2	0.511	0.001
CIT	0.838	0	ZBTB8OS	0.629	0	DPH2	0.576	0.005	ENY2	0.51	0
RPS15A	0.836	0.002	TUSC2	0.627	0.009	VKORC1L1	0.575	0.055	NMD3	0.51	0
SLC25A36	0.829	0.118	SLBP	0.625	0.017	NEXN	0.572	0.047	CMTR1	0.508	0
C10orf2	0.806	0	ZDHHC18	0.623	0.049	EMC6	0.571	0	ERCC6L	0.508	0.078
CENPC	0.802	0	TMEM230	0.621	0.015	CD8B	0.571	0.024	C2orf49	0.507	0.078
TMED10	0.8	0	R3HCC1	0.621	0.06	TECR	0.57	0.177	PLA2R1	0.506	0.053
C16orf72	0.799	0.011	MED18	0.618	0	NIPBL	0.567	0	XRCC6	0.505	0.005
CASC5	0.782	0	INTS8	0.618	0.004	SUCLG2	0.567	0.127	HDGFRP3	0.505	0.021
DDA1	0.771	0.004	WHAMM	0.617	0.003	COPS5	0.559	0	MEF2B	0.504	0.141
MPLKIP	0.768	0.118	SIN3A	0.615	0	MAD1L1	0.558	0.001	SPCS2	0.503	0.001
DTYMK	0.743	0	UBE2Q1	0.615	0.116	SPN	0.558	0.052	KIF23	0.502	0.001
CNOT4	0.732	0	CIAO1	0.613	0.011	MPV17	0.557	0.116	FAM69A	0.501	0.058
KDM1A	0.728	0.123	CDK2	0.609	0	ATPAF1	0.556	0.06	UTP18	0.5	0
EIF4B	0.724	0	ATRAID	0.606	0.137	KIF20B	0.554	0.142	CD3EAP	0.5	0.006
PCBP2	0.722	0.014	MARCH5	0.602	0.018	MAP3K19	0.547	0.009	AVIL	0.5	0.129
NRD1	0.722	0.024	E2F7	0.601	0.165	HAL	0.543	0.039	CLCN6	0.5	0.146
PPIA	0.715	0.019	CLSPN	0.597	0	GPX2	0.539	0.089			

Appendix C - Yeast synthetic lethal screen results

Table C.1 – Results of the synthetic lethal screen with *yCHL1*

Yeast systematic name	Yeast standard name	Vector Set 1	Vector Set 2	Vector Set 3	Vector Avg.	yCHL1 Set 1	yCHL1 Set 2	yCHL1 Set 3	yCHL1 Avg.	E-C[a]	GC Validations (plasmid expression)[b]	Validations (hetero-allelic haploids)[c]
YDR364C	CDC40	0.8496	0.9967	0.8605	0.9023	0.0000	0.0000	0.7768	0.2589	-0.6433		
YMR048W	CSM3	0.8673	0.8975	0.9149	0.8932	0.4675	0.4417	0.5226	0.4772	-0.4160	No interaction	
YBR289W	SNF5	0.4602	0.4747	0.9388	0.6246	0.2639	0.2132	0.2124	0.2298	-0.3947		
YNL307C	MCK1	1.0222	0.9542	0.8540	0.9435	0.5470	0.4874	0.6539	0.5627	-0.3807		
YNL273W	TOF1	0.7434	0.7322	0.8301	0.7686	0.4420	0.3472	0.3856	0.3916	-0.3769	No interaction	
YAL021C	CCR4	0.7390	0.7180	0.8040	0.7537	0.4929	0.3320	0.5226	0.4492	-0.3045		
YLR240W	VPS34	0.8142	0.8196	0.8540	0.8293	0.4961	0.5391	0.5393	0.5248	-0.3044	No interaction	
YJL065C	DLS1	0.9094	0.9660	0.9866	0.9540	0.7219	0.6031	0.6790	0.6680	-0.2860		
YBR272C	HSM3	1.0001	1.0723	0.9974	1.0233	0.6996	0.6701	0.8495	0.7397	-0.2835		
YER016W	BIM1	1.0377	1.0463	0.9149	0.9996	0.7123	0.6305	0.8523	0.7317	-0.2679	No interaction	No interaction
YJR082C	EAF6	0.9315	0.9565	0.8649	0.9176	0.5024	0.8529	0.6259	0.6604	-0.2572		
YDR079C-A	TFB5	1.0112	0.0638	0.6367	0.5705	0.3307	0.3320	0.2850	0.3159	-0.2546		
YJR090C	GRR1	0.7678	0.7038	0.6171	0.6962	0.4516	0.3381	0.5477	0.4458	-0.2505		
YJR104C	SOD1	0.3983	0.3283	0.2673	0.3313	0.0382	0.0487	0.1565	0.0811	-0.2502		
YMR186W	HSC82	1.0908	1.0770	0.9561	1.0413	0.8364	0.6001	0.9501	0.7955	-0.2458		
YGR188C	BUB1	0.7987	0.9022	0.7910	0.8307	0.6328	0.6001	0.5673	0.6001	-0.2306	No interaction	No interaction
YNL136W	EAF7	1.1218	1.0345	1.1148	1.0903	0.7887	0.8376	0.9613	0.8625	-0.2278		
YMR137C	PSO2	0.8474	0.8503	0.8736	0.8571	0.5979	0.5726	0.7405	0.6370	-0.2201		
YIL018W	RPL2B	1.0466	1.1077	1.0800	1.0781	0.9667	0.7463	0.8858	0.8663	-0.2118		
YIR002C	MPH1	0.8496	0.8975	0.9344	0.8938	0.6169	0.6945	0.7489	0.6868	-0.2071	No interaction	
YBR158W	AMN1	1.1417	1.1998	1.1995	1.1803	0.9222	0.9473	1.0507	0.9734	-0.2069	No interaction	
YKL113C	RAD27	0.9492	0.8219	0.9214	0.8975	0.6519	0.7341	0.6902	0.6921	-0.2054		
YMR216C	SKY1	1.0731	1.1006	0.8975	1.0237	0.9127	0.5818	0.9669	0.8204	-0.2033	No interaction	
YNR052C	POP2	0.4381	0.3732	0.4411	0.4175	0.2194	0.2132	0.2124	0.2150	-0.2025		
YBR245C	ISW1	0.8386	0.9636	0.9149	0.9057	0.6710	0.8194	0.6231	0.7045	-0.2012		
YBR034C	HMT1	1.0089	1.0746	1.1083	1.0639	0.7187	0.9108	0.9669	0.8654	-0.1985		
YNL068C	FKH2	0.8341	0.8573	0.9149	0.8688	0.6456	0.6366	0.7293	0.6705	-0.1983		
YHR115C	DMA1	1.1550	0.8550	1.1300	1.0466	0.6646	1.0113	0.8802	0.8520	-0.1946		
YBR089C-A	NHP6B	1.0510	1.0817	0.9953	1.0427	0.7378	0.7889	1.0200	0.8489	-0.1938		
YDL216C	RRI1	0.9094	0.9140	0.9866	0.9367	0.6456	0.7067	0.8830	0.7451	-0.1916		
YIL139C	REV7	1.0510	1.0274	1.0518	1.0434	0.8554	1.0295	0.6734	0.8528	-0.1906		
YER164W	CHD1	0.7810	0.6755	0.8062	0.7542	0.5438	0.7036	0.4499	0.5658	-0.1885		
YMR036C	MIH1	0.7788	0.8172	0.9149	0.8370	0.5883	0.6305	0.7321	0.6503	-0.1866		
YDR289C	RTT103	0.5974	0.6117	0.5889	0.5993	0.3943	0.4630	0.3912	0.4162	-0.1832		
YLR107W	REX3	1.1240	1.1502	0.9279	1.0674	0.8809	0.7219	1.0591	0.8873	-0.1801	No interaction	
YER116C	SLX8	0.9226	1.0203	1.0192	0.9874	0.6519	0.8468	0.9333	0.8107	-0.1767		
YMR199W	CLN1	0.8341	0.7959	0.8779	0.8360	0.6201	0.6397	0.7182	0.6593	-0.1767		
YER169W	RPH1	0.8872	0.9565	0.9236	0.9224	0.7473	0.7615	0.7489	0.7526	-0.1699		
YGR271W	SLH1	1.0643	1.0794	1.0735	1.0724	1.0017	0.7432	0.9641	0.9030	-0.1694		
YLR394W	CST9	0.9979	0.8621	1.0170	0.9590	0.7378	0.6975	0.9417	0.7923	-0.1666		

Yeast systematic name	Yeast standard name	Vector Set 1	Vector Set 2	Vector Set 3	Vector Avg.	yCHL1 Set 1	yCHL1 Set 2	yCHL1 Set 3	yCHL1 Avg.	E-C[a]	GC Validations (plasmid expression)[b]	Validations (hetero-allelic haploids)[c]
YML032C	RAD52	0.6062	0.6519	0.5672	0.6084	0.4039	0.4478	0.4778	0.4432	-0.1653	No interaction	No interaction
YIL153W	RRD1	0.6881	0.7109	0.7388	0.7126	0.5788	0.4721	0.5952	0.5487	-0.1639	No interaction	
YGL175C	SAE2	0.9580	0.8526	0.9366	0.9158	0.6615	0.7615	0.8327	0.7519	-0.1639		
YGL094C	PAN2	1.0598	1.0770	1.1539	1.0969	0.8936	1.0600	0.8467	0.9334	-0.1635		
YDR217C	RAD9	0.9448	1.0061	0.9409	0.9640	0.6106	0.9473	0.8467	0.8015	-0.1624		
YML011C	RAD33	1.0488	1.0156	0.8671	0.9771	0.8300	0.6945	0.9361	0.8202	-0.1569		
YER142C	MAG1	0.8939	1.0109	0.9996	0.9681	0.7664	0.8346	0.8411	0.8140	-0.1541		
YMR173W	DDR48	1.0289	0.9447	1.0083	0.9940	0.8395	0.6640	1.0172	0.8402	-0.1537		
YDR279W	RNH202	1.0266	0.9613	0.9149	0.9676	0.8268	0.6549	0.9613	0.8143	-0.1533		
YOL087C	DUF1	0.8142	0.8951	0.8323	0.8472	0.6074	0.7676	0.7070	0.6940	-0.1532		
YJL176C	SWI3	0.1505	0.1346	0.1782	0.1544	0.0000	0.0000	0.0224	0.0075	-0.1470		
YJL013C	MAD3	1.0355	1.0652	1.0474	1.0494	0.9540	0.9808	0.7796	0.9048	-0.1445	No interaction	
YDL013W	SLX5	0.9603	1.0085	1.0235	0.9974	0.8618	0.9351	0.7629	0.8533	-0.1442		
YER098W	UBP9	0.9182	0.9660	0.9496	0.9446	0.7855	0.8437	0.7740	0.8011	-0.1435		
YKL213C	DOA1	0.7102	0.7723	0.7497	0.7441	0.5820	0.5970	0.6259	0.6016	-0.1425		
YEL061C	CIN8	0.9226	0.9684	0.8605	0.9172	0.9159	0.7676	0.6455	0.7763	-0.1409	No interaction	
YDL074C	BRE1	0.5089	0.4558	0.5715	0.5121	0.3657	0.3625	0.3856	0.3713	-0.1408		
YDL042C	SIR2	1.0156	1.1101	0.9887	1.0381	0.8809	0.9686	0.8439	0.8978	-0.1403	No interaction	
YNL330C	RPD3	0.5620	0.5031	0.5932	0.5528	0.3848	0.4569	0.3968	0.4128	-0.1399		
YPL241C	CIN2	1.0089	1.0416	0.9648	1.0051	0.8904	0.9229	0.7880	0.8671	-0.1380	No interaction	
YJL030W	MAD2	0.7191	0.7487	0.8888	0.7855	0.4738	0.7371	0.7405	0.6505	-0.1350		
YDL154W	MSH5	0.8983	0.9991	0.9953	0.9642	0.7728	0.8437	0.8718	0.8294	-0.1348		
YCR065W	HCM1	0.8629	1.0203	0.9909	0.9580	0.7219	0.8437	0.9054	0.8237	-0.1344		
YDL082W	RPL13A	0.8961	0.9117	0.9561	0.9213	0.8904	0.6214	0.8523	0.7880	-0.1333		
YML095C	RAD10	1.0222	0.9684	0.8127	0.9344	0.7600	0.7036	0.9417	0.8018	-0.1326		
YDR440W	DOT1	0.9912	0.9849	0.8888	0.9550	0.8332	0.6732	0.9669	0.8244	-0.1306		
YNL116W	DMA2	1.1948	1.1148	1.0235	1.1110	0.9445	0.8833	1.1178	0.9819	-0.1292		
YIL066C	RNR3	1.1373	1.1124	0.9388	1.0628	0.8777	0.8559	1.0675	0.9337	-0.1291		
YBR010W	HHT1	0.8961	0.9542	0.9692	0.9398	0.7632	0.8041	0.8663	0.8112	-0.1286		
YMR127C	SAS2	0.9116	0.9731	0.9866	0.9571	0.8300	0.7767	0.8914	0.8327	-0.1244		
YCR008W	SAT4	0.7855	0.7133	0.8279	0.7756	0.6933	0.5239	0.7405	0.6526	-0.1230		
YDL116W	NUP84	0.6948	0.7511	0.8171	0.7543	0.5183	0.7189	0.6567	0.6313	-0.1230		
YBR026C	ETR1	0.6616	0.6826	0.5867	0.6436	0.5597	0.5300	0.4723	0.5206	-0.1230		
YDL200C	MGT1	0.9514	0.9754	1.0040	0.9769	0.7950	0.8681	0.9054	0.8562	-0.1208		
YER179W	DMC1	0.8740	0.9376	0.8975	0.9030	0.8713	0.7402	0.7377	0.7831	-0.1200		
YGL115W	SNF4	0.6129	0.6660	0.7410	0.6733	0.5056	0.5726	0.5840	0.5541	-0.1192		
YBR098W	MMS4	0.8895	0.8054	0.9887	0.8945	0.7537	0.8102	0.7629	0.7756	-0.1189		
YBR278W	DPB3	0.9647	1.0416	1.0387	1.0150	0.7441	0.9077	1.0367	0.8962	-0.1188		
YDR369C	XRS2	0.6549	0.6519	0.6693	0.6587	0.5724	0.5117	0.5393	0.5412	-0.1175		
YIL009C-A	EST3	0.8297	0.9471	0.8714	0.8827	0.6392	0.8681	0.7908	0.7660	-0.1167		
YOL054W	PSH1	1.0665	0.9235	0.7627	0.9176	0.7696	0.7432	0.8942	0.8023	-0.1152		
YER173W	RAD24	0.7965	0.9447	0.8714	0.8709	0.5565	0.9077	0.8076	0.7573	-0.1136	No interaction	
YBL002W	HTB2	1.0797	0.9684	0.8127	0.9536	0.8014	0.8133	0.9054	0.8400	-0.1136		
YLR233C	EST1	0.9868	1.0038	0.9909	0.9938	0.7537	0.9869	0.9082	0.8829	-0.1109		
YBR009C	HHF1	0.8076	0.8526	0.8127	0.8243	0.7537	0.6914	0.7014	0.7155	-0.1088		
YKL139W	CTK1	0.8054	0.8810	0.8258	0.8374	0.7410	0.7554	0.6902	0.7289	-0.1085		
YPR023C	EAF3	0.8430	0.7511	0.7953	0.7965	0.7155	0.5696	0.7796	0.6882	-0.1082		

Yeast systematic name	Yeast standard name	Vector Set 1	Vector Set 2	Vector Set 3	Vector Avg.	yCHL1 Set 1	yCHL1 Set 2	yCHL1 Set 3	yCHL1 Avg.	E-C[a]	GC Validations (plasmid expression)[b]	Validations (hetero-allelic haploids)[c]
YPL256C	CLN2	0.8142	0.8030	0.9887	0.8687	0.6583	0.8285	0.7964	0.7611	-0.1076		
YPL181W	CTI6	0.8828	0.9258	0.8975	0.9020	0.9063	0.7036	0.7740	0.7947	-0.1074		
YBL003C	HTA2	0.8341	0.8621	0.9127	0.8696	0.7155	0.8407	0.7321	0.7628	-0.1069		
YHR120W	MSH1	0.8518	0.8668	0.8975	0.8720	0.8300	0.6793	0.7908	0.7667	-0.1053		
YDL070W	BDF2	0.9514	0.9967	0.9801	0.9761	0.8300	0.9595	0.8243	0.8713	-0.1048	No interaction	
YLL019C	KNS1	1.1705	1.2400	1.1669	1.1925	1.0653	1.0966	1.1038	1.0886	-0.1039	No interaction	
YLR032W	RAD5	0.6704	0.8266	0.8236	0.7735	0.5915	0.7889	0.6287	0.6697	-0.1038		
YJL006C	CTK2	0.4868	0.5361	0.5563	0.5264	0.4706	0.4051	0.3968	0.4242	-0.1022		
YLR085C	ARP6	1.1174	1.1219	1.0561	1.0984	1.0208	0.9168	1.0535	0.9970	-0.1014		
YPL024W	RMI1	0.7213	0.8101	0.9496	0.8270	0.7505	0.6793	0.7489	0.7262	-0.1008		
YBR274W	CHK1	0.8209	0.7983	0.9301	0.8497	0.7187	0.7006	0.8299	0.7497	-0.1000		
YLR234W	TOP3	0.8651	0.7487	0.9518	0.8552	0.7950	0.6732	0.8020	0.7567	-0.0985		
YNL250W	RAD50	0.6195	0.6849	0.6758	0.6601	0.5692	0.5970	0.5365	0.5676	-0.0925	No interaction	
YDR225W	HTA1	0.6881	0.7463	0.6954	0.7099	0.5597	0.6275	0.6679	0.6183	-0.0916		
YGR171C	MSM1	0.1682	0.2078	0.2477	0.2079	0.0000	0.3533	0.0000	0.1178	-0.0901		
YOR290C	SNF2	0.7899	0.8857	0.9496	0.8751	0.7155	0.7402	0.8998	0.7852	-0.0899		
YDR386W	MUS81	0.8895	0.8762	0.9627	0.9095	0.7950	0.8559	0.8104	0.8204	-0.0890		
YER176W	ECM32	0.9912	0.9896	0.8627	0.9479	0.8300	0.7067	1.0423	0.8597	-0.0882		
YOR191W	ULS1	0.8518	0.9117	0.8671	0.8769	0.8109	0.8011	0.7545	0.7888	-0.0880		
YDR363W-A	SEM1	0.4757	0.5574	0.5215	0.5182	0.4770	0.4752	0.3409	0.4310	-0.0872		
YHR064C	SSZ1	0.3695	0.4960	0.4151	0.4268	0.2989	0.3290	0.3912	0.3397	-0.0871		
YCR066W	RAD18	0.7810	0.7770	0.8823	0.8134	0.7187	0.7859	0.6762	0.7269	-0.0865		
YLR320W	MMS22	0.6328	0.6471	0.6237	0.6345	0.4706	0.6183	0.5617	0.5502	-0.0843		
YDR030C	RAD28	0.8850	0.8904	0.9561	0.9105	0.7187	0.8742	0.8858	0.8262	-0.0843		
YPL096W	PNG1	0.9846	1.0605	1.0235	1.0229	1.0335	0.7798	1.0032	0.9388	-0.0840		
YPL194W	DDC1	0.8762	0.9849	0.9149	0.9253	0.7664	0.9351	0.8243	0.8420	-0.0834	No interaction	
YGL100W	SEH1	0.8762	0.9188	0.8866	0.8938	0.8268	0.8620	0.7489	0.8126	-0.0813		
YOR386W	PHR1	1.0045	0.9471	0.9322	0.9613	0.8395	0.8041	0.9976	0.8804	-0.0809		
YOR156C	NFI1	0.8076	0.8030	1.0257	0.8788	0.6837	0.8925	0.8243	0.8002	-0.0786		
YDL230W	PTP1	0.8253	0.9235	0.8584	0.8690	0.7759	0.7249	0.8718	0.7909	-0.0781		
YLR154C	RNH203	1.0997	0.9306	0.9409	0.9904	0.8682	0.8620	1.0116	0.9139	-0.0765		
YGL070C	RPB9	0.5996	0.6660	0.6997	0.6551	0.5215	0.5940	0.6231	0.5795	-0.0756		
YNL030W	HHF2	0.9094	0.8479	0.9018	0.8864	0.7537	0.8529	0.8327	0.8131	-0.0733		
YPL022W	RAD1	0.8010	0.8290	0.8301	0.8200	0.7823	0.8864	0.5728	0.7472	-0.0728		
YGL211W	NCS6	0.6151	0.6873	0.6302	0.6442	0.5247	0.6001	0.5896	0.5715	-0.0727		
YGL033W	HOP2	0.8607	0.9093	0.8475	0.8725	0.9286	0.9229	0.5505	0.8007	-0.0718		
YBR186W	PCH2	0.9160	0.9731	0.9453	0.9448	1.0303	1.0478	0.5421	0.8734	-0.0714		
YLL039C	UBI4	0.8563	0.7487	1.0974	0.9008	0.6869	1.0570	0.7489	0.8309	-0.0699		
YDR263C	DIN7	0.9713	1.0557	1.0170	1.0147	0.7569	1.0113	1.0703	0.9461	-0.0686		
YNL201C	PSY2	0.6992	0.8077	0.7236	0.7435	0.6551	0.6853	0.6846	0.6750	-0.0685		
YOR304W	ISW2	0.8010	0.8880	0.8171	0.8354	0.7728	0.8163	0.7126	0.7672	-0.0681		
YGL086W	MAD1	0.7479	0.8479	0.7671	0.7876	0.6742	0.7463	0.7405	0.7203	-0.0673	No interaction	No interaction
YJR043C	POL32	0.7523	0.8196	0.7671	0.7796	0.7569	0.6853	0.6958	0.7127	-0.0670		
YMR167W	MLH1	0.7633	0.8337	0.8171	0.8047	0.8173	0.7432	0.6539	0.7381	-0.0666		
YPR164W	MMS1	0.6372	0.7558	0.6932	0.6954	0.4738	0.6853	0.7321	0.6304	-0.0650		
YGL240W	DOC1	0.8850	0.9565	0.8866	0.9094	0.9095	0.9504	0.6790	0.8463	-0.0631		
YPL008W	CHL1	0.8164	0.9022	0.9388	0.8858	0.7918	0.7463	0.9305	0.8229	-0.0629		
YPR052C	NHP6A	0.8364	0.8999	0.9518	0.8960	0.7378	0.8651	0.8998	0.8342	-0.0618		

Yeast systematic name	Yeast standard name	Vector Set 1	Vector Set 2	Vector Set 3	Vector Avg.	yCHL1 Set 1	yCHL1 Set 2	yCHL1 Set 3	yCHL1 Avg.	E-C[a]	GC Validations (plasmid expression)[b]	Validations (hetero-allelic haploids)[c]
YGR270W	YTA7	0.7965	0.8644	0.8279	0.8296	0.8141	0.8041	0.6874	0.7686	-0.0611		
YJR066W	TOR1	0.6372	0.7322	0.7062	0.6919	0.5406	0.6823	0.6734	0.6321	-0.0598		
YNL230C	ELA1	0.8408	0.7794	1.0126	0.8776	0.7728	0.8011	0.8802	0.8180	-0.0596		
YIL128W	MET18	0.6505	0.6897	0.6715	0.6705	0.5724	0.6640	0.5980	0.6115	-0.0591		
YBL046W	PSY4	0.8253	0.9306	0.9127	0.8895	0.8205	0.7493	0.9277	0.8325	-0.0570		
YGL173C	KEM1	0.5111	0.5243	0.5346	0.5233	0.5215	0.4203	0.4583	0.4667	-0.0566		
YOR368W	RAD17	0.9027	0.9778	0.9496	0.9434	0.9826	0.8620	0.8160	0.8869	-0.0565	No interaction	
YDL047W	SIT4	0.1195	0.0236	0.0587	0.0673	0.0000	0.0000	0.0335	0.0112	-0.0561		
YDR359C	EAF1	1.0266	0.9754	1.0800	1.0274	0.9095	0.9290	1.0758	0.9715	-0.0559		
YDR363W	ESC2	0.9005	0.8692	0.8562	0.8753	0.8427	0.8437	0.7740	0.8202	-0.0551		
YNL072W	RNH201	1.0266	0.9991	1.0909	1.0389	0.9349	0.9717	1.0479	0.9848	-0.0540		
YLR306W	UBC12	0.7678	0.8337	0.7758	0.7924	0.7060	0.7615	0.7489	0.7388	-0.0536		
YGR163W	GTR2	0.7788	0.8904	0.8431	0.8375	0.8968	0.6366	0.8188	0.7840	-0.0534		
YGL229C	SAP4	0.9403	0.9991	0.9453	0.9616	0.9795	0.8651	0.8802	0.9083	-0.0533		
YHL025W	SNF6	0.3828	0.4110	0.5128	0.4355	0.4261	0.2284	0.4974	0.3840	-0.0515		
YMR224C	MRE11	0.5354	0.6212	0.6019	0.5862	0.4579	0.6153	0.5309	0.5347	-0.0515		
YNL138W	SRV2	0.7501	0.9613	0.7323	0.8146	0.7569	0.7767	0.7573	0.7636	-0.0509		
YHR031C	RRM3	0.9249	0.9140	0.9040	0.9143	0.8650	0.8407	0.8858	0.8638	-0.0505		
YMR080C	NAM7	0.8364	0.9353	0.8931	0.8883	0.7887	0.8986	0.8299	0.8391	-0.0492		
YHR191C	CTF8	0.8076	0.7676	0.9561	0.8438	0.7155	0.8833	0.7908	0.7966	-0.0472	No interaction	No interaction
YCR044C	PER1	0.8142	0.9188	0.8518	0.8616	0.8141	0.8468	0.7824	0.8144	-0.0472		
YGR252W	GCN5	0.7412	0.1724	0.6780	0.5305	0.4452	0.6092	0.3996	0.4847	-0.0459		
YBL067C	UBP13	0.8032	0.7629	0.9714	0.8458	0.7505	0.7676	0.8830	0.8004	-0.0454		
YHL022C	SPO11	0.8253	0.8975	0.8301	0.8510	0.8745	0.7859	0.7573	0.8059	-0.0451		
YCL016C	DCC1	0.9271	0.8361	0.9583	0.9072	0.8682	0.8498	0.8691	0.8623	-0.0448	No interaction	No interaction
YKL017C	HCS1	0.8231	0.9093	0.8540	0.8621	0.7473	0.9108	0.7964	0.8182	-0.0440		
YML028W	TSA1	0.8319	0.8857	0.8410	0.8529	0.8586	0.8224	0.7461	0.8090	-0.0438		
YOL004W	SIN3	0.4381	0.4133	0.4694	0.4403	0.4420	0.4203	0.3297	0.3974	-0.0429		
YEL003W	GIM4	0.9492	0.9684	0.9257	0.9478	0.9445	0.9108	0.8607	0.9053	-0.0425		
YDR379W	RGA2	0.9470	0.9258	0.8953	0.9227	0.8968	0.9321	0.8132	0.8807	-0.0420		
YOR014W	RTS1	0.6571	0.6826	0.7128	0.6842	0.6138	0.5909	0.7293	0.6447	-0.0395		
YHR082C	KSP1	0.7987	0.8857	0.7953	0.8266	0.7823	0.8072	0.7740	0.7878	-0.0387		
YNL031C	HHT2	1.0178	1.0699	0.9931	1.0269	0.7887	0.9839	1.1960	0.9895	-0.0374		
YPR141C	KAR3	0.7191	0.7936	0.7541	0.7556	0.7251	0.7615	0.6707	0.7191	-0.0365	No interaction	
YKL190W	CNB1	0.9072	0.8880	0.9953	0.9302	0.8332	0.9229	0.9249	0.8937	-0.0365		
YJR074W	MOG1	0.9580	0.9188	1.0648	0.9805	0.9540	0.8955	0.9836	0.9444	-0.0361		
YER162C	RAD4	0.8408	0.8857	0.8866	0.8710	0.7887	0.9168	0.8020	0.8358	-0.0352		
YMR078C	CTF18	0.8695	0.9140	1.0040	0.9292	0.7759	0.8955	1.0116	0.8943	-0.0348		No interaction
YGR184C	UBR1	0.9536	1.0368	0.9974	0.9960	1.0590	0.9412	0.8914	0.9639	-0.0321	No interaction	
YAL015C	NTG1	0.7633	0.8479	0.8040	0.8051	0.7473	0.8316	0.7405	0.7731	-0.0320		
YOL068C	HST1	0.9138	0.9424	0.9366	0.9309	0.9477	0.9260	0.8243	0.8993	-0.0316		
YPL183W-A	RTC6	0.3607	0.4464	0.4933	0.4334	0.5342	0.3503	0.3214	0.4020	-0.0315		
YKL057C	NUP120	0.6793	0.6873	0.7606	0.7090	0.6964	0.7219	0.6148	0.6777	-0.0313		
YLR270W	DCS1	0.8120	0.8692	0.7953	0.8255	0.8077	0.8285	0.7489	0.7950	-0.0305		
YER177W	BMH1	0.4425	0.4676	0.4281	0.4461	0.3943	0.4782	0.3744	0.4157	-0.0304		
YCR014C	POL4	0.8563	0.9447	0.8757	0.8922	0.8936	0.9108	0.7824	0.8623	-0.0300		
YJR047C	ANB1	0.9536	0.9754	0.8888	0.9393	0.9477	0.7128	1.0675	0.9093	-0.0300		
YER095W	RAD51	0.7036	0.7652	0.7236	0.7308	0.7918	0.7158	0.5952	0.7009	-0.0299		

Yeast systematic name	Yeast standard name	Vector Set 1	Vector Set 2	Vector Set 3	Vector Avg.	yCHL1 Set 1	yCHL1 Set 2	yCHL1 Set 3	yCHL1 Avg.	E-C[a]	GC Validations (plasmid expression)[b]	Validations (hetero-allelic haploids)[c]
YKL025C	PAN3	0.9072	1.0014	0.9518	0.9535	0.9254	0.9656	0.8830	0.9247	-0.0288		
YNL025C	SSN8	0.0553	0.0638	0.0522	0.0571	0.0382	0.0000	0.0475	0.0286	-0.0285		
YGL090W	LIF1	0.8187	0.8479	0.9822	0.8829	0.7028	0.8894	0.9724	0.8549	-0.0280		
YHR066W	SSF1	0.8895	0.9849	0.9409	0.9384	0.9254	0.9290	0.8802	0.9116	-0.0269		
YNR023W	SNF12	0.8341	0.9400	0.9257	0.9000	0.9477	0.9473	0.7265	0.8738	-0.0261		
YGR258C	RAD2	0.9160	0.9495	0.9388	0.9347	0.9381	0.9656	0.8271	0.9103	-0.0245		
YGL194C	HOS2	0.7744	0.8573	0.8149	0.8155	0.6901	0.8742	0.8104	0.7915	-0.0240		
YHR086W	NAM8	0.9005	0.9731	1.0474	0.9737	0.9890	0.8742	0.9892	0.9508	-0.0229		
YCL029C	BIK1	0.8784	0.9754	0.8823	0.9120	0.9445	0.9443	0.7796	0.8895	-0.0226		
YLR376C	PSY3	0.7346	0.7841	0.7062	0.7417	0.7123	0.7615	0.6846	0.7195	-0.0222		
YDL059C	RAD59	0.8386	0.8715	1.0083	0.9061	0.7855	0.8772	0.9892	0.8840	-0.0222		
YDR075W	PPH3	0.8253	0.9188	0.8475	0.8638	0.8872	0.8864	0.7517	0.8418	-0.0221		
YBL088C	TEL1	0.8541	0.9117	0.8692	0.8783	0.8841	0.8955	0.7936	0.8577	-0.0206		
YPL164C	MLH3	0.9116	0.9754	0.8975	0.9282	0.9763	0.9351	0.8132	0.9082	-0.0200		
YNL246W	VPS75	0.8386	0.8833	0.8584	0.8601	0.9636	0.7402	0.8216	0.8418	-0.0183		
YPR135W	CTF4	0.7833	0.7109	0.9105	0.8016	0.7823	0.7615	0.8104	0.7847	-0.0168		
YML021C	UNG1	0.7855	0.8573	0.7627	0.8019	0.8236	0.7950	0.7405	0.7864	-0.0155		
YLL002W	RTT109	0.7479	0.6684	0.6324	0.6829	0.7123	0.7828	0.5086	0.6679	-0.0150		
YLR288C	MEC3	0.7810	0.8526	0.7932	0.8089	0.7537	0.8498	0.7852	0.7962	-0.0127		
YOL043C	NTG2	0.8917	0.9353	0.9257	0.9176	0.9667	0.9382	0.8132	0.9060	-0.0115		
YLR135W	SLX4	0.6704	0.7487	0.6780	0.6990	0.6742	0.7189	0.6707	0.6879	-0.0111		
YNL299W	TRF5	0.9514	0.9754	0.9822	0.9697	1.0526	0.9564	0.8691	0.9594	-0.0103		
YGR129W	SYF2	0.8452	0.9518	0.8931	0.8967	0.8872	0.9199	0.8551	0.8874	-0.0093		
YMR201C	RAD14	0.8895	0.9235	0.9322	0.9151	0.9636	0.9199	0.8355	0.9063	-0.0087		
YDR004W	RAD57	0.7302	0.8148	0.7323	0.7591	0.7791	0.7128	0.7601	0.7506	-0.0085		
YOR144C	ELG1	0.6195	0.8290	0.7497	0.7327	0.8236	0.8559	0.4946	0.7247	-0.0080		
YOR080W	DIA2	0.9758	0.9778	0.9561	0.9699	1.0144	0.9382	0.9361	0.9629	-0.0070		
YBR195C	MSI1	0.8718	0.9258	0.8779	0.8918	0.9286	0.9412	0.7852	0.8850	-0.0068		
YOL090W	MSH2	0.6439	0.7487	0.6715	0.6880	0.6933	0.6732	0.6790	0.6818	-0.0062		
YNL252C	MRPL17	0.0000	0.0000	0.0174	0.0058	0.0000	0.0000	0.0000	0.0000	-0.0058		
YBR189W	RPS9B	0.8518	0.9046	0.8714	0.8759	0.9858	0.7889	0.8383	0.8710	-0.0049		
YML102W	CAC2	0.6771	0.7322	0.7062	0.7052	0.7441	0.6945	0.6623	0.7003	-0.0049		
YLR265C	NEJ1	0.7390	0.8314	0.7475	0.7726	0.7219	0.8011	0.7824	0.7685	-0.0042		
YNL218W	MGS1	0.9580	1.0014	0.9409	0.9668	0.9890	0.9930	0.9110	0.9643	-0.0025		
YMR190C	SGS1	0.8518	0.8810	0.8757	0.8695	0.9190	0.8864	0.7964	0.8673	-0.0022		
YNL082W	PMS1	0.7744	0.9046	0.8127	0.8306	0.8777	0.8224	0.7880	0.8294	-0.0012		
YGL066W	SGF73	0.8430	0.8951	0.8127	0.8503	0.9063	0.8651	0.7768	0.8494	-0.0009		
YOR005C	DNL4	0.7833	0.8692	0.8127	0.8217	0.7537	0.8742	0.8355	0.8211	-0.0006		
YFR031C-A	RPL2A	0.8297	0.9093	0.8106	0.8499	0.8904	0.8346	0.8243	0.8498	-0.0001		
YLR418C	CDC73	0.0000	0.0000	0.0000	0.0000	0.0000	0.0000	0.0000	0.0000	0.0000		
YAR002W	NUP60	0.0000	0.0000	0.0000	0.0000	0.0000	0.0000	0.0000	0.0000	0.0000		
YAL040C	CLN3	0.7545	0.8337	0.7671	0.7851	0.8236	0.8194	0.7126	0.7852	0.0001		
YKL203C	TOR2	0.7633	0.7581	0.9301	0.8172	0.7028	1.0143	0.7349	0.8173	0.0002		
YGR108W	CLB1	0.7921	0.8739	0.8431	0.8364	0.8618	0.8833	0.7657	0.8369	0.0006		
YHR154W	RTT107	0.6771	0.7062	0.6802	0.6878	0.7028	0.7128	0.6511	0.6889	0.0011		
YJL101C	GSH1	0.0000	0.0000	0.0261	0.0087	0.0000	0.0305	0.0000	0.0102	0.0015		
YDR523C	SPS1	1.0134	1.0605	1.0105	1.0281	1.0876	1.0295	0.9752	1.0308	0.0027		
YGL003C	CDH1	0.6771	0.7889	0.6845	0.7168	0.6901	0.7676	0.7014	0.7197	0.0029		
YFR034C	PHO4	0.8784	0.9542	0.8844	0.9057	0.9699	0.8894	0.8691	0.9095	0.0038		
YKR024C	DBP7	0.7279	0.7109	0.6997	0.7129	0.7441	0.7889	0.6176	0.7169	0.0040		
YIL132C	CSM2	0.8364	0.9353	0.8475	0.8730	0.8332	0.9534	0.8467	0.8778	0.0047		
YIL112W	HOS4	0.8651	0.9353	0.8953	0.8986	0.8936	0.9686	0.8579	0.9067	0.0081		
YBR223C	TDP1	0.8651	0.9447	0.8562	0.8887	0.9413	0.9595	0.7908	0.8972	0.0085		
YOR026W	BUB3	0.8961	0.9400	0.9366	0.9242	1.0971	0.7432	0.9585	0.9329	0.0087		

Yeast systematic name	Yeast standard name	Vector Set 1	Vector Set 2	Vector Set 3	Vector Avg.	yCHL1 Set 1	yCHL1 Set 2	yCHL1 Set 3	yCHL1 Avg.	E-C[a]	GC Validations (plasmid expression)[b]	Validations (hetero-allelic haploids)[c]
YML061C	PIF1	0.8939	0.9565	0.9192	0.9232	0.9381	1.0387	0.8216	0.9328	0.0096		
YBR228W	SLX1	0.8452	0.9329	0.8518	0.8767	0.9286	0.9321	0.7992	0.8866	0.0100		
YOR073W	SGO1	0.8607	0.9329	0.8518	0.8818	0.8713	1.0021	0.8020	0.8918	0.0100	No interaction	
YKL210W	UBA1	0.8253	0.8573	1.0366	0.9064	0.7600	0.9534	1.0367	0.9167	0.0103		
YJR035W	RAD26	0.8518	0.8503	0.9779	0.8933	0.8173	0.9016	0.9948	0.9046	0.0112		
YGL087C	MMS2	0.7678	0.8550	0.7454	0.7894	0.7791	0.8590	0.7657	0.8012	0.0119		
YML124C	TUB3	0.8275	0.8904	0.8649	0.8609	0.9222	0.8833	0.8132	0.8729	0.0120		
YKR092C	SRP40	0.7766	0.8692	0.8127	0.8195	0.8141	0.8559	0.8327	0.8342	0.0147		
YKL117W	SBA1	0.8408	0.9447	0.8671	0.8842	0.9699	0.9321	0.7964	0.8995	0.0153		
YBR073W	RDH54	0.8651	0.9754	0.8366	0.8924	0.8364	0.9656	0.9249	0.9090	0.0166		
YER045C	ACA1	0.7589	0.8621	0.7953	0.8054	0.8586	0.8133	0.7964	0.8228	0.0173		
YAL019W	FUN30	0.7899	0.8715	0.8149	0.8254	0.8427	0.8803	0.8076	0.8435	0.0181		
YOR351C	MEK1	0.8364	0.8762	0.8431	0.8519	0.8904	0.9016	0.8188	0.8703	0.0183		
YPR018W	RLF2	0.6328	0.6991	0.6280	0.6533	0.7155	0.6579	0.6483	0.6739	0.0206		
YDR097C	MSH6	0.7191	0.7936	0.6910	0.7346	0.7537	0.7889	0.7237	0.7554	0.0209		
YJR063W	RPA12	0.7412	0.7865	0.7780	0.7686	0.8395	0.8102	0.7210	0.7902	0.0217		
YOR308C	SNU66	0.8430	0.8999	0.8888	0.8772	0.8968	0.9960	0.8076	0.9001	0.0229		
YBL058W	SHP1	0.8010	0.8526	0.8279	0.8272	0.8300	0.9047	0.8160	0.8502	0.0230		
YFR040W	SAP155	0.7191	0.7912	0.6867	0.7323	0.8046	0.7006	0.7629	0.7560	0.0237		
YDR076W	RAD55	0.7456	0.8196	0.7171	0.7608	0.8173	0.7950	0.7433	0.7852	0.0244		
YPL042C	SSN3	0.6151	0.7062	0.6454	0.6556	1.0081	0.5148	0.5226	0.6818	0.0262		
YGL163C	RAD54	0.7169	0.7747	0.7171	0.7362	0.8109	0.7585	0.7210	0.7634	0.0272		
YGL251C	HFM1	0.7656	0.8739	0.7888	0.8094	0.8268	0.8590	0.8243	0.8367	0.0273		
YEL056W	HAT2	0.7766	0.8007	0.7866	0.7880	0.8046	0.8590	0.7824	0.8153	0.0273		
YOR346W	REV1	0.8452	0.9400	0.8823	0.8892	0.9477	0.8955	0.9110	0.9180	0.0289		
YLR399C	BDF1	0.6018	0.4747	0.1782	0.4182	0.3212	0.1157	0.9054	0.4474	0.0292		
YLR210W	CLB4	0.7412	0.8007	0.7606	0.7675	0.7982	0.8224	0.7713	0.7973	0.0298		
YML060W	OGG1	0.8032	0.8975	0.8040	0.8349	0.8459	0.9351	0.8132	0.8647	0.0298		
YMR156C	TPP1	0.7678	0.8786	0.8106	0.8190	0.8682	0.8285	0.8523	0.8497	0.0307		
YBL019W	APN2	0.8651	0.9140	0.8649	0.8813	0.9349	0.9564	0.8495	0.9136	0.0323		
YKR056W	TRM2	0.8673	0.9117	0.8671	0.8820	0.9922	0.9047	0.8467	0.9145	0.0325		
YGL058W	RAD6	0.9138	0.9518	0.9540	0.9399	0.9763	0.9778	0.9641	0.9727	0.0328		
YOL115W	PAP2	0.8784	0.9400	0.9040	0.9075	1.0272	0.9077	0.8886	0.9412	0.0337		
YER070W	RNR1	0.9603	0.9731	0.9757	0.9697	1.1003	0.8651	1.0451	1.0035	0.0338		
YPR101W	SNT309	0.7014	0.7723	0.6650	0.7129	0.7791	0.7432	0.7182	0.7468	0.0339		
YDR419W	RAD30	0.8297	0.9188	0.8258	0.8581	0.9063	0.9077	0.8635	0.8925	0.0344		
YGR063C	SPT4	0.3540	0.4842	0.0304	0.2895	0.0572	0.8681	0.0475	0.3243	0.0347		
YPL240C	HSP82	0.8784	0.9424	0.9431	0.9213	1.0621	0.9047	0.9026	0.9565	0.0352		
YLR247C	IRC20	1.2059	1.1786	1.2039	1.1961	1.2466	1.1940	1.2547	1.2318	0.0357	No interaction	
YER041W	YEN1	0.9138	0.9660	0.9127	0.9308	1.0176	0.9534	0.9305	0.9672	0.0364		
YDR092W	UBC13	0.6129	0.6944	0.6085	0.6386	0.6742	0.7219	0.6287	0.6749	0.0364		
YDR078C	SHU2	0.8541	0.9471	0.9018	0.9010	0.9954	0.9625	0.8551	0.9377	0.0367		
YLR318W	EST2	0.8762	0.9589	0.8910	0.9087	0.9699	0.9534	0.9138	0.9457	0.0370		
YFL003C	MSH4	1.0134	1.1053	1.0170	1.0452	1.1989	1.0509	1.0004	1.0834	0.0381		
YCR092C	MSH3	0.7921	0.8786	0.7910	0.8206	0.8745	0.8833	0.8188	0.8589	0.0383		
YOL012C	HTZ1	0.8695	0.8975	0.8410	0.8693	0.9381	0.9412	0.8439	0.9077	0.0384		
YKR028W	SAP190	0.8120	0.8880	0.8801	0.8601	0.9731	0.9717	0.7545	0.8998	0.0397		
YLR035C	MLH2	0.9072	0.9376	0.8996	0.9148	1.0208	0.9595	0.8858	0.9554	0.0406		
YDR121W	DPB4	0.7611	0.7912	0.7475	0.7666	0.8236	0.8559	0.7433	0.8076	0.0410		
YHL006C	SHU1	0.8253	0.8904	0.8584	0.8580	0.8872	0.9382	0.8718	0.8991	0.0411		
YGR109C	CLB6	0.7877	0.8762	0.8692	0.8444	0.9445	0.8376	0.8774	0.8865	0.0421		
YKL114C	APN1	0.8917	0.9707	0.9366	0.9330	1.0208	1.0082	0.8970	0.9753	0.0423		

Yeast systematic name	Yeast standard name	Vector Set 1	Vector Set 2	Vector Set 3	Vector Avg.	yCHL1 Set 1	yCHL1 Set 2	yCHL1 Set 3	yCHL1 Avg.	E-C[a]	GC Validations (plasmid expression)[b]	Validations (hetero-allelic haploids)[c]
YJL115W	ASF1	0.6726	0.6519	0.6476	0.6574	0.7505	0.7128	0.6371	0.7001	0.0428		
YDR314C	RAD34	0.7744	0.8928	0.7693	0.8121	0.9477	0.8407	0.7796	0.8560	0.0438		
YPL046C	ELC1	0.6903	0.8101	0.7258	0.7421	0.8491	0.7737	0.7405	0.7878	0.0457		
YLR176C	RFX1	0.7855	0.7463	0.8149	0.7822	0.8554	0.7615	0.8691	0.8287	0.0464		
YPL127C	HHO1	1.0797	1.0250	1.1843	1.0964	1.1893	1.0844	1.1708	1.1482	0.0518		
YIR019C	MUC1	0.7833	0.8904	0.8279	0.8339	0.9604	0.8376	0.8635	0.8872	0.0533		
YDL155W	CLB3	1.1859	1.2282	1.2234	1.2125	1.3261	1.2428	1.2351	1.2680	0.0555		
YFR014C	CMK1	0.7877	0.8739	0.7736	0.8117	0.8968	0.8498	0.8551	0.8672	0.0555		
YOR025W	HST3	0.9448	0.6991	0.8323	0.8254	0.9445	0.8651	0.8355	0.8817	0.0563		
YOL072W	THP1	0.8098	0.8007	0.8106	0.8070	0.8014	0.8468	0.9473	0.8652	0.0581		
YBR231C	SWC5	0.8541	0.9164	0.8671	0.8792	1.0272	0.9930	0.7992	0.9398	0.0606		
YJL092W	SRS2	0.8895	0.9636	0.8562	0.9031	1.0462	0.9138	0.9333	0.9645	0.0614	No interaction	
YOL006C	TOP1	0.8518	0.9022	0.8584	0.8708	0.9922	0.9747	0.8299	0.9323	0.0615		
YJL047C	RTT101	0.7678	0.7865	0.7454	0.7665	0.8650	0.8316	0.7992	0.8319	0.0654		
YPL129W	TAF14	0.5399	0.2929	0.5063	0.4464	1.0749	0.2650	0.2152	0.5183	0.0720		
YEL037C	RAD23	0.8120	0.8786	0.8323	0.8410	0.9763	0.9473	0.8216	0.9150	0.0741		
YPL167C	REV3	0.8607	0.9211	0.8866	0.8895	1.0367	0.9382	0.9194	0.9647	0.0753		
YLR357W	RSC2	0.7678	0.4180	0.5628	0.5829	0.7918	0.9382	0.2515	0.6605	0.0776		
YDL101C	DUN1	0.8275	0.8692	0.8692	0.8553	0.9667	0.8864	0.9473	0.9335	0.0782		
YOR033C	EXO1	0.8563	0.9400	0.8627	0.8863	1.0653	0.9443	0.8858	0.9651	0.0788		
YGL043W	DST1	0.7036	0.7369	0.6954	0.7120	0.8650	0.7767	0.7601	0.8006	0.0886		
YDR334W	SWR1	0.7899	0.8786	0.7758	0.8148	0.9636	0.8955	0.8635	0.9075	0.0928		
YNL021W	HDA1	0.5266	0.4511	0.6802	0.5526	0.5692	0.6701	0.6986	0.6460	0.0934		
YPL001W	HAT1	0.8076	0.8408	0.7801	0.8095	0.9985	0.8407	0.8802	0.9065	0.0970		
YMR284W	YKU70	0.9868	0.9164	0.9518	0.9517	1.1257	1.1118	0.9166	1.0514	0.0997		
YGR180C	RNR4	0.5708	0.6188	0.6715	0.6204	0.7473	0.7036	0.7237	0.7249	0.1045		
YCL061C	MRC1	0.7766	0.7511	0.8279	0.7852	1.0272	0.7463	0.9026	0.8920	0.1068		
YGR003W	CUL3	0.7766	0.8573	0.7584	0.7975	0.9731	0.8651	0.8830	0.9071	0.1096		
YDR014W	RAD61	0.9558	1.0109	0.8910	0.9526	1.1703	0.9625	1.0563	1.0630	0.1105		No interaction
YOR258W	HNT3	0.7855	0.9211	0.7084	0.8050	0.9826	1.0265	0.7629	0.9240	0.1190		
YMR234W	RNH1	0.7102	0.7322	0.8149	0.7524	0.9286	0.9930	0.7070	0.8762	0.1237		
YDR378C	LSM6	0.9603	1.0203	0.9714	0.9840	1.1607	1.1879	1.0116	1.1201	0.1361		
YPR119W	CLB2	0.8054	0.8644	0.8518	0.8406	0.9890	1.0295	0.9138	0.9774	0.1369		
YGR285C	ZUO1	0.3673	0.3708	0.3738	0.3706	0.9127	0.2071	0.4136	0.5111	0.1405		
YJL187C	SWE1	0.7036	0.7794	0.8497	0.7776	1.0367	0.9869	0.7433	0.9223	0.1447		
YHR200W	RPN10	0.4868	0.5102	0.5737	0.5235	0.7855	0.7706	0.4611	0.6724	0.1489		
YNL107W	YAF9	0.6748	0.7605	0.6389	0.6914	0.9508	0.7615	0.8607	0.8577	0.1663		
YDR176W	NGG1	0.1770	0.2055	0.1782	0.1869	0.0000	0.3747	0.7070	0.3605	0.1737		
YER051W	JHD1	1.1417	1.0746	1.1452	1.1205	1.3897	1.3585	1.1960	1.3147	0.1942		
YGR056W	RSC1	0.4536	0.7251	0.4955	0.5580	0.4261	0.9991	0.8467	0.7573	0.1993		
YPR120C	CLB5	0.7390	0.7369	0.8562	0.7774	1.0844	1.0813	0.7852	0.9836	0.2063		
YGR276C	RNH70	0.9271	0.8077	0.9670	0.9006	1.2593	1.1758	0.8858	1.1070	0.2063		
YMR106C	YKU80	0.6594	0.6094	0.5150	0.5946	0.7918	0.8742	0.8439	0.8366	0.2421		

[a]Experimental-control or (yCHL1 average)-(vector average). For each mutant, area of pinned spot was normalized to the average of WT spots on the same plate.

[b]Growth curve validations using plasmid expression. Top hits with yK48R and some selected mutants were chosen for validations by growth curves using plasmid-based ectopic expression. "No interaction" indicates no SDL interaction was observed.

[c]Validations using integrated hetero-allelic haploids. Selected mutants were tested by integrating a GAL-inducible CHL1 ORF at the ura3Δ0 locus. "No interaction" indicates no SDL interaction was observed.

Table C.2 - Results of the dominant synthetic lethal screen for *CHL1*^{K48R}

Yeast systematic name	Yeast standard name	Vector Set 1	Vector Set 2	Vector Set 3	Vector Avg.	yK48R Set 1	yK48R Set 2	yK48R Set 3	yK48R Avg.	E-C[a]	GC Validations (plasmid expression)[b]	Validations (hetero-allelic haploids)[c]
YDR364C	CDC40	0.8496	0.9967	0.8605	0.9023	0.0000	0.1644	0.0000	0.0548	-0.8475		
YER016W	BIM1	1.0377	1.0463	0.9149	0.9996	0.1805	0.1918	0.2201	0.1975	-0.8021	Negative	Negative
YGR188C	BUB1	0.7987	0.9022	0.7910	0.8307	0.1316	0.0914	0.2406	0.1545	-0.6761	Negative	Negative
YPR141C	KAR3	0.7191	0.7936	0.7541	0.7556	0.1102	0.1523	0.1497	0.1374	-0.6182	No interaction	
YEL061C	CIN8	0.9226	0.9684	0.8605	0.9172	0.3642	0.3532	0.3697	0.3624	-0.5548	No interaction	
YMR048W	CSM3	0.8673	0.8975	0.9149	0.8932	0.4101	0.3197	0.3521	0.3606	-0.5326	No interaction	
YNL273W	TOF1	0.7434	0.7322	0.8301	0.7686	0.2295	0.2832	0.2700	0.2609	-0.5077	No interaction	
YCL016C	DCC1	0.9271	0.8361	0.9583	0.9072	0.7467	0.3380	0.1291	0.4046	-0.5026	Negative	Negative
YLR240W	VPS34	0.8142	0.8196	0.8540	0.8293	0.3733	0.3593	0.4050	0.3792	-0.4501	No interaction	
YBR158W	AMN1	1.1417	1.1998	1.1995	1.1803	0.7773	0.7186	0.7659	0.7539	-0.4264	No interaction	
YDL042C	SIR2	1.0156	1.1101	0.9887	1.0381	0.6732	0.6181	0.5663	0.6192	-0.4189	No interaction	
YLL019C	KNS1	1.1705	1.2400	1.1669	1.1925	0.8171	0.7917	0.7630	0.7906	-0.4019	No interaction	
YLR399C	BDF1	0.6018	0.4747	0.1782	0.4182	0.0000	0.0000	0.1350	0.0450	-0.3733		
YGR184C	UBR1	0.9536	1.0368	0.9974	0.9960	0.6977	0.5877	0.5840	0.6231	-0.3728	No interaction	
YDL070W	BDF2	0.9514	0.9967	0.9801	0.9761	0.6212	0.6608	0.5634	0.6151	-0.3609	No interaction	
YOR386W	PHR1	1.0045	0.9471	0.9322	0.9613	0.9487	0.8739	0.0000	0.6075	-0.3538		
YER173W	RAD24	0.7965	0.9447	0.8714	0.8709	0.5294	0.5572	0.4695	0.5187	-0.3522	No interaction	
YMR186W	HSC82	1.0908	1.0770	0.9561	1.0413	0.5967	0.6456	0.8304	0.6909	-0.3504		
YOR073W	SGO1	0.8607	0.9329	0.8518	0.8818	0.5141	0.6121	0.4754	0.5338	-0.3480	No interaction	
YJL013C	MAD3	1.0355	1.0652	1.0474	1.0494	0.7161	0.8009	0.6045	0.7071	-0.3422	No interaction	
YER164W	CHD1	0.7810	0.6755	0.8062	0.7542	0.3886	0.4141	0.4372	0.4133	-0.3409		
YHR191C	CTF8	0.8076	0.7676	0.9561	0.8438	0.5019	0.5329	0.4871	0.5073	-0.3365	Negative	Negative
YLR107W	REX3	1.1240	1.1502	0.9279	1.0674	0.6824	0.7217	0.7952	0.7331	-0.3343	No interaction	
YPL241C	CIN2	1.0089	1.0416	0.9648	1.0051	0.7314	0.7887	0.5077	0.6759	-0.3292	No interaction	
YBR289W	SNF5	0.4602	0.4747	0.9388	0.6246	0.2234	0.3867	0.3022	0.3041	-0.3204		
YIL153W	RRD1	0.6881	0.7109	0.7388	0.7126	0.3886	0.4324	0.3697	0.3969	-0.3157	No interaction	
YOR258W	HNT3	0.7855	0.9211	0.7084	0.8050	0.0000	0.7278	0.7806	0.5028	-0.3022		
YGL086W	MAD1	0.7479	0.8479	0.7671	0.7876	0.4927	0.4963	0.4871	0.4920	-0.2956	No interaction	No interaction
YMR216C	SKY1	1.0731	1.1006	0.8975	1.0237	0.6977	0.5816	0.9185	0.7326	-0.2911	No interaction	
YPL194W	DDC1	0.8762	0.9849	0.9149	0.9253	0.7161	0.6181	0.5752	0.6365	-0.2888	No interaction	
YLR247C	IRC20	1.2059	1.1786	1.2039	1.1961	0.9456	0.8557	0.9361	0.9124	-0.2836	No interaction	
YOR368W	RAD17	0.9027	0.9778	0.9496	0.9434	0.7038	0.6364	0.6573	0.6659	-0.2775	No interaction	
YNL136W	EAF7	1.1218	1.0345	1.1148	1.0903	0.7559	0.9227	0.7600	0.8128	-0.2775		
YNL250W	RAD50	0.6195	0.6849	0.6758	0.6601	0.3856	0.3532	0.4138	0.3842	-0.2759	No interaction	
YPL129W	TAF14	0.5399	0.2929	0.5063	0.4464	0.5172	0.0000	0.0000	0.1724	-0.2740		
YBR245C	ISW1	0.8386	0.9636	0.9149	0.9057	0.6947	0.7125	0.5018	0.6363	-0.2694		
YIR002C	MPH1	0.8496	0.8975	0.9344	0.8938	0.6579	0.6181	0.6074	0.6278	-0.2660	No interaction	
YJL092W	SRS2	0.8895	0.9636	0.8562	0.9031	0.6579	0.5755	0.7013	0.6449	-0.2582	No interaction	
YML032C	RAD52	0.6062	0.6519	0.5672	0.6084	0.3458	0.3959	0.3257	0.3558	-0.2526	No interaction	No interaction
YER162C	RAD4	0.8408	0.8857	0.8866	0.8710	0.5631	0.6577	0.6456	0.6221	-0.2489		
YDL013W	SLX5	0.9603	1.0085	1.0235	0.9974	0.7283	0.7704	0.7512	0.7500	-0.2474		
YOL072W	THP1	0.8098	0.8007	0.8106	0.8070	0.5845	0.6060	0.4901	0.5602	-0.2468		
YJL030W	MAD2	0.7191	0.7487	0.8888	0.7855	0.5080	0.6151	0.5165	0.5465	-0.2390		
YML011C	RAD33	1.0488	1.0156	0.8671	0.9771	0.6518	0.7734	0.7952	0.7402	-0.2370		
YNR052C	POP2	0.4381	0.3732	0.4411	0.4175	0.3060	0.1309	0.1086	0.1818	-0.2356		
YDR279W	RNH202	1.0266	0.9613	0.9149	0.9676	0.7069	0.6821	0.8158	0.7349	-0.2327		
YDR369C	XRS2	0.6549	0.6519	0.6693	0.6587	0.4345	0.4476	0.4020	0.4281	-0.2306		
YMR173W	DDR48	1.0289	0.9447	1.0083	0.9940	0.7375	0.6608	0.8979	0.7654	-0.2286		
YOR025W	HST3	0.9448	0.6991	0.8323	0.8254	0.6885	0.5664	0.5575	0.6042	-0.2212		

Yeast systematic name	Yeast standard name	Vector Set 1	Vector Set 2	Vector Set 3	Vector Avg.	yK48R Set 1	yK48R Set 2	yK48R Set 3	yK48R Avg.	E-C[a]	GC Validations (plasmid expression)[b]	Validations (hetero-allelic haploids)[c]
YKL113C	RAD27	0.9492	0.8219	0.9214	0.8975	0.6977	0.5542	0.7776	0.6765	-0.2210		
YKL139W	CTK1	0.8054	0.8810	0.8258	0.8374	0.5723	0.5146	0.7747	0.6205	-0.2168		
YNL116W	DMA2	1.1948	1.1148	1.0235	1.1110	0.9027	0.8496	0.9390	0.8971	-0.2139		
YEL003W	GIM4	0.9492	0.9684	0.9257	0.9478	0.7681	0.8191	0.6221	0.7364	-0.2113		
YNL107W	YAF9	0.6748	0.7605	0.6389	0.6914	0.9640	0.4781	0.0000	0.4807	-0.2107		
YNL068C	FKH2	0.8341	0.8573	0.9149	0.8688	0.5661	0.6151	0.7982	0.6598	-0.2090		
YLR394W	CST9	0.9979	0.8621	1.0170	0.9590	0.6610	0.7491	0.8422	0.7508	-0.2082		
YHR066W	SSF1	0.8895	0.9849	0.9409	0.9384	0.4988	0.8892	0.8040	0.7307	-0.2078		
YOL087C	DUF1	0.8142	0.8951	0.8323	0.8472	0.6671	0.6516	0.6104	0.6430	-0.2042		
YDR440W	DOT1	0.9912	0.9849	0.8888	0.9550	0.6671	0.6638	0.9244	0.7518	-0.2032		
YLR320W	MMS22	0.6328	0.6471	0.6237	0.6345	0.4345	0.4415	0.4372	0.4378	-0.1968		
YIL018W	RPL2B	1.0466	1.1077	1.0800	1.0781	0.9793	0.7704	0.8950	0.8816	-0.1965		
YLR085C	ARP6	1.1174	1.1219	1.0561	1.0984	0.8752	0.8678	0.9654	0.9028	-0.1956		
YDR014W	RAD61	0.9558	1.0109	0.8910	0.9526	0.7406	0.7156	0.8216	0.7593	-0.1933		No interaction
YMR224C	MRE11	0.5354	0.6212	0.6019	0.5862	0.3886	0.4324	0.3727	0.3979	-0.1883		
YNL330C	RPD3	0.5620	0.5031	0.5932	0.5528	0.3978	0.4324	0.2729	0.3677	-0.1851		
YDL074C	BRE1	0.5089	0.4558	0.5715	0.5121	0.3213	0.3015	0.3756	0.3328	-0.1793		
YER051W	JHD1	1.1417	1.0746	1.1452	1.1205	1.0007	0.9440	0.8833	0.9426	-0.1779		
YPL024W	RMI1	0.7213	0.8101	0.9496	0.8270	0.5478	0.6151	0.7952	0.6527	-0.1743		
YGL003C	CDH1	0.6771	0.7889	0.6845	0.7168	0.5386	0.5329	0.5575	0.5430	-0.1738		
YDR289C	RTT103	0.5974	0.6117	0.5889	0.5993	0.4407	0.4141	0.4284	0.4277	-0.1716		
YDL154W	MSH5	0.8983	0.9991	0.9953	0.9642	0.8477	0.7065	0.8246	0.7929	-0.1713		
YGL066W	SGF73	0.8430	0.8951	0.8127	0.8503	0.7375	0.7552	0.5458	0.6795	-0.1708		
YDL155W	CLB3	1.1859	1.2282	1.2234	1.2125	1.1384	0.9805	1.0065	1.0418	-0.1707		
YGR063C	SPT4	0.3540	0.4842	0.0304	0.2895	0.0520	0.0731	0.2318	0.1190	-0.1706		
YGR271W	SLH1	1.0643	1.0794	1.0735	1.0724	1.0282	0.7978	0.8891	0.9051	-0.1673		
YDR176W	NGG1	0.1770	0.2055	0.1782	0.1869	0.0000	0.0274	0.0323	0.0199	-0.1670		
YBL046W	PSY4	0.8253	0.9306	0.9127	0.8895	0.6579	0.7125	0.8099	0.7268	-0.1627		
YGR270W	YTA7	0.7965	0.8644	0.8279	0.8296	0.7100	0.6699	0.6221	0.6673	-0.1623		
YBR009C	HHF1	0.8076	0.8526	0.8127	0.8243	0.6824	0.6486	0.6573	0.6628	-0.1615		
YBR089C-A	NHP6B	1.0510	1.0817	0.9953	1.0427	0.8232	1.0688	0.7571	0.8830	-0.1596		
YDL116W	NUP84	0.6948	0.7511	0.8171	0.7543	0.6182	0.6212	0.5546	0.5980	-0.1563		
YDR079C-A	TFB5	1.0112	0.0638	0.6367	0.5705	0.2724	0.8861	0.0910	0.4165	-0.1541		
YGR171C	MSM1	0.1682	0.2078	0.2477	0.2079	0.1102	0.0000	0.0528	0.0543	-0.1536		
YDR379W	RGA2	0.9470	0.9258	0.8953	0.9227	0.7987	0.7795	0.7336	0.7706	-0.1521		
YBR010W	HHT1	0.8961	0.9542	0.9692	0.9398	0.8079	0.7460	0.8128	0.7889	-0.1509		
YJL065C	DLS1	0.9094	0.9660	0.9866	0.9540	0.6426	0.8130	0.9537	0.8031	-0.1509		
YDR225W	HTA1	0.6881	0.7463	0.6954	0.7099	0.5753	0.5694	0.5341	0.5596	-0.1503		
YIL139C	REV7	1.0510	1.0274	1.0518	1.0434	0.8354	0.8739	0.9742	0.8945	-0.1488		
YDL200C	MGT1	0.9514	0.9754	1.0040	0.9769	0.7314	0.7552	1.0006	0.8291	-0.1479		
YLR032W	RAD5	0.6704	0.8266	0.8236	0.7735	0.5508	0.6790	0.6544	0.6281	-0.1455		
YJR082C	EAF6	0.9315	0.9565	0.8649	0.9176	0.7344	0.8222	0.7600	0.7722	-0.1454		
YLR288C	MEC3	0.7810	0.8526	0.7932	0.8089	0.6182	0.7034	0.6720	0.6645	-0.1444		
YPR164W	MMS1	0.6372	0.7558	0.6932	0.6954	0.6120	0.6121	0.4314	0.5518	-0.1436		
YER169W	RPH1	0.8872	0.9565	0.9236	0.9224	0.7283	0.8404	0.7688	0.7792	-0.1433		
YBR034C	HMT1	1.0089	1.0746	1.1083	1.0639	0.8477	1.1206	0.7982	0.9221	-0.1418		
YDR363W	ESC2	0.9005	0.8692	0.8562	0.8753	0.7620	0.7552	0.7013	0.7395	-0.1358		
YML061C	PIF1	0.8939	0.9565	0.9192	0.9232	0.8354	0.8252	0.7072	0.7893	-0.1339		
YER116C	SLX8	0.9226	1.0203	1.0192	0.9874	0.8109	0.9531	0.8011	0.8551	-0.1323		
YCR065W	HCM1	0.8629	1.0203	0.9909	0.9580	0.8048	0.9013	0.7776	0.8279	-0.1301		
YOR351C	MEK1	0.8364	0.8762	0.8431	0.8519	0.8783	0.5512	0.7365	0.7220	-0.1299		
YER179W	DMC1	0.8740	0.9376	0.8975	0.9030	0.7803	0.7400	0.8011	0.7738	-0.1292		
YLR357W	RSC2	0.7678	0.4180	0.5628	0.5829	0.9242	0.2345	0.2025	0.4537	-0.1292		

Yeast systematic name	Yeast standard name	Vector Set 1	Vector Set 2	Vector Set 3	Vector Avg.	yK48R Set 1	yK48R Set 2	yK48R Set 3	yK48R Avg.	E-C[a]	GC Validations (plasmid expression)[b]	Validations (hetero-allelic haploids)[c]
YOR080W	DIA2	0.9758	0.9778	0.9561	0.9699	0.8844	0.8557	0.7835	0.8412	-0.1287		
YBR272C	HSM3	1.0001	1.0723	0.9974	1.0233	0.7436	0.9470	1.0036	0.8981	-0.1252		
YPL042C	SSN3	0.6151	0.7062	0.6454	0.6556	0.5141	0.5725	0.5077	0.5314	-0.1241		
YNL031C	HHT2	1.0178	1.0699	0.9931	1.0269	1.0068	0.8039	0.8979	0.9029	-0.1241		
YBR195C	MSI1	0.8718	0.9258	0.8779	0.8918	0.7956	0.8618	0.6485	0.7686	-0.1232		
YLL002W	RTT109	0.7479	0.6684	0.6324	0.6829	0.5569	0.6181	0.5047	0.5599	-0.1229		
YMR127C	SAS2	0.9116	0.9731	0.9866	0.9571	0.8293	0.7552	0.9244	0.8363	-0.1208		
YDL216C	RRI1	0.9094	0.9140	0.9866	0.9367	0.7222	0.7552	0.9713	0.8162	-0.1204		
YJR090C	GRR1	0.7678	0.7038	0.6171	0.6962	0.3580	0.5451	0.8275	0.5769	-0.1194		
YER177W	BMH1	0.4425	0.4676	0.4281	0.4461	0.3183	0.3258	0.3404	0.3282	-0.1179		
YML124C	TUB3	0.8275	0.8904	0.8649	0.8609	0.7528	0.7643	0.7189	0.7454	-0.1156		
YOR304W	ISW2	0.8010	0.8880	0.8171	0.8354	0.8171	0.7795	0.5634	0.7200	-0.1154		
YGL094C	PAN2	1.0598	1.0770	1.1539	1.0969	0.8783	0.9592	1.1122	0.9832	-0.1137		
YOR144C	ELG1	0.6195	0.8290	0.7497	0.7327	0.5355	0.6486	0.6779	0.6207	-0.1121		
YPL164C	MLH3	0.9116	0.9754	0.8975	0.9282	0.7314	0.8952	0.8216	0.8161	-0.1121		
YJR104C	SOD1	0.3983	0.3283	0.2673	0.3313	0.0000	0.0000	0.6632	0.2211	-0.1102		
YJR047C	ANB1	0.9536	0.9754	0.8888	0.9393	0.7773	0.7582	0.9537	0.8297	-0.1095		
YDR217C	RAD9	0.9448	1.0061	0.9409	0.9640	0.8018	0.9227	0.8451	0.8565	-0.1074		
YOL068C	HST1	0.9138	0.9424	0.9366	0.9309	0.9058	0.8039	0.7718	0.8272	-0.1038		
YGL100W	SEH1	0.8762	0.9188	0.8866	0.8938	0.7956	0.8739	0.7043	0.7913	-0.1026		
YGL033W	HOP2	0.8607	0.9093	0.8475	0.8725	0.6579	0.7247	0.9420	0.7749	-0.0976		
YJR043C	POL32	0.7523	0.8196	0.7671	0.7796	0.6885	0.6395	0.7219	0.6833	-0.0964		
YOR191W	ULS1	0.8518	0.9117	0.8671	0.8769	0.7344	0.7734	0.8363	0.7814	-0.0955		
YBR026C	ETR1	0.6616	0.6826	0.5867	0.6436	0.5631	0.5359	0.5458	0.5483	-0.0954		
YKL213C	DOA1	0.7102	0.7723	0.7497	0.7441	0.6212	0.6334	0.6925	0.6490	-0.0950		
YPL181W	CTI6	0.8828	0.9258	0.8975	0.9020	0.7895	0.8343	0.8011	0.8083	-0.0937		
YMR201C	RAD14	0.8895	0.9235	0.9322	0.9151	0.8905	0.8191	0.7630	0.8242	-0.0909		
YJL115W	ASF1	0.6726	0.6519	0.6476	0.6574	0.5906	0.5938	0.5194	0.5679	-0.0894		
YKR024C	DBP7	0.7279	0.7109	0.6997	0.7129	0.6335	0.6730	0.5663	0.6243	-0.0886		
YJR074W	MOG1	0.9580	0.9188	1.0648	0.9805	1.0252	0.9227	0.7336	0.8938	-0.0867		
YCR008W	SAT4	0.7855	0.7133	0.8279	0.7756	0.7589	0.5420	0.7659	0.6889	-0.0866		
YHR120W	MSH1	0.8518	0.8668	0.8975	0.8720	0.8140	0.7734	0.7688	0.7854	-0.0866		
YNL138W	SRV2	0.7501	0.9613	0.7323	0.8146	0.7773	0.4598	0.9508	0.7293	-0.0853		
YMR137C	PSO2	0.8474	0.8503	0.8736	0.8571	0.7008	0.7369	0.8803	0.7727	-0.0844		
YNR023W	SNF12	0.8341	0.9400	0.9257	0.9000	0.7987	0.8678	0.7806	0.8157	-0.0843		
YDR030C	RAD28	0.8850	0.8904	0.9561	0.9105	0.7559	0.7552	0.9684	0.8265	-0.0841		
YBL003C	HTA2	0.8341	0.8621	0.9127	0.8696	0.6396	0.7917	0.9273	0.7862	-0.0834		
YGL211W	NCS6	0.6151	0.6873	0.6302	0.6442	0.5508	0.5359	0.5957	0.5608	-0.0834		
YDL230W	PTP1	0.8253	0.9235	0.8584	0.8690	0.6916	0.7795	0.8891	0.7868	-0.0823		
YCL029C	BIK1	0.8784	0.9754	0.8823	0.9120	0.8018	0.8161	0.8715	0.8298	-0.0822		
YMR190C	SGS1	0.8518	0.8810	0.8757	0.8695	0.8354	0.7948	0.7336	0.7879	-0.0816		
YOR290C	SNF2	0.7899	0.8857	0.9496	0.8751	0.6885	0.8922	0.8040	0.7949	-0.0801		
YER098W	UBP9	0.9182	0.9660	0.9496	0.9446	0.8630	0.8313	0.9009	0.8650	-0.0796		
YLR233C	EST1	0.9868	1.0038	0.9909	0.9938	0.8783	0.9531	0.9126	0.9147	-0.0792		
YHL022C	SPO11	0.8253	0.8975	0.8301	0.8510	0.7528	0.7674	0.8011	0.7738	-0.0772		
YMR284W	YKU70	0.9868	0.9164	0.9518	0.9517	0.9333	0.8831	0.8070	0.8745	-0.0772		
YER095W	RAD51	0.7036	0.7652	0.7236	0.7308	0.6855	0.5877	0.6955	0.6562	-0.0746		
YNL299W	TRF5	0.9514	0.9754	0.9822	0.9697	0.9548	0.8861	0.8451	0.8953	-0.0744		
YBR223C	TDP1	0.8651	0.9447	0.8562	0.8887	0.8293	0.8252	0.7894	0.8146	-0.0741		
YDL082W	RPL13A	0.8961	0.9117	0.9561	0.9213	0.8446	0.8465	0.8539	0.8484	-0.0730		
YCR066W	RAD18	0.7810	0.7770	0.8823	0.8134	0.6641	0.7308	0.8275	0.7408	-0.0727		
YDR363W-A	SEM1	0.4757	0.5574	0.5215	0.5182	0.3795	0.4689	0.4901	0.4462	-0.0721		
YOR156C	NFI1	0.8076	0.8030	1.0257	0.8788	0.8140	0.8465	0.7600	0.8069	-0.0719		

Yeast systematic name	Yeast standard name	Vector Set 1	Vector Set 2	Vector Set 3	Vector Avg.	yK48R Set 1	yK48R Set 2	yK48R Set 3	yK48R Avg.	E-C[a]	GC Validations (plasmid expression)[b]	Validations (hetero-allelic haploids)[c]
YKR092C	SRP40	0.7766	0.8692	0.8127	0.8195	0.7742	0.6516	0.8216	0.7492	-0.0703		
YOL012C	HTZ1	0.8695	0.8975	0.8410	0.8693	0.8140	0.7887	0.7952	0.7993	-0.0700		
YNL218W	MGS1	0.9580	1.0014	0.9409	0.9668	0.7712	0.9318	0.9889	0.8973	-0.0695		
YHR086W	NAM8	0.9005	0.9731	1.0474	0.9737	1.0007	0.9409	0.7718	0.9045	-0.0692		
YPR119W	CLB2	0.8054	0.8644	0.8518	0.8406	0.7497	0.7704	0.7952	0.7718	-0.0688		
YGL240W	DOC1	0.8850	0.9565	0.8866	0.9094	0.8507	0.8496	0.8216	0.8406	-0.0687		
YPL096W	PNG1	0.9846	1.0605	1.0235	1.0229	0.9333	0.9744	0.9566	0.9548	-0.0681		
YKL057C	NUP120	0.6793	0.6873	0.7606	0.7090	0.6335	0.6943	0.5986	0.6421	-0.0669		
YKL017C	HCS1	0.8231	0.9093	0.8540	0.8621	0.7681	0.8526	0.7688	0.7965	-0.0656		
YML028W	TSA1	0.8319	0.8857	0.8410	0.8529	0.7987	0.7978	0.7659	0.7875	-0.0654		
YMR080C	NAM7	0.8364	0.9353	0.8931	0.8883	0.8354	0.8130	0.8216	0.8234	-0.0649		
YJL176C	SWI3	0.1505	0.1346	0.1782	0.1544	0.1928	0.0000	0.0763	0.0897	-0.0647		
YPL256C	CLN2	0.8142	0.8030	0.9887	0.8687	0.8874	0.8465	0.6808	0.8049	-0.0637		
YLR270W	DCS1	0.8120	0.8692	0.7953	0.8255	0.7467	0.7917	0.7512	0.7632	-0.0623		
YHR154W	RTT107	0.6771	0.7062	0.6802	0.6878	0.6212	0.6577	0.5986	0.6259	-0.0619		
YOR308C	SNU66	0.8430	0.8999	0.8888	0.8772	0.8018	0.8861	0.7600	0.8160	-0.0612		
YBR073W	RDH54	0.8651	0.9754	0.8366	0.8924	0.8660	0.6943	0.9361	0.8321	-0.0603		
YKL190W	CNB1	0.9072	0.8880	0.9953	0.9302	0.9487	0.8983	0.7659	0.8709	-0.0592		
YDR386W	MUS81	0.8895	0.8762	0.9627	0.9095	0.7620	0.8374	0.9566	0.8520	-0.0575		
YDL047W	SIT4	0.1195	0.0236	0.0587	0.0673	0.0000	0.0305	0.0000	0.0102	-0.0571		
YDR263C	DIN7	0.9713	1.0557	1.0170	1.0147	0.8752	1.0566	0.9420	0.9579	-0.0568		
YNL201C	PSY2	0.6992	0.8077	0.7236	0.7435	0.6763	0.6943	0.6925	0.6877	-0.0558		
YMR036C	MIH1	0.7788	0.8172	0.9149	0.8370	0.7681	0.7247	0.8627	0.7852	-0.0518		
YGL229C	SAP4	0.9403	0.9991	0.9453	0.9616	0.9027	0.9501	0.8774	0.9101	-0.0515		
YAL040C	CLN3	0.7545	0.8337	0.7671	0.7851	0.7038	0.7521	0.7453	0.7338	-0.0513		
YDR523C	SPS1	1.0134	1.0605	1.0105	1.0281	0.9976	0.9653	0.9684	0.9771	-0.0510		
YLR210W	CLB4	0.7412	0.8007	0.7606	0.7675	0.7038	0.7795	0.6691	0.7175	-0.0500		
YLR135W	SLX4	0.6704	0.7487	0.6780	0.6990	0.6763	0.6669	0.6045	0.6492	-0.0498		
YGL070C	RPB9	0.5996	0.6660	0.6997	0.6551	0.5692	0.6425	0.6074	0.6064	-0.0487		
YDR075W	PPH3	0.8253	0.9188	0.8475	0.8638	0.8140	0.8313	0.8011	0.8155	-0.0484		
YGL163C	RAD54	0.7169	0.7747	0.7171	0.7362	0.6273	0.6821	0.7542	0.6879	-0.0484		
YNL025C	SSN8	0.0553	0.0638	0.0522	0.0571	0.0000	0.0000	0.0323	0.0108	-0.0463		
YGR129W	SYF2	0.8452	0.9518	0.8931	0.8967	0.8109	0.8952	0.8451	0.8504	-0.0463		
YER142C	MAG1	0.8939	1.0109	0.9996	0.9681	0.8813	1.0018	0.8833	0.9221	-0.0460		
YIL128W	MET18	0.6505	0.6897	0.6715	0.6705	0.5937	0.5633	0.7219	0.6263	-0.0442		
YLR234W	TOP3	0.8651	0.7487	0.9518	0.8552	0.8538	0.7065	0.8745	0.8116	-0.0436		
YJR063W	RPA12	0.7412	0.7865	0.7780	0.7686	0.7497	0.7552	0.6749	0.7266	-0.0419		
YJL006C	CTK2	0.4868	0.5361	0.5563	0.5264	0.3642	0.7674	0.3228	0.4848	-0.0416		
YOL004W	SIN3	0.4381	0.4133	0.4694	0.4403	0.4498	0.4172	0.3345	0.4005	-0.0397		
YML021C	UNG1	0.7855	0.8573	0.7627	0.8019	0.7742	0.7247	0.7894	0.7628	-0.0391		
YJR066W	TOR1	0.6372	0.7322	0.7062	0.6919	0.6549	0.6790	0.6250	0.6530	-0.0389		
YHR064C	SSZ1	0.3695	0.4960	0.4151	0.4268	0.4070	0.4080	0.3521	0.3891	-0.0378		
YAL019W	FUN30	0.7899	0.8715	0.8149	0.8254	0.7436	0.8435	0.7776	0.7882	-0.0372		
YPL183W-A	RTC6	0.3607	0.4464	0.4933	0.4334	0.3764	0.4720	0.3404	0.3963	-0.0372		
YGR258C	RAD2	0.9160	0.9495	0.9388	0.9347	0.8171	0.9257	0.9508	0.8978	-0.0369		
YEL056W	HAT2	0.7766	0.8007	0.7866	0.7880	0.7375	0.8283	0.6896	0.7518	-0.0362		
YPL240C	HSP82	0.8784	0.9424	0.9431	0.9213	0.9333	0.8618	0.8715	0.8889	-0.0324		
YGL090W	LIF1	0.8187	0.8479	0.9822	0.8829	0.8293	0.8404	0.8833	0.8510	-0.0319		
YKL025C	PAN3	0.9072	1.0014	0.9518	0.9535	0.8966	0.9348	0.9361	0.9225	-0.0309		
YDL059C	RAD59	0.8386	0.8715	1.0083	0.9061	1.0282	0.8648	0.7336	0.8755	-0.0306		
YDR004W	RAD57	0.7302	0.8148	0.7323	0.7591	0.7038	0.7034	0.7806	0.7293	-0.0298		
YFL003C	MSH4	1.0134	1.1053	1.0170	1.0452	1.0741	0.9775	0.9948	1.0155	-0.0298		
YML102W	CAC2	0.6771	0.7322	0.7062	0.7052	0.6120	0.6851	0.7365	0.6779	-0.0272		
YIL009C-A	EST3	0.8297	0.9471	0.8714	0.8827	0.8997	0.8496	0.8246	0.8579	-0.0248		

Yeast systematic name	Yeast standard name	Vector Set 1	Vector Set 2	Vector Set 3	Vector Avg.	yK48R Set 1	yK48R Set 2	yK48R Set 3	yK48R Avg.	E-C[a]	GC Validations (plasmid expression)[b]	Validations (hetero-allelic haploids)[c]
YOL043C	NTG2	0.8917	0.9353	0.9257	0.9176	0.9364	0.9348	0.8128	0.8947	-0.0229		
YNL307C	MCK1	1.0222	0.9542	0.8540	0.9435	0.8813	0.7460	1.1386	0.9220	-0.0215		
YHR115C	DMA1	1.1550	0.8550	1.1300	1.0466	0.9517	1.1480	0.9772	1.0256	-0.0210		
YGR108W	CLB1	0.7921	0.8739	0.8431	0.8364	0.7895	0.8526	0.8040	0.8154	-0.0210		
YAL015C	NTG1	0.7633	0.8479	0.8040	0.8051	0.7742	0.8039	0.7747	0.7843	-0.0208		
YBR186W	PCH2	0.9160	0.9731	0.9453	0.9448	0.9425	0.9775	0.8598	0.9266	-0.0182		
YMR106C	YKU80	0.6594	0.6094	0.5150	0.5946	0.5937	0.6638	0.4754	0.5776	-0.0169		
YBL058W	SHP1	0.8010	0.8526	0.8279	0.8272	0.7956	0.8739	0.7630	0.8108	-0.0163		
YNL072W	RNH201	1.0266	0.9991	1.0909	1.0389	1.1231	1.1419	0.8040	1.0230	-0.0159		
YDR092W	UBC13	0.6129	0.6944	0.6085	0.6386	0.6518	0.6456	0.5722	0.6232	-0.0154		
YAL021C	CCR4	0.7390	0.7180	0.8040	0.7537	0.5784	0.7095	0.9273	0.7384	-0.0153		
YCR044C	PER1	0.8142	0.9188	0.8518	0.8616	0.8109	0.8618	0.8686	0.8471	-0.0145		
YBR098W	MMS4	0.8895	0.8054	0.9887	0.8945	0.8262	0.8770	0.9390	0.8807	-0.0138		
YPL008W	CHL1	0.8164	0.9022	0.9388	0.8858	0.9333	0.8983	0.7864	0.8727	-0.0131		No interaction
YDR121W	DPB4	0.7611	0.7912	0.7475	0.7666	0.7283	0.8069	0.7277	0.7543	-0.0123		
YML095C	RAD10	1.0222	0.9684	0.8127	0.9344	0.8905	0.8343	1.0417	0.9222	-0.0122		
YDR359C	EAF1	1.0266	0.9754	1.0800	1.0274	1.1170	1.1389	0.7923	1.0160	-0.0113		
YMR167W	MLH1	0.7633	0.8337	0.8171	0.8047	0.8201	0.8831	0.6779	0.7937	-0.0110		
YGR180C	RNR4	0.5708	0.6188	0.6715	0.6204	0.5508	0.6882	0.5898	0.6096	-0.0108		
YGR109C	CLB6	0.7877	0.8762	0.8692	0.8444	0.8446	0.7734	0.8833	0.8338	-0.0106		
YGR285C	ZUO1	0.3673	0.3708	0.3738	0.3706	0.5692	0.1462	0.3668	0.3607	-0.0099		
YJL101C	GSH1	0.0000	0.0000	0.0261	0.0087	0.0000	0.0000	0.0000	0.0000	-0.0087		
YNL246W	VPS75	0.8386	0.8833	0.8584	0.8601	0.8721	0.8404	0.8422	0.8516	-0.0085		
YGL087C	MMS2	0.7678	0.8550	0.7454	0.7894	0.7497	0.8222	0.7718	0.7812	-0.0081		
YDR076W	RAD55	0.7456	0.8196	0.7171	0.7608	0.7314	0.7400	0.7894	0.7536	-0.0072		
YNL252C	MRPL17	0.0000	0.0000	0.0174	0.0058	0.0000	0.0000	0.0000	0.0000	-0.0058		
YPR052C	NHP6A	0.8364	0.8999	0.9518	0.8960	0.7865	0.9379	0.9478	0.8907	-0.0053		
YCR014C	POL4	0.8563	0.9447	0.8757	0.8922	0.8721	0.8892	0.9038	0.8884	-0.0039		
YHR082C	KSP1	0.7987	0.8857	0.7953	0.8266	0.7987	0.8831	0.7894	0.8237	-0.0029		
YLR376C	PSY3	0.7346	0.7841	0.7062	0.7417	0.7344	0.7704	0.7131	0.7393	-0.0023		
YBR189W	RPS9B	0.8518	0.9046	0.8714	0.8759	0.8874	0.9287	0.8070	0.8744	-0.0016		
YLR035C	MLH2	0.9072	0.9376	0.8996	0.9148	0.8752	0.8831	0.9830	0.9138	-0.0010		
YLR418C	CDC73	0.0000	0.0000	0.0000	0.0000	0.0000	0.0000	0.0000	0.0000	0.0000		
YAR002W	NUP60	0.0000	0.0000	0.0000	0.0000	0.0000	0.0000	0.0000	0.0000	0.0000		
YBL088C	TEL1	0.8541	0.9117	0.8692	0.8783	0.8599	0.8831	0.8921	0.8783	0.0000		
YBR231C	SWC5	0.8541	0.9164	0.8671	0.8792	0.8477	0.8283	0.9625	0.8795	0.0003		
YBR228W	SLX1	0.8452	0.9329	0.8518	0.8767	0.8660	0.8618	0.9067	0.8782	0.0015		
YLR306W	UBC12	0.7678	0.8337	0.7758	0.7924	0.7436	0.8404	0.8040	0.7960	0.0036		
YPL022W	RAD1	0.8010	0.8290	0.8301	0.8200	0.7375	0.8800	0.8539	0.8238	0.0038		
YGL175C	SAE2	0.9580	0.8526	0.9366	0.9158	0.8997	0.9470	0.9214	0.9227	0.0070		
YOR026W	BUB3	0.8961	0.9400	0.9366	0.9242	0.9456	0.9470	0.9038	0.9321	0.0079		
YGR163W	GTR2	0.7788	0.8904	0.8431	0.8375	0.8262	0.8374	0.8745	0.8460	0.0086		
YNL082W	PMS1	0.7744	0.9046	0.8127	0.8306	0.8507	0.8191	0.8481	0.8393	0.0087		
YOR005C	DNL4	0.7833	0.8692	0.8127	0.8217	0.7865	0.8861	0.8216	0.8314	0.0097		
YGL194C	HOS2	0.7744	0.8573	0.8149	0.8155	0.8018	0.8709	0.8070	0.8265	0.0110		
YBL067C	UBP13	0.8032	0.7629	0.9714	0.8458	0.6947	0.9074	0.9684	0.8568	0.0110		
YIL132C	CSM2	0.8364	0.9353	0.8475	0.8730	0.8385	0.9257	0.8921	0.8854	0.0124		
YGR276C	RNH70	0.9271	0.8077	0.9670	0.9006	0.9793	0.9044	0.8598	0.9145	0.0139		
YOR014W	RTS1	0.6571	0.6826	0.7128	0.6842	0.7008	0.7034	0.6925	0.6989	0.0147		
YHL025W	SNF6	0.3828	0.4110	0.5128	0.4355	0.4560	0.4354	0.4607	0.4507	0.0152		
YFR034C	PHO4	0.8784	0.9542	0.8844	0.9057	0.8997	0.9074	0.9566	0.9212	0.0156		
YER070W	RNR1	0.9603	0.9731	0.9757	0.9697	1.0619	0.8252	1.0711	0.9861	0.0164		
YGL043W	DST1	0.7036	0.7369	0.6954	0.7120	0.7620	0.7095	0.7160	0.7292	0.0172		

Yeast systematic name	Yeast standard name	Vector Set 1	Vector Set 2	Vector Set 3	Vector Avg.	yK48R Set 1	yK48R Set 2	yK48R Set 3	yK48R Avg.	E-C[a]	GC Validations (plasmid expression)[b]	Validations (hetero-allelic haploids)[c]
YER176W	ECM32	0.9912	0.9896	0.8627	0.9479	0.7559	1.1480	0.9918	0.9652	0.0174		
YIL066C	RNR3	1.1373	1.1124	0.9388	1.0628	1.1353	0.9562	1.1503	1.0806	0.0178		
YGR056W	RSC1	0.4536	0.7251	0.4955	0.5580	0.0306	0.6060	1.0916	0.5761	0.0180		
YPR018W	RLF2	0.6328	0.6991	0.6280	0.6533	0.6732	0.6699	0.6720	0.6717	0.0184		
YLR318W	EST2	0.8762	0.9589	0.8910	0.9087	0.9272	0.8922	0.9625	0.9273	0.0186		
YPR101W	SNT309	0.7014	0.7723	0.6650	0.7129	0.7497	0.6943	0.7542	0.7327	0.0198		
YKL117W	SBA1	0.8408	0.9447	0.8671	0.8842	0.8783	0.9105	0.9244	0.9044	0.0202		
YBR278W	DPB3	0.9647	1.0416	1.0387	1.0150	0.9884	1.0688	1.0505	1.0359	0.0209		
YDL101C	DUN1	0.8275	0.8692	0.8692	0.8553	0.8844	0.8739	0.8803	0.8796	0.0243		
YPR135W	CTF4	0.7833	0.7109	0.9105	0.8016	0.7803	0.8069	0.8921	0.8265	0.0249		
YIR019C	MUC1	0.7833	0.8904	0.8279	0.8339	0.8385	0.8709	0.8715	0.8603	0.0264		
YKR028W	SAP190	0.8120	0.8880	0.8801	0.8601	0.8232	0.9013	0.9390	0.8878	0.0278		
YFR031C-A	RPL2A	0.8297	0.9093	0.8106	0.8499	0.8385	0.8983	0.9009	0.8792	0.0294		
YGL058W	RAD6	0.9138	0.9518	0.9540	0.9399	0.9731	0.9896	0.9566	0.9731	0.0333		
YER041W	YEN1	0.9138	0.9660	0.9127	0.9308	0.9272	0.9836	0.9830	0.9646	0.0338		
YGL173C	KEM1	0.5111	0.5243	0.5346	0.5233	0.5508	0.4629	0.6632	0.5590	0.0356		
YML060W	OGG1	0.8032	0.8975	0.8040	0.8349	0.8568	0.9196	0.8393	0.8719	0.0370		
YLR265C	NEJ1	0.7390	0.8314	0.7475	0.7726	0.7467	0.9166	0.7747	0.8126	0.0400		
YPL046C	ELC1	0.6903	0.8101	0.7258	0.7421	0.7528	0.8222	0.7747	0.7832	0.0411		
YCL061C	MRC1	0.7766	0.7511	0.8279	0.7852	0.8201	0.8374	0.8246	0.8274	0.0422		
YDR314C	RAD34	0.7744	0.8928	0.7693	0.8121	0.8477	0.8739	0.8422	0.8546	0.0424		
YDR378C	LSM6	0.9603	1.0203	0.9714	0.9840	1.0374	1.1358	0.9067	1.0266	0.0427		
YKR056W	TRM2	0.8673	0.9117	0.8671	0.8820	0.8721	0.9653	0.9420	0.9265	0.0444		
YIL112W	HOS4	0.8651	0.9353	0.8953	0.8986	0.9211	0.9592	0.9537	0.9447	0.0461		
YJL047C	RTT101	0.7678	0.7865	0.7454	0.7665	0.7528	0.8770	0.8099	0.8132	0.0467		
YDR078C	SHU2	0.8541	0.9471	0.9018	0.9010	0.9119	0.9714	0.9625	0.9486	0.0476		
YHL006C	SHU1	0.8253	0.8904	0.8584	0.8580	0.8752	0.9166	0.9302	0.9073	0.0493		
YOL090W	MSH2	0.6439	0.7487	0.6715	0.6880	0.7956	0.7339	0.6867	0.7387	0.0507		
YPR023C	EAF3	0.8430	0.7511	0.7953	0.7965	0.8140	0.7856	0.9420	0.8472	0.0507		
YOR033C	EXO1	0.8563	0.9400	0.8627	0.8863	0.9119	0.9714	0.9449	0.9427	0.0564		
YPL127C	HHO1	1.0797	1.0250	1.1843	1.0964	1.2791	0.8892	1.2941	1.1541	0.0578		
YER045C	ACA1	0.7589	0.8621	0.7953	0.8054	0.9333	0.8191	0.8393	0.8639	0.0585		
YFR040W	SAP155	0.7191	0.7912	0.6867	0.7323	0.7834	0.6912	0.8979	0.7909	0.0585		
YOR346W	REV1	0.8452	0.9400	0.8823	0.8892	0.9303	0.9622	0.9537	0.9487	0.0596		
YBL019W	APN2	0.8651	0.9140	0.8649	0.8813	0.9303	0.9683	0.9244	0.9410	0.0596		
YLR176C	RFX1	0.7855	0.7463	0.8149	0.7822	0.9058	0.6699	0.9508	0.8422	0.0599		
YOL006C	TOP1	0.8518	0.9022	0.8584	0.8708	0.9762	0.9257	0.8921	0.9313	0.0605		
YFR014C	CMK1	0.7877	0.8739	0.7736	0.8117	0.8354	0.9166	0.8657	0.8726	0.0608		
YEL037C	RAD23	0.8120	0.8786	0.8323	0.8410	0.8415	0.9409	0.9273	0.9033	0.0623		
YOL115W	PAP2	0.8784	0.9400	0.9040	0.9075	0.9548	0.9775	0.9772	0.9698	0.0623		
YMR156C	TPP1	0.7678	0.8786	0.8106	0.8190	0.8324	0.9166	0.9067	0.8852	0.0663		
YNL230C	ELA1	0.8408	0.7794	1.0126	0.8776	0.8997	1.0079	0.9273	0.9450	0.0674		
YGL251C	HFM1	0.7656	0.8739	0.7888	0.8094	0.8262	0.9105	0.8979	0.8782	0.0688		
YNL021W	HDA1	0.5266	0.4511	0.6802	0.5526	0.6029	0.6760	0.5898	0.6229	0.0703		
YCR092C	MSH3	0.7921	0.8786	0.7910	0.8206	0.8660	0.9318	0.8774	0.8917	0.0712		
YKL210W	UBA1	0.8253	0.8573	1.0366	0.9064	0.9854	1.1297	0.8246	0.9799	0.0735		
YGL115W	SNF4	0.6129	0.6660	0.7410	0.6733	0.7712	0.7156	0.7542	0.7470	0.0737		
YDR097C	MSH6	0.7191	0.7936	0.6910	0.7346	0.7406	0.9227	0.7630	0.8087	0.0742		
YMR078C	CTF18	0.8695	0.9140	1.0040	0.9292	1.0313	1.1784	0.8011	1.0036	0.0744		Negative
YPL167C	REV3	0.8607	0.9211	0.8866	0.8895	0.9425	0.9866	0.9654	0.9649	0.0754		
YKL203C	TOR2	0.7633	0.7581	0.9301	0.8172	0.7253	1.0414	0.9449	0.9039	0.0867		
YLL039C	UBI4	0.8563	0.7487	1.0974	0.9008	0.8599	1.1297	0.9742	0.9880	0.0872		
YGR003W	CUL3	0.7766	0.8573	0.7584	0.7975	0.8477	0.9227	0.8979	0.8894	0.0920		
YKL114C	APN1	0.8917	0.9707	0.9366	0.9330	1.0007	1.0445	1.0300	1.0250	0.0920		

Yeast systematic name	Yeast standard name	Vector Set 1	Vector Set 2	Vector Set 3	Vector Avg.	yK48R Set 1	yK48R Set 2	yK48R Set 3	yK48R Avg.	E-C[a]	GC Validations (plasmid expression)[b]	Validations (hetero-allelic haploids)[c]
YDR334W	SWR1	0.7899	0.8786	0.7758	0.8148	0.8844	0.9409	0.8979	0.9078	0.0930		
YJL187C	SWE1	0.7036	0.7794	0.8497	0.7776	0.7773	0.9562	0.9097	0.8810	0.1035		
YDR419W	RAD30	0.8297	0.9188	0.8258	0.8581	0.9303	0.9775	0.9772	0.9616	0.1036		
YHR031C	RRM3	0.9249	0.9140	0.9040	0.9143	1.0282	0.9592	1.0681	1.0185	0.1042		
YNL030W	HHF2	0.9094	0.8479	0.9018	0.8864	0.9517	1.0171	1.0271	0.9986	0.1122		
YGR252W	GCN5	0.7412	0.1724	0.6780	0.5305	0.6212	0.2132	1.1004	0.6449	0.1144		
YPL001W	HAT1	0.8076	0.8408	0.7801	0.8095	0.8936	0.9775	0.9038	0.9249	0.1154		
YBR274W	CHK1	0.8209	0.7983	0.9301	0.8497	0.9364	0.9744	0.9860	0.9656	0.1159		
YOL054W	PSH1	1.0665	0.9235	0.7627	0.9176	1.0619	0.9409	1.1122	1.0383	0.1208		
YMR234W	RNH1	0.7102	0.7322	0.8149	0.7524	0.7589	0.9866	0.8803	0.8753	0.1228		
YJR035W	RAD26	0.8518	0.8503	0.9779	0.8933	1.0068	1.2180	0.8833	1.0360	0.1427		
YPR120C	CLB5	0.7390	0.7369	0.8562	0.7774	0.9793	0.8952	0.8921	0.9222	0.1448		
YBL002W	HTB2	1.0797	0.9684	0.8127	0.9536	1.1506	1.0049	1.2061	1.1205	0.1669		
YMR199W	CLN1	0.8341	0.7959	0.8779	0.8360	0.9731	1.0110	1.0300	1.0047	0.1687		
YLR154C	RNH203	1.0997	0.9306	0.9409	0.9904	1.1629	1.2089	1.1268	1.1662	0.1758		
YHR200W	RPN10	0.4868	0.5102	0.5737	0.5235	0.7130	0.7125	0.6925	0.7060	0.1825		

[a]Experimental-control or (yK48R average)-(vector average). For each mutant, area of pinned spot was normalized to the average of WT spots on the same plate.

[b]Growth curve validations using plasmid expression. Top hits and some selected mutants were chosen for validations by growth curves using plasmid-based ectopic expression. No interaction" indicates no dominant synthetic lethality was observed. "Negative" and highlighted in yellow indicates that growth curves validated the dominant synthetic lethality of that deletion mutant

[c]Validations using integrated hetero-allelic haploids. Plasmid validated strains and some additional strains of interest were selected for re-testing. Mutants were tested by integrating a GAL-inducible CHL1K48R ORF at the ura3Δ0 locus. No interaction" indicates no dominant synthetic lethality was observed. "Negative" and highlighted in yellow indicates that growth assays validated the dominant synthetic lethality of that deletion mutant.

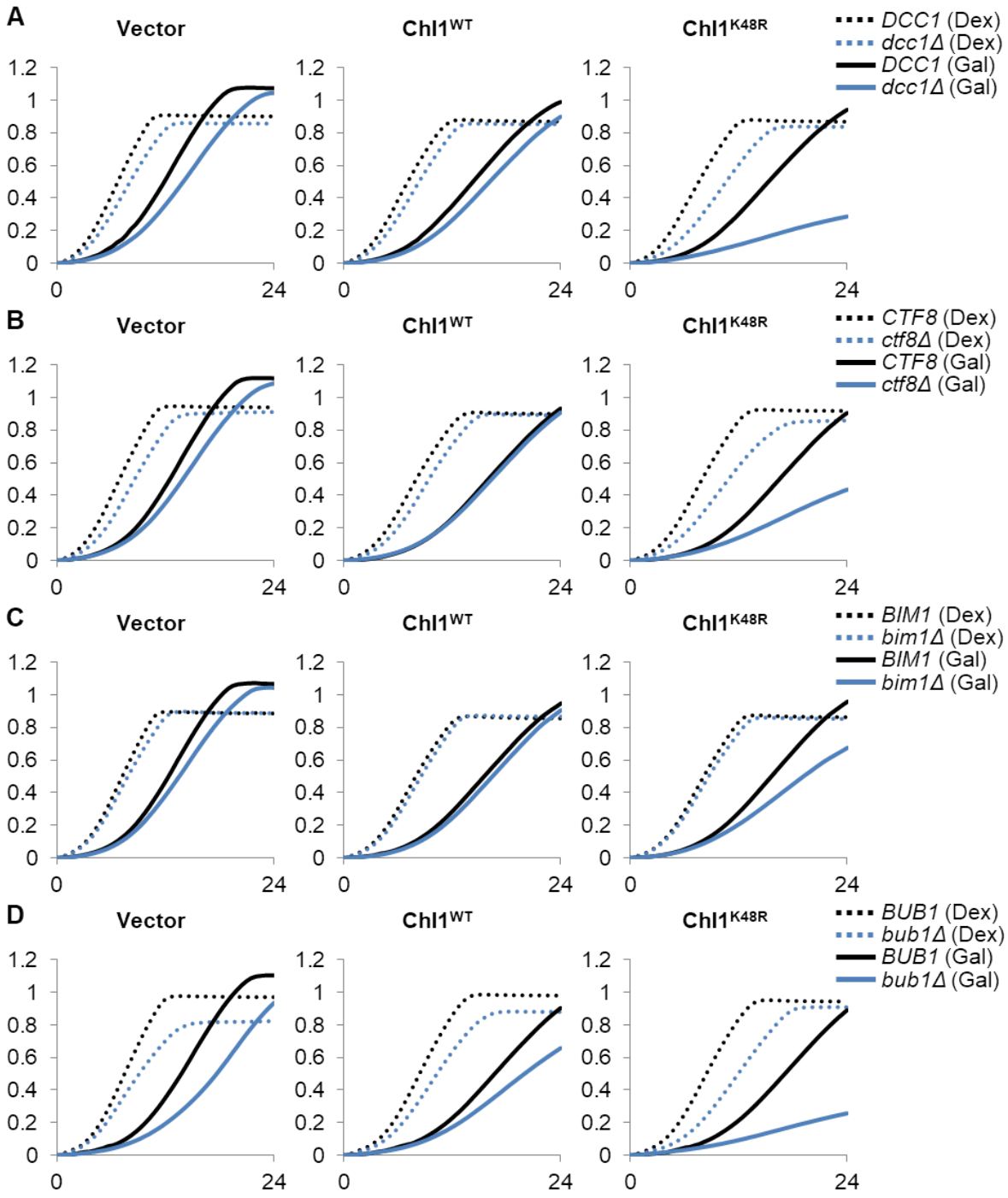

Figure C.1 - Growth curve assays for validation of the yeast *CHL1*^{K48R} dominant SL screen. Yeast strains (wild-type or knock-out mutants) containing a vector control or indicated yeast ORF cloned in a yeast expression vector were grown in dextrose or galactose media. Each represented curve is the average of 3 replicates per media condition. For each panel, x axis represents time in hours, while y-axis represents OD_{600} readings. Quantification of strain fitness is shown in Figure 3.2. **(A)** *dcc1Δ* **(B)** *ctf8Δ* **(C)** *bim1Δ* **(D)** *bub1Δ.*

Appendix D - Alignment of DDX11, DDX12P and LOC642846

Blue text = exons Green = ATG/TGA
Yellow highlights = insertions/deletions Red =sgRNAs

```
                                                                  Exon 1
DDX11      --------GTTGTTCCGGCTGCCTTTCACTGAGGGGACCCGCCAGTTTCTAACTCAGTGG     52
LOC642846 CGGCGGGG..........A.............CC.............A..T.......     60
DDX12P    ----------------------------------------------A..T.......     11

DDX11     CGTTTGCCCTGATTCCCGGGGCCTGGCTTTCAGCGTAGCAATTCTGCCGGCGAAGAAGGT    112
LOC642846 ....................................................            120
DDX12P    ....................................................             71

DDX11     GAGCGCAGTGCTGTGTGGCAGCAGAGCTCCTTAGGACGAGGAGCAGCGGGACGAGGAAGG    172
LOC642846 ........................G.............A.................    180
DDX12P    ........................G.............................    131

DDX11     GCAGACTGGTGAAATCGCAAACTGGGCGTCTGTTCCGGCGCCGGACCCCTATTTGCAAAG    232
LOC642846 ....................................A..........G.........    240
DDX12P    ................................................G.........    191

DDX11     GTGGGTGGCCCGTCCGGAGCGGGAAAACATTCCGGAAGTGGAGGGCCGGGCCAGCGTGAT    292
LOC642846 ....................A.....................................    300
DDX12P    ................................G.........T.............    251

DDX11     TGACAAGCGGGAACCCCTGTGTGGGGAC-GGGTAGGCCTAGGAAGGTTGTGCCTGCGGTG    351
LOC642846 ........................G...CC.........................    360
DDX12P    ........................G...C..........................    311

DDX11     GAACTGGGCGGTGCGCAGAAGTGGGCATTAACAGCAGCCGCGTGTCTGGGTCTTAGATTT    411
LOC642846 ....G.C...........G...C.....................................    420
DDX12P    ....G.C...........G.....................................    371

DDX11     GGCCCAGCTGTGTTGAGCTTTTCATGGATTATCTTACGTAGATAAGACACTGCAACAGTG    471
LOC642846 ....T........................G.........................    480
DDX12P    ....T........................G.........................    431

DDX11     AGTGAGCGCTTGTAACCCACCTGTCTCTTACGGAAACTGAGCCCCAGCGATGCTAACTTT    531
LOC642846 ............................A...................A........    540
DDX12P    ............................A...................A........    491

DDX11     AGCAAGGATACAGCTGGGATCCTAAACTTGGCAATCAGAGCCCAGAGCCGATAAAGTTAG    591
LOC642846 ............................G.........................    600
DDX12P    ............................G.........................    551

DDX11     CTGCATGAGTCTAGCTTCCCCCAGGGCGGGAATCGAGGCGGAGCAGGGTACAGTACGGAG    651
LOC642846 ....G..............G.....................................    660
DDX12P    ....G.....................................................    611

DDX11     GCCAGGAATGAGTGCACTTGACCAGATTGTTGACGGAAGTGTCATAAAAATGGACTTAAA    711
LOC642846 ......G.........G.............................G..........    720
DDX12P    ......G.........G.............................G..........    671
```

```
DDX11      TGCTGATAAGCAGCTGTTTGGGTTCCACACAGGGTGCGAGCTCAGGATGCACGTTGGAGG    771
LOC642846 ..T.............G................T.........................    780
DDX12P    ..T.............G.........................................    731

DDX11      GGACACAGGGCCAGAGCAAGGTGGGAATGCGGGTATTATGGGCCAGGCCATCCTCCAGCT    831
LOC642846 ..............................................................    840
DDX12P    ..............................................................    791

DDX11      GGTGGAGCACCGCAGTACTGCAGTGTGTGGCCCTGGCTTAACAGCAGTGCGGAAAAGCTT    891
LOC642846 ..............C...............................................    900
DDX12P    ..............C........A.....................................    851

DDX11      TTTTCTTGGGGCTGTGGTGCTTTCCAGGTGTGTGAAGTTAAAACATTTTAGGGCCATACG    951
LOC642846 ..C..........................................................    960
DDX12P    ..C..........................................................    911

DDX11      GTAGATAGTACCTGCCACATAGTTGTCTTGGTCAGCCCCGGCTGCCATGACAAAATACCA   1011
LOC642846 ....G.....................................G.............    1020
DDX12P    ....G...C.................................T..............    971

DDX11      TAAACTGGGTGGCTTAGACACAGAAATGTGTTTTCTCACAGTCCCAGAGGCTTGGGATGT   1071
LOC642846 ..............................................................   1080
DDX12P    ..............................................................   1031

DDX11      CCAAGATCAATGTGGGGAGGACACAACTGAGCCCACAACAATAGTCTGTACTCAGTAATG   1131
LOC642846 ..........................................................G.....   1140
DDX12P    ...G........................................................G.....   1091

DDX11      AGTGATAATTGGGGACTGAAGAAAATGAACACGTTAAGAACTAATATGTTCCTGAAGTGC   1191
LOC642846 ..............................................................   1200
DDX12P    ..............................................................   1151

DDX11      TTTCACAACTCTAACCTCGTTTTATGAGCGTGAGCTTTGCTGTCCTGGTGTGTGCCTTGG   1251
LOC642846 ..............................................................   1260
DDX12P    ............................A.................................   1211

DDX11      CACTGGGAGGTGATGGTTGTCCTCCACACAGCCAACCTGAAGAGGGCTGAACAAGTCACT   1311
LOC642846 ..........................................................G..   1320
DDX12P    ..............................................................   1271

DDX11      GCAAATGTTTTTAATAGGGCTTAGTGAATCCGTTATACTCAGATTTATCTAAACCTCTAT   1371
LOC642846 ..............................................................   1380
DDX12P    ..............................................................   1331

DDX11      GATTTAGCCTGTGCTGCTTCTGGAATAATGAGATCCATAATTACCACTGATGGGGAAGTG   1431
LOC642846 ..............................................................   1440
DDX12P    ..............................................................   1391

DDX11      AAATAATACTT-ACGTTTCTTCTGTATTGTTTAGTGTTGTCATTCTAGAGTTTGGTAACC   1490
LOC642846 ...........A..............................................C...   1500
DDX12P    .G.........A..A.....................................C...   1451

DDX11      AAGTCTGTCTTTTTTATCCCACTTATCCTGGTGGGAGGAAAAGTGAGGAGATAGAAAGTT   1550
LOC642846 ..A.....................C.................................   1560
DDX12P    ..A.....................C.................................   1511
```

```
DDX11     TCAGGTGGCTTGGGGGTCTGGCAGATGTGGTTCAAATCCTGAGTTCAAGCACTTGCTGAG   1610
LOC642846 ............................................................   1620
DDX12P    ............................................................   1571

DDX11     TGACCTTGGGCAAGTCATATAAGTTTACTGAGTCTCAGTTTCTTTCTCTATAAAATAGAG   1670
LOC642846 ............................................................   1680
DDX12P    ............................................................   1631

DDX11     CTTATAAAAATACCACACAGGGTTTTTGTGGGGTTATCTGAAAACGGTTTGAAACCATTA   1730
LOC642846 ............................................................   1740
DDX12P    ............................................................   1691

DDX11     AAGAACTGGCCATTTAACTAATAGGTATTCAAGTCATGGGACCTCCGTTACCCAGCCTCG   1790
LOC642846 ............................................................   1800
DDX12P    ............................................................   1751

DDX11     GAAGAGAAACCTTCACTTACAGCCCCGATGTCTGGCTGGCTACTCATTCGTTCATCAGAT   1850
LOC642846 ............T...........................C.......A..........   1860
DDX12P    ............T...........................C.......A..........   1811

DDX11     TTTTGTTGAATGCCTATGAGGTGTCGAAGCACCTAGTTCTGAGTCCTGGAGCCAGAGAAG   1910
LOC642846 ........................T.................................   1920
DDX12P    ........................T.................................   1871

DDX11     AGCAAGACAGACAAGGTTCCTCTATTTATGGAACGTATATTCCAGTGAGGAAGAATAAAT   1970
LOC642846 ..............................T.............................   1980
DDX12P    ..............................T.............................   1931

DDX11     AGGTTCAGATGGTGCTAAGAGCTATGAATAAATTAAATACAGAGTAATGTGATTTTTTAA   2030
LOC642846 ............................................................A..   2040
DDX12P    ............................................................A..   1991

DDX11     AAGTGACTTAGAGCAAGCTAGGGGGTGAGGAGTGGGGGTGGTGTTTGACCACTGTCCAGC   2090
LOC642846 ............................................................   2100
DDX12P    ............................................................   2051

DDX11     GGCCAGACAGCCGGAGAGGCTTCTCTGAGGAGGTGAGCCAAAGCCTGGATATTGAGGAGG   2150
LOC642846 ............................................................   2160
DDX12P    ............................................................   2111

DDX11     ACTCCTTCTCCAGGCCAAGGGGAGCAGCAAGTGCAAGGCCCGAGCTGAGTAGATGAGGCT   2210
LOC642846 ............................................................   2220
DDX12P    ............................................................   2171

DDX11     GGGAGCCTGACCAGTCTCAGGCTGACCAGTGCTCTGTCTTGAGAGGAGCTGCTGGTCAGC   2270
LOC642846 .......A.........T...........................................   2280
DDX12P    .......A.....................................................   2231

DDX11     TTTTTGTCTTGGGATTCAGAACGAGGAGACATGAAGACTTTTTACTTGGCAGTGGGAGCT   2330
LOC642846 ..............................A.............................   2340
DDX12P    ............................................................   2291
```

```
DDX11     GAAGCTGAAAGGTCCAGGGGCTGATGAGGCCACGTGTAAGCGAAAGTTTGGGATAAGCAG   2390
LOC642846 ............................................................   2400
DDX12P    ............................................................   2351

DDX11     AAACCGAGTGCGCTGAGGGAGTGAGATTGTGGCTGTATCCGGCACCTGGCTGAGCAGGAG   2450
LOC642846 ..........................................G.................   2460
DDX12P    ..........................................G.................   2411

DDX11     AGTGAACCCCGTGGGTGTGTGTTTGCTGGTGACGTTCCTGGAGCTGTCTTGAAGTCCGAG   2510
LOC642846 ............................................................   2520
DDX12P    ............................................................   2471

DDX11     CTGCCTTGCAGCTTGTAGTCTGCCTCTGTTTTTGGCTTTCCCAGATAGTTTCAATTCTTA   2570
LOC642846 ............C-........T.....................................   2579
DDX12P    ............C-........T.....................................   2530

DDX11     CTCTCAGTTTGTGAACCTCCCTTCAGTGAACCTCCCTTCACTTATGCTGGATATCTCTTG   2630
LOC642846 ....................................T.......................   2639
DDX12P    ....................................T.......................   2590

DDX11     CAACCGGATGAGCTTCACTAAAGCAGAGTCATTTGGACCTGGATTCGAATCCCTGGTTTT   2690
LOC642846 .G..T.....................C...........T.....................   2699
DDX12P    .G..T.....................C.................................   2650

DDX11     CCACTTTTTAGCTGTGACTTTGAGCAATTATTTAATTTCTGTAAGCATCAGTATCCAGTA   2750
LOC642846 ..................G.........................................   2759
DDX12P    ..................G.........................................   2710

DDX11     GCTGTATCCTTATAGTGTTGTACAGATTAAATGAGATAATAAAAGCAAAAGACCACTGTA   2810
LOC642846 ............................................................   2819
DDX12P    ............................................................   2770

DDX11     GAGTGTTTAACACATAGGAGGTACTCAAAAATTTGTTAGGTACCTTTCTTCCCCTTTCCT   2870
LOC642846 ...................................................C........   2879
DDX12P    ...................................................C........   2830

DDX11     TCATGTGTTAAAGCTTTTTCAGTACATACCCCTCTCTCAGGATTGAATTGTAAATCATGT   2930
LOC642846 ...........................................................G....A.   2939
DDX12P    ...........................................................G....A.   2890

DDX11     TTTTTGATTACCCTTCTTGTAATAATTCCTCTACCTCTGTAGTCATGTTTTTCTTTTTTC   2990
LOC642846 .....A......................................................   2999
DDX12P    .....A......................................................   2950

DDX11     ATTTTTTCTTGTCCCCAGAATGTCTAACAAAACAGCCAAATATACCTCTGTGAAGACAGA   3050
LOC642846 ..................................................A.........   3059
DDX12P    ..........................................C.........A.........   3010

DDX11     GGGTAAAATAATGCTAGTTCTGTGAGTTCTCTCTTCTTGTGCAAATCCATAAACTGCCAC   3110
LOC642846 ............................................................   3119
DDX12P    ..........................--..............................   3068

DDX11     CAATCTGTAGTCATTTTAATTGCCCCTAAACCGAAGAGCATCGTGGCAACTACCTTTCCC   3170
LOC642846 ..........................................A.................   3179
DDX12P    ......................T...................A.................   3128
```

```
DDX11     CTCGTAAATAGAGTGACACTATCACTAGTCTTATTGAGGCCAAAGTTATAAAGATGGGCT   3230
LOC642846 ....----.........................C.........................   3235
DDX12P    ....----.....................................................   3184

DDX11     CTCGATCTACTAATATTAGTAAAATGGGTTTGGGACTTACTAACATTTGTGCTTAGAAGA   3290
LOC642846 .............................................................   3295
DDX12P    .............................................................   3244

DDX11     GACAGACCTGGCAAAGAGCTTGGAGAAGTGAGTTCCAAAGAGAGAGGTGTGGGAACCAGG   3350
LOC642846 .............................................................   3355
DDX12P    .............................................................   3304

DDX11     ATGGAAGAGTCAGGCCTCCAGATAGCGTTTACTTCTCCTTTCTTCCTTGAATCACTGTCT   3410
LOC642846 .............................................................   3415
DDX12P    .............................................................   3364

DDX11     CAGAGATAATTAGGTTCAGGAGAGGAGAAAAAAAAAAGATGACGTCAACGTGGAGCAGAGT   3470
LOC642846 ..................A.......G.....................A...........   3475
DDX12P    ..C.............A.............................A...........   3424

DDX11     TTTTCTTAGACCTTAGCCTAGCAAGGAAAGAGAAATGCCTGGTCTCAGTACTGGGAAGCT   3530
LOC642846 ...................................................G.........   3535
DDX12P    ...................................................G.........   3484

DDX11     GTTCCAGCCAGAGCCCCGTGGCTGTGAAGAGAGCTCTCCTGTCTGGAACCAAACAGAAAG   3590
LOC642846 ...T.........................................G.............   3595
DDX12P    .............................................G.............   3544

DDX11     CTCATAGGTCTAGAGGCCAGAAAAGTTAGTAGGTGGTGGCTCTGTTCGGTGCTGGAAATG   3650
LOC642846 ..........T.......................C.......G...............   3655
DDX12P    ..........T.......................C.......G...............   3604

DDX11     GAGGCCAGGATGAACTAAGAAGCAAACTAAAGATACTTGTAAGATAAGGACGTGTAGGCC   3710
LOC642846 ...........................................T.................T   3715
DDX12P    .............................................................T   3664

DDX11     GGGTGCGGTGGCTCACGCCTGTAATCCCAGCACTTCGGGAGGCCAAGGCGGGCGGATCAC   3770
LOC642846 .............................................................   3775
DDX12P    .............................................................   3724

DDX11     GAGGTCAGGAGATCGAGACCATCCTGGCTAACACGGTGAAACCCCGTCTCTACC------   3824
LOC642846 .....................................................AAAAAA   3835
DDX12P    .....................................................----AA   3780

DDX11     ----AAAAAAAAAATTAGCTGGGCGTGGTGGCGGGCACCTGTAGTCCCAGCTACTCGGG   3880
LOC642846 AAAA.............C..C.............G.....................   3895
DDX12P    AAAA.............C..C.............G.................T...   3840

DDX11     AGGCTGAGGCAGGAGAATGGTGTGAACCCGGGAGGCGGAGCGTGCAGTGAGCCGAGATTG   3940
LOC642846 ...................................-....T.............C.   3954
DDX12P    ...................................-....T.............C.   3899
```

```
DDX11      CGCCACTGCACTCCAGCCTGGGCGACAGAGTGAGACTCTGTCTCG------AAAAAAAAA   3994
LOC642846  ......................T.....................G.GAAAAA.........   4014
DDX12P     ......................T.....................G.GAAAAA.........   3959

DDX11      AAAAAAAAGATAGGGACGTGTATGTTAACTTGCGCTATCCAAACAACAAGCTGTGCTTAT   4054
LOC642846  ............A.............................---.................   4071
DDX12P     ............A.............................---.................   4016

DDX11      GGTCCTCTGCCTGTGCGTCATGATTTTCCAGGACTTCACAACGGGATAAAGTGAAGTAGC   4114
LOC642846  ............................................................   4131
DDX12P     ............................................................   4076

DDX11      TTCGGCTTGTGAATGTGCATTGCAGAGACGTGGGAGAAGAAAGCTGCAAAAGTCATTATA   4174
LOC642846  ............................................................G   4191
DDX12P     ............................................................G   4136

DDX11      AGCAACACCCTTGATCTTAGGGGTGCTGGTCTGTGAGAAGAGAGCTCTAAGCCTTTTGTA   4234
LOC642846  ................................T...........................   4251
DDX12P     ................................T...........................   4196

DDX11      GAGGCATTAGAAAGGTATCGGAGCCACGGTGAAATGCAGGGGAGATTGGGTTTAGGGGCT   4294
LOC642846  ......................C.....................................   4311
DDX12P     ......................C.....................................   4256

DDX11      TTCCTGGTCTGCATTCTGCTACAGCCGTTAAATGCCGCTAGATGGAGTGCGTGATTCTGG   4354
LOC642846  ............................................................   4371
DDX12P     ............................................................   4316

DDX11      TATGGCCTCACGTGGACCTGCTGCGAAGGATGGAGAGAACATGGTCTCTGCTTCCCAG-A   4413
LOC642846  ..........T......---.....................................A.   4428
DDX12P     ..........T......---.....................................A.   4373

DDX11      AAAAAGGAGAAATTTGGTAATAAGTGTGGAGACTGCTCTTAAATAATGCTCCAGATTTCA   4473
LOC642846  ......................C.....................................   4488
DDX12P     ......................C.....................................   4433
                                                                 Exon 2
DDX11      AGCCACTTCTTCCTGGACCATGAGAGAGCTCCCTAATGTTGTATTTATTTTTCCTAGGTC   4533
LOC642846  ............................................................   4548
DDX12P     ............................................................   4493

DDX11      CATGGCTAATGAAACACAGAAGGTTGGTGCCATCCATTTTCCTTTTCCCTTCACACCCTA   4593
LOC642846  ............................................................   4608
DDX12P     ............................................................   4553

DDX11      TTCCATCCAGGAAGACTTCATGGCAGAGCTGTACCGGGTTTTGGAGGCTGGCAAGATTGG   4653
LOC642846  ............................................................   4668
DDX12P     ............................................................   4613

DDX11      GATATTTGAGAGTCCAACTGGCACTGTGAGTATGAACAGTGAGAGATACTGAAAAGGACA   4713
LOC642846  ............................................................   4728
DDX12P     ............................................................   4673

DDX11      ACTTAACAGCAGCCGTACTAGCTTTTCCTGTTTGCCTATCCAGAGATTTTCATAGTTTGA   4773
LOC642846  .......G.....T..G.................C.........................   4788
DDX12P     ....T..G.....T..G.................C.........................   4733
```

```
DDX11     AGTTGGGCAGAGTAGTCTCT----GTTTA----TCTGAGTAATAGTCACTTCCTCTATTA   4825
LOC642846 ..................CTCA.....TCTT.............G............   4848
DDX12P    ..................CTCA.....TCTT...........C..............   4793

DDX11     AAGTCTTTTTTTT----------TTTTTTTTGAGACGGAGTCTCGCTGTGTCGCCCAGGC   4875
LOC642846 ..A.........TTTTTTTTTT.................................   4908
DDX12P    ............-------------------------------------.......   4814

DDX11     CAGAGTGCAGTGGGACGATCTCGGCTCACTGCAAGCTCCGCCTCCCGGGTTCACGCCATT   4935
LOC642846 .G.....................................................T....   4968
DDX12P    .G.....................................................T....   4874

DDX11     CTCCTGCCTCAGCCTCTTGAGTTGCTGGGACTACAGGTGCCCGCCGCCACGCCCGGCTAA   4995
LOC642846 ..............C..............G.........................   5028
DDX12P    ..............C.....................................   4934

DDX11     TTTTTTGTAGTTTTAATAGAGACAGGGTTTCACCGTGTTAGCCAGGATGATCTCAGTCTT   5055
LOC642846 ...............................A.......................C   5088
DDX12P    .....................................................C   4994

DDX11     CTGACCTCGTGATCCGCCCGCTTCGGCCTCCCAAAGTGCTAGGATTACAGGCATGAGTCA   5115
LOC642846 ..................A.....................................C..   5148
DDX12P    ..................AT.....................................C..   5054

DDX11     CCGTGCCCGGCCTAAAGTCTTAAACATAGCTCTGTGGTCTGAGAAAAATTAGGCTGAAGT   5175
LOC642846 ....-----.....................................................   5203
DDX12P    .....-.....................................................   5113

DDX11     CATTGGTGCCTACCTATTACGGTAGATGAGACGGCTTTCTTACCAACTCTTTTCCCTCCC   5235
LOC642846 ............................T.........................G   5263
DDX12P    ............................T.........................G   5173

DDX11     GTTCCCCATCCTTCAAATATAATTCTAAGTTTTAGTCTCTGCTGAGTGAACCAGTGTGTT   5295
LOC642846 .....................................................C...   5323
DDX12P    .....................................................C...   5233

DDX11     ATGATTATGTTTTGAACATAATTTTGTCTTGAACAATATGTCTTAATATTCTGTTTTTTC   5355
LOC642846 .....................................................C..   5383
DDX12P    .....................................................   5293

DDX11     TAGTTAATAATTGCCCTTTTAAAGTTAGTTTAGTTTTTAATATACCTATGCCAGTTCCTC   5415
LOC642846 .....................................................   5443
DDX12P    .....................................................   5353

DDX11     CCACATCATCCAGTGGCCTCTCAATATGATTTTCCATACAGATAACTCCTGTCTTAGTCG   5475
LOC642846 .....................................................   5503
DDX12P    .....................................................   5413

DDX11     GCCAGGACTGCCATAGTAAAATACCATAGACTGGGTGACTTAACAGGAATTTATTTTCTC   5535
LOC642846 .....................................................   5563
DDX12P    .....................................................   5473
```

```
DDX11     ACCATTCTGGAGGCTGGAAAGTTGAAGATCCAGATTCTGGCAGGGTTCTGGTTCTGGGGA   5595
LOC642846 ............................................................   5623
DDX12P    ............................................................   5533

DDX11     GGGGGTCTCTTCCTGGCTTGCAGATGGCTGCGTTCTTACTGTGGAGCAAGAAAAGACGAG   5655
LOC642846 ...........................................................G...   5683
DDX12P    ....................................T.....................G...   5593

DDX11     GAGGAGAAAAACAAATCTTTGGTGTCTCTTTCTCTTTTATGAGGACAAGGGCTGCTCCCT   5715
LOC642846 ............................................................   5743
DDX12P    ............................................................   5653

DDX11     TATGGCTGCTCCGTTATGACCTCCTTTACCCTTGAAGGCCAGATCTGTAGTAGAGTCACA   5775
LOC642846 ............T.....................................C.......   5803
DDX12P    ............T.....................................C.......   5713

DDX11     TGGCGGGGTTAGGATTTCAACATATGTTTGTTTGTTAAGATGGGCAGTCTCACTATGTGG   5835
LOC642846 ............................................................   5863
DDX12P    ....A.................................................G.....   5773

DDX11     CCCAGGCTGGTCTCGAACTCAAGCGATCCTCCCCTCTCAGCCTCCCAAGTACCTGGTGGC   5895
LOC642846 ..........................T.................................   5923
DDX12P    ............A.............................................   5833

DDX11     TGGCAAGATCCAAGATTACTGGTGCACACCACCATACACAGCTTCTTTTGTTTTGTTTTT   5955
LOC642846 ...........................................................G......   5983
DDX12P    ............................................................   5893

DDX11     GTTCTTTAAAAACATTTTTTTAACATGCATTTTGGTGGGGATACAATTCAGTCCACAGCA   6015
LOC642846 ............T.....................................................   6043
DDX12P    ............................................................   5953

DDX11     GTGACCAATTCCATTTTTACCTTGGAGCCCTCCTGGAATCCTCCATCCTTTCCCTGTCAT   6075
LOC642846 ............................................................   6103
DDX12P    ....................................A.......................   6013

DDX11     TTGAATTAGTTGCTCCTCAGACTGACTTGACAGATTTCAGCATGAGTGTTAATGGGGACA   6135
LOC642846 ...........................................................G........   6163
DDX12P    ...........................................................G........   6073

DDX11     GACGGCCGCACCCACACCACATCAGGGTATACGTCCGTTTGGAGGCTTTCCTCAAACGTC   6195
LOC642846 ..............................T.............................   6223
DDX12P    ..............................T.............................   6133

DDX11     TGGCAGCCCTGGACTGCCTGTGTATGCTGAAGAACAGGGCACAGAAAGGCTGAGTCTGCA   6255
LOC642846 ................................G...........................   6283
DDX12P    ................................G...........................   6193

DDX11     GGGCA--CTGGCTGTGGCTGCCAGGCTGGGCTCCTTTGTTGGGGGCCTCCAGTTGCCAGC   6313
LOC642846 .....GG.....................................................   6343
DDX12P    .....GG.....................................................   6253

DDX11     ACATCTGTGGGATTTTCCCTAGAGTCTTCAGTCTCTCCAGAGCAGGTGCCTCTGAGCCCT   6373
LOC642846 ............................G.............................T..   6403
DDX12P    ............................G.............................T..   6313
```

```
DDX11     GGCCCAGCAGGTACAGACGCTGAAGCCCAATAGCCGGTCTTCCGGGAGGTGGTCTGGGGA   6433
LOC642846 ............................................................   6463
DDX12P    ............................................................   6373

DDX11     AGGGGATCCAGGTGGAGAGTCCCCCTCAGTGCCTGCTTTCAGCCTGGCCCTCCTCCCCCT   6493
LOC642846 ..............................................A.........T....   6523
DDX12P    ..............................................A.........T....   6433

DDX11     CCCTCTTGCCTCCTCAATCTGCCGGTTGCCTCCAGGGCTCTCCTAGCTCAGCTTCCACTT   6553
LOC642846 ........................A.....................................   6583
DDX12P    ........................A.............T.......................   6493

DDX11     AGAGCCCACTTCCTGTCTTCTGCAAGGAGCAGGAGCAGGGATTGCAACCTGAGAATCTAA   6613
LOC642846 ................G.....................................G........   6643
DDX12P    ....................................................G........   6553

DDX11     TTGTTCTTAAAAAGAATTTCAACCCGTCCCTTTGTTTTCAGTGGCCTGCTGTGTTCCTAC   6673
LOC642846 ...........C..................................................   6703
DDX12P    ...........C..................................................   6613

DDX11     CACTTCCTGAGTCTTTCTGAGAATGAGTGGGGGAGATCTCTGGGGACACTTGGGCTTGAG   6733
LOC642846 ............................................................   6763
DDX12P    ............................................................   6673

DDX11     TGTCTCTGCCGAAATCACTTCCATGTCTCTGCCTTCTTTCCCTCTCTCCTAAAACATATT   6793
LOC642846 ...........-..................................................   6822
DDX12P    ...........-..................................................   6732

DDX11     ACTCCTTCCACTTTC----TTTTTGTGGGTGTAAGCCTCCATATTACTTTGGTTAATTTT   6849
LOC642846 ..............TTTG..............................................   6882
DDX12P    ..............TTTG..............................................   6792

DDX11     AGTGTGCTTTGGAACACAGATGAGTGCATGTTCATTCTGCCTTGTTTAATTTTAGAGACA   6909
LOC642846 ............................................................   6942
DDX12P    ............................................................   6852

DDX11     GGGTGTTGCTCTGTTGCCCAGGGCCGAGTGCAGTGTTAAGATCATGGTTTACTGCAGCCT   6969
LOC642846 ......C.....................................C.........C.....   7002
DDX12P    ......C.....................................C.........C.....   6912

DDX11     CAACCTTCTGGCAACAAGTGATCTTCCCACGTCAGCCTCCTGAGCAGCTGGGACTACAGG   7029
LOC642846 .G...........T..............................................   7062
DDX12P    .G...........T..............................................   6972

DDX11     TGTGCACCATCACACCTAGCTAATTTTTTAATTTGTAGAAATGAGATCTCACTATGCTGC   7089
LOC642846 .....G...........A..........................................   7122
DDX12P    .....G........................................................   7032

DDX11     TCAGGCCGGTGGTCTTAAACCCCTAGGCTCAAGCAATCCTCCCTCCTTGGCCTCCCATAG   7149
LOC642846 ............................................................   7182
DDX12P    ......T.........G..............................................   7092

DDX11     TGCTGAGATTACAGGCATGAGCCACTGTACCTGACCCCTTTCACCTTGTTTAGCCTGACA   7209
LOC642846 .........G......G.......................T.....................   7242
DDX12P    .........G......G.......................T.....................   7152
```

```
DDX11     ACCCATCTTCTCCCTCTCAGGTCTTTCCATCTCAGTCTTCTGCACTCCAGGCTTCTGCGT   7269
LOC642846 ..........................................................A.   7302
DDX12P    ..........G..................................................A.   7212

DDX11     CTTCTTCCTCTGCTCAGCCTTTAATTGTCGATGTTTCTGGTTCTATAGCTTCATCTTCTT   7329
LOC642846 ....C....A.....................................................   7362
DDX12P    ....C....A.....................................................   7272

DDX11     GTGTGCAGTCTCTGTGAATGTACCCTGTGGCTTTATTACCTTTGACATTCTTCTGTCTTC   7389
LOC642846 .......C.....................................................   7422
DDX12P    .......C.....................................................   7332

DDX11     TAAATCATCTCCTGAATAGAGTGTTTTCTCCTGTCCTGGGTGTCCCGCAGCCCATAGAAG   7449
LOC642846 ..............................................C..........G..   7482
DDX12P    ..............................................C..........G..   7392

DDX11     CAGCCATGCTGTGGGACACCCTGAGTGGGGTTTGTGTTACCTGTTGTGCCTACCATGCCC   7509
LOC642846 ............................C.....................................   7542
DDX12P    ............................C.....................................   7452

DDX11     TTCCCCGCCGTGGATGCACAGGTGCCCCACCTTAGCTGCCCCAGATGCTGTTTATCCTTG   7569
LOC642846 .........T..............................G.....................   7602
DDX12P    .........T..............................G.....................   7512

DDX11     ATAGTCACCTTTTAAGCCTTATACAGGTCTATCAAGTTGAGTCACCATTACCACTTGGTG   7629
LOC642846 ...................C.....................................   7662
DDX12P    .........................................................   7572

DDX11     TGTGCTGTGCCTTGTGTAATACTGCAGTTCCGGGAGTCATCCAACCTGGAATGCATGCTT   7689
LOC642846 ...................C...................C.....................   7722
DDX12P    ...................C...................C.....................   7632

DDX11     TGCGGGGATCTATGATGCCCTCGAATTGTATGTTACATGTGAACCTGTGAGCATTTTCTA   7749
LOC642846 .........................................................   7782
DDX12P    ..........................................T................   7692

DDX11     GGGGCTCTGCACCTTTGTGTCCTCAGCTCTGAGCCCCATGCTTGCTGCAACCAGCAGGTG   7809
LOC642846 ...................T.....................................   7842
DDX12P    ...................T.....................................   7752

DDX11     TTCAGAGTGAATGAATTTGCTTATCTTGGCATAAATCATGTAACTGTTGATGATACCCCA   7869
LOC642846 .........................................................   7902
DDX12P    .........................................................   7812

DDX11     GGAAGGTGAGCCTTTGGTTATAAATCCTTTTAACATTTTCCAGTCTAAAAGTTTTGTGGT   7929
LOC642846 .........................................................   7962
DDX12P    .........................................................   7872

DDX11     CTTATTACACGATGTAGAAAACAGTGGGCCTCAGTTATTCTTTTGCTGTTGTGCCGGAGT   7989
LOC642846 .........G.....................................................   8022
DDX12P    .........G.....................................................   7932
```

```
DDX11     ATACCACGGTTGTTTTTGAAAGATAACTTTGACCATACCCTTAGGAACTTCCTCAGCTCA   8049
LOC642846 ............................................................   8082
DDX12P    ............................................................   7992

DDX11     CTTTCAAATGGAGGGCACTGGCTTTCTAACCATTGTGTCTCCCAGCCCAGTGACAGCTGA   8109
LOC642846 ............................................................   8142
DDX12P    ............................................................   8052

DDX11     AGCTGACTGCTTCCGATATCACAGACAGCACAGAAGAGCCGCCCTCCAGGTGCTGCTGGG   8169
LOC642846 .....T..................G.....................................   8202
DDX12P    .....T..................G.....................................   8112

DDX11     AAATGCTGCCTGGAACTCTTTGCCATTTACTTTCTATCAAAAGCTGAGGGAAATGGTACA   8229
LOC642846 ................C...........................................   8262
DDX12P    ............................................................   8172

DDX11     TATGGGGCTTTCCTAAAAATATGGGATCCATCCATTTGTCAACAATGTCATTCTATCCTA   8289
LOC642846 ........................................G.....................   8322
DDX12P    ........................................G.....................   8232

DDX11     TCCCAGGGCCTTTCAAGATTTTGATGAAAACTAATAGATCCCATATTCCAGAATAATGCT   8349
LOC642846 ......................G.....................................   8382
DDX12P    ......................G.....................................   8292

DDX11     ATTAATAATTTTATTATTATTACTTAATGATAGCAAAAAGTTAGCTAACTCCAACCGCTC   8409
LOC642846 ............................................................   8442
DDX12P    ............................................................   8352

DDX11     ACTTGTTATTTGCCAGGTAATCCTCTAATCCAGAGGATTTGGCCTTTTGTGTGTGTTAAT   8469
LOC642846 ........................G...................................   8502
DDX12P    ............................................................   8412

DDX11     GTCCTGCTTGCACCAGCTCTATGAGGAAGGTGCCGCTGTTGTCATTTCCATTTCTGCACT   8529
LOC642846 ................G.............A.............................   8562
DDX12P    ..............................T.............................   8472

DDX11     CGTGGAAACAAGCGTAGTGAGGCCAGCCTGAGCCACAGAGCTGCAGGTGGGGGAGACAGC   8589
LOC642846 ..............................................A......G....   8622
DDX12P    ..............................................A......G....   8532

DDX11     TGGAACCCTGGCACCTGGCTGTGGAGTTTGAGACTCTGACTCCTGCGCCGCGCTGCTGCC   8649
LOC642846 ...........G................G.....................................   8682
DDX12P    ...........G................G.....................................   8592

DDX11     CCAACCGTAGTCATACGAGGTGTTTCACCCCGCCCTGGATACTCTGAGATCCCCTCTGGG   8709
LOC642846 ......C.....................................................   8742
DDX12P    ......C.....................................................   8652

DDX11     TTCAGCAGGCTCAGAGAGCTGACTGCCTGGAGCAGAAGGCATGGGGTCCTCCAGAGACTC   8769
LOC642846 ............................................................   8802
DDX12P    ............................................................   8712

DDX11     CCCTGAGCTGAGTTCCCCTGTGGACACCAGGGCCGCCTCCTTGTGGCGCTCCCTGAAGGG   8829
LOC642846 ............................................................   8862
DDX12P    ............................................................   8772
```

```
DDX11     TCCTCTCTGGAAGAACTGTATTGGTTCCCTGGGGCTGCTAGAGGAAAGCTTCACAAACTG   8889
LOC642846 ............................................................   8922
DDX12P    ............................................................   8832

DDX11     GGGCTTAAACAACAGAAACTGACATCCCACAGCGCTGGAGGCTGGAGTCCGAGATCAAGG   8949
LOC642846 ............................................................   8982
DDX12P    ............................................................   8892

DDX11     TGTCAGCATGCTTGGTCCCTTCTGAGGGTCGTGAGGGAAAGATCTCTTCAGGCCCCTTTC   9009
LOC642846 ..............................C.............................   9042
DDX12P    ..............................C.............................   8952

DDX11     CTTGGCTTATAGGTGGCGTGTTCTCCTTGGGTATCATCACATCGCCTGCCTTCTGTGCAT   9069
LOC642846 ............-.......................G......................   9101
DDX12P    ............-.......................G......................   9011

DDX11     GTCTGCATCCACGTGTCCCCTTTCCAATAAGGATATTAGCCCTTTAGGCTGGGTCCCGTC   9129
LOC642846 ............................................................   9161
DDX12P    ............................................................   9071

DDX11     CTAGTAGTCTCATCTTAACTAATTACATTTGCGACAGTCCTATTTCCAGATCAGGCCACA   9189
LOC642846 ..............................T.....................A........   9221
DDX12P    ..............................T.....................A........   9131

DDX11     TTCTGAGATGCTGGGGGTTAGGATTTCAACACAGGAATTTGGAGGAATACAACTCAATCA   9249
LOC642846 ....................................................T.......   9281
DDX12P    ....................................................T.......   9191

DDX11     GGCTTATGGAAAATTCTGGTCTTAAGTCAAGGGTAGTGTTCTCCAGTCTGTATATGGAGG   9309
LOC642846 ..........C......................A......................G......   9341
DDX12P    ..........C......................A.....C................G......   9251

DDX11     CGCACACCTATGGTCCCAGCCACTTGGGAGGCTGAGGCCAGAGAACTGTGTGAGCCC---   9366
LOC642846 ..............................................T...........AGG   9401
DDX12P    ..............................................T...........AGG   9311

DDX11     AGGAGTTCCATACCAGCCTGGGCAACATAGCAAGACCTCCTCTCAAAAACAGAC----AG   9422
LOC642846 ..........................................................AAAA.A   9461
DDX12P    ..........................................................AAAA.A   9371

DDX11     AGTGGTGTCTTCCAGAGTGATTAGTTTGCTT---AAAAAAAAAAAAAC----------   9467
LOC642846 .......--.......................TAA..............AAAAAAACAAAA   9519
DDX12P    .......--.......................T--..............AAAAAAACAAAA   9427

DDX11     AAAACAAAACACAAACCGTAAGCACTGGCGCTCATGACTGATCATCCTGTATCCACGCAC   9527
LOC642846 ....A.................A.......A...G..........................   9579
DDX12P    ....A.................A.......A...G..........................   9487

DDX11     GAGCTGCACGAAGGCCGCGCGGTCACTCTGGCTCCCTGTTGGCGAGTACCTGGGATTTCT   9587
LOC642846 ............................G........C.......................   9639
DDX12P    ............................G........C.......................   9547
```

```
DDX11      TGCTCAGCATTTTGGGGCCTTAATTCTTTTAGGGGACTTTTTGTCTAATGTCTCCCCTTC   9647
LOC642846 .........G.................................................   9699
DDX12P    .........G.................................................   9607

DDX11      TTCTAATTATGTGCGATATTTACATAGAATCTGATAAACTGCTTCAAATTTGTTTTCAGA   9707
LOC642846 .........G.................................................   9759
DDX12P    .........G.................................................   9667

DDX11      ACAGTGAGCTGGATAATTAAAGAAGCTTTTTCCTGCTTCTTGGGCCCAGTTTCCATTTCT   9767
LOC642846 .........G.................................................   9819
DDX12P    .........G.................................................   9727

DDX11      TTCTTTTTTCTGTTTTTCCTGGCTATTCTAGTGCTAATTTCCTTCCTTTCCTTTCCTAGG   9827
LOC642846 .C.....................................G.....................   9879
DDX12P    .C.....................................G.....................   9787

DDX11      CTGGTCTTAGAGCATCCTCTCCTATGTACAGCCAGACCTTCTTTCAAGCTTTTATTAAAA   9887
LOC642846 ....C.....................................G.....................   9939
DDX12P    ....C.....................................G.....................   9847

DDX11      TGGGGAAAGGTCATTTGGGAGGCTTTGTTGTTTTCCTGTTTCTAAAGATCATTTTTCTTC   9947
LOC642846 .....................................G.....................   9999
DDX12P    .....................................G.....................   9907

                 Exon 3                                    gRNA exon 3
DDX11      CTGCAGGGGAAGTCCTTAAGTCTTATTTGTGGGGCCCTCTCTTGGCTCCGTGACTTTGAA  10007
LOC642846 .....................................C.....................  10059
DDX12P    .....................................C.....................   9967

DDX11      CAGAAGAAGCGTGAAGAAGAGGCACGACTCCTTGAAACTGGAACTGGCCCCTTACATGAT  10067
LOC642846 .....................................G.....................  10119
DDX12P    .....................................G.....................  10027

DDX11      GAGAAAGATGAATCCCTGTGTCTGTCTTCTTCCTGCGAAGGGGCTGCAGGCACCCCGAGG  10127
LOC642846 ..........................C..........................G.....  10179
DDX12P    ..........................C..........................G.....  10087

DDX11      CCTGCTGGAGAACCGGCCTGGGTTACTCAGTTTGTGCAGAAGAAAGAAGAGAGGGACCTG  10187
LOC642846 .....................................G.....................  10239
DDX12P    .....................................G.....................  10147

DDX11      GTGGACCGACTAAAGGTGAGACCTGGGGTATCCGGAAGTGGGAGTACTGGAGGAAACAGG  10247
LOC642846 ..........G.....................................G.....G.....  10299
DDX12P    ...A.......G.....................................G.....G.....  10207

DDX11      GCTTCAGCGATTGTTCTGGGGCGATTCCGAGACTCAGGCAGTGCATGCTCCCCTGCCGTT  10307
LOC642846 ..............G.....................................G.....G.....  10359
DDX12P    ..............G.....................................G.....G.....  10267

DDX11      GCCGTGCCTCTCAGCTCTTCCCTCAGCTCCTTGGGTCTATGGTGCTGCCGCTGTGCTGTC  10367
LOC642846 ..T.....................................G.....G.....G.....G.....  10419
DDX12P    ..T.....................................G.....G.....G.....G.....  10327

DDX11      TTTTTTGAGCTGGAGGTCAGCA-GGCCTTCTCCACATAAGGAACTGTTGGTGCCCATTTA  10426
LOC642846 .C.....................G.....C.....G.....C.....G.....C.....  10479
DDX12P    .C.....................G.....C.....G.....C.....G.....C.....  10387
```

```
DDX11      TTACTCACCTGGGAAAGGACCTGATCATTGCCATTGGCAGCATGGTTCAATGGCTGCAAA  10486
LOC642846 ..........................G.................................  10539
DDX12P    ..........................G.....................G..........  10447

DDX11      TGGATCTGATGGAGAGCGTGTGGCTTTGGGAGGAGTGTGCCGCCTTCCGCAGTGAGCAGC  10546
LOC642846 ....................................C............A...........  10599
DDX12P    ..............................................A...........  10507

DDX11      GAGGCTGGGACCGGCAGGGATGAGGTCCCGGGAGGGGATGCGGCAGCCCTTGAGTGCTGG  10606
LOC642846 ............T.............................................  10659
DDX12P    ............T.............................................  10567

DDX11      CCGGGGAAGGAGAGATGCCCCCAGTGAGGAGGCGCCGGGCTGAGTGGCCCAGACTCCTTA  10666
LOC642846 T............C.....G.....................................  10719
DDX12P    TT..A.........C......................A.....................  10627

                                                    Exon 4   gRNA exon 4
DDX11      GGAGAGGCCTGGTTTTGGGCTTCCTTGGTGATTTTCCTTCATGTCTGCCTCCTGTAGGCG  10726
LOC642846 ........................-................................T.  10778
DDX12P    ........................-.................................  10686
           gRNA exon 4
DDX11      GAGCAGGCCAGGAGGAAGCAGCGAGAAGAACGCCTGCAGCAGCTGCAGCACAGGGTGCAG  10786
LOC642846 ..........................................................  10838
DDX12P    ..........................................................  10746

DDX11      CTCAAGTATGCAGCCAAGCGCCTGGTGAGCCTCATTTCTTGGGGGGCAGGATTATGTCCA  10846
LOC642846 ..........................................................  10898
DDX12P    ..........................................................  10806

DDX11      GGCAGGGTTGCTCTGCTTGGAGGCTCATGGGTGCGTGGTCAGGGCCTTGGTCTCCCCTCC  10906
LOC642846 ........C..C.........................C.....T...............  10958
DDX12P    ........C..C.........................C.....T...............  10866

DDX11      GTGACCCTCACTGGCTATGTGCTCCCGTACAGAAGCTGGGCTGTGAGTGGTTGAGGCGTG  10966
LOC642846 A.........................................................  11018
DDX12P    A.........................................................  10926

DDX11      GATCCTAGGAGTCGACCTCTCTCCAGCCAGGCAGCCAGGCCTATGTGAATGGGGCGTGGT  11026
LOC642846 ..................................................-.........  11077
DDX12P    ..................................................-.........  10985

DDX11      GTGCTTTGTCTCTGGCATGTGGGGAGGTGGGTACTGGTGCTGAGACTTCTTCCTCCCTCA  11086
LOC642846 ................C.........................................C  11137
DDX12P    ................C.........................................C  11045
                                  Exon 5
DDX11      CCACCTCCACTACCCCTGTCCAGAGGCAGGAAGAAGAAGAAAGAGAGAATCTCCTCCGCC  11146
LOC642846 ..........G.............................C.................  11197
DDX12P    ..........G.........................................................  11105

DDX11      TCAGCAGGGAGATGCTAGAGACAGGCCCGGAGGCTGAGCGGCTGGAGCAGCTGGAGTCTG  11206
LOC642846 ................................C.........................  11257
DDX12P    ..........................................C.................  11165
```

```
DDX11     GGGAGGAGGAGCTGGTCCTCGCCGAATACGAGAGTGATGAGGAGAAAAAGGTGGCGAGCA  11266
LOC642846 ............................................................G  11317
DDX12P    ............................................................G  11225

DDX11     GGTGAGACAGAGGCGGTAGCACTACCCTGCCCCAGGCCAGGGGACACCCTTGAAGACAGC  11326
LOC642846 .............................................................  11377
DDX12P    .............................................................  11285

DDX11     TCTTTCCCTCATGCCACAGATGCCATGAAGCACCTGGCAAGAGGCATGGTGGCCTCTGCC  11386
LOC642846 .............................................................  11437
DDX12P    .............................................................  11345

DDX11     CTCTGCTCTAAGCCGGGTCCTTCCTAGGGTCCATGAGTGCCAGTGGCAGTGAGGACAGTC  11446
LOC642846 ...................C.........................................  11497
DDX12P    ............A.................................................  11405

DDX11     ACCGGCCTGGCCTGTGTCCTCTCAGCTGTCCTCACGGCAGCTCAGGCAGGGCAGGAACAT  11506
LOC642846 .................................A...........................  11557
DDX12P    .................................A...........................  11465

DDX11     TTGTGTCTGCGCCTTATACACAAGGAGGCTGCAGCCCCACAAGGAGAGACTCCTTGGCTG  11566
LOC642846 ..........A..........................................................  11617
DDX12P    ..........A..........................................................  11525

DDX11     AGGCCACAAGCCTCGGCAGTGGAGAGCTGGGCTAGAACTCAGCTGGCCTGGCTCTAGATC  11626
LOC642846 ..........................................C............C...  11677
DDX12P    ..........................................C..............  11585

DDX11     TCAGGCTCTGAGGCAGCTGACTGCACTGGGTAACCTGTGAGGTGCCAACCATCAAGGCGT  11686
LOC642846 .................................T............G.........  11737
DDX12P    .................................T............G.........  11645

DDX11     CCTTAGCCTGAGCTTTCCTTCTCCCATAAAGCCTCTGTTGGTCCAGACTCAAGGTTTCCA  11746
LOC642846 .............................................................  11797
DDX12P    .............................................................  11705

DDX11     CTTGATGAGCCATGAGCTGCTGGGTGACTTAGCCCTGAGCAGGCCACCCAGGCCATTTCG  11806
LOC642846 .............................................................  11857
DDX12P    .............................................................  11765

DDX11     GGCCCACAGGATCCCTGGTCACAGCCCTGTTCCCATTCACACTGGAACCTCACCACCATC  11866
LOC642846 ..................G.......C...T.........................  11917
DDX12P    ..................G.......C...T.........................  11825

DDX11     CCTGAGTGTCTGCTCTGAGTATGGCACTGTCCAGATGCTGTGGACATAGAAGGGAAGAAG  11926
LOC642846 ..........................................G..............  11977
DDX12P    .............................................................  11885

DDX11     ACATGGAGGGGACAGTTAATAGACATGAAAACAAATAGCACCTATGTGAAGTCAGCATGT  11986
LOC642846 .............................................................  12037
DDX12P    .............................................................  11945

DDX11     TTGCCTACAAGGAAAACAAAATGGTGATGTGGATGGGGTGGGGGGCTGCACCTGATGATG  12046
LOC642846 .............................................................  12097
DDX12P    .............................................................  12005
```

```
DDX11     AGTCCCGTGTGTCCTGTGACATCCTGGCCACCACATCTGTCGGAGGGTAACTGCAAGACC  12106
LOC642846 ....................................G..................  12157
DDX12P    ....................................G..................  12065

DDX11     AGAGACCCTCCATGGATATTCCTGAAGGTTCATCCCCGGCCTTCACAGTCTGTCTGCAGG  12166
LOC642846 ..........G................................G............  12217
DDX12P    ..........G................................G............  12125

DDX11     GCGCCTTCTGATGCCACCTCCAGCCGCCATCCACCAGACGCCAGCTTCCCCGCTGCCCTG  12226
LOC642846 ..........C..............................................  12277
DDX12P    ..........C..............................................  12185

DDX11     AACTTCCTCCAGCGCACCAGGCCTTCCTCTGTCCTGTCTGAGGATTTGCTCATGCAACGT  12286
LOC642846 ..........................................................  12337
DDX12P    ..........................................................  12245

DDX11     GCTGTGGCCAAACACCCTGCCCTCCTCCCTTGGCAGATGTCTTCCTCTCCTTTAAGGCCT  12346
LOC642846 ..........................................................  12397
DDX12P    ............................C.............................  12305

DDX11     GGCTCAGGTGTCGTCTTGGTGGCTTCGGGTGTCAGCTGCTCTGTTTTGCTCATGCACCTG  12406
LOC642846 ..................................................C.......  12457
DDX12P    ..................................................C.......  12365

DDX11     CTTGTGCTTCTGTTGTTGCCTCCTCTCCCTGGCTGGGCTCGAGCTGCTTCAGGGCAGGAA  12466
LOC642846 ..........................................................  12517
DDX12P    ..........................................................  12425

DDX11     CCACGTCTTTATAGTTTGATGTTCCCAGAGCTGACCCAGTGTTTGGCATAGGGGTGTGCT  12526
LOC642846 ..........C..............................................  12577
DDX12P    ..........C..............................................  12485

DDX11     CAATAAAATCGAGTTGACATGAATGAGCAGATGCTGCCTCGTTGCAGTCTGGTAGTGTAA  12586
LOC642846 ..........................................................  12637
DDX12P    .....C..................................................A...  12545

DDX11     TTCCAGGCTGCGCATGTGAACTTCGACTTCTGCCCCTGCCCAGGGCAGAGACCACCGTGT  12646
LOC642846 ..........C......G........................................  12697
DDX12P    ................G..C.........G........G..............A..C  12605

DDX11     TGCTTTATGCCTCGCTGGTGAGAGGGGGTCATAAACAGTTTGTGCTCCATGAACCCTTCC  12706
LOC642846 ..................................................G....  12757
DDX12P    ..................................................G....  12665

DDX11     TGCCCGCCTCCGAGGTCATGTTTCTGCTCCCTCTCTTCTCCCTTAGAGCCCGTGGGGACA  12766
LOC642846 .....A.....A.....G................................A........  12817
DDX12P    .....A.....A.....G................................A........  12725

DDX11     AGGCAGAGAACTTGAGTGGAGATGGAGGTGGTGAATATTAAAGGAACAAAGTGCTCCTTC  12826
LOC642846 ........................A..............G..................  12877
DDX12P    ........................A..............G..................  12785
```

```
DDX11     AGGTCTGGGCAAGAGCCATGGATCCTGTAGGTCAGCTTCTGGGGCTTCCCATGCCCTCAC  12886
LOC642846 ................G.....................C...................  12937
DDX12P    ................G.....................C...................  12845

DDX11     GTTTCAGGAGATAACGTGAGCCTCGGAGGACCTGAGTTCTGAATAGAAAATTTTTGCTCT  12946
LOC642846 ......................A...............................  12997
DDX12P    ............T.........A...............................  12905

DDX11     TCATTTCTTCACACACCCAGCCTCTCAGTGAGCTCCTGCTGGCTTTGTCCAGCATGCGAC  13006
LOC642846 ............................................................  13057
DDX12P    ............................................................  12965

DDX11     ATAAGATTGAATCCAAGCCTTTTAAGATAGAGCCGCCTGCTCTTTAGTGACCATGAAGCC  13066
LOC642846 ............................................................  13117
DDX12P    ............................................................  13025

DDX11     AAGCCTGTAATAATTACTCTTCTGATAGCCCAAGACAATTGTATTCTGTTTTGTTAGAAA  13126
LOC642846 ..............................................C.............  13177
DDX12P    ..............................................C.............  13085

DDX11     GGAATTTCGAGGTGAACAAAAATGTTTTCTTTTTATGTGATGTTGCCATAGGTAGCGTGT  13186
LOC642846 ..........................................................G.....  13237
DDX12P    ..........................................................G.....  13145

DDX11     GCCTGTCAGATGGTTTTGTGTTTTCTGAGGAGCATAGACTAGTAGAGCTAGCTCAGCTTC  13246
LOC642846 ............................................................  13297
DDX12P    ............................................................  13205

DDX11     AGGCCATGGGATGCAGGGCTGGCTTCCCTGCCAACGCCTGGCGCTGATGGATTCTTCCCG  13306
LOC642846 ............................................................  13357
DDX12P    ............................................................  13265

DDX11     CATTGCTGGGAAGGGCAGACTGAGGCACTGACACAAGAAGAGTTGTAGCTGGTCATAAGT  13366
LOC642846 .........A................G......A...........C..............  13417
DDX12P    .........A................G......A...........C..............  13325

DDX11     GACAGCATCCTCTGTTCACTCGATTGGTCAGTTGTAGCTTCATCCAGGAGATGGTCATGG  13426
LOC642846 ............................................................  13477
DDX12P    ............................................................  13385

DDX11     GGTTCCTGCTGCATACCAAGCTCTAGGTGAGGCCACGGGGACTCAGCAGAAACAAGGCCG  13486
LOC642846 ............................................................  13537
DDX12P    ..................................T.........................  13445

DDX11     ACCTGGGTCCTCCCTTGTGGACATGACAGTCTGGGGAGATAGACCGAGAGGAAGCGATTT  13546
LOC642846 ..........................................................A....  13597
DDX12P    ..........................................................A....  13505

DDX11     TGAATGAGATGGGTGTGAAGAGCAGGGGCCATGAATCTGTGTCAGAGCAGCCAGGCCTAC  13606
LOC642846 ................-----.............................A.....  13652
DDX12P    ................-----.............................A.....  13560

DDX11     CAGGGAAGGTCAAAGAAGGCTTCCTGGAGGAGGTGATGTTTCTGCTGCTATCTCAGAGTT  13666
LOC642846 ............................................................  13712
DDX12P    ............................................................  13620
```

```
DDX11     GACTGGGAGCTGGTGAGGGGAGACAACATTCCAGGCACAGAACATCCGAAGGCCTGAGAT  13726
LOC642846 ..........................................................C.....  13772
DDX12P    ..........................................................  13680

DDX11     GATGAAGAGCAAATATCCGCCCTGGGGCCTCAGAGGGGTCCAGCTTGCTGGAGGGAGGGC  13786
LOC642846 ..................C.........................................  13832
DDX12P    ..................C.........................................  13740

DDX11     AGAGAGGAGAGCAGCCTGCCATGAGTCCCGAGGCTTCCGACTCAAGACTTGGGTTGGGGG  13846
LOC642846 .....................................A................T....  13892
DDX12P    .....................................A................T....  13800
                                                gRNA 5/6.2
DDX11     TGCTGAGCCCCTTTCTCCTTTTTACATTTCCCTACCCACAGACCTGAGCGGCCATGGGAG  13906
LOC642846 ........T.A.G.....................................C.....  13952
DDX12P    ........T.A.G.....................................C.....  13860

DDX11     GTTGGGGTTGGCATTTGCCTGGGGGAGTTTCTGAGCGAGCAGCACCTGCTACCTTGGTGG  13966
LOC642846 ..................................A.......................  14012
DDX12P    ..................................A.......................  13920

DDX11     AACCCATTGCTGGGAATGGCCAGGGCTCAGCACCAGCGCTCAGCAGATGCTCAGTGCGTT  14026
LOC642846 ..........................................................  14072
DDX12P    ..........................................................  13980
                                                          Exon 6
DDX11     TTGCTGAGTTTGCTGAGGGAAGACTGTTTTCTGTTCTCTCTCACACACACAGAGTGGATG  14086
LOC642846 ............................A.............................  14132
DDX12P    ..........................................................  14040

DDX11     AGGATGAGGATGACCTGGAGGAAGAACACATAACTAAGGTAACACAAGTGTCCTCAGCTG  14146
LOC642846 .........................................G................  14192
DDX12P    .........................................G................  14100

DDX11     GTGCTGTGCTGGGGG-TATAGGCTGGGCTGTGCACCCCTGGGGAGGAGGCTGGAGTCACT  14205
LOC642846 ..............C.G.G...........T....T......A...............  14252
DDX12P    ..............C...G..............T......A...............  14160

DDX11     TGGCTACTTCTCACCCTCCTCTCCACAAAGGAGGAGCTTCCAGCACTTGGACTCCGTTGC  14265
LOC642846 C.....................................................T.....  14312
DDX12P    C.....................................................T.....  14220

DDX11     TTCTTGCACACAACCCTGGTCCTAAGTTGCTCCCTTGGCCAGCTGCAGTGGACCCTGGAG  14325
LOC642846 .........G............G............T.....................  14372
DDX12P    .........G............G.............................T.....  14280

DDX11     TCCTCTCCTGGGGTCAGGGCCTGGGGAGTCCTCTCCTGGGGAGACCTTTCCTGGGAACAG  14385
LOC642846 ...........................................................----  14428
DDX12P    ...........................................................G...  14340

DDX11     GGACCTGAGGAGACCTCTCTTGAGTTTGGGGCCTGGGGAGACATCTCCTGGGTTCGGGGC  14445
LOC642846 ---------------------------------------------------------------  14428
DDX12P    ...........................................................  14400
```

```
DDX11      CTGGGGAGACCTCTCCTGGGGGCAGGGCCATGCTTGCCACCCCAGGGCATCGAGGAACAG  14505
LOC642846  ----------------------..............................A.........  14467
DDX12P     ..................................................A.........  14460

DDX11      CTGTTCTGGGCTGAAATCTGGGTGTTTTCTGTCCCTGCTGGGTGGTACGGGTAGGACAGA  14565
LOC642846  ..............G.............................--------------  14513
DDX12P     ..............G.............................--------------  14506

DDX11      CATGAGTCCCCTGCCCTTTGGGTCTCTCATGGTGTGCTTCTCCCTTTGTCTGTGTTCCCA  14625
LOC642846  ------------------------------------------------------------  14513
DDX12P     ------------------------------------------------------------  14506

DDX11      TTTGCATGGAGGGCTATGGGTTGTGTATGGTCTGACATTTCCCATTTGGTTTCATTGATT  14685
LOC642846  ------------------------------------------------------------  14513
DDX12P     ------------------------------------------------------------  14506

                    gRNA 6/7.1
DDX11      TATGACTTGTTTTCTGTCGGAAGTAGGTATTTTCTTTGTATTTTCTTTTTTTCTCCCTTC  14745
LOC642846  ------------------------------------------------------------  14513
DDX12P     ------------------------------------------------------------  14506

DDX11      ACTCTTGCCTTAGAGGAGTAGAGAGAGGGTATTCTGGTCAGCCTTCCTTTTTCCCTTTGG  14805
LOC642846  ------------------------------------------------------------  14513
DDX12P     ------------------------------------------------------------  14506

DDX11      GGATGTGTGTGACACACTCCCTCCCCTCCCACCAACAACCCACCCTCCCCAAGTGGGGAC  14865
LOC642846  ------------------------------------------------------------  14513
DDX12P     ------------------------------------------------------------  14506

DDX11      CCTTTGCCACGGGAGATGGTCACCCATGTCCAAAGATTGGCCAACCCCCCAAAAGCGGTT  14925
LOC642846  ------------------------------------------------------------  14513
DDX12P     ------------------------------------------------------------  14506

DDX11      GATTAGAGGCTGGATATGACTCGTGGAAGGAGCTGCCTTTGGGGCATTCCCTTGAACTTC  14985
LOC642846  --------..............................G.....................  14565
DDX12P     --------..............................G.....................  14558

DDX11      TGGAGCTGTGGGTGACTTGGGAATCCCTGGGTCCCTCGATAGATGCCTGACATGGGACAT  15045
LOC642846  ............................................................  14625
DDX12P     ............................................................  14618

DDX11      TGCTGTCCTGCCTCGGCTTTGTGCATTGGGAGCCACTCCCTTTCCCTCAGCCTCTCAGGC  15105
LOC642846  ............................................................  14685
DDX12P     ............................................................  14678

DDX11      CCTGGCGTGCCTTGATGTTAGAGAATGCTGTGGGATGTTTTGGTTCTCTCTTTGAAGCGC  15165
LOC642846  ..............................................C..........T..  14745
DDX12P     ..............................................C..........T..  14738

                                Exon 7
DDX11      CTTTCTTTCTCTCTGCTAGATTTATTACTGTAGTCGGACACACTCCCAGCTGGCCCAGTT  15225
LOC642846  ........................C.................................  14805
DDX12P     ........................C.................................  14798

DDX11      TGTGCATGAGGTGAAGAAGAGCCCCTTTGGCAAGGATGTTCGGCTGGTCTCCCTTGGCTC  15285
LOC642846  ..................................................C.........  14865
DDX12P     ..................................................C.........  14858
```

```
DDX11     CCGGCAGGTAAACAGTAGCCAGTATTTCCACCAGGGGCCATCCTGCTCCTTTCGCCACAA  15345
LOC642846 ..................................................C.......  14925
DDX12P    ..................................................C.......  14918

DDX11     CTTTGTCCTGCTCGTCCAGGCCTTGGGAGACGCTGGGTCTGTGACAGGCTGAACCGTGTG  15405
LOC642846 ....................-.....................................  14984
DDX12P    ....................-.....................................  14977

DDX11     AGGAGCAGCCCCCTCCCTGACCTGGCCGGCCCAGCACTGGAAGGCAAAGGAGAGGTGGC-  15464
LOC642846 ..................G.............T........................G  15044
DDX12P    ..................G.............T........................G  15037

DDX11     GGGGCAGGTCCACGTGTGTTGGTAGGATGTCATTTAGCTGGCACCATCTTTTTGCCTCTT  15524
LOC642846 ..................................................C.........  15104
DDX12P    ..................................................C.........  15097
                                  Exon 8
DDX11     TCTTTCTCCTTTGCTGCAGAACCTTTGTGTAAATGAAGACGTGAAAAGCCTAGGTTCTGT  15584
LOC642846 ............T...............................G..............  15164
DDX12P    ............T...............................G..............  15157

DDX11     GCAGCTTATCAACGACCGCTGTGTGGACATGCAGAGAAGCAGGCACGGTAGCCACTGGGA  15644
LOC642846 ..................C................................C....  15224
DDX12P    ............A.......C................................CA...  15217

DDX11     CCATGGTGTAGCCGCAGGTGGTCTGGAGAGAGTGAGGCAGGGGTGGCAGTGACTGAAGAC  15704
LOC642846 ............................................................  15284
DDX12P    ............................................................  15277

DDX11     CATTAAGTGTCTTTCATAGAAAGAATGGCAGAGGAGACCCCAGTTCCTTCCTGAGTCCCC  15764
LOC642846 ....C.....................................................  15344
DDX12P    ....C.....................................................  15337

DDX11     TCTCCTTGGGAAAAAGTGTTCCTACTCTCTGGGTCAGTGTCTGGTCCGAATCCTTGGCTT  15824
LOC642846 ................................G..C.............G.......  15404
DDX12P    ................................G..C.............G.......  15397

DDX11     GGAGATGATTTTACGGGCTCTTTCTGGAGAACAGAAGTAAAACCTTACAGTGTTCCGATG  15884
LOC642846 ................................A...........--............  15462
DDX12P    ................................A.........G................  15457

DDX11     AGACCACAGTAGGCAGTACTTGGGAGGGTCTTATAGACCCTACCCCATGGAAGTGGGTCT  15944
LOC642846 ...-.....................................C....TG............  15521
DDX12P    ...-.....................................C....TG............  15516

DDX11     CAACATTACACAACCCCCTCTTGGGCCCGTGGACAGTTGCTGTCCTCTCTGTTTTCTCTC  16004
LOC642846 ....................C.....................T...............  15581
DDX12P    ....................C.....................................  15576
                                  Exon 9
DDX11     TTTGTGCCTGTGCCACCCTCAGAGAAGAAGAAAGGAGCTGAGGAGGAGAAGCCAAAGAGG  16064
LOC642846 ............................................................  15641
DDX12P    ..............C.............................................  15636
```

```
DDX11     AGGAGGCAGGAGAAGCAGGCAGCCTGCCCCTTCTACAACCACGAGCAGATGGGCCTTCTC  16124
LOC642846 ............................................................  15701
DDX12P    ............................................................  15696

DDX11     CGGGATGAGGCCCTGGCAGAGGTGAAGGACATGGAGCAGCTGCTGGCCCTTGGGAAGGAG  16184
LOC642846 ............................................................  15761
DDX12P    ............................................................  15756

DDX11     GCCCGGGCCTGTCCCTATTACGGGAGCCGCCTTGCCATCCCTGCAGCCCAGGTGAGGGCC  16244
LOC642846 ......................A.............................A..........  15821
DDX12P    ............................................................  15816

DDX11     CTGCAGGGCCAGAAAGCCGCTCTTGACTCTCACTGTGGTCTAGGCCATGAGGGGGGTCCT  16304
LOC642846 ........................G.............................C.....  15881
DDX12P    ........................G.................................  15876

DDX11     CATCACACTGTAGTTTGGGGGATGCCCCCCACCGTGGTCAGGTTGATGGCACCTTAACCC  16364
LOC642846 ............................................................  15941
DDX12P    ............................................................  15936

DDX11     ATTCTCTCCTGATGTGTGAGTTGGAGGAGGCGCGTGGGATCCCTTGGGGTCTCCAGGCAG  16424
LOC642846 ..............C.............................................  16001
DDX12P    ............G.C.............................................  15996

DDX11     CAGGGCCAGTTGGCATTACTGGGGATGGTATTTAGGAGCCAGGAAAGCCGGTGCATTCCT  16484
LOC642846 ............................................................  16061
DDX12P    ............................................................  16056

DDX11     AGTGAAACCACAGGGAGAGGGGGGATGCCAGGAGCTGAGAAGAGTGTGCTGCATACATCT  16544
LOC642846 ............................................................  16121
DDX12P    ............................................................  16116

DDX11     ATTTACAAATGGCTTTCCAAGTGATGCTCCCAACTTCCATGCCTATGATGTGATGGAGGA  16604
LOC642846 ............................................................  16181
DDX12P    ............................................................  16176

DDX11     TGTCAGTGATAGAACCATTCAGTTTTCCAGTTTTTCCTTTTTGTAATATCAGTACTCTTA  16664
LOC642846 ............................................................  16241
DDX12P    ............................................................  16236

DDX11     ACTGGAAAGCTTTCCCTAACTTACACCTACCTGCAGCACGTGAGAATACTGTCTTCTCTG  16724
LOC642846 ............................................................  16301
DDX12P    ............................................................  16296

DDX11     CCTCAACTTCTCTTGATTTTTAAACAGAAGGAAGAACTGCTAATGTAGCAGATCAAAAGT  16784
LOC642846 ..A.........................................................G......  16361
DDX12P    ..A.........................................................G......  16356

DDX11     AGTATCTCACTGTTATTTGGTGGGTGCAGTTTCACTATTTCCTTGCTACTTCTTTAATTT  16844
LOC642846 ..............C.........................................C..  16421
DDX12P    ..............C.........................................C..  16416

DDX11     GAGTGACTTTGGAAACGGGATATCACTAGTGGAAAATTCTGTATAATCCAGAAAAAAATG  16904
LOC642846 ............................................................  16481
DDX12P    ............................................................  16476
```

```
DDX11     TAAGGTTTTAAAAGATTCAGGGAACTAAGTAACCATTTGCACAGCAGCTAAATGCTCACC  16964
LOC642846 ................................G.......................  16541
DDX12P    ................................G.......................  16536

DDX11     AGCATACCTGCTGAGCTGTGTGGGCACTGGCAGAGAAACTGAGGAAAGCTGCCAGGCCCC  17024
LOC642846 ........................G.................................  16601
DDX12P    ........................G.................................  16596

DDX11     ATGGTGTCCCAGGCCTTCCCTCCCGTCTGTTTGCCTTTAGAGCAAGATTAGTGCTATAGG  17084
LOC642846 .....T.................G.................................  16661
DDX12P    ......................G.................................  16656

DDX11     CATTTATACACAAATACCATAATATGGCCCAAAATCTTTACAATTTTTGAATTTTTAAAG  17144
LOC642846 ....................................G............G.....  16721
DDX12P    ....................................G............G.....  16716

DDX11     TACTTTGACCATATTTTGCTTTTATGTTAATAGTATTCCAGTGAAATTCTGTGCATGGGG  17204
LOC642846 ...............................................C.........  16781
DDX12P    ...............................................C.........  16776

DDX11     ACACTGGAGCCCAGAAAAGTTAAGTGACTCATATTTTCTCACCAAGCGTGGGTGATGGAG  17264
LOC642846 ............................................................  16841
DDX12P    ..G.........................................................  16836

DDX11     CCATTCAGTTTTCCGATATTTTATTTTTTATATGAGTATTCCTTTAACTGGAAACTTTCC  17324
LOC642846 ............................................................  16901
DDX12P    ........................C...................................  16896

DDX11     TAACAACAAACACCTAAAGATGTGCAGAGTTGCTTTTATTTTTGTTACCCCAGCTCCACG  17384
LOC642846 ..................CC........................................  16961
DDX12P    ..................CC........................................  16956

DDX11     CCTTAACCCTCACTTTGAAATAGGATGTATCAACCCTATTTTGCAGATGAGGAAAGCAAG  17444
LOC642846 ............................................................  17021
DDX12P    ...........................G................................  17016

DDX11     AGTCAGAGAGGTTAGACAACTCTTCCAGAGTCACACAGCTGGGGAGTAGCAGCTCCAGGA  17504
LOC642846 G.........................................A................  17081
DDX12P    G.........................................A................  17076

DDX11     GTAGAAGCTGGGGCCGCTTCCTGGTGCACCGATGGTCTGCAGGTG-TTTGTGGAAACTCG  17563
LOC642846 .C.....................................T......T.............  17141
DDX12P    .C.....................................T......T.............  17136

DDX11     GGGGCCTCCGGGGCGACCTTGAGGACATGGACAAGGCTAAGCAGGGGTTCCCTTCACCCA  17623
LOC642846 ............................................................  17201
DDX12P    ............................................................  17196

DDX11     GCCCTGCCCTTGGTTTACTCAGGAGTCAGACCAGCCCTAGTTTCCTGTGTTTCATGTATT  17683
LOC642846 ............................................................  17261
DDX12P    ............................................................  17256
```

```
DDX11     GGCTTTTCATGTGAAACTCGAGGAGAGCTTGTCCGTTGCCACAAGCTGTTTTTCGAATGT  17743
LOC642846 ....................................T..G..........T...C..  17321
DDX12P    ....................................T.............T......  17316

DDX11     CTCTACACAGTCCAGGCAGGAAATAGAAGCACTCACATCAGGAGCTCAGTGTCAGGCAGG  17803
LOC642846 ............................................................  17381
DDX12P    ....................G.....................................  17376
                                                            Exon 10
DDX11     CAAGGCTCCTGCAGGGGAGCCCCGCCCTGCTCAGGTGGCCTCATCTCCCCTCCCAGCTGG  17863
LOC642846 ....C.....................................................  17441
DDX12P    ....C.....................................................  17436

DDX11     TGGTGCTGCCCTATCAGATGCTGCTGCATGCGGCCACTCGGCAGGCCGCGGGCATCCGGC  17923
LOC642846 ...............................................C..........  17501
DDX12P    ...............................................T..........  17496

DDX11     TGCAGGACCAGGTGGTGATCATCGACGAGGCGCACAACCTGATCGACACCATCACGGGCA  17983
LOC642846 ............................................................  17561
DDX12P    ...............................................C....A...  17556

DDX11     TGCACAGCGTGGAGGTCAGCGGCTCCCAGGTGTGTGGGCCTCCCCTCCCCGGGCCAGGGC  18043
LOC642846 ..............................C.................A.........  17621
DDX12P    ..............................C..........................  17616

DDX11     CTGCTGTGACGTAAAGGGACTTGGATGGTTCCTCCAGACACCTGGGCCAAGAGTTCCTCC  18103
LOC642846 ....C....G..............................C.........A.......  17681
DDX12P    ....C....G.....................................A.......  17676

DDX11     GGAGGTGGGGCTTGATAGAGGGTGCACGAGTCAAGGCGGTGACCTCATCGGAGGCTGACC  18163
LOC642846 ..............C..C.....................................  17741
DDX12P    ..............C..C.................T.....................  17736

DDX11     ATGGCTTTCCAGTGCA---------TCGGGGGACCCCGCTATGACAGAGTGCCTCATTTC  18214
LOC642846 ................TCCCAGAAC..T.............................  17801
DDX12P    ................TCCCAGAAC..T.............................  17796

DDX11     CCTGCACCTCATCTGCCCCCATGCTCCTGAGTCCCTCCAGCCCTGGATGCCAGCAGCCAG  18274
LOC642846 ...........C.....................................................  17861
DDX12P    ...........C.....................................................  17856

DDX11     TTCTGTAAGCCAGGGAGATGGCATGTGTGAGGCAGAAGTCCCCTCAGGATTGGATTTTGT  18334
LOC642846 .....C.....................................................  17921
DDX12P    .....C.....................................................  17916

DDX11     CATTACTGAAGTTGTCTGGAGGGGACTGAATTGAGGAATGCTCAAGATCAGCGCAGGCTC  18394
LOC642846 ...................................................T........  17981
DDX12P    ...................................................T........  17976

DDX11     CTCCTGCTGCCCTATCATGCGCCATGCATGGCACCAGGTGTCTCTGGTCTTCACGCTGAC  18454
LOC642846 ............................................................  18041
DDX12P    ............................................................  18036

DDX11     TCTGCCATGGGTGTGGTGTTCCTGTTTTACATTGGAAACTTGGAGATTCAAAGATGGTCA  18514
LOC642846 ...........G.....................................................  18101
DDX12P    ...........G.........................G..........G.........  18096
```

```
DDX11     AGCTCTGTCCTGAGGTCATGCAGCTCATGAGTGTGGAGCTGGGGTGTGCCCACTGGTTTC  18574
LOC642846 ............................................................  18161
DDX12P    ............................................................  18156

DDX11     TGACTGTGAAAACCCCCACGACATCCCACCAGCTCTACTGACCTGTGCCTGGGCTGAATT  18634
LOC642846 ........-...................................................  18220
DDX12P    ........-...................................................  18215

DDX11     GAGGCTGGGATGTGATGGTGGCCTTGAACCATCACTCTTTGTAGACTCCAGGTCTTTTCC  18694
LOC642846 ..................A.........................................  18280
DDX12P    ..................A.........................T...........  18275

DDX11     CAACCCGGTGGAAACTTAGCAGGGAGATTCCATACTTGAGGAATTCAGCCTCTTGCTTTT  18754
LOC642846 ..............-.......C.....................................  18339
DDX12P    ..............-.............................................  18334

DDX11     TCTCTGACCCACAGTGGACACTGGAGGAAAACTTCCCTTCCTTCCCTTTTCTCTTAGCTC  18814
LOC642846 ............................C...............................  18399
DDX12P    ............................C...............................  18394

DDX11     CCACCAGCCTAAGGGCTGTGGAAACCCGTACCTTTTGTCTGCAGCCAGCCCCCTCTCCTC  18874
LOC642846 ........................A.................C.................  18459
DDX12P    ........................A.................C.................  18454

DDX11     CCTTTGGTGGCTTCCTGTGTGTCCAGGGCCAGCATCTTCTAGGTGAATCTAAGATGTCAG  18934
LOC642846 ............................T...............................  18519
DDX12P    ............................T...G...........................  18514

                                                          Exon 11
DDX11     TACCTTAGCCCTCAGCTGCTTGCTCAGAGCCTGGTTTGTGTTCTTTCCCCAGCTCTGCCA  18994
LOC642846 ............G.....................................................  18579
DDX12P    ............G.....................................................  18574

DDX11     GGCCCATTCCCAGCTGCTGCAGTACGTGGAGCGATACGGGTGAGATGTGACCCTCTGAGG  19054
LOC642846 ........................A.........................T........  18639
DDX12P    ........................A.........................T........  18634

DDX11     TAGTGGGACAGTCCCTTGGTGGCCCCCTGCGTGGGCCTCTGAGAGGCAGGCAGCACTTTG  19114
LOC642846 ............................A............----.............  18695
DDX12P    ............................A............----.............  18690

DDX11     GTTCCCACCTCTGGCCCGGGCTGTGGCGGGGTGGAGCTGCATGCCATTCATGTCCTAGGC  19174
LOC642846 ................T...........................................  18755
DDX12P    ............................................................  18750

DDX11     ACATCATGGTGTGTGCTGCACACAGACCTGGAAGGCTGGGGACTGACCGCTGGCTCTGAG  19234
LOC642846 ....G.......................................................  18815
DDX12P    ............................................................  18810

DDX11     GCCTGGGGCCGTGGCCAGCCTGCTCTCTGGGAAAGGATTTGTAGCTTGTGACCCAGTTTG  19294
LOC642846 ............................................................  18875
DDX12P    ............................................................  18870
```

```
DDX11      AGAGGCACCGGGCAGCAAGGCTTCCACTGGGGTGGGCGGGGCGAGTCGCCATCAGGGCAC  19354
LOC642846 ............................................................  18935
DDX12P    ............................................................  18930

                                      Exon 12
DDX11      CACCACTTAATGTCCGTTGGCTTCTTCTCAGGAAGCGTTTGAAGGCCAAGAACCTGATGT  19414
LOC642846 ............................................................  18995
DDX12P    ............................................................  18990

DDX11      ACCTGAAGCAGATCCTGTATTTGCTGGAGAAATTCGTGGCTGTGCTAGGGGGTGAGAGCC  19474
LOC642846 ............................................................  19055
DDX12P    ............................................................  19050

DDX11      TCG-TCCCCCTGCTGACCCCGGGCCTGCAAAACTCGCTGGGCTGCTTTTTCCTTGGATGC  19533
LOC642846 ...-C.....G...A.....C.............C.A.C.....................  19114
DDX12P    ...TC.....G.........C.............C...C.....................  19110

DDX11      CCATCAGGACACCTCAGTTCTCTGTGTTTTTAAGAAGGGTCGGCCGGGTGCGGTGGCTCA  19593
LOC642846 ..........G.......................................T.........  19174
DDX12P    ..........G.....................................A....T.........  19170

DDX11      CGCCTGTAATCCCAGCACTTGGGAGGCCGAGGCAGGTGGTTCACCTGAGGTTAGGAGTTT  19653
LOC642846 .A..............C.....................................C.......  19234
DDX12P    ..............C.....................................C.......  19230

DDX11      TGAGACCAGCCTGGCCAACATGGTGAAATCCCATCTCTACTAAAAATACAAAAAAATTAG  19713
LOC642846 ..............T.......A.....................................  19294
DDX12P    ..............T.......A.....................................  19290

DDX11      CTGGGAGTGTTGCCGTGGCCTGTAGTCCCAGCTGCTCCAGAGGCTGAGACAAGAGAATTG  19773
LOC642846 ...........................................A..................  19354
DDX12P    ...........................................A..................  19350

DDX11      CTTGCTCAAACCCGGGAGGCGGAGGTTGCAGTGAGCCGAGATTGTGCCACTGCAGTCCAG  19833
LOC642846 ............................................................  19414
DDX12P    ....................A.....................................  19410

DDX11      TCTGGGCGACAGAGTGAGAATCAGTCTCAAAAAAAAAAAAAAA----AAAAAAAAAGAAG  19889
LOC642846 ..................G.....................GAACC..............  19474
DDX12P    ..............A...G...................--------..............  19462

DDX11      GGTCTTGGTCATTGATTTAGAAAATTCTTGTTCTTTGTAGCTTAGTTGAGTTGTCTGACT  19949
LOC642846 ............................................................  19534
DDX12P    ............................................................  19522

DDX11      TGAGCTTTATTTAGACCCATGGGTTCTTTGCCCATGTTCTGAGGACTTTTTATTTCAGGC  20009
LOC642846 ........T...................................................  19594
DDX12P    ........T...................................................  19582

DDX11      CCTGCTCTGGGGGGATATTAAGGATACAGCATCACATAGACACACGGTGTTTCCGTGATA  20069
LOC642846 G.....................................G......................  19654
DDX12P    G.....................................G......................  19642

DDX11      GGCATAGTTCTGTGGGTTGTTCGAAGCACTTGCATATGCGGTTTTGTGTGCCCTGTGAGA  20129
LOC642846 ............................................................  19714
DDX12P    ............................................................  19702
```

```
DDX11     ACGCAGTGCTGGTATTTGAATCCTTGTTGATAGACGCATAAACTAGAGCTCGGAGCAAGG  20189
LOC642846 ............................................................  19774
DDX12P    ............................................................  19762

DDX11     GCTGCTCCCAGCACGGGAGCCTGGGATCTTCTGACTCCAGCTCCCACGCCTCTTTGCATG  20249
LOC642846 ...........................................................G..  19834
DDX12P    ............................................................  19822

DDX11     ACCCTGTCACGTCCCCTTCTTTTATGATGGGGCACCCCCT---TGGAAGGCGTCTGTGGA  20306
LOC642846 ....................................TGC.......T.........  19894
DDX12P    ..........A.........................TGT.....A.T.........  19882

DDX11     AGTGGAAGCTGCAGAAAGCCTGTGGGAGCTCCTGGCGGGAGCTGGTCTCGTGTTGCTGCT  20366
LOC642846 ............................................................  19954
DDX12P    ............................................................  19942

DDX11     CTGAGCCACCAGCTCTGCTTTGCCTCAGGCTCACCAGTGGCCTGGGCAGCTCCTCTGTGC  20426
LOC642846 .......G....................................................  20014
DDX12P    .......G....................................................  20002

DDX11     TCCGGTGCCCTGCATACCTTGGTCTGGCTGCTGTGTCCCGGCCTCCTGGAGAAGGGGTGA  20486
LOC642846 ............................................................  20074
DDX12P    ............................................................  20062

DDX11     AAAACATGAAC-TTACAGGGCTTTGGGTTCCACGTGCAAGCACGTGAGTCAGACATGGGA  20545
LOC642846 ...........-.....................................G.....  20133
DDX12P    .......A...T.....................................G.....  20122

DDX11     GGCTCCTGGACCCACCTGCCCTCTCAGTGGGTCCGTTGCATGCTATAAACAGTGAAAAGC  20605
LOC642846 ........................A.......................................  20193
DDX12P    ........................A.................A.....................  20182

DDX11     AAAACAAAGCCATTTAAATACAGATGCTCTTCTTACTTGATGTGCAGTGTGGAGGGAGAG  20665
LOC642846 ...........G..C.....................................................  20253
DDX12P    ...........G..C.....................................................  20242

DDX11     AAGATAGGGAAGGGTTGGGGGTCCTGAGAACCAGCATTGTGACCTATTTCCATTCTCTTT  20725
LOC642846 ....................G...........C.....................  20313
DDX12P    ....................G...........C.....................  20302

                Exon 13
DDX11     TTTAGGGAACATTAAGCAAAATCCCAATACACAGAGTCTGTCACAGACAGGTAAGAGAGT  20785
LOC642846 ............................................................  20373
DDX12P    ............................................................  20362

DDX11     TGCCCTCAGAGGGCCCAGAGCTGATCTGAGCCACTTCCGAGCTTAACCCTGGGACTGAAA  20845
LOC642846 ............................................................  20433
DDX12P    ............................................................  20422

                                                          Exon 14
DDX11     CCTGAGGCTTAGGGTGAAGCTCCCAAGGCCCTTCATGTGTTTGTTCTCAGGGACGGAGCT  20905
LOC642846 ............................................................  20493
DDX12P    ..........................................................T.....  20482
```

```
DDX11     GAAGACCATCAACGACTTTCTCTTCCAGAGCCAGATCGACAACATCAACCTGTTCAAGGT  20965
LOC642846 ..........................................................  20553
DDX12P    ......T.....................................................  20542

DDX11     AGAGGTTTCCACCTTTCCACATTCCACATCCAATTTCCTTCCTGTCACCACCTGTGGGTA  21025
LOC642846 ..............G...TG...........G.............................  20613
DDX12P    ..........................................................  20602

DDX11     AAGTACTATGTTAAGACTGTAGAAGGAAGAAAAAGCAAAACAGATGTGTAATTACTTAAC  21085
LOC642846 G.................A.........................C................  20673
DDX12P    G.................A.........................C................  20662

DDX11     CCTTAACGCAACATGCCTGTGAGACAAAAGTCATCTTCTTTTAGAGTGAAGGCCACAGGG  21145
LOC642846 ............C.....................A.......................  20733
DDX12P    ............C.....................A.......................  20722

DDX11     ATGAGGGATGGGTGAGAAAGGGACCTTTCTTGGTGCCCCATAGAACAGATAGAGACTCCA  21205
LOC642846 ..........................................................  20793
DDX12P    ..........................................................  20782

DDX11     GGTCCTTGCTCTCTCACTCCGTCTTCTGGCACAGTCTCCCTCAGGCTTATGGACAGGAAT  21265
LOC642846 ..........G......C..A.....................................  20853
DDX12P    ..........G.G.......A.....................................  20842

DDX11     AGGACGTTGATTTGTTCTGTGCAACCCCTGTCACGTCTTCCCACTTGGGCCTTGGGTCTG  21325
LOC642846 ....................................G................G..  20913
DDX12P    ....T.......................................................  20902

DDX11     GTTGCAGCCTCAGACCTCTGCTCACTCCAGGTCTGTGTACCCAGCGCTCCCCAGATGAAA  21385
LOC642846 ......................G...................................  20973
DDX12P    ......................G...................................  20962

DDX11     CACGGCCACTGCCGCCTGAACCCCAAGCTCGTAACTCAAATCAGCAACAGTGACTGCCCC  21445
LOC642846 ......................C...................................  21033
DDX12P    ......................C...................................  21022

DDX11     CGGGTACAGGGTTCTGCCTCTGTTGTAGGCGGCATGCCATGTGCTGTGCTCTGAGCTAGG  21505
LOC642846 T.....................C.............C....................  21093
DDX12P    T.....................C......C.......C....................  21082

DDX11     ATATCCTTTTGCCCCAGCAAGGAAAGCAAACAGGCCCGTGGAGGTGACTTCAGGAGGGTG  21565
LOC642846 ..............G.....................A.....................  21153
DDX12P    ..............G.....................A.....................  21142

DDX11     GCGAGCACAGGCTTCCCACAAGTGAGCCAATAGCAAGTGGCAGAGACAGCGTCCAAACCT  21625
LOC642846 ..........................................................  21213
DDX12P    .......T....................................................  21202

DDX11     GGCTGCACTGACTTGGGGCCCCACATTCTTCCCATCCTGCCTGCCTTTTTTTTCTTAAAA  21685
LOC642846 ..................................G.......................  21273
DDX12P    ..........................................................  21262

DDX11     CCAGCTTTTCCCCTGAATTACACATTTGGGTCACTGTCACTGCCGCCATCCCTGCCAGAC  21745
LOC642846 ..........................................A...............  21333
DDX12P    ..........................................A...............  21322
```

```
DDX11     AGGCTGGATCCAGGTCATCCTTGATGCCTTTCTCCCCTTGTCTCCCACATGCCTGTGACA  21805
LOC642846 ............C.............................................  21393
DDX12P    ..........................................................  21382

DDX11     GCCGCCAGGCCTGACAGCCTGAGACAGTCCTGCCGTCCCTGCGCTTCTCCCACAGCTGGG  21865
LOC642846 ..................C...............C.....................  21453
DDX12P    ..................C...............C.....................  21442

DDX11     ACATGGGTGCAGGCACTCCTTCTCTCGCCTTCCCTTTGCCCTCCTTGCTTTCCTTCTCCC  21925
LOC642846 ..........................................................-  21512
DDX12P    ..........................................................  21502

DDX11     CTCTTCTTCCCATGGGTCTCGGGTCTCATCACTCACCATTGAGGGAATCCTCATCGAAGG  21985
LOC642846 --.........................C.............................  21570
DDX12P    ..........................................................  21562

DDX11     ACGTCGCTCTTTTTAGAAACCGGTTTAAAGGCTCCAAACTCCTCATCTCTGCATCCCAAG  22045
LOC642846 ............................C.............................  21630
DDX12P    ..A.......................................................  21622

DDX11     CTAAGATCTGGCACCAAACCACACACATTGGATGCACCGACTGAGTGGCACTGCCCCAGC  22105
LOC642846 .......G..................................................  21690
DDX12P    ....................................T.....................  21682

DDX11     CCCTGAGCAGGTCCCAGCCATCATCTCCTCTGTGGCTTTGCTCATAGAAGTTCCTTTTTT  22165
LOC642846 ..................................................----..  21746
DDX12P    ..................................................----..  21738

DDX11     TTTTTTAACTCTTTGTCACCTGGAAGGAAAGCCAAGGGGAACTGGATTTTACTGAGCACT  22225
LOC642846 .G.........C.........................C..A.........G.....  21806
DDX12P    .G......--..C.........................C..A....G...........  21796

DDX11     CTTAGACTTGAGAGAGACATTTGGAAAGAGGGTCTCCACCCTGAGGAGGACACTGCGTTG  22285
LOC642846 ..........G.........................C......................  21866
DDX12P    ....................................C......................  21856

DDX11     TGGGCAGGGGCAGTAGAGGAGGGGGTGGCCTCGGAGAGGAGATGACAAGGTTGGTGGCAA  22345
LOC642846 ....................................G.....................  21926
DDX12P    ....................................G.....................  21916

DDX11     GGAGGCTCCAGGTGCCTCAGAAGGTAGCACTGCGTTGTGCTGCCTGGGTGGTAGAAGTGG  22405
LOC642846 ..........................................................  21986
DDX12P    ..........................................................  21976

DDX11     TGTTTTTTGTTTTGTTTTTAAGATTATAGCTTGCTCAGTTTGCACTCATGCCTACAGCTG  22465
LOC642846 ..............G..........C...................A..............  22046
DDX12P    ..............G..........C...................A..............  22036
                        Exon 15
DDX11     GGCTTGGTTTTTGCAGGTGCAGCGATACTGTGAGAAGAGCATGATCAGCAGAAAGGTAAC  22525
LOC642846 ..........................................................  22106
DDX12P    ..........................................................  22096
```

```
DDX11     TGCTCCCATCTTGTGGTCCTGAACAAGACCCAGCTGTGCCCCAACCCCCTGCCCTTGCCA  22585
LOC642846 ..................................................G......  22166
DDX12P    ..................................................G......  22156

DDX11     TGCTTTCCTCCCCTGCCCTCAGGGAACTCCAGAGTCCCCTTCGTCTCCACTCTCCTTGGT  22645
LOC642846 ..................................................C.....  22226
DDX12P    ....................A..................A.......C.....  22216

DDX11     GCAGTGGGCCTTGCTGGGGTGGTGGGATGTGTGCTGCAGGTGTCTTGGGCCTGGCAGAGC  22705
LOC642846 ..............................C...T...........A..........  22286
DDX12P    ..............A............C.........................  22276

DDX11     CTCCGATCCACCCAGCCTCTCTCTCATGGCTGTACCTCGTTCCTCTCCACTGCTCTCTCT  22765
LOC642846 ..............................T.....................  22346
DDX12P    ..............................T.....................  22336
                        Exon 16
DDX11     CATCCCACCCAGCTCTTTGGATTCACTGAACGGTACGGAGCAGTGTTCTCATCCCGGGAG  22825
LOC642846 ..................C.....................................  22406
DDX12P    ..................C.....................................  22396

DDX11     CAGCCCAAACTGGCTGGGTTTCAGCAATTCCTGCAGAGCCTGCAGCCCAGGACGACTGAA  22885
LOC642846 ..........................................................  22466
DDX12P    ..........................................................  22456

DDX11     GGTGAGGCAGGAGGGTGGGCAGGCAGAGCCGGCTGCACGCATGGGCAAGGACTTCTGTTC  22945
LOC642846 ..............A..................G.....................  22526
DDX12P    ..............A.....................................  22516
                                                        Exon 17
DDX11     CTCATGTGTGGACCTGACCAGAGGGAGGCCTCCTCCCCGTTCTGCTCTGTGCAGCTCTTG  23005
LOC642846 ..............T..................A.....................  22586
DDX12P    ..............A..................A.....................  22576

DDX11     CAGCCCCTGCAGACGAGAGTCAGGCCAGCACCCTGCGACCAGCTTCTCCACTGATGCACA  23065
LOC642846 ........................GT..C..A.........C.....A.......  22646
DDX12P    ........................GT..C..A.........C.............  22636

DDX11     TCCAAGGCTTCCTGGCAGCTCTCACTACGGCCAACCAGGACGGCAGGGTCATCCTGAGCC  23125
LOC642846 ..G.......................................................  22706
DDX12P    ..G.......................................................  22696

DDX11     GCCAAGGTAATCAGGTGGTTCTTGGCCAGGTTCAGTTCCCAGGAAGGAGCCAAGCTGAGC  23185
LOC642846 ..........................................................  22766
DDX12P    ..........................................................  22756

DDX11     CCGGGAGCCGCAGCGTGAAAGGATTCTTTCCTTCCATCCTGGGAACTTCCTGGGTTAGGA  23245
LOC642846 ............A.....................................................  22826
DDX12P    ............A.................................C.....  22816

DDX11     GGAAGCAGTGCAGTGGGCACTGGCCTGCTGTGACCTGGGCAAGCAGTGGAGGTGGATGGG  23305
LOC642846 ....................................------------------  22866
DDX12P    ....................................------------------  22856

DDX11     AGGAGATCGAAGGGCTGGGATGGGGGTCCCGTGACCAGGGTAAGCAGTGGAGGTGGACGG  23365
LOC642846 ------------------------------------..................  22885
DDX12P    ------------------------------------..................  22875
```

```
DDX11      GAGGAGATCGAGGAGCTGGGATGGGGGTCCTCTAGGGCAGGGGTCCTAGGGAAACTTCTA  23425
LOC642846 ............G.........A.................................G..  22945
DDX12P    ............G.........A.................................G..  22935

DDX11      CTGTGGGGTAGGTGGGCTTTGGTTTGGGTCATGATTTTGTCATCTATGAGCCTTGTGATT  23485
LOC642846 T.....................................................  23005
DDX12P    T.....................................................  22995

DDX11      TGGACTATTTTCTTTCTCAACTTCAGTTTCTTCATATGAAAATGGAGAGGATAGGCCGGG  23545
LOC642846 ............................C.........................  23065
DDX12P    ............................C.........................  23055

DDX11      CGCGGTGGCTCACGCCTATAATCCCAGCACTTTGGGAGGCTGAGGGGGGGCGGATCGTGA  23605
LOC642846 ................G.......................-.............  23124
DDX12P    ................G...........G...........-.............  23114

DDX11      GTTCAGGAGATCGAG-ACCATCCTGGCTAACACAGTGAAACCCCGTCTCTACTAAAAATA  23664
LOC642846 .G............A.........................................  23184
DDX12P    .G............-.........................................  23173

DDX11      CAAAAAATTAGCAGGGTGTGGTGGTGGGTGCCTGTAGTCCCAGCTACTCGGGAGGCTGAG  23724
LOC642846 .....................................................  23244
DDX12P    .....................................................  23233

DDX11      GCAGGAAAATTGCTTGAACCCAGGAGGCGGAGGTTGCAGGGAGCCGAGATTGAGCCACTG  23784
LOC642846 .....................................................  23304
DDX12P    ..........................T..........................  23293

DDX11      CACTCCAGCCTGGGCAACAGATCGAGACTCCATCTCAAAAAAAAAAAAAA-AAAAGGATG  23843
LOC642846 ............................-..............G.G.GA....  23363
DDX12P    ..............................................---..A....  23350

DDX11      GAGAGGACAGTGTGGTCCACCTCTGTGGGCTGGTTGTCCTAGAGATTAAATGGTGTTTAA  23903
LOC642846 ..........A......................................................  23423
DDX12P    ..........A......................................................  23410

DDX11      TTTAAAGAGAAAGCACTAGCACTTGTGCCTCAGACCTGGACTCACCTGGGGGACCCCCTT  23963
LOC642846 .....................................................  23483
DDX12P    ..........................................A..-.T.....  23469

DDX11      TGCTGGGACGACAGAAGTGTCTGTTGGGCTTGCACTCACCT-CCCACCGATCTGTTTTTC  24022
LOC642846 ..........T.........................-.................  23542
DDX12P    ..........T.......................T..C......A..........  23529
```

Exon 18

```
DDX11      CAGGCAGCCTCAGTCAGAGCACCCTGAAGTTTTTGCTCCTGAATCCAGCTGTGCACTTTG  24082
LOC642846 ............G.....................................................  23602
DDX12P    .......T.....................................................  23589

DDX11      CCCAAGTGGTGAAGGAATGCCGGGCAGTGGTCATTGCGGGGGGTACCATGCAGCCGGTAA  24142
LOC642846 ..........................................G................  23662
DDX12P    ..................................C.....G................  23649
```

```
DDX11     GGACACCTTTCCCAGCCCCTCGTGCCCCAGGTGTTGGGATGAGATGGGGGCTTGGGAGAG  24202
LOC642846 ..................................................A.........  23722
DDX12P    ......................T.......................A...........  23709

DDX11     ATGCATTATCAGTCCTGTTCTCTCCTGGGGCCCCAAGCCAGAAAGGGTCAGCTCGAGCAG  24262
LOC642846 ............................................................  23782
DDX12P    ....G.........................G.............................  23769

DDX11     GCCCAGTGGTGTCCGCTGGGTGACACTGCTATTCTCTCACTGCTGTGCCTTTTAGGCTGC  24322
LOC642846 ..............A.............................................  23842
DDX12P    ..............A.............................................  23829

DDX11     AGGAGCAGTGGAGACTCCTCTGCTGCTCCATTCTGTAGCCCCAGGATCACATGTCTCCCA  24382
LOC642846 ..........C.........................................CT.......  23902
DDX12P    ............................................................  23889

DDX11     GAGAAAGCTGTTCTGTGGTTTCAAACTCAAGGAAAAAAATCATGATTCCACTTTTAAAAG  24442
LOC642846 ............................................................  23962
DDX12P    ............................................................  23949

DDX11     GTTCATTTTGATGTATATGAATATAATAGTCTTTGTAGGCGTAATTTTTACTTATGTGCA  24502
LOC642846 ........................................A...................  24022
DDX12P    ....G.....................................A...................  24009

DDX11     TAGCTGTTTTAAAAACAAAAGTACGGCTCCCTCCATGTGCTGTCACTGGAACTTGCTCTT  24562
LOC642846 .....A.................G.....................................  24082
DDX12P    ......................---TT.TAAAA...........................  24066

DDX11     TTCACTCAGCAGCCAGAGGGTCATAAACCCTGTCTCCTTGTCAGCAAGCATGCACGTATT  24622
LOC642846 ............................................................  24142
DDX12P    ...............................................T.....T.....  24126

DDX11     TCAGTATCCCAGCTGTGCTGGATTCCAGTTACACAGATATATAGCATTTCATGTAGCTGC  24682
LOC642846 ..............................C........C............C..C.  24202
DDX12P    ............................................................  24186

DDX11     TTCTCTCTTGTTAGGTGTGCAAGCTATTTGCAGTTTTCTGTTTTGAGCATGACTGTGATA  24742
LOC642846 ......T......................T...........................G  24262
DDX12P    ............................................................  24246

DDX11     AATATAACCGCATTTCTGCACAGTGGTGACTCCTACCTAGCGAAGGGCCTCCTGGACAAA  24802
LOC642846 ................C.........................A.................  24322
DDX12P    ..............................T........A.................  24306

DDX11     AAGCTGCTGGGAATCCTGAAGCAGTGCTTCCCAGCCCCAGCTGCCTTAGCTTTTGATTTT  24862
LOC642846 ............................................................  24382
DDX12P    ............................................................  24366

DDX11     TATATTTTTGTATGGATAGATTCATAGTTTTATTCATTCGGCATATTAAAAGTTGTTTAC  24922
LOC642846 ............................................................  24442
DDX12P    ...............................................-............  24425

DDX11     AGTAATTATTGTTTCTGACGTTCACATTGTGAGAGCCCCTTCCTGCTAGCTCAGGTCCTC  24982
LOC642846 ...C......................G.............................  24502
DDX12P    ...C..............A.......G.............................  24485
```

```
DDX11     CCCGTGGCCCGGTCAGTCTCGCCTCCAGCACAGCAGAATGTCATGGGATCACCATGGGTG  25042
LOC642846 ............................................................  24562
DDX12P    ............................................................  24545

DDX11     TCCTTTCCCCACACTGGATTGATTCATTTCTCCAAGCTGCTCTGGTTTCTTGTAATGGGG  25102
LOC642846 .....G..G.....................................................  24622
DDX12P    .....G..G.............................C.........................  24605

DDX11     AATGACATTTAGAAGTCAAGCTGTGGGTGCTAGGGTGTTTGTCGTGCTCCTGGGGCGTTT  25162
LOC642846 ..........................................................A...  24682
DDX12P    ..........G................................A............A...  24665

DDX11     TGGTAGACAGATCTAGGAAATGTTTTCAGAATGAATCCATACTGGTATTTCTTTCTTTCT  25222
LOC642846 ...............................G............................  24742
DDX12P    .A..........................................................  24725

DDX11     TTC----TTTTTTTTTTTTTTTTTTTGAGACACAGTCTCGCTCTGTCTCCCAGGCTGG  25278
LOC642846 ...---------..................................................  24794
DDX12P    ...TTTC............................G.........................  24785

DDX11     AGCGCAGTG-ACCTGATCACGGCTCTCTGCAACCTCTGCCTCCGGGGTTCAAGCGATTCT  25337
LOC642846 ..........-...C.................................................  24853
DDX12P    ..........A...C.................................................  24845

DDX11     CATGCCTCAACCTCCTGAGTAGCTGTGATTACAGGCATGTGCCACCACACCCAGCTAATT  25397
LOC642846 ............................................................  24913
DDX12P    ............................................................  24905

DDX11     TTTGTATTTTAGTAGAGATGGGGTTTTACCATGTTGGCCAGGCTGGTCTTGAAATCAGGT  25457
LOC642846 ...................A..................................T....T.  24973
DDX12P    ..................................................C.......  24965

DDX11     GATCCGCCAGCCTTGGCATCCCAAAGAGCTGGGATTACAGGCATGAGCCACCACGCCTGG  25517
LOC642846 ............................................................  25033
DDX12P    ............................................................  25025

DDX11     CCCATATTGGTGTTTCTAAGTAAAAATCAAAGGATTTGTTTACTTGACCTTTTATTGTAC  25577
LOC642846 ............................................................  25093
DDX12P    ............................G...............................T  25085

DDX11     CTCTTTTTCTCTTAAGCCTGAACATGTGTGCTACATTAACATACTTATCTGCTCTATCCT  25637
LOC642846 ............................................................  25153
DDX12P    ........................................T...................  25145

DDX11     ATAATATACTTAAAAGTTTTGAAATCATAGTACCAATATTACTTCTAACAATAGATCTGA  25697
LOC642846 ............................................................  25213
DDX12P    ..........................................A.................  25205

DDX11     TTGAAATTGCCTTTCCTCTTTGCCTTTAGAGTGTAACCCACTAAGGATGCCTGGTCACTA  25757
LOC642846 ........................C...................................  25273
DDX12P    ........................C...................................  25265
```

```
DDX11     GGCTCTAAAGTCACGTGGAACCAGGCTTCTCTCCGTGTGCTTCTGTTGTCAGTTTCATAG  25817
LOC642846 ............................................................  25333
DDX12P    ............................................................  25325

DDX11     ATAACTAGGCTGTTTTTGTTTCATTTTCTTTTCAATTTTAGAATTTGCTTTTTTCTTTTC  25877
LOC642846 ...G.....................................................C....  25393
DDX12P    ...G.....................................................C....  25385

DDX11     TGACTTGTAGTTTTTAAATATGTAAATATTTGTATGGCTCAAAAGTCAAAGCAATATAAA  25937
LOC642846 ............................................................  25453
DDX12P    ............................................................  25445

DDX11     AAGATCTATTCAGGAAAGCCTCACTCTCATCCCTTTCCAGCCCATTCCCCACCCCCATAG  25997
LOC642846 ............................................................  25513
DDX12P    ............................................................  25505

DDX11     GGAATCCGTTTTACTAGCTTATCCTTTCAGTCTTTCTTTTTCCCCTAAATAAGCAAAAAC  26057
LOC642846 ............................................................  25573
DDX12P    ..................................--......................  25563

DDX11     GTGTCTTCATTTTTCCCTTTCCTGTTTTATTTACACAGAAGGCATCTTAGTCAGTTGTCT  26117
LOC642846 ...C....T.........................G.......................  25633
DDX12P    ...................C....................................  25623

DDX11     GACCATCGCTCCTCTAGTGGGCTGCGTGGTTCTCTGTTGGACAGATGTAGGGAGCTTATC  26177
LOC642846 .G.................................................A........  25693
DDX12P    ............................................................  25683

DDX11     CAACCAGTACCCTCTGGATAGGCAGGCGCATGATTACAGGGAAAGGTCCGGGGGCACATG  26237
LOC642846 ............................................................  25753
DDX12P    ..........................T.....................T...........  25743

DDX11     CTGTTTGGTATTTGTGGGCTGTATCTTCTCACTGGACTCCTAAATATGGGATTCCTGGGT  26297
LOC642846 ............................................................  25813
DDX12P    ............................................................  25803

DDX11     TAAAAAGTATAAATATGTTTAATTTGTTAACTACTGTGAAATTTCATGAGAATTGTACCA  26357
LOC642846 ............................................................  25873
DDX12P    ............C...............................................  25863

DDX11     TTCTGTATCCCACCAGTACTGTCTAGGAATGCCTGTTTCTCCAGAGTGGTTACTTTTGGA  26417
LOC642846 ............................................................  25933
DDX12P    ..................................................A.........  25923

DDX11     TTTTTGCCAGTCTAACAGGTGAAAGCCTGGAGATTCTTATTCAGTAGTTTGGGCTGGGGC  26477
LOC642846 ..............G.....................G.......................  25993
DDX12P    ..............G...........T........G.......................  25983

DDX11     CTGGCCATGTG-TATTTTTGAAAATTTTCGCTGGTGATTTTGCTGCATGGCCAGGGTTGA  26536
LOC642846 .......C...-.....................................................  26052
DDX12P    .......C...T.....................................................  26043

DDX11     TAATGACTGTGCCAGATTTGCTGGATTTCCTTTGCTGTTCCTGCACATAGTTTAAACGAG  26596
LOC642846 ....................................A.......................  26112
DDX12P    ............................................................  26103
```


DDX11 ACTGCCAGCACTGGGTATCAGTCACCATTTTTCTTTTTGTTAGTTTGCCATCAGCCTTTT 26656
LOC642846 .....G..... 26172
DDX12P .....G..... 26163
DDX11 CTTTGACCTCTTCTTTCAGTTTGTGTGTACTTGCTGTCTCTTAGCCCAGACTTCTCGCTT 26716
LOC642846 .....G..... 26232
DDX12P .....G..... 26223
Exon 19
DDX11 CCTTTCTGCTGGGCCTCTGAGGGGTCATGGGGCCGTGACGCTGTGGCCTTGGTCTACAGG 26776
LOC642846 .....A.....C..... 26292
DDX12P .....A..... 26283
DDX11 TGTCTGACTTCCGGCAGCAGCTGCTGGCCTGTGCCGGGGTGGAAGCTGAGCGCGTGGTGG 26836
LOC642846 .....T..... 26352
DDX12P .....A..... 26343
DDX11 AGTTTTCCTGTGGTGAGAAGCTGTGCCCAGGGTGGGGCAGGCTAGAGGTCAGGTTCTGGC 26896
LOC642846 26412
DDX12P 26403
DDX11 CCCCGTTTTCTGTGGGTAATACCTCATACTGCGACCAGGCACAGGGGCGGAGGAGACCCC 26956
LOC642846 .....C.T.....A..... 26472
DDX12P .....A.....A..... 26463
DDX11 GGGGTGGGAGCCTCACCCTTCGTGCGCTCGCCCAGGCTCTCCTGCTTTGCTCCCTGCTGC 27016
LOC642846 ...A..... 26532
DDX12P ...A.....A.....A..... 26523
DDX11 C-------TGCTGCCCAGTGTGACTGGTGATGGTGGGCGGGTGAGCGCTGTCAGTCGCTG 27069
LOC642846 .-------.....C.....T..... 26585
DDX12P .TGCTGCG.....C.....T..... 26583
DDX11 TTCCTGTGCTGGATGATGGGGCAGGGAAATGCCCTCTCTGCAGTGTCTTGCAGCACACCT 27129
LOC642846 .....T.....A..... 26645
DDX12P .....T.....A..... 26643
Exon 20
DDX11 GCATCTCCAGTTTTCGGCCCCTCCCTGGCTCTTACCAGGTCACGTGATCCCTCCAGACAA 27189
LOC642846 .....A-..... 26704
DDX12P .....T..... 26703
DDX11 CATCCTGCCCCTCGTCATCTGCAGCGGGATCTCCAACCAGCCGCTGGAATTCACGTTCCA 27249
LOC642846 ...-.....T.....C..... 26763
DDX12P .....T.....G.....A..... 26763
DDX11 GAAAAGAGAGCTGCCTCAGATGGTCAGTCCCAGCCAGCTCGCCGCACCACAGCCTGGCCT 27309
LOC642846 .....C.....T..... 26823
DDX12P ...G.....C.....T..... 26823
DDX11 CAGGCAGCAAAGGGTTTTCTGGGGCAGGGGCGCTCTGGCCCACCCTGAGTGTTTTCA-GT 27368
LOC642846 .....A.....G.. 26883
DDX12P .C.....G.. 26883

```
DDX11     GTTGGGGAAATTGCACAGGGACACCCGCTTAGAGCCACACAGAATGAGCGGCGTCGATCT  27428
LOC642846 ..........................A.................................  26943
DDX12P    ..........................A.................................  26943

DDX11     AGATGCTTATGGAGGAAGGTCTGAGCTTCCCCGCCCCTCACGCCTTAGGCTGCGAAATAT  27488
LOC642846 ....................................T.....A.................  27003
DDX12P    ...........................................................  27003

DDX11     GTATTCATAAAACCTCCAGGCATCCTCTGAGGACGCCTCACACAGGAGAAAGCTGCTAGT  27548
LOC642846 ........................T.................G.................  27063
DDX12P    ..........................................T...C.............  27063

DDX11     TCCCTTTGGCTCTCTTGCCCTTTGGTTATATCTGCCCCTGCCGGGGGTAGGGATGTGGGG  27608
LOC642846 ..........................................T.....C............  27123
DDX12P    ................................................C............  27123

DDX11     CTTGGGGGCATCTCCTGTGGTGTGCCTGGGGTGTGCAGCCCCTGATTGTCGTTGTGGTGC  27668
LOC642846 ................................................A.........  27183
DDX12P    ................................................A.........  27183

DDX11     CCATCAGGACCCTGGACAGAAGAAGGGAGGACTCAGTGCCAGGGCAATAGGGAGGCCCCC  27728
LOC642846 ...........................................................  27243
DDX12P    ............................C..............................  27243

DDX11     TAGGGACGCTAGTGCTGTGACATGTGTCAGAAAGGCGCAGTCAGCAGCAGCGGCTGGGTG  27788
LOC642846 C..........................................................  27303
DDX12P    C...........................G.....................T.........  27303

DDX11     TGTTTGGTGGGAGGTGGCACCTACCACCCCGTGGTTCCCACCCAGGGGAGCCAAGTCCTC  27848
LOC642846 ...........................................................  27363
DDX12P    ...........................................................  27363

DDX11     TTCCTTGGCTGTAGTCCTGCCGAGGGTCTCTCCTCAGTTTTGAGTCTCAAGGTGAAGACG  27908
LOC642846 ......................A....................................  27423
DDX12P    ...T........................................................  27423

DDX11     CGGTTTGTGGGTGGCTGAGGGGTTGCTCCATGGGGGCTCCCTCCCTCCCTC---------  27959
LOC642846 ..............................................-------------  27470
DDX12P    .......C.................................................CCTTCCTTC  27483

                                  Exon 21
DDX11     -----------CTTTCCTTCCTTAGATGGACGAGGTGGGTCGCATTCTCTGTAACCTGTG  28008
LOC642846 -----------.C.................................C.............  27519
DDX12P    CTTCCTTCCTT.C.............................C.............  27543

DDX11     CGGTGTGGTTCCTGGAGGGGTGGTCTGTTTCTTCCCCTCCTACGAGTACCTGCGCCAGGT  28068
LOC642846 ..........T.....................T.........................  27579
DDX12P    ..........T...........................................  27603

DDX11     CCATGCCCACTGGGAGAAGGGTGGCCTGCTGGGCCGTCTGGCTGCCAGGAAGAAGGTGAG  28128
LOC642846 ...........................................................  27639
DDX12P    ...........................................................  27663

DDX11     TGGCCTGTCGGCAGCCTTCCCACTTGTGAGGACAGTGCCACTGAGTCCTCCTGGGAGCTC  28188
LOC642846 ..................G........................................  27699
DDX12P    ...........................................................  27723
```

```
DDX11     TCGTGCTCATCGGGTCAGGACAGGCTTCTGGCTCCTCATCCCCACCGCTCCCAGTCCCTG  28248
LOC642846 .T.............G............................T.............  27759
DDX12P    .T.........................................A.............  27783

DDX11     ACTACAGAGGATTTCCCCCAAAGTCCCTGGCTGTGAGGTTCTCCAGTCCCCTGGCCAGAA  28308
LOC642846 ............-.................................G.........  27818
DDX12P    ............-.............................................  27842

DDX11     AACACAAGGCCACGAGCAGACTCGAGACCTGGCACCCTGAACCTGTCTCTGGGAAATGTC  28368
LOC642846 ....................C.................A.....................  27878
DDX12P    ....................C.....................................  27902
                              Exon 22
DDX11     CTCTGTCTTTCTCAGATATTCCAGGAACCTAAGAGCGCACACCAGGTGGAGCAGGTGCTG  28428
LOC642846 ............................................................  27938
DDX12P    ............................................................  27962

DDX11     CTGGCATATTCCAGGTGCATCCAGGTGCGGGCGTCATGCTGGGCTTGGGTCTGAGATCGT  28488
LOC642846 .....G.................................A..............C.A.  27998
DDX12P    .....G...----------.....................A........A.....C.A.  28012

DDX11     GTGGGGGTGGCAGCTGGAAACGTTGTGGGTGTCATCCAAGTTTTGGCTCAGCAACTCAGC  28548
LOC642846 ......................---.................................  28055
DDX12P    ............................................................  28072
                                    Exon 23
DDX11     GTCTGGGTTTCTCCTACAGGCCTGTGGCCAGGAGAGAGGCCAGGTGACAGGGGCCCTGCT  28608
LOC642846 ................................................A.........  28115
DDX12P    ..........................................CC..............  28132

DDX11     CCTCTCTGTGGTTGGAGGAAAGATGAGTGAAGGGATCAACTTCTCTGACAACCTAGGCCG  28668
LOC642846 ............................................................  28175
DDX12P    ............................................................  28192

DDX11     GTAAGTAGTGGTTCTGCTCGTCTCCTGGGCCGTGATACATGGCCGGCCCTCACTCCCAGC  28728
LOC642846 ..................A.........T...............................  28235
DDX12P    ..................A.......................A......T.......  28252

DDX11     AGCTGGGCCCCTGCCTGCTCTCTGCTGCCATTAGAGCCCACAGCTGGGCTGCGACTGCTC  28788
LOC642846 ..................G.........................................  28295
DDX12P    ..................G.........................................  28312

DDX11     AGACCAGCCAGCTGGAGGGAGGGGCTCAGCAGCTCTGGGTTTGGTCCTGGGAGAGCAGTT  28848
LOC642846 ..........................................C....A.....T....  28355
DDX12P    ..........................................C...............  28372

DDX11     GGATTTTAGGCTACCCATTGCTGTATCAGGACCCAGTCAATTGGCCTAGACGGGATCTCT  28908
LOC642846 ............GG.....................A.......................  28415
DDX12P    ............GG.....................A.......................  28432

DDX11     CAGCCGAACAAGCCCTCTCCAGGTGGTAGGTACAGAGTGGAGAGAGGCTGAGTTTTGATC  28968
LOC642846 .....TT..........................................................  28475
DDX12P    .....TT..........................................................  28492
```

```
DDX11      ACAGTCGGAGA-GGCTGAGGGAAGGGGTAGAACGGAGCAGCTGGTGACGTGGGTGATGAC  29027
LOC642846  ...........G......C.............................A...........  28535
DDX12P     ...........G......C.............T..............A...........  28552

                                                          Exon 24
DDX11      CCGGGAGGTCCTGACGTCCACCTGCTGGGCTCTTGTCTCCCCCGCCCAGGTGTGTGGTGA  29087
LOC642846  .......T.............CA..................--....C...........  28593
DDX12P     ......................C.................--..............  28610

DDX11      TGGTGGGCATGCCCTTCCCCAACATCAGGTCTGCAGAGCTGCAGGAGAAGATGGCCTACT  29147
LOC642846  ............................................................  28653
DDX12P     ............................................................  28670

DDX11      TGGATCAAACCCTCGTGAGTGACCCCAGTGTCACAGA--GGGTGACAGGAGAGTAGGCAG  29205
LOC642846  ......................................--.......---...........  28708
DDX12P     ....................................GG......................  28730

DDX11      TGGGTGGGAGTGGCATCACCCCCAGGGCTGATACAGCCAGGCCTTCCCCGCTGCGCTGGC  29265
LOC642846  ................................................A.........T  28768
DDX12P     ................................................A.........T  28790

DDX11      GTCTCCTGCCCCCTCCGGAAGCTTGGATGCCCCTCCACACCCTCTTGATCTTCCCTGTGA  29325
LOC642846  ............................................................  28828
DDX12P     ............................................................  28850

DDX11      TGTCACCTGGACCCCTGCTGCTGGCATTGGCCACGAAGCCTCCTGGTCTGGCTCCAAAGC  29385
LOC642846  ................................A...........................  28888
DDX12P     ............................................................  28910

DDX11      CTGGCAGGGTCTTTTCCCAGGGGGAGCTGCAGGCAGGGAACAGTCCTGATGGGTCTTCCC  29445
LOC642846  ................C.....................................A....  28948
DDX12P     .......C.........C.....................................A....  28970

                      Exon 25
DDX11      CTTCACTCCCAGCCCAGAGCCCCCGGCCAGGCACCCCCAGGGAAGGCTCTGGTGGAGAAC  29505
LOC642846  ............................................................  29008
DDX12P     ................................A...........................  29030

DDX11      CTGTGCATGAAGGCCGTCAACCAGTCCATAGGTGAGCCTGGCTGCCTCCAGCTGGGTGGA  29565
LOC642846  ............................................................  29068
DDX12P     ............................................................  29090

DDX11      CAGATGGGGGCTGGAGAAAGGGAGAACAGGAAAGAGGGGTTGCCTGCCCTGTTTCCTATA  29625
LOC642846  ................G...........................................  29128
DDX12P     ........A.........G.........................................  29150

DDX11      TAAGTCTGAGGAAGGGGA--GGGGGTCGCCGTGGGAATGTGCTGTAGGGGGGAGGCAGGT  29683
LOC642846  ................--.........A.............--.................  29184
DDX12P     ..............T..GG.........A.............-.................  29209

                                                  Exon 26
DDX11      GTTGCTCGGAGCCCCAGCCTCTGTTCCTATGCAGGCAGGGCCATCAGGCACCAGAAGGAT  29743
LOC642846  ............................................................  29244
DDX12P     ...........G................................................  29269

DDX11      TTTGCCAGCGTAGTGCTCCTGGACCAGCGATATGCCCGGCCCCCTGTCCTGGCCAAGCTG  29803
LOC642846  .........A.....................C..............................  29304
DDX12P     .........A.....................C..............................  29329
```

```
DDX11     CCGGCCTGGATCCGAGCCCGTGTGGAGGTCAAAGCTACCTTTGGCCCCGCCATTGCTGCT  29863
LOC642846 ..................A.......................................  29364
DDX12P    ..................C.......................................  29389

DDX11     GTGCAGAAGGTCAGTCCTACCTTTTTCTTTCTGAGAGCCTCCCCACCCCGAGATCACATT  29923
LOC642846 ..........................................A................  29424
DDX12P    ..........................................A................  29449
                                    Exon 27
DDX11     TCTCACTGCCTTCTGTCTGCCCAGTTTCACCGGGAGAAGTCGGCCTCTTCCTGATGGGCA  29983
LOC642846 ...........................................................  29484
DDX12P    ...........................................................  29509

DDX11     ACCACACCACTGCCTGGCGCCGTGCCCTTCCTTTGTCCTGCCCGCTGGAGACAGTGTTTG  30043
LOC642846 ..........C...C............................T................  29544
DDX12P    ..........C...C............................T................  29569

DDX11     TCGTGGGCGTGGTCTGCGGGGATCCTGTTACAAAGGTGAAACCCAGGAGGAGAGTGTGGA  30103
LOC642846 ..................A........................................  29604
DDX12P    ..................A........................................  29629

DDX11     GTCCAGAGTGCTGCCAGGACCCAGGCACAGGCGTTAGCTCCCGTAGGAGAAAATGGGGGA  30163
LOC642846 .........C......G.....................................C....  29664
DDX12P    .........C.....................................................  29689

DDX11     ATCCTGAATGTACAGTGGGTCCTGGCTGTCCTTGGGGCGTTCCAGGGCAGCTCCCCTCCT  30223
LOC642846 ...........................................................  29724
DDX12P    ...........................................................  29749

DDX11     GGAATAGAATCTTTCTTTCCATCCTGCATGGCTGAGAGCCAGGCTTCCTTCCTGGTCTCC  30283
LOC642846 ...............................................G.T...AG...  29784
DDX12P    ...........................................C...CG.T........  29809

DDX11     GCAGGAGGCTGTGGCAGCTGTGGCATCCACTGTGGCATCTCCGTCCTGCCCACCTTCTTA  30343
LOC642846 ..................A.....................................---....  29841
DDX12P    A...........................................................  29869

DDX11     AGAGGCGAGATGGAGCAGGCCCATCTGCCTCTGCCCTTTCTAGCCAAGGTTATAGCTGCC  30403
LOC642846 ..................T........................................  29901
DDX12P    ...........................................................  29929

DDX11     CTGGACTGCTCACTCTCTGGTCTCAATTTAAAATGAT-CCATGGCCACAGGGCTCCTGCC  30462
LOC642846 ....................................C..G...................  29961
DDX12P    ......................T.............C......................  29989

DDX11     CAGGGGCTTGTCACCTTCCCCTCCTCCTTCCTGAGTCACTCCTTCAGTAGAAGGCCCTGC  30522
LOC642846 ...........................................................  30021
DDX12P    ...........................................................  30049

DDX11     TCCCTATCCTGTCCCACAGCCCTGCCTGGATTTGTATCCTTGGCTTCGTGCCAGTTCCTC  30582
LOC642846 ..T........C.....................................................  30081
DDX12P    ..T........C....T.....................................................  30109
```

```
DDX11      CAAGTCTATGGCACCTCCCTCCCTCTCAACCACTTGAGCAAACTCCAAGACACCTTCTAC  30642
LOC642846  ............................................................  30141
DDX12P     ............................................................  30169

DDX11      CCCAACACCAGCAATTATGCCAAGGGCCGTTAGGCTCTCAACATGACTATAGAGACCCCG  30702
LOC642846  ...G.....................A.....................................  30201
DDX12P     ...G.....................A.....................................  30229

DDX11      TGTCATCACGGAGACCTTTGTTCCTGTGGGAAAATATCCCTCCCACCTGCAACAGCTGCC  30762
LOC642846  .A......T.........................A.............................  30261
DDX12P     .A......T.....................................................  30289

DDX11      CCTGCTGACTGCGCCTGTCTTCTCCCTCTGACCCCAGAGAAAGGGGCTGTGGTCAGCTGG  30822
LOC642846  ..............................................C.............  30321
DDX12P     ..............................................C.............  30349

DDX11      GATCTTCTGCCACCATCAGGGACAAA-CGGGGGCAGGAGGAAAGTCACTGATGCCCAGAT  30881
LOC642846  ........................C.................................C.  30381
DDX12P     ........................C.................................C.  30409

DDX11      GTTTGCATCCTGCACAGCTATAGGTCCTTAAATAAAAGTGTGCTGTTGGTTTCTGCTGA-  30941
LOC642846  ..................C..........T.........A.........---------   30441
DDX12P     ..................C..........T.........A.................G  30469
```